Joint Defra/EA Flood and Coastal Erosion Risk Management R&D Programme

Absolute Fixing of Tide Gauge Benchmarks and Land Levels:

Measuring Changes in Land and Sea Levels around the coast of Great Britain and along the Thames Estuary and River Thames using GPS, Absolute Gravimetry, Persistent Scatterer Interferometry and Tide Gauges

R&D Technical Report FD2319/TR

Environment Agency

defra
Department for Environment Food and Rural Affairs

Joint Defra/EA Flood and Coastal Erosion Risk Management R&D Programme

Absolute Fixing of Tide Gauge Benchmarks and Land Levels:

Measuring Changes in Land and Sea Levels around the coast of Great Britain and along the Thames Estuary and River Thames using GPS, Absolute Gravimetry, Persistent Scatterer Interferometry and Tide Gauges

R&D Technical Report FD2319/TR

Produced: April 2007

Authors: R M Bingley, F N Teferle, E J Orliac, A H Dodson, (IESSG)
S D P Williams, D L Blackman, T F Baker, (POL)
M Riedmann, M Haynes, (NPA)
D T Aldiss, H C Burke, B C Chacksfield and D G Tragheim (BGS)

Statement of use

Dissemination status

Internal: Released Internally.
External: Released to Public Domain.

Keywords: Land Level; Sea Level; Great Britain; Thames Estuary; Global Positioning System (GPS); Absolute Gravimetry (AG); Persistent Scatterer Interferometry (PSI); Tide Gauge (TG)

Research contractors: this report was produced by the Institute of Engineering Surveying and Space Geodesy (IESSG), University of Nottingham, University Park, Nottingham, NG7 2RD (Responsible person: Dr Richard M Bingley, richard.bingley@nottingham.ac.uk), with input from Proudman Oceanographic Laboratory (POL), Nigel Press Associates Ltd. (NPA) and British Geological Survey (BGS).

The research work reported on in this Technical Report was carried out as a national study, funded by the Joint Defra/EA Flood and Coastal Erosion Risk Management R&D Programme as FD2319, and a regional study, funded by the Environment Agency Thames Estuary 2100 project, Phase 2, Estuary Processes Theme, study ref. EP20. The national study was carried out jointly by POL and IESSG. The regional study was led by IESSG and carried out jointly by IESSG, POL, NPA and BGS.

Defra/EA and EA TE2100 project officers: Ian Meadowcroft, Environmental Policy – Risk & Forecasting, Environment Agency, Kings Meadow House, Kings Meadow Road, Reading, RG1 8DQ. (ian.meadowcroft@environment-agency.gov.uk). Owen Tarrant, Environment Agency Thames Estuary 2100 project, Thames Barrier, Eastmoor Street, Charlton, London, SE7 8LX. (owen.tarrant@environment-agency.gov.uk).

Publishing organisation

Department for Environment, Food and Rural Affairs
Flood Management Division,
Ergon House,
Horseferry Road
London SW1P 2AL

Tel: 020 7238 3000 Fax: 020 7238 6187

www.defra.gov.uk/environ/fcd

Published by the Department of Environment, Food and Rural Affairs, July 2007. Printed on material that contains a minimum of 100% recycled fibre for uncoated paper and 75% recycled fibre for coated paper.

PB No. 12643

Executive summary

Since 1997, Defra and the Environment Agency (EA) have been funding research to measure long term changes in land and sea levels around the coast of Great Britain and along the Thames Estuary and River Thames:

- to monitor current changes in land level due to ‘land tilt' and regional/local geological effects;
- to improve estimates of climate driven changes in sea level based on tide gauges;
- to help in predicting future sea level rise;
- to carry out more refined regional studies to support planning for flood risk management for the Thames Estuary and River Thames.

The aims of these measurements are to obtain direct estimates of current changes in land level on the scale of millimetres per year, in a stable reference frame, both at tide gauges and at other specific locations, and to use these to obtain estimates of changes in sea level (decoupled from changes in land level). Such measurements represent a major challenge and the research carried out has essentially included three complementary monitoring techniques: the Global Positioning System (GPS); Absolute Gravimetry (AG); and Persistent Scatterer Interferometry (PSI).

The objectives of the research work reported in this Technical Report were to investigate how best to combine the information from these three complementary monitoring techniques to meet these aims.

From 2003 to 2006, the research work was carried out as a national study, funded by the Joint Defra/EA Flood and Coastal Erosion Risk Management R&D Programme as FD2319, and a regional study, funded by the Environment Agency Thames Estuary 2100 project. The national study was carried out jointly by the Proudman Oceanographic Laboratory (POL) and the University of Nottingham’s Institute of Engineering Surveying and Space Geodesy (IESSG). The regional study was led by IESSG and carried out jointly by IESSG, POL, Nigel Press Associates Ltd. (NPA) and British Geological Survey (BGS). For the national study, continuous GPS (CGPS) stations have been established at ten tide gauges around the coast of Great Britain and AG measurements have been made at three of these. For the regional study, episodic GPS (EGPS) data from a network of stations in the Thames Region and PSI data for hundreds of thousands of persistent scatterer (PS) points in the Thames Region have been analysed and the changes in land level interpreted using various geoscience data sets.

The report presents the results from all three monitoring techniques, including the estimates and uncertainties obtained for the changing land and sea levels.

The results for the national study demonstrate how:

- the combined CGPS and AG estimates of changes in land level
  - correlate with long term geological and geophysical evidence for the 'tilt' of Great Britain, which have Scotland rising by 1 to 2mm/yr and the South of England subsiding by up to 1.2mm/yr.
  - are in general agreement with long term geological and geophysical evidence, in terms of whether there is subsidence or uplift at individual stations, although in some cases there are differences which are of the same order as the changes in land level themselves and are, therefore, significant in relation to any assumptions made regarding future changes in land level.
- when the combined AG and CGPS results are considered along with tide gauge estimates of changes in sea level, our 'best' current estimate for the average change in sea level (decoupled from changes in land level) around the coast of Great Britain over the past few decades/past century suggests that sea level has risen by 0.9 to 1.2mm/yr.
- the direct estimates of changes in land level at specific tide gauges can be combined with predictions of future changes in sea level to provide an assessment of future changes in sea level around the coast of Great Britain.

The results for the regional study demonstrate how:

- when the CGPS and AG estimates of changes in land level from the national study are combined with the EGPS and PSI estimates of changes in land level from the regional study, the estimates of changes in land level for the Thames Region, which range from approximately 0.3mm/yr uplift to 2.1mm/yr subsidence, correlate with certain aspects of the geoscience data sets to explain the pattern of land movements observed on a regional scale.
- when the CGPS and AG estimates of changes in land level from the national study are combined with the EGPS and PSI estimates of changes in land level from the regional study and considered along with the results of a new analysis of the tide gauge data for the Thames Estuary and River Thames
  - the estimates for the changes in sea level (decoupled from changes in land level) along the Thames Estuary and River Thames are consistent with those obtained around the coast of Great Britain.
  - our 'best' current estimate for the combined effect of changes in land and sea levels is a 1.8 to 3.3mm/yr rise in sea level with respect to the land along the Thames Estuary and River Thames over the past few decades/past century.

The report concludes that the national and regional studies were extremely successful and have greatly improved our knowledge of changes in land and sea levels around the coast of Great Britain and along the Thames Estuary and River Thames well beyond what was known at the start of the studies in 2003. They have provided new estimates of changes in land level due to 'land tilt' and regional/local geological effects, new estimates of climate driven changes in sea level based on tide gauges and a new assessment of future sea level rise. The results are, therefore, of direct relevance to the Joint Defra/EA Flood and Coastal Erosion Risk Management R&D Programme Modelling and Risk (MAR) Theme, in providing information and knowledge to support decision making in terms of coastal flood risk management and climate change, as part of the

cross cutting risk based knowledge and methods sub-theme. The results are also a direct input to the Environment Agency Thames Estuary 2100 project.

A number of recommendations are then given, both for improving the confidence we can place on the current results, and for further long term monitoring. Together, these will enable the validation of climate change model predictions of sea level rise around Great Britain, particularly as the various IPCC scenario predictions are likely to remain uncertain. This will lead to a better assessment of risk and more informed decisions on planning and managing flood risk at the coast and in our estuaries.

The recommendations for long term monitoring on a national scale are particularly important in the context of policy needs from the sciences over the next 10 years (Defra 2004). These include the need for key long-term evidence relating to climate change and the specific requirements for monitoring, reliable regional predictions and a comprehensive understanding of the range of climate change impacts, including sea level rise.

The recommendations for long term monitoring on a regional scale aim to provide a monitoring solution for the Thames Estuary and River Thames. This would be part of an adaptive strategy for the long term planning of flood and coastal defences in that region, established as a result of the Environment Agency Thames Estuary 2100 project.

Foreword and acknowledgements

The research work reported on in this Technical Report was carried out as a national study, funded by the Joint Defra/EA Flood and Coastal Erosion Risk Management R&D Programme as FD2319, and a regional study, funded by the Environment Agency Thames Estuary 2100 project. The national study was carried out jointly by the Proudman Oceanographic Laboratory (POL) and the University of Nottingham's Institute of Engineering Surveying and Space Geodesy (IESSG). The regional study was led by IESSG and carried out jointly by IESSG, POL, Nigel Press Associates Ltd. (NPA) and British Geological Survey (BGS).

The results detailed in this report are based on data that was observed and/or collated during the periods of the national and regional studies, i.e. from 2003 to 2006, but also on data which was observed earlier. For the national study, Global Positioning System (GPS) and Absolute Gravimetry (AG) data were observed between 1996 and 2003 as part of MAFF project FD0305 and Defra project FD2301. For the regional study, GPS data was observed between 1997 and 1999 as part of Natural Environment Research Council (NERC) CONNECT Scheme grant GR3/C003 and Environment Agency R&D Project W5-i698.

Apart from the author and co-authors listed, many other persons, past and present, from the funding organisations and the contracting organisations have contributed to the results detailed in this report in one way or another and are hereby acknowledged as:

- persons who contributed to the earlier projects: Tony Polson, formerly of MAFF/Defra, and Peter Allen-Williams formerly of Defra now of the Environment Agency; Dick Greenaway, formerly of the Environment Agency, and Mervyn Bramley, Keith Nursey and Mike Sutton, from the Environment Agency; Glen Beamson, Simon Booth, Pete Clarke, Andy Evans, Kenny Gibson, Andrew Nesbitt, Nigel Penna, Leighton Symons, Theo Veneboer and Vidal Ashkenazi, formerly of IESSG; Bob Edge and Graham Jeffries, formerly of POL; Tony Morigi, from BGS.
- persons who contributed to both the earlier and the latest projects: John Goudie and David Richardson, from Defra; Samantha Waugh, from IESSG; Steve Booth, Richard Ellison and John Rees, from BGS.
- persons who contributed to the latest projects: Richard Groom, Ian Meadowcroft, Tim Reeder, Suresh Surendran, Simon Tanner and Owen Tarrant, from the Environment Agency; Emily Cosser, Chris Hide, Sean Ince, Oluropo Ogundipe and Jock Souter, formerly of IESSG, and Stephen Blake, Jon Leighton, Caroline Noakes, Andy Sowter and Mark Warren, from IESSG; Daniel McLaughlin, from POL; Geraint Cooksley, formerly of NPA, and Ren Capes, Kim Culver, Nigel Press and Adam Thomas from NPA; Emma Bee, Stephen Brearley, David Entwisle, Lee Jones, John Ludden, Andrew McKenzie, David Morgan, Bruce Napier, Helen Rutter, Ricky Terrington and Gerry Wildman from BGS; Mervyn Littlewood from HR Wallingford.

Finally, we would like to acknowledge: the data and products provided by the International GNSS Service (IGS); the services of the NERC British Isles GPS

archive Facility (BIGF), which provided data for continuous GPS (CGPS) stations in Great Britain that were not directly funded by Defra or the Environment Agency; the services of the NERC British Oceanographic Data Centre (BODC), which provided some data for some tide gauges on the Thames Estuary and River Thames; the Permanent Service for Mean Sea Level (PSMSL), which provided up-to-date estimates of changes in sea level for British tide gauges; the Port of London Authority, which provided some data for some tide gauges on the Thames Estuary and River Thames; and all of the landowners who gave their permission for the establishment of the CGPS stations on a national scale and the episodic GPS (EGPS) stations in the Thames Region, and for allowing us access to observe at those stations over the last 9 years.

Contents

Contents

Figures

Contents

Tables

Contents

Appendices

Glossary

Acronyms

AG	Absolute Gravimetry
AOI	Area Of Interest
ArcMap9.1	GIS employing the ESRI software system ArcMap 9.1, used by BGS in the regional study
BGS	British Geological Survey
BIGF	NERC British Isles GPS archive Facility
BODC	NERC British Oceanographic Data Centre
BSM	Berntsen Survey Monument
BSW5.0	Bernese GPS Software (version 5.0); developed by the Astronomic Institute, University of Berne and used by IESSG in the national study
CATS	Create and Analyse Time Series software; developed by POL and used by IESSG in the national study
CGPS	Continuous GPS
CGPS@TG	Continuous GPS at Tide Gauge
CTSAna	Coordinate Time Series Analysis tools for CATS; developed by IESSG and used by IESSG in the national study
DD	Double Differencing
Defra	Department for Environment, Food and Rural Affairs
DInSAR	Differential Synthetic Aperture Radar Interferometry
DEM	Digital Elevation Model
DTM	Digital Terrain Model
EA	Environment Agency
EABM	EA BenchMark
EDTEVA	The principal program within TEVA
EGPS	Episodic GPS
EGPS@TG	Episodic GPS at Tide Gauge
ENVISAT	Environmental Satellite
ERS	European Remote Sensing
ESA	European Space Agency
ETM	Enhanced Thematic Mapper
ETRS89	European Terrestrial Reference System 1989
FBM	Fundamental BenchMark
FN	Flicker Noise
GALILEO	The European equivalent GNSS to GPS
GAS2.4	GPS Analysis Software (version 2.4); developed by IESSG and used by IESSG in the national and regional study
GEV	Generalised Extreme Value
GIA	Glacial Isostatic Adjustment
GIS	Geographic Information System
GLONASS	The Russian GNSS equivalent to GPS
GLOSS	Global Sea Level Observing System
GMT	Generic Mapping Tools, used by IESSG in the national study
GNS	Global Network Solution
GNSS	Global Navigation Satellite System
GPS	Global Positioning System; the American GNSS

GTS	Globally Transformed Solution
IAG	International Association of Geodesy
ICAG	Intercomparison of Absolute Gravimeters experiment
IERS	International Earth Rotation Service
IESSG	The University of Nottingham's Institute of Engineering Surveying and Space Geodesy
IGb00	The IGS realisation of ITRF2000 based on a global GPS network
iGNSS	interactive GNSS processing tools for BSW5.0; developed by IESSG and used by IESSG in the national study
IGS	International GNSS Service
InSAR	Synthetic Aperture Radar Interferometry
IOC	Intergovernmental Oceanographic Commission
IPCC	Intergovernmental Panel on Climate Change
IPTA	Interferometric Point Target Analysis software (version October 2005); developed by GAMMA Remote Sensing, Switzerland and used by NPA in the regional study
ITRF	International Terrestrial Reference Frame
ITRF2000	International Terrestrial Reference Frame 2000
ITRF2005	International Terrestrial Reference Frame 2005
LGM	Last Glacial Maximum
MA	Mean Amplitude
MAN	Mean Amplitude Neaps
MAS	Mean Amplitude Springs
MD	Mean Duration
MF	Mapping function
MHW	Mean High Water
MHWI	Mean High Water Interval
MHWN	Mean High Water Neaps
MHWS	Mean High Water Springs
MI	Mean Interval
MLE	Maximum-Likelihood estimation
MLW	Mean Low Water
MLWI	Mean Low Water Interval
MLWN	Mean Low Water Neaps
MLWS	Mean Low Water Springs
MSL	Mean Sea Level
MTA	Mean Tide Amplitude
MTL	Mean Tide Level
MTLN	Mean Tide Level Neaps
MTLS	Mean Tide Level Springs
NERC	Natural Environment Research Council
NGS	United States National Geodetic Survey
NOAA	United States National Oceanographic and Atmospheric Administration
NPA	Nigel Press Associates Ltd.
NTSLF	National Tidal and Sea Level Facility

ODN	Ordnance Datum Newlyn
OSGB	Ordnance Survey of Great Britain
OSGB36NG	Ordnance Survey of Great Britain 1936 National Grid
OSGM02	Ordnance Survey Geoid Model 2002
OSTN02	Ordnance Survey Transformation 2002
PCV	Phase Centre Variations
POL	Proudman Oceanographic Laboratory
PLA	Port of London Authority
PLN	Power Law Noise
PPP	Precise Point Positioning
PS	Persistent Scatterer
PSI	Persistent Scatterer Interferometry
PSMSL	Permanent Service for Mean Sea Level
PTGBM	Primary TGBM
QCGPS	Quasi-continuous GPS
RINEX	Receiver INdependent EXchange format
RLR	Revised Local Reference
RMS	Root-Mean-Square
RNS	Regional Network Solution
RTS	Regionally Transformed Solution
SAR	Synthetic Aperture Radar
SD	Standard Deviation
SLC	Single Look Complex
SLR	Satellite Laser Ranging
SRTM	Shuttle Radar Topography Mission
TEQC	Translation, Editing and Quality Check software; developed by UNAVCO and used by IESSG in the national study
TEVA	Tidal data, Editing, Visualisation and Analysis software; developed by POL and used by POL in the regional study
TG	Tide Gauge
TGBM	Tide Gauge BenchMark
TMGO	Table Mountain Geophysical Observatory
TRF	Terrestrial Reference Frame
UKCIP	United Kingdom Climate Impacts Programme
UNAVCO	Universities Navstar Consortium
VLBI	Very Long Baseline Interferometry
VLM	Vertical Land Movement
WN	White noise
ZHD	Zenith Hydrostatic Delay
ZWD	Zenith Wet Delay

Glossary

Frequently used terms

Absolute gravity time series: Values of absolute gravity, computed from AG data on an epochal basis, and the epoch to which they refer.

Absolute gravity time series analysis strategy: A procedure for using absolute gravity time series in a particular software, in order to compute AG vertical station velocities and their uncertainties.

Accuracy: A measure of the closeness to the true value of an estimated parameter.

AG data: Time-tagged, absolute gravity observations from AG measurements made at an AG station.

AG data processing strategy: A procedure for using AG data in a particular software, along with specific models and/or methods for mitigating systematic errors that affect AG, in order to compute absolute gravity values on an epochal basis.

AG measurements: The process of temporarily setting up an absolute gravimeter instrument over a permanent survey marker and recording AG data for a certain period of time, whilst the absolute gravimeter instrument is maintained at a fixed height above the survey marker.

AG station: A permanent survey marker, over which an absolute gravimeter instrument can be positioned for AG measurements.

AG-aligned CGPS estimates of vertical station velocity: Values for the vertical velocity of a CGPS station based on a combination of CGPS and AG.

AG-aligned EGPS estimates of vertical station velocity: Values for the vertical velocity of an EGPS station based on a combination of CGPS/EGPS and AG.

AGGPS-aligned PSI estimates of vertical velocity: Values for the vertical velocity of a PS point based on a combination of CGPS/EGPS, AG, and PSI.

CGPS coordinate time series: Values of the change in latitude, longitude and height, computed from CGPS data on a daily basis, and the epoch to which they refer.

CGPS coordinate time series analysis strategy: A procedure for using CGPS coordinate time series in a particular software, along with specific methods for noise analysis and the mitigation of periodic signals, in order to compute CGPS estimates of station velocities and their uncertainties.

CGPS data: Time-tagged, pseudo-range and carrier phase observations made continuously at a CGPS station.

CGPS data processing strategy: A procedure for using CGPS data in a particular software, along with specific models and/or methods for mitigating systematic errors that affect GPS positioning, in order to compute CGPS station coordinates, in a particular terrestrial reference frame, on a daily basis.

CGPS estimates of vertical station velocity: Values for the vertical velocity of a CGPS station based purely on GPS.

CGPS height time series: Values of the change in height, computed from CGPS data on a daily basis, and the epoch to which they refer.

CGPS station: A GPS antenna, mounted on a permanent monument which is positioned at a fixed height over a permanent survey marker, and connected to a GPS receiver which observes and records the CGPS data and has some form of communications to transfer the CGPS data from the remote site.

CGPS@TG station: A CGPS station located at or close to a tide gauge.

Changes in land level: Estimated parameters based on a GIA model, geological studies or measurements using GPS, AG and/or PSI, e.g. CGPS estimates of changes in land level.

Changes in sea level: Estimated parameters based on measurements using tide gauges, i.e. tide gauge estimates of changes in sea level.

Changes in sea level (decoupled from changes in land level): Estimated parameters based on a combination of tide gauge measurements and either a GIA model, geological studies or measurement using GPS, AG and/or PSI.

EGPS campaign: The process of making simultaneous EGPS measurements at several EGPS stations.

EGPS coordinate time series: Values of the change in latitude, longitude and height, computed from EGPS data on an epochal basis, and the epoch to which they refer.

EGPS coordinate time series analysis strategy: A procedure for using EGPS coordinate time series in a particular software, in order to compute EGPS estimates of station velocities and their uncertainties.

EGPS data: Time-tagged, pseudo-range and carrier phase observations from EGPS measurements made at an EGPS station.

EGPS data processing strategy: A procedure for using EGPS data in a particular software, along with specific models and/or methods for mitigating systematic errors that affect GPS positioning, in order to compute EGPS station coordinates, in a particular terrestrial reference frame, on an epochal basis.

EGPS estimates of vertical station velocity: Values for the vertical velocity of a EGPS station based purely on GPS.

EGPS height time series: Values of the change in height, computed from EGPS data on a daily basis, and the epoch to which they refer.

EGPS measurements: The process of temporarily setting up a GPS receiver-antenna over a permanent survey marker and recording EGPS data for a certain period of time, whilst the GPS receiver-antenna is maintained at a fixed height above the survey marker.

EGPS station: A permanent survey marker, over which a GPS receiver-antenna can be positioned for EGPS measurements.

EGPS@TG station: An EGPS station located at or close to a tide gauge.

IGS data processing strategy: The procedure adopted by the IGS for using CGPS data in a particular software, along with specific models and/or methods for mitigating systematic errors that affect GPS signals, in order to compute CGPS station coordinates for the global network of IGS stations on a daily basis.

National study: The part of the research work detailed in this Technical Report which was funded by the Joint Defra/EA Flood and Coastal Erosion Risk Management R&D Programme as FD2319, and focussed on changes in land and sea levels around the coast of Great Britain.

Net sea level change: An estimate of the change in sea level relative to the land over a specified time period.

Precision: A statistical measure indicating the spread or uncertainty of an estimated parameter.

PSI processing strategy: A procedure for using SAR data in a particular software, along with specific models and/or methods for mitigating systematic errors that affect PSI, in order to compute satellite-point ranges for PS points, on an epochal basis.

PS point time series: Values of the change in satellite-point range for a PS point, computed on an epochal basis, and the epoch to which they refer.

PS point time series analysis: A procedure for using PS point time series in a particular software, in order to compute the velocities of PS points, both along the line-of-sight to the satellite and in the vertical (with some assumptions).

Regional study: The part of the research work detailed in this Technical Report which was funded by the funded by the Environment Agency Thames Estuary 2100 project, and focussed on changes in land and sea levels for the Thames Region.

Systematic bias: The difference between the value for an estimated parameter and the true value for that parameter.

Systematic error: An error source within an estimation procedure which has the potential to cause a systematic bias in an estimated parameter.

Systematic offset: The difference between two alternative values for the same estimated parameter.

Tide gauge: A device for measuring sea level at the coast or on tidal estuaries, with some form of communications to transfer the tide gauge data from a remote site.

Tide gauge annual MSL time series: Values of MSL, computed from quality controlled tide gauge data as annual means, and the epoch to which they refer.

Tide gauge data: Values of the height of instantaneous sea level and the time at which they were recorded.

Tide gauge data analysis: A procedure for using tide gauge data in a particular software in order to compute estimates of tidal parameters and their uncertainties.

Tide gauge monthly MSL time series: Values of MSL, computed from quality controlled tide gauge data as monthly means, and the epoch to which they refer.

Tide gauge quality control and validation: A procedure for inspecting and editing ‘raw tide gauge data’ to account for unphysical values and instrumental faults.

1. Introduction

Since 1997, Defra and the Environment Agency (EA) have been funding research to measure long term changes in land and sea levels around the coast of Great Britain and along the Thames Estuary and River Thames:

- to monitor current changes in land level due to 'land tilt' and regional/local geological effects;
- to improve estimates of climate driven changes in sea level based on tide gauges;
- to help in predicting future sea level rise;
- to carry out more refined regional studies to support planning for flood risk management for the Thames Estuary and River Thames.

The aims of these measurements are to obtain direct estimates of current changes in land level on the scale of millimetres per year, in a stable reference frame, both at tide gauges and at other specific locations, and to use these to obtain estimates of changes in sea level (decoupled from changes in land level). Such measurements represent a major challenge and the research carried out has essentially included three complementary monitoring techniques:

- The Global Positioning System (GPS), which enables the measurement of vertical land movement at a specific station, in a GPS reference frame (essentially a geometrical model of the Earth), and can be used in continuous or episodic modes.
- Absolute Gravimetry (AG), which enables the measurement of absolute gravity, as an independent measurement of vertical land movement at a specific station, with reference to the centre of the Earth; but a highly sensitive instrument is needed and can only be deployed by specialists, in short, episodic campaigns.
- Persistent Scatterer Interferometry (PSI) analysis, which can provide good spatial coverage and refinement over a regional scale, but gives relative rather than absolute movements and is limited to periods for which suitable satellite images exist for the study area.

The objectives of the research work reported in this Technical Report were to investigate how best to combine the information from these three complementary monitoring to meet these aims.

From 2003 to 2006, the research work was carried out as a national study, funded by the Joint Defra/EA Flood and Coastal Erosion Risk Management R&D Programme as FD2319, and a regional study, funded by the Environment Agency Thames Estuary 2100 project. The national study was carried out jointly by the Proudman Oceanographic Laboratory (POL) and the University of Nottingham's Institute of Engineering Surveying and Space Geodesy (IESSG). The regional study was led by IESSG and carried out jointly by IESSG, POL, Nigel Press Associates Ltd. (NPA) and British Geological Survey (BGS).

The report presents the results from all three monitoring techniques, including the estimates and uncertainties obtained for the changing land and sea levels.

The report starts by providing brief details of the technology behind the measurements made at tide gauges and the use of GPS, AG and PSI for monitoring long term changes in land level, which are given in Chapter 2. The report then focuses on the national and regional studies separately in Chapters 3, 4, 5 and 6, before providing conclusions in Chapter 7 and recommendations in Chapter 8. References cited in the text are listed in Chapter 9 and a series of Appendices are provided to show the results from all parts of the studies.

1.1 The national study

For the national study, continuous GPS (CGPS) stations have been established at ten tide gauges around the coast of Great Britain and AG measurements have been made at three of these. A background to the national study is given in Chapter 3, including details on published changes in sea level from British tide gauges, published changes in the land level of Great Britain, and the GPS and AG data sets used. The results of the national study are then presented in Chapter 5, firstly as the independent results from CGPS and AG, then as the results from combining the two techniques and lastly as the estimates of changes in land and sea levels computed for Great Britain.

1.2 The regional study

For the regional study, CGPS and episodic GPS (EGPS) data from a network of stations in the Thames Region and SAR data for hundreds of thousands of persistent scatterer (PS) points in the Thames Region have been analysed and the changes in land level interpreted using various geoscience data sets. A background to the regional study is given in Chapter 4, including details on published changes in sea level from Thames tide gauges, the geological setting of the Thames Region and the tide gauge, GPS, PSI and geoscience data sets used. The results of the regional study are then presented in Chapter 6, firstly as the independent results from PSI and GPS, then as the results from combining the two techniques in the framework of the national study. Chapter 6 also provides geological interpretations based on the geoscience data sets, then goes on to consider the new analysis of the tide gauge data for the Thames Estuary and River Thames carried out as part of the regional study, and finally presents the estimates of changes in land and sea levels for the Thames Region.

2. The monitoring techniques used

In this chapter, brief details of the technology behind the measurements made by tide gauges and the use of GPS, AG and PSI for monitoring long term changes in land level are given. Where appropriate, references to more detailed information on each technique are given as sources of further technical information.

2.1 Tide gauges

A tide gauge is a device for measuring sea level at the coast or on tidal estuaries. At their most basic level tide gauges can be used to facilitate navigation within coastal and estuarine environments but on a more advanced level they can also be used for oceanographic and hydraulic/hydrological applications ranging from real-time, such as storm tide or storm surge warning, to longer term studies of mean sea level (MSL) and other tidal parameters.

This section focuses on the use of tide gauges for longer term studies. The section begins with a subsection on tide gauge basics, which is followed by subsections on tide gauge data, tide gauge data quality control and validation, and tide gauge data analysis.

2.1.1 Tide gauge basics

Up to the 1980s, most tide gauges were 'float gauges' consisting of a stilling well, designed to remove high frequency effects such as waves, containing a float which is mechanically connected to a pen and rotating chart, so that as the float rises and falls due to the combined effect of various tidal constituents, the height of instantaneous sea level with respect to a 'measuring point' is recorded on the chart. A photograph of the pen and chart arrangement for a Munro float gauge is given as Figure 2.1.

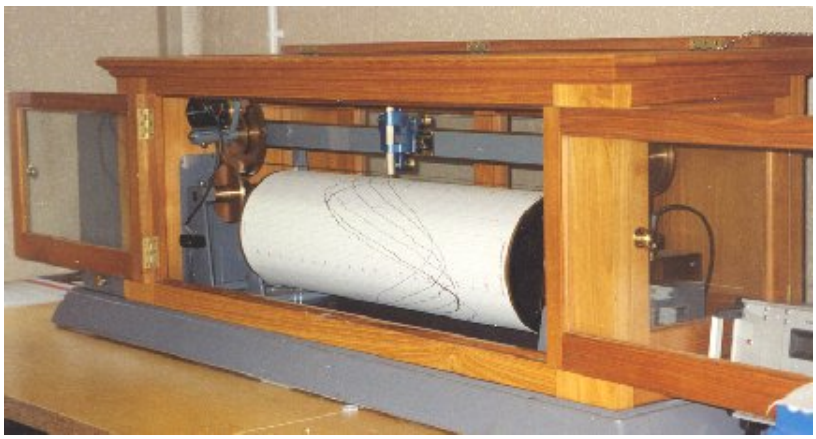

Figure 2.1 Photograph of the pen and chart arrangement for a Munro float gauge*: taken from http://www.pol.ac.uk/ntslf/tgi/gauges.html#MR*

With developments in electronics, the mechanical pen and chart were replaced by encoders which translate the analogue signal to a digital value for the height of instantaneous sea level, but the float and stilling well remained as the main part of the tide gauge.

More recently, float gauges have been replaced by alternative devices which use pressure, acoustic or radar sensors to effectively achieve the same measurements of the height of instantaneous sea level. In the British Isles, the 44 'Class A' tide gauges which form the national tide gauge network as part of the National Tidal and Sea Level Facility (NTSLF) were originally float devices but have now been replaced by a particular type of pressure sensor, referred to as a 'bubbler gauge', with each tide gauge having a number of sensors for redundancy. Some of these are housed in the stilling wells originally installed for the operation of the float gauges, but these stilling wells are not essential to the operation of the bubbler gauge and others are simply placed in the open. Photographs of a 'full bubbler gauge' and a 'mid tide bubbler gauge' are given as Figure 2.2.

Figure 2.2 Photographs of a full tide bubbler gauge (left) and a mid tide bubbler gauge (right)*: taken from* *http://www.pol.ac.uk/ntslf/tgi/bubbler.html#FT and* *http://www.pol.ac.uk/ntslf/tgi/bubbler.html#MT*

With respect to the two types of tide gauge shown in Figure 2.2, NTSLF (2006) states that:

“The full tide bubbler system normally consists of two independent measuring points ... The pressure points which you can see mounted underwater in the photograph are similar in appearance to an inverted bucket with a copper nozzle mounted on the side. This nozzle is the actual ‘measuring point’. A low flow of dry air (normally 7cm per min) is fed down an air tube to the top of the pressure point. When the air pressure in the air line equals the pressure exerted by the column of water above it, then the excess air is released as bubbles through the copper nozzle. This means that the pressure in the air line is proportional to the weight of the water column.

The operation of the mid tide bubbler is similar to that of the full tide system, except that the measuring point is mounted at the mid tide height. That means that the pressure point is only immersed for half of the tidal cycle. The reason for this is that when the measuring point is exposed … it can be accurately levelled into the [national] geodetic network. Once this is accomplished the full tide pressure points can be fitted to match the tidal curve produced by the mid tide pressure point, thereby connecting them to the geodetic network.”

When considering the use of tide gauges for longer term studies the use of a tide gauge benchmark (TGBM) becomes the final essential component in a tide gauge set up. Through a spirit levelling connection between the TGBM and the measuring point, it is possible to calculate the height of instantaneous sea level with respect to the national geodetic datum or a chart datum or both. Clearly this is useful in terms of representation; however, it also enables modifications to or upgrading of the tide gauge sensor to be controlled through a re-connection to the TGBM, thus ensuring the continuity of long term time series.

Information on the historical and current set ups for the 44 tide gauges in the British Isles, which form the national tide gauge network as part of the NTSLF, can be found at NTSLF (2006).

2.1.2 Tide gauge data

Modern tide gauges typically output a value of the height of instantaneous sea level at a pre-defined interval (typically anything from 1 to 15 minutes). It is these values, along with the time at which they were recorded, which then constitute ‘raw tide gauge data’. For longer term studies, raw tide gauge data at 15 minute intervals is usually archived; although it is important to note that historical tide gauge data has not always been archived at such high data rates and may only be archived as hourly values, for example, especially if it was subject to digitisation from paper charts.

Clearly, the operators of a tide gauge have the initial responsibility for the archival of raw tide gauge data. In the case of the regional study detailed in this Technical Report, raw tide gauge data archived by EA and the Port of London Authority (PLA), for a number of tide gauges on the Thames Estuary and River Thames, have been used, as detailed in Section 4.3.

2.1.3 Tide gauge data quality control and validation

Before any analysis for longer term studies, it is essential to carry out quality control and validation of the raw tide gauge data. The basis of quality control is the inspection of raw tide gauge data and residuals, computed through tidal analysis. This enables the detection of unphysical values and instrumental faults such as timing errors, spikes, gaps, etc.. Tide gauge data that has been subject to different levels of quality control levels are typically defined as 'Level 0', 'Level 1' and 'Level 2' (Rickards and Kilonsky 1997). Level 0 data are raw tide gauge data. Level 1 data have undergone basic quality control and are provided with flags (e.g. missing, suspect, interpolated values, datum changes, etc.), but no raw tide gauge data is changed and the original sampling interval is preserved. Level 2 data are fully quality controlled and written in a standard format; included in a Level 2 data set would be hourly values of instantaneous sea level that form a continuous time series and are given with respect to a TGBM, and computed data, such as daily and monthly mean sea levels, together with a full documentation.

In the British Isles, the 44 tide gauges which form the national tide gauge network as part of the NTSLF are subject to quality control and validation by the British Oceanographic Data Centre (BODC), which is also responsible for the archival of the 'quality controlled tide gauge data'. In addition to this, the Permanent Service for Mean Sea Level (PSMSL) archives historical and current quality controlled tide gauge data made available for any high quality tide gauges around the world; which includes all data for the 44 tide gauges mentioned above and a number of others, notably Southend, Tilbury and Tower Pier tide gauges on the Thames Estuary and River Thames for the period from 1929 to 1982/3.

In the case of the national study detailed in this Technical Report, quality controlled tide gauge data archived by PSMSL for a selection of the 44 tide gauges which form the national tide gauge network as part of the NTSLF was considered, as detailed in Sections 3.1 and 5.4. In the case of the regional study detailed in this Technical Report, quality controlled tide gauge data archived by BODC for a number of tide gauges on the Thames Estuary and River Thames was considered, as detailed in Section 4.3. In addition to this, quality control and validation was also carried out on raw tide gauge data supplied by the EA and PLA for a number of tide gauges on the Thames Estuary and River Thames, as also detailed in Section 4.3.

2.1.4 Tide gauge data analysis

Following quality control and validation, the quality-controlled tide gauge data can then be used to calculate tidal parameters such as MSL, mean high water (MHW), mean low water (MLW), mean tide level (MTL) and mean tide amplitude (MTA) or mean amplitude (MA). Such tidal parameters are typically calculated as either monthly or annual means which can be used to form time series, an example of which is given in Figure 2.3.

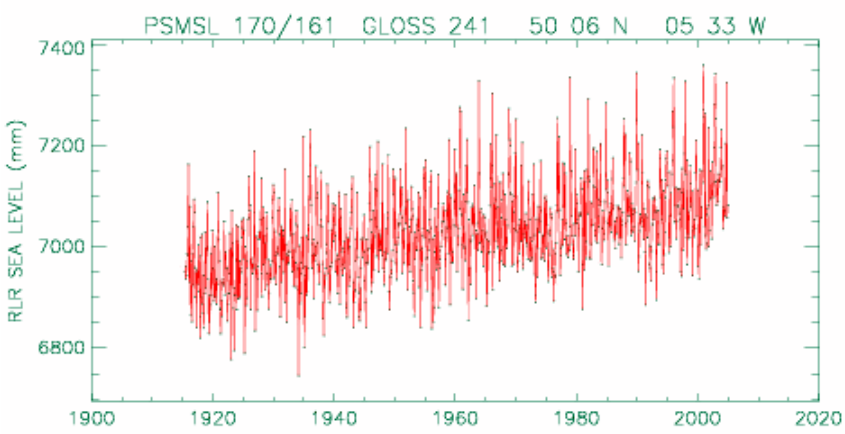

Figure 2.3 Example tide gauge monthly MSL time series for Newlyn*: taken from http://www.pol.ac.uk/ntslf/trends.php*

Using the monthly or annual tidal parameter time series it is then possible to carry out a regression analysis in order to obtain estimates of changes in the tidal parameters. For annual data, it is normal to carry out the regression analysis by solving for a linear trend and accounting for coefficients related to the nodal (approximately 18.6 years) cycle and semi-nodal (approximately 9.3 years) cycle. For monthly data, it is normal to carry out the regression in the same manner as for the annual data but to also include annual and semi-annual terms to account for seasonal variations. For tide gauges in river and estuarine environments an additional term to account for mean freshwater flow can also be included in the analysis.

In this respect, it should be noted that it is generally accepted that a high quality tide gauge record can enable the secular change of MSL to be estimated with an acceptable level of uncertainty if 30 to 50 years or more of data are used (Woodworth et. al. 1999). Considering this further, a similar statement can also be applied to MHW, MLW, MTL, MA and other tidal parameters.

MSL estimation

For MSL estimation, the standard POL method employed is to rate reduce the equal interval quality controlled tide gauge data to hourly values and then apply the Doodson X0 filter to obtain daily MSL values; with any missing data resulting in a missing daily MSL value. Daily MSL values are then averaged to monthly and annual MSL values; with monthly and annual MSL values levels only included if there are at least 80% of days in the month or year available.

MHW, MLW, MTL and MA estimation

For MHW, MLW, MTL and MA, the method employed is to compute the high and low water times and heights from the quality controlled tide gauge data. For this, equal interval heights of instantaneous sea level are interpolated, e.g. using a cubic spline fitted to four consecutive interval heights as interpolation function, in order to provide the heights and times of high and low waters. Turning point values are subsequently added together and averaged to

estimate monthly or annual MHW, MLW, MTL and MA with the proviso that an acceptable mean has to include data from at least 80% of the days in the month or year, in order to avoid distortion to the mean from missing data and the seasonal cycle of these levels. Based on the above estimates it is also possible to then compute Mean High Water Interval (MHWI), Mean Low Water Interval (MLWI), Mean Interval (MI) and Mean Duration (MD).

Other tidal parameters estimation

Considering the estimates of MHW, MLW, MTL and MA, other parameters can be estimated, including Mean High Water Springs (MHWS), Mean High Water Neaps (MHWN), Mean Low Water Neaps (MLWN), Mean Low Water Springs (MLWS), Mean Tidal Level Spring (MTLS), Mean Tidal Level Neaps (MTLN), Mean Amplitude Springs (MAS) and Mean Amplitude Neaps (MAN). These require a consideration of the dates and times of the moon's meridian passage and are only calculated based on annual values.

To obtain mean tidal curves in stages of the moon's transit the method for processing each year's data entails preparing 12 tables listing the dates and times of the moon's meridian passage – the times between 00 and 01 hrs and 12 and 13 hrs for the first table, between 01 and 02 hrs and 13 and 14 hrs for the second and so on. Each tide is then listed in the appropriate table, first the high water nearest to the time of the moon's transit followed by the succeeding low water. At the end of the year each table is totalled and the mean times and levels obtained; the group of tides with the highest and lowest levels are taken as MHWS and MLWS, and the group with the smallest range as MHWN and MLWN.

To obtain Lunitidal intervals in stages of the moon's transit, the mean time of transit in each of the moon's 12 transit time bands e.g. 00 to 01 hrs and 12 to 13 hrs, is subtracted from the mean high or low water time in the corresponding transit time band for each tide gauge in order to estimate the time of high or low water related to the time of lunar transit and the corresponding intervals.

The mean high or low water time in the corresponding transit time band for one tide gauge can then be subtracted from the corresponding value for the next nearest tide gauge to estimate the high or low water time difference between tide gauges related to the time of lunar transit. The time and height differences between the observed and predicted times and heights of high and low water can also be computed.

Summary

More details on the specific tide gauge data analysis for the national and regional studies detailed in this Technical Report are given in Sections 3.1 and 6.5.

2.2 The Global Positioning System

GPS, or 'the Global Positioning System', is the American Global Navigation Satellite System (GNSS) primarily designed to meet the metric and decimetric positioning accuracy requirements of military and transport applications. However, at its most advanced level it can be used for high accuracy positioning to millimetric accuracies and has revolutionised surveying and geodesy.

In this section, the use of GPS for monitoring long term changes in station heights and land level is described. The section begins with a subsection on GPS and GNSS basics, which is followed by a subsection on high accuracy positioning using GPS, including details on the mitigation of systematic errors associated with GPS, a subsection on GPS data processing, and a subsection on GPS coordinate time series analysis.

2.2.1 GPS and GNSS basics

GPS has been operational since the 1980s and is one of three GNSSs that will be available for such applications in the future; the other two being GLONASS, the Russian equivalent to GPS which has been operational for about the same amount of time as GPS but has always had a limited satellite constellation, and GALILEO, the European equivalent to GPS which is due to become operational some time after 2008.

A GNSS comprises a space segment, a ground segment and a user segment. For GPS, the space segment consists of a constellation of (currently) 30 mid-Earth orbiting satellites organised in six orbital planes with each satellite at an approximate altitude of 20,200km, as shown schematically in Figure 2.4. The basic design of the constellation is such that at least four satellites are visible in an open environment at all locations on the Earth for 24 hours a day.

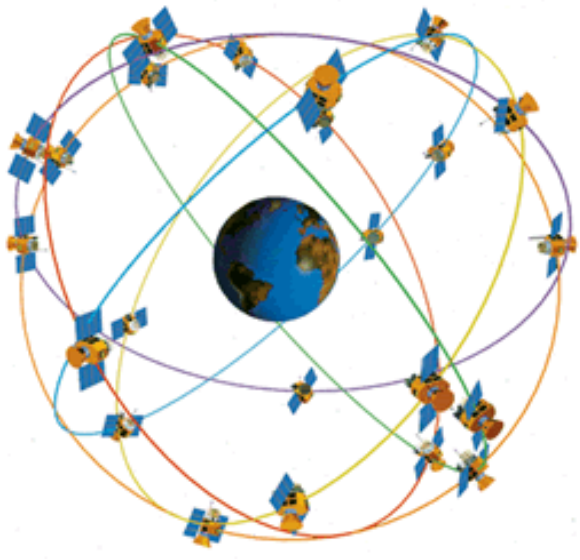

Figure 2.4 Schematic of the GPS satellite constellation

The ground segment consists of the infrastructure which monitors the GPS satellites and uploads information on the satellite positions and the state of their satellite clocks (as the broadcast ephemeris which is part of the navigation message) as well as information on their health (as another part of the navigation message). The user segment consists of an unlimited number of users equipped with a GPS antenna and GPS receiver; unlimited by the fact that GPS is a passive system whereby a user receives all of the information required to accurately position themselves without the need to transmit any information. An example of a GPS antenna and monument set up at the Dover tide gauge is shown in Figure 2.5.

Figure 2.5 Photograph of a GPS antenna and monument*: the photograph shows the equipment installed at the Dover tide gauge.*

2.2.2 High accuracy positioning using GPS

For high accuracy positioning using GPS, a station is established with a user receiver programmed to observe GPS data (time-tagged, pseudo-ranges and carrier phase) for a certain period of time whilst a user receiver-antenna is maintained at a fixed height above a survey marker. The data recorded by the user receiver is then combined with concurrent data from a number of other receivers (at least one, but usually many more) and GPS products (information on satellite positions, satellite clocks and Earth orientation parameters) and post-processed using software which attempts to mitigate the various systematic errors that affect GPS positioning. For discussion purposes, the systematic errors can be separated into satellite-related, atmospheric-related and station-related.

Satellite-related systematic errors

Satellite-related systematic errors include those in the satellite positions and the satellite clocks. As stated previously, information on these is provided as part of the broadcast ephemeris; however, due to their method of computation and prediction forward in time by the ground segment, the information in the broadcast ephemeris is generally considered to be unacceptable for high accuracy GPS positioning when using station separations (or baseline lengths) of greater than a few kilometres. To overcome this limitation the international scientific community (primarily led by NASA centres) provide a series of post-processed GPS products of varying latency and quality (where quality is generally a trade-off against latency). The current products provided by the International GNSS Service (IGS) include ultra-rapid, rapid and final. The first two are generally used for high latency applications such as space weather, meteorology, earthquakes and other seismological studies; whereas the final products (which are the most accurate, with satellite positions computed to an accuracy of less than 5cm and satellite clocks to an accuracy of less than 0.1ns, but are not available until 11 days after observation) are used for low latency applications and long-term studies, including, but not limited to, climate-related changes in the atmosphere, plate tectonics and the monitoring of changes in land level. It is, therefore, these IGS final products which have been used in the GPS data processing for both the national and regional studies detailed in this Technical Report.

Atmospheric-related systematic errors

Atmospheric-related systematic errors include effects on the satellite signals as they pass through the Earth's atmosphere. In terms of GPS, the signals are considered to be unaffected as they travel through space (considered to be a vacuum) from the satellite some 20,000+ kilometres away until they reach about 100km from the Earth's surface. At this point, for GPS the Earth's atmosphere is considered to comprise of two general layers, referred to as the ionosphere (from approximately 100km above the Earth's surface to approximately 10 to 20km above the Earth's surface) and the troposphere (from approximately 10 to 20km above, down to, the Earth's surface).

The ionosphere effectively consists of a series of charged particles which behave in ways that depend on the solar activity, so are less active at night and at times of solar minima, e.g. 1998 and 2008, and conversely more active at local mid-day and at times of solar maxima, e.g. 2003 and 2014. However, for the frequencies of the two GPS signals (L1 = 1575MHz; L2=1240MHz) the effect of the ionosphere on the signals is frequency dependent, such that if these two frequencies are combined in a certain way, first-order ionospheric effects, which account for about 98% of the total effect, are completely mitigated. Such a combination of observables has, therefore, been used in the GPS data processing for both the national and regional studies detailed in this Technical Report.

Unfortunately, the troposphere does not behave in this way and causes delays to the signals which mainly depend on pressure and relative humidity and are,

therefore, more difficult to mitigate as these parameters vary both spatially and temporally, just as our weather does. For GPS data processing, the effects of the troposphere are generally considered to be a combination of a hydrostatic component, which is related to pressure and, hence, station altitude, and a ‘wet; component, which is related to relative humidity or, more precisely, the amount of water vapour in the atmosphere above the station; in this respect it is important to note that GPS is not affected by rain or snow, as it is the amount of water vapour, i.e. prior to precipitation, that is stored in the atmosphere which does not necessarily vary in a predictable manner on a daily or seasonal basis. For the hydrostatic component, physical models of the atmosphere have been developed which, based on the difference in station altitude between two stations (which form a baseline) and an assumption about the change in pressure with altitude, can be used to compute the tropospheric zenith hydrostatic delay (ZHD); this is then mapped down to the elevation angle between a satellite and a station using an appropriate tropospheric mapping function (MF) and effectively removes about 80 to 90% of the total tropospheric delay. For high accuracy GPS positioning, the remaining 10 to 20% of the tropospheric total delay is then estimated (along with the station coordinates and carrier phase ambiguities) by the GPS data processing software as part of the solution; this effectively results in an estimate of the zenith wet delay (ZWD), which includes both the delay due to the actual wet component of the atmosphere and any errors in the calculation of the delay due to the hydrostatic component, and can also be mapped down to the elevation angle between a satellite and a station using an appropriate tropospheric MF. Using this approach most of the tropospheric delay is mitigated during processing, but all of it can never be mitigated as the estimation process described above integrates the delays over a large portion of atmosphere above the station, due to satellites being at varying zenith or elevation angles to create the geometry of the GPS satellite constellation required for positioning itself; however, comparisons of the ZWD with meteorological estimates based on radiosondes does suggest that the estimation process is accurate to an equivalent of less than 10mm systematic bias in height for GPS data processed on a daily basis. Such a mitigation strategy has, therefore, been used in the GPS data processing for both the national and regional studies detailed in this Technical Report.

Station-related systematic errors

Station-related systematic errors include effects on the GPS signals either just before or as they arrive at the GPS antenna, notably interference and multipath and receiver-antenna phase centre variations (PCVs), and effects on the instantaneous station location which appear as permanent and periodic ‘loading’ of the Earth’s crust, due to solid Earth tides, ocean tides, atmospheric pressure and hydrological factors.

Interference and multipath are site-specific and depend, respectively, on the presence of any interfering radio sources and any reflecting sources (such as buildings) close to the GPS antenna. When establishing CGPS or EGPS stations a thorough reconnaissance is always carried out in order to select a location for the station which is free from interference and multipath; however,

the need to site the station as close as possible to the tide gauge, in order to decouple the changes in land and sea level, sometimes means that there has to be a trade-off between an ideal location for the station that is free from interference and multipath and this need. Later in this Technical Report, the influence of interference at the tide gauge sites of Aberdeen, in East Scotland, and Tilbury on the Thames Estuary, and multipath at the tide gauge site of North Shields, in North-East England, will be discussed.

Receiver-antenna PCVs are an electrical phenomenon whereby the signals from GPS satellites appear to arrive at a different point (over a range of millimetres) within the receiver-antenna, depending on the elevation angle between the station and the satellite. Such effects have been understood since the early 1990s and models of the receiver-antenna PCVs with respect to elevation angle are available for all different GPS receiver-antenna types, notably from the United States National Geodetic Survey (NGS) and the United States National Oceanographic and Atmospheric Administration (NOAA). The critical point here is that although such PCVs have an absolute nature, i.e. all antennas have electrical variations with respect to a physical antenna 'patch', as the IGS had started their generation of GPS products in 1992 without using receiver-antenna PCVs a decision was made in 1995 that the IGS GPS data processing strategy would continue in a way that assumed the Dorne-Margolin 'choke ring' receiver-antenna used at all IGS CGPS stations to be a 'standard' and to have zero PCVs. As such all GPS data processing softwares that allow the use of other types of receiver-antennas have used models for relative receiver-antenna PCVs, i.e. the difference between the absolute PCVs for a particular receiver-antenna and the absolute PCVs for a Dorne-margolin choke ring receiver-antenna. In the case of the GPS data processing for the national and regional studies detailed in this report, all observations carried out since 1997 have been made using Dorne-margolin choke ring receiver-antennas to avoid the use of such relative receiver-antenna PCV models. Quite recently, however, the IGS have assessed the changes in the quality of their products from the last 15 years or so, due to improvements in the GPS satellite constellation and their GPS data processing strategy, and concluded that the use of the relative antenna PCV models has effectively degraded the quality of their products and IGS station coordinates and velocities. The outcome being that the new IGS GPS data processing strategy (with effect from 26 November 2006) includes the use of absolute antenna PCV models for both receiver-antennas and satellite-antennas. Later in this Technical Report, the impact of these different antenna PCV models will be discussed.

In terms of loading processes, the effects of solid Earth tides and ocean tide loading are relatively easy to mitigate as they are tidal in nature and models to provide station-specific corrections for these effects have been produced and are made available through the International Earth Rotation Service (IERS). Such models have, therefore, been used in the GPS data processing for both the national and regional studies detailed in this Technical Report. Here it should be noted that the current (prior to 26 November 2006) IGS GPS data processing strategy only used models for solid Earth tides, based on the assumption that as they process daily (24-hour) data from the global network the dominant diurnal and semi-diurnal ocean tide loading effects are mitigated

through averaging. Although not incorporated in the current IGS GPS data processing strategy, models for ocean tide loading were used in the national and regional studies because, firstly, we do not have daily data at all stations, notably in the regional study, and, secondly, the effects of ocean tide loading in the South-West of England are quite large. As a point of note, the new IGS GPS data processing strategy (with effect from 26 November 2006) also includes the use of models for ocean tide loading.

The other two loading processes mentioned previously were atmospheric loading and hydrological loading. In comparison to the tidal loading effects these are relatively 'new' and were effectively 'discovered' from the processing and analysis of data from global GPS networks. They have a long wavelength nature, effectively exhibiting variations in loading between the Northern and Southern hemispheres of the Earth, and both require external data sets of either global atmospheric pressure or global water storage in their modelling. As such, neither of these is modelled in the current or new IGS GPS data processing strategies and, therefore, they have not been modelled in the GPS data processing for either the national or regional studies detailed in this Technical Report. They are, however, considered as part of the reason for the periodic signals which are apparent in all current CGPS height time series and are, therefore, effectively mitigated at the GPS coordinate time series analysis stage.

Summary

More details on the specific mitigation of systematic errors in the GPS data processing for the national and regional studies detailed in this Technical Report are given in Sections 5.1 and 6.2.

2.2.3 GPS data processing

As stated at the start of Subsection 2.2.2, "for high accuracy positioning using GPS, a station is established with a user receiver programmed to observe GPS data (pseudo-ranges and carrier phase) for a certain period of time whilst a user receiver-antenna is maintained at a fixed height above a survey marker. The data recorded by the user receiver is then combined with concurrent data from a number of other receivers (at least one, but usually many more) and GPS products (information on satellite positions, satellite clocks and Earth orientation parameters) and post-processed using software which attempts to mitigate the various systematic errors that affect GPS positioning."

A discussion of the systematic errors was given in Subsection 2.2.2, along with some information on the mitigation strategies employed in the GPS data processing for both the IGS products and for the national and regional studies detailed in this Technical Report. The other aspect of GPS data processing is to compute the coordinates of stations in a particular datum or, more strictly speaking, particular terrestrial reference frame (TRF). In this respect, GPS is unlike any other survey technique as, with appropriate GPS data processing software, it is possible to compute coordinates in a global TRF. This is

particularly important for the national and regional studies detailed in this Technical Report as it enables the computation of changes in sea level (decoupled from changes in land level) to be effectively referred to the origin of the TRF and have an absolute nature, rather than being relative to any benchmarks or points on land that are then assumed to be 'stable'.

In the GPS data processing for the national and regional studies detailed in this Technical Report, the TRF used was the International Terrestrial Reference Frame (ITRF) 2000 (ITRF2000). ITRF2000 is a global TRF realised using space geodetic observations and data from various techniques, notably Satellite Laser Ranging (SLR), which defines the origin of the TRF and contributes to the definition of the orientation and scale of the TRF, Very Long Baseline Interferometry (VLBI), which contributes to the definition of the scale of the TRF, and GPS itself, based on the weekly solutions of station coordinates computed by the IGS for their global network of CGPS stations (as shown in Figure 2.6), which contributes to the definition of the orientation of the TRF.

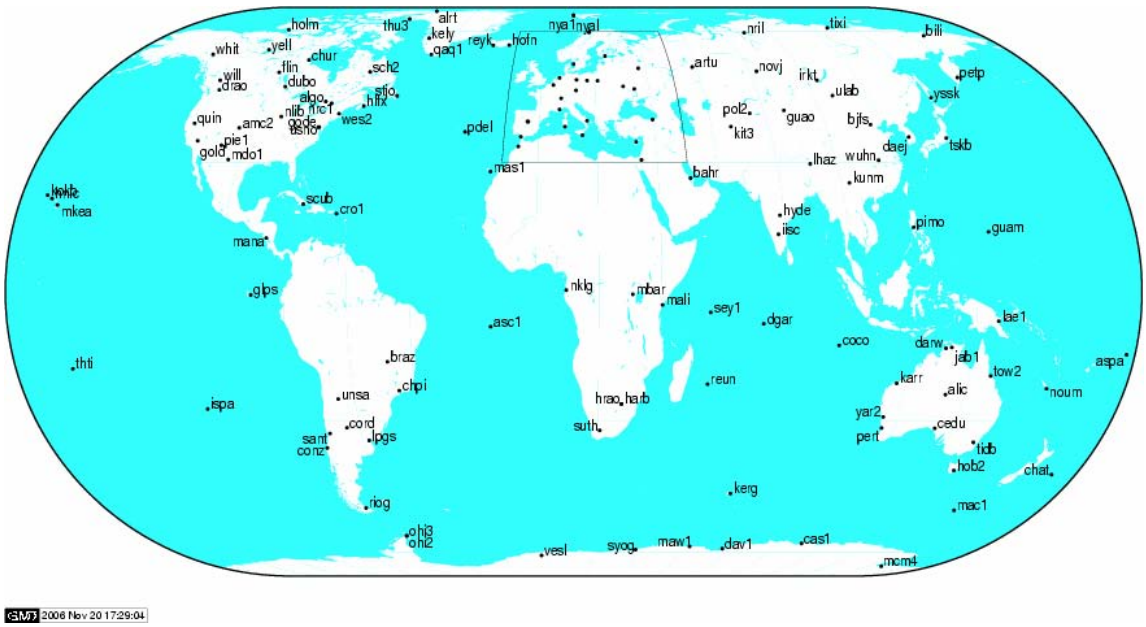

Figure 2.6 The IGS global network of CGPS stations

Through GPS data processing, the data recorded by receivers at stations with 'unknown' coordinates are combined with concurrent data from a number of other receivers at reference stations with 'known' coordinates and the IGS final products, with the primary output from the processing being the coordinates of stations in a particular TRF. In this respect there are two distinctly different approaches available when forming the 'observation equations':

- the first approach is to use double-differencing (DD) whereby the observations from two receivers (that form a baseline) and a pair of satellites are differenced in order to eliminate the satellite clock and receiver clock terms and solve for the vector (difference in latitude, longitude and ellipsoidal height between the stations) along with the double-difference carrier phase ambiguities and any additional unknowns included to account for the un-modelled tropospheric delay. For a network of m stations and n

satellites, observation equations for m-1 baselines and n-1 satellite pairs can be formed with loose constraints applied to the known coordinates of a number of reference stations. The resultant vectors can then be adjusted by constraining the known coordinates of the reference stations and solving for a four-parameter (three translations and a scale) transformation and the coordinates of the unconstrained stations in the same TRF as the reference stations. Depending on the scale of the network of reference stations used in this process, the solution is either termed a global network solution (GNS) or a regional network solution (RNS).

- the second approach is to use precise point positioning (PPP) whereby the observations from one receiver to each satellite are processed in order to estimate the station coordinates along with the receiver clock term, the carrier phase ambiguities and any additional unknowns included to account for the un-modelled tropospheric delay. A comparison of the resultant coordinates and the known coordinates for a number of reference stations are then used to solve for a four-parameter (three translations and a scale) or seven-parameter (three translations, three rotations and a scale) transformation, which is applied to the coordinates of the other stations to transform them into the same TRF as the reference stations. Depending on the scale of the network of reference stations used to compute the transformation parameters, the solution is either termed a regionally transformed solution (RTS) or a globally transformed solution (GTS).

More details on the specific reference frame definition in the GPS data processing for the national and regional studies detailed in this Technical Report are given in Sections 5.1 and 6.2.

2.2.4 GPS coordinate time series analysis

In the GPS data processing for the national and regional studies detailed in this Technical Report, the coordinates (latitude, longitude and ellipsoidal height) for our stations are either daily coordinates for the CGPS stations or epochal coordinates for the EGPS stations. Both of these can be represented as time series, i.e. a data set of changes in coordinates with respect to time. Example height time series from these different types of station are illustrated in Figure 2.7.

Such time series are then subject to an analysis through which either a ‘best fit’ linear plus periodic trend or best fit linear trend are obtained, with the linear component being an estimate of the station velocity in a particular coordinate component. At this stage it is also possible to account for any ‘jumps’ in the time series or coordinate offsets, which are due to changes in equipment (usually the antenna) at the specific station or at one of the IGS stations used to define the reference frame, as illustrated by the dashed vertical lines corresponding to jumps in the CGPS height time series in 1998 and 1999.

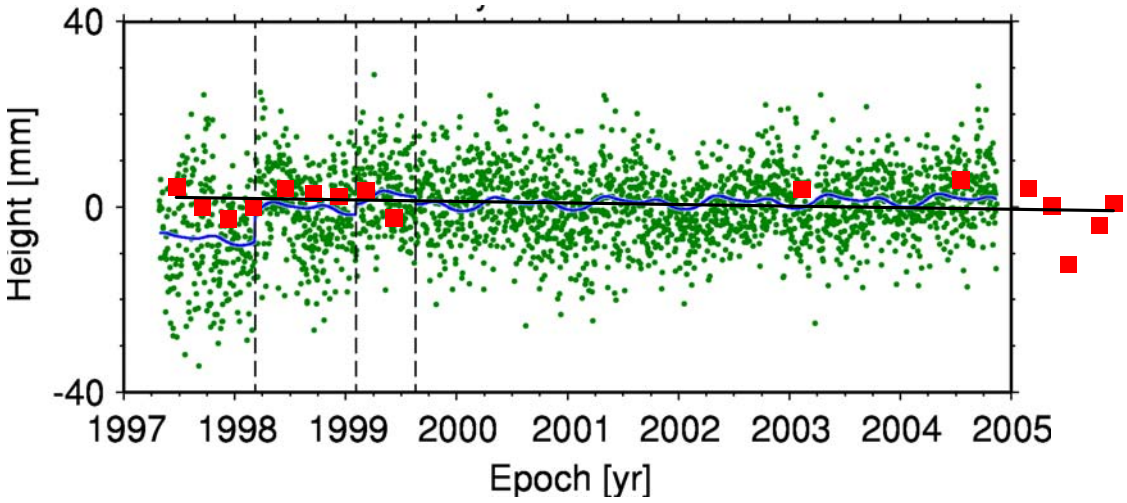

Figure 2.7 Example CGPS/EGPS height time series

In Figure 2.7, the CGPS estimates of the changes in height for one station are shown as green dots, on a daily basis; EGPS estimates of the change in height for another station are shown as red dots, at intervals of 1 to 3 months for two separate monitoring periods; the best fit linear plus periodic trend in the CGPS estimates is shown by the blue line, from which estimates of vertical station velocity can be inferred; the best fit linear trend in the EGPS estimates is shown by the black line, from which vertical station velocity can be inferred.

As part of the coordinate time series analysis a measure of the uncertainty in any station velocity estimate is also obtained.

For EGPS estimates this is a relatively straightforward procedure as a white noise (random error) only model can be used in which the uncertainty in a velocity estimate σ_v (mm/yr) is a function of the uncertainty in the input data σ_d (mm), the time interval between data points Δt (years) and the total time span of the time series T (years). A formula for this was presented by Dixon (1991), and is given as Equation 2.1 where, in the case of EGPS estimates, the standard deviation of the epochal coordinate estimates can be used as a measure of the uncertainty in the input data.

$$\sigma_v = \frac{\sigma_d}{T}\left[\frac{12T/\Delta t}{(1+T/\Delta t)(2+T/\Delta t)}\right]^{1/2} \qquad \text{[Equation 2.1]}$$

For CGPS estimates this is not as straightforward as such daily coordinate estimates have been shown to contain temporal correlations, meaning that the time series contain both white noise and coloured noise (temporally correlated errors), which must be taken into account in order to obtain a realistic estimate of the velocity uncertainty.

For CGPS estimates, daily coordinate time series have also been shown to contain spatial correlations, meaning that the time series from all stations in a region contain common periodic signals, due to systematic errors arising from

such things as loading processes that are not modelled in the CGPS data processing. It is common practice, therefore, for the 'raw coordinate time series' to be subjected to a regional filtering, which attempts to remove such periodic signals before coordinate time series analysis is carried out, resulting in two estimates of vertical station velocities and their uncertainties: one based on the raw or unfiltered coordinate time series and one based on the filtered coordinate time series, which will typically have vertical station velocities with a reduced uncertainty.

More details on the specific coordinate time series analysis applied to obtain vertical station velocities and changes in land level for the national and regional studies detailed in this Technical Report are given in Sections 5.1 and 6.2.

2.3 Absolute Gravimetry

The measurement of absolute gravity can be traced back to the Dutch astronomer Huygens (1629-1695), who used a pendulum, and Captain Henry Kater (1817), who used a reversible pendulum. More recently, due to advances in geometrical optics and interferometry, it has become possible to use 'free fall methods' to obtain measurements of absolute gravity to an unsurpassed level of precision and accuracy. In this context, AG, or 'Absolute Gravimetry', is the measurement of the acceleration due to gravity ("g") from distance and time measurements. In this respect, an absolute gravimeter instrument must have a unique feature in that the quantities it measures (distance and time) must directly define gravity, so that the calibration of the instrument comes only through the metrological control of these measured quantities.

In this section, the use of AG for monitoring long term changes in absolute gravity and land level is described. The section begins with a subsection on AG basics, which is followed by a subsection on the FG5 absolute gravimeter instrument, a subsection on AG data processing, including details on the mitigation of systematic errors associated with AG, and a subsection on absolute gravity time series analysis.

2.3.1 AG basics

Absolute gravity is measured in units of μgal, where 1μgal = $1 \times 10^{-8} m/s^2$. To put this into context, if two objects were allowed to fall with a 1μgal difference in gravity between them, one object would be ahead of the other by the thickness of a sheet of paper after traveling a distance of 248km!

In the case of the Earth, based on Newton's law, the acceleration due to g is given by

$$g = \frac{GM_e}{R_e^2} \approx 9.8\, ms^{-2} \qquad \text{[Equation 2.2]}$$

where G is the gravitational constant and M_e and R_e are the mass and radius of the Earth respectively.

Free fall methods involve the measurement of time-distance pairs. Considering that if $\ddot{x} = g$ then integrating this equation with respect to time, gives the following equation of motion

$$x = x_0 + v_0 t + \tfrac{1}{2} g t^2 \qquad \text{[Equation 2.3]}$$

where x_0 and v_0 are the initial height and velocity respectively (at the top of the drop), and x is the new height after time t. Therefore, by accurately measuring t and the distance fallen from x_0 to x, a value of g can be obtained.

However, if measurements of absolute gravity at the sub-milligal level or less are required, it is also necessary to consider the variation of gravity with height. The variation of gravity with respect to height is somewhere between -3.1μgal/cm and -1.7μgal/cm. So over a 20cm drop this is a significant variation that has to be accounted for. Including the (known or estimated) variation of gravity with height in the equation of motion, this then becomes

$$x = x_0\left(\frac{\gamma t^2}{2} + 1\right) + v_0 t\left(\frac{\gamma t^2}{6} + 1\right) + \tfrac{1}{2} g_0 t^2\left(\frac{\gamma t^2}{12} + 1\right) \qquad \text{[Equation 2.4]}$$

where x_0 and v_0 are the initial height and velocity respectively (at the top of the drop), and x is the new height after time t, but also g_0 is the absolute gravity at x_0 and γ is the change in gravity with height. In this case, by accurately measuring t and the distance fallen from x_0 to x, a value of g_0 can then be obtained (referred to the top of the drop).

2.3.2 The FG5 absolute gravimeter instrument

The FG5 absolute gravimeter instrument developed by the company, Micro-g Solutions Inc., USA uses the free fall method to determine absolute gravity with a precision and accuracy of the μgal level, through the use of three critical components: a dropping chamber, a laser interferometer and a superspring. A schematic diagram of the components of an FG5 absolute gravimeter instrument is provided as Figure 2.8.

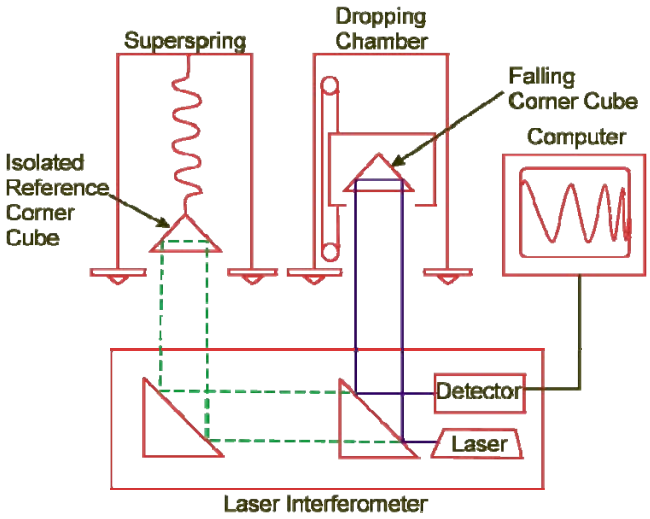

Figure 2.8 Schematic diagram of the components of an FG5 absolute gravimeter instrument

A cross-sectional diagram and photograph of an FG5 absolute gravimeter instrument is provided as Figure 2.9.

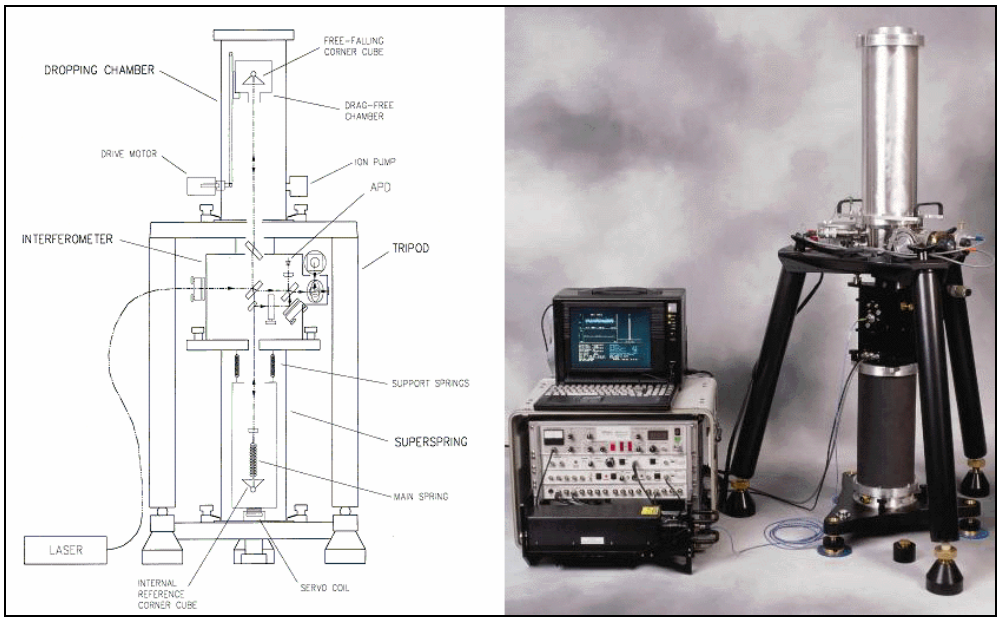

Figure 2.9 Cross-sectional diagram and photograph of an FG5 absolute gravimeter instrument

The dropping chamber is in fact a 'drag free' dropping chamber, which houses a free-falling corner cube reflector. It reduces drag due to residual gas molecules, follows the dropped corner cube, then gently arrests and lifts it, and shields the corner cube from external electrostatic forces.

The laser interferometer carries out the distance measurement to the free-falling corner cube reflector, and the superspring provides an inertial reference frame. This enables the instrument to avoid any microseismic noise, which would

otherwise reduce the precision of the instrument from μgals to tens or hundreds of μgals.

Through inter-comparisons between FG5 absolute gravimeter instruments it is generally accepted that the instrument accuracy is about 2μgal and precision (based on a 10 second drop interval, at a quiet site) is about ±1μgal (over a 3.75 minutes observation period) or ±0.1μgal (over a 6.25 hour observation period). The FG5 can be used anywhere in the world, but requires an environment with a stable operating temperature in the range of 10 to 30°C.

2.3.3 AG data processing

As with GPS, AG is affected by 'Earth processes' including polar motion, solid Earth tides, ocean tides and changes in atmospheric pressure. In addition to these, the nature of AG means that there are also instrument-specific corrections that need to be applied, namely: comparator response correction, speed of light correction, gradient correction and reference height correction.

Corrections for Earth processes

Polar motion causes shifts in the rotation axis of the Earth, which causes changes in the geodetic latitude of a site and therefore a change in gravity; however, standard models are available to correct for this. Solid Earth tides affect gravity by causing a change in gravity field and a change in the gravity gradient, as the loading redistributes the mass of the Earth; however, standard models are available to correct for this.

In terms of the other two Earth processes, these have both a direct and an indirect effect on gravity. From the ocean tides there is a direct gravitational attraction due to the mass of the water plus a change in the gravity field and gravity gradient as the loading redistributes the mass of the Earth. For the atmospheric pressure there is also a combined effect from a direct attraction of the air mass and loading of the Earth's surface.

Considering ocean tides, it is not normal practice to establish AG stations at tide gauges but rather to establish them in quiet locations, inland from the tide gauge. This means that standard models can then be used to correct for ocean tide effects.

Considering atmospheric pressure, the total effect on absolute gravity could be calculated if the global distribution of air mass is known, from global datasets of air pressure that are now routinely available, however this method is not used as these global datasets can be prone to errors in certain regions (different data sets disagree with each other). Fortunately, it can be shown that about 90% of the gravity signal is due to the air mass within 50km of a site; which can be approximated by local atmospheric pressure values (except when fronts are passing overhead). Based on this, therefore, a correction computed from local atmospheric pressure, and an assumed linear relationship between gravity and atmospheric pressure, is applied.

Instrument-specific corrections

The high-speed comparator produces digital pulses, from the laser interferometer, as the fringe signal crosses zero. Clearly, any delay between the zero fringe signal detection and the digital pulse produced can change the value of the distance measured and hence the value of absolute gravity. For this reason, a comparator response correction is applied to the values, depending on the fringe voltage measured.

In addition to this, it must be considered that within the FG5 absolute gravimeter instrument, the laser light takes a finite time to traverse around the system. As the free-falling corner cube reflector drops, the time for the distance measured to it decreases, whilst the time for the distance measured to the isolated reference corner cube reflector does not. To account for this, a 'speed of light correction' is applied.

The correction due to the gravity gradient at the site is automatically accounted for through the FG5 absolute gravimeter instrument using Equation 2.4 presented in the previous subsection. The final correction applied is then a reference height correction, to transfer the absolute gravity value observed (which is referred to the top of the drop) to some reference height, e.g. the survey marker for the AG station.

More information on the specific corrections applied in the absolute gravity data processing for the national study detailed in this Technical Report are given in Section 5.2.

2.3.4 Absolute gravity time series analysis

In the AG data processing for the national study detailed in this Technical Report, the absolute gravity values for our AG stations are episodic. Through the use of a reference height correction at each epoch of measurements, these values can be represented as time series, i.e. a data set of changes in absolute gravity with respect to time. An example AG time series is illustrated in Figure 2.10.

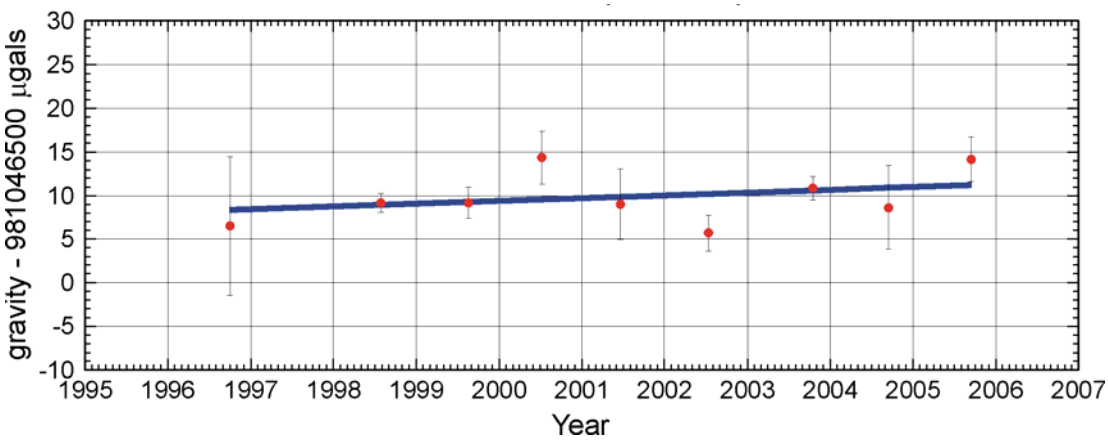

Figure 2.10 Example absolute gravity time series

In Figure 2.10, the AG estimates of absolute gravity for a station are shown as red dots, at approximately annual intervals. The figure also shows the best fit linear trend in the absolute gravity estimates (as a blue line) from which the rate of change of absolute gravity and its uncertainty can be computed. Based on these, and applying a conversion factor of -2μgal/cm or -5mm/μgal, consistent with the Bouger model described in Subsection 2.3.1, the equivalent vertical station velocity and uncertainty can then be inferred as an estimate of the change in land level.

More details on the specific absolute gravity time series analysis applied in the national study detailed in this Technical Report are given in Section 5.2.

2.4 Persistent Scatterer Interferometry

Synthetic Aperture Radar (SAR) is a kind of radar that is often used for Earth imaging purposes. Satellite-based SAR Interferometry (InSAR) is a method of using two or more SAR images, primarily for topographic mapping or digital elevation model (DEM) generation. With further processing it is possible to allow the identification of surface changes through a technique known as Differential InSAR (DInSAR). In this context, several processing methods have been developed which use PSI, or 'Persistent Scatterer Interferometry'.

In this section, the use of PSI for monitoring long term changes in PS point location and land level is described. The section begins with subsections on InSAR and DInSAR basics, followed by a subsection on PSI processing methods, all of which include details on the mitigation of associated systematic errors. The section then ends with a subsection on PS point time series analysis.

2.4.1 InSAR basics

InSAR basically involves the combination of the phase measurements from two SAR images to create an interference pattern. This is called the interferogram (or interferometric phase). When viewed, the interferogram appears as a series of 'fringes' denoting where the interferometric phase completes a full cycle (0-2π radians). The interferometric phase is a measure of the difference in the phase between the two SAR images, which in turn can be related to difference in radar signal path length. Using satellite positions, given as precise orbits, it is then possible to relate this path difference to surface topography.

An important part of InSAR history was when the European Space Agency (ESA) launched the European Remote Sensing (ERS) satellite ERS-1 in 1991, which had an onboard SAR. Having only one antenna on board, interferometric analyses are carried out using repeat passes: this is where the satellite images the area twice on separate orbital passes. During different phases of its lifetime, ERS-1 had different orbital repeat periods, but the nominal repeat period was 35 days. In 1995, ESA launched a second SAR capable satellite, ERS-2, with the same instrument characteristics as ERS-1 and in a similar orbit

to ERS-1. Then in 2002, ESA launched their Environmental Satellite (ENVISAT).

Figure 2.11 shows a typical spaceborne InSAR configuration. S1 and S2 denote the satellite positions when the first and second SAR images were taken. The three-dimensional distance between them is called the (geometric) baseline and is denoted as B in Figure 2.11. The perpendicular baseline, $B_\perp$, is the component of B in the direction perpendicular to the S1 look direction, and R1 and R2 denote the ranges to the target T from satellite positions S1 and S2 respectively (Warren 2007).

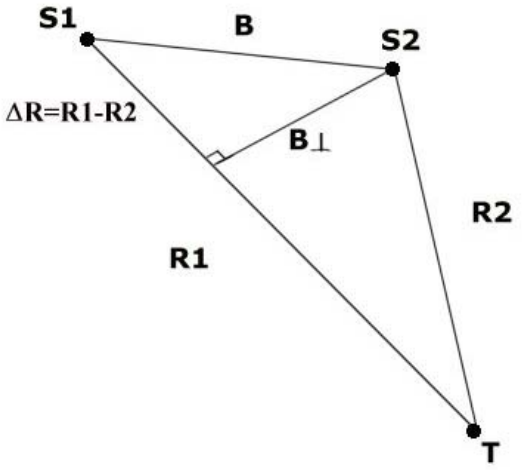

Figure 2.11 Schematic of a typical spaceborne InSAR configuration*: reproduced from Warren (2007)*

The difference between the two ranges is denoted ΔR and is related to the interferometric phase, ϕ, as

$$\phi = \frac{4\pi}{\lambda}\Delta R \qquad \text{[Equation 2.5]}$$

For InSAR, the interferometric processing chain can be split up into several different stages. The processing chain, starting from SLC (Single Look Complex) data, basically comprises image coregistration, resampling, interferogram formation, filtering and noise reduction, phase flattening and phase unwrapping. This subsection presents a brief overview of each of these stages. More information on these can be found in Hanssen (2001).

Image coregistration

As the two images (master and slave) are taken at different times, on slightly different orbits and with different start-stop times, they will not be of exactly the same area. Due to the satellite geometry they will almost certainly have some small rotation between them. This must be addressed since for InSAR it is vital that the two images are registered to sub-pixel accuracy. Coregistration is

usually split up into a coarse registration, to find the approximate line and pixel offset, and a fine registration to get the sub-pixel accurate offsets.

Resampling

This stage uses the 'coregistration equation' derived from the previous step and an interpolation kernel to resample the slave image. This is required so that the two SAR images are on the same grid in order to form the interferogram.

Interferogram formation

The interferogram can now be formed using the master and resampled slave images. An example of an interferogram, formed by Warren (2007) from an ERS-1 and ERS-2 tandem pair on 9th and 10th November 1995, using the DORIS software available from Delft University (Kampes and Usai 1999), is shown below in Figure 2.12.

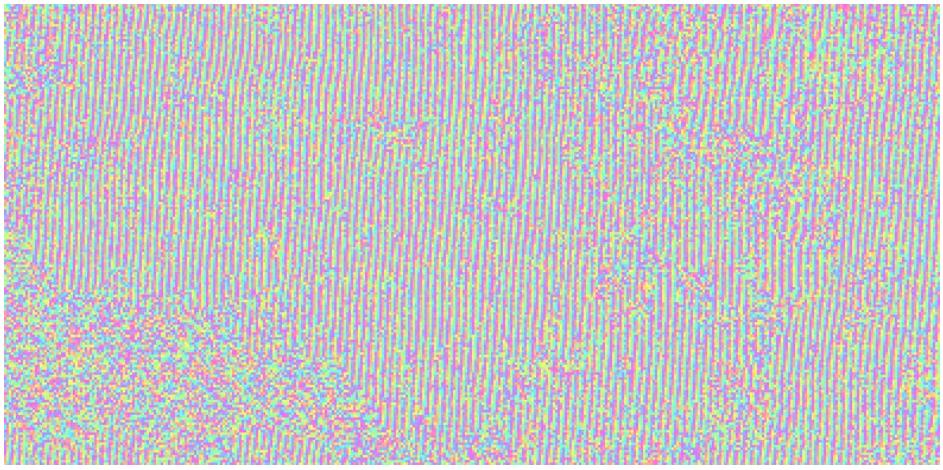

Figure 2.12 An example InSAR interferogram*: reproduced from Warren (2007)*

Filtering and noise reduction

Filtering and noise reduction techniques are then commonly applied to the interferogram to 'clean up' the product for easier interpretation and future processing (such as phase unwrapping). In this context, it is common to apply some a-priori filtering during the coregistration and resampling stages, i.e. before interferogram formation, and then some a-posteriori filtering after the interferogram is formed.

Phase flattening

Usually before a-posteriori filtering or multilooking the phase, it is "flattened". This is where a reference phase is subtracted from the interferometric phase. The reference phase is usually produced from a DEM of the scene area, or if no ground truth is available, a satellite-ellipsoid model. This is undertaken to reduce the fringe rate of the interferogram and is essential for phase unwrapping methods because of the need for small phase gradients. The

example from Figure 2.12 is shown below as Figure 2.13, where the WGS84 ellipsoid has been used as the Earth model and some noise filtering has been carried out (Warren 2007).

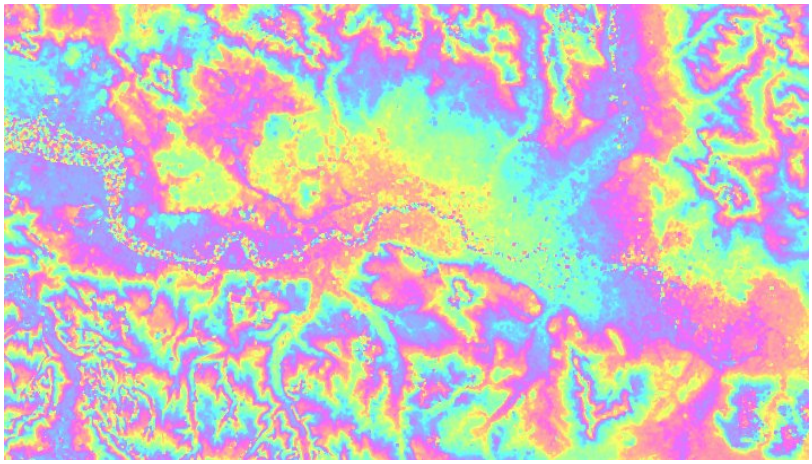

Figure 2.13 An example InSAR flattened interferogram*: reproduced from Warren (2007) and covering the same area as Figure 2.12.*

Phase unwrapping

The interferometric phase is ambiguous, i.e. it is only known modulo 2π and there is no information on the number of wavelengths (cycles) that have preceded it. Phase unwrapping is carried out to calculate the unknown integer number of cycles, either absolutely or relatively to a point on the image.

The coherence image

The coherence image (or complex correlation) is an important by-product of the interferogram formation. The one that relates to the InSAR interferograms from Figures 2.12 and 2.13 is shown below as Figure 2.14 (Warren 2007).

Figure 2.14 An example InSAR coherence image*: reproduced from Warren (2007) and corresponding to the interferograms given in Figures 2.12 and 2.13.*

The coherence image is basically the result of a correlation test between the two SAR images and gives an evaluation of the reliability of the phase values. The two main causes of decorrelation in interferograms are temporal and geometric. Values for coherence range between 0 and 1 where a value of 0 means there is no correlation and 1 means perfect correlation between the two signals. If the pixel has a high correlation value then the scattering properties of the pixel have not changed much between the two SAR images, giving more confidence in the phase value. Often these areas tend to be in urban environments. Areas of low coherence have low phase reliability. Such areas could be due to expanses of water, agricultural activity, or other regions that could change between SAR acquisitions.

Summary

As previously stated, the interferometric phase is related to the topography of the scene. In an ideal world this would be exact and there would be no phase corruption. Unfortunately this is not true and the phase will be erroneous, probably due to a number of sources including (but not limited to): speckle noise, temporal decorrelation, geometric decorrelation, orbital inaccuracies and atmospheric perturbations.

Speckle noise is usually dealt with by averaging pixels, known as complex multilooking, and temporal and geometric decorrelation effects can be minimised by selecting suitable SAR images to construct the interferogram. In general, temporal decorrelation can be minimised by selecting SAR images with a short temporal baseline and geometric decorrelation can be minimised by selecting SAR images that have small geometric baselines; however, the size of the geometric baseline has an affect on how sensitive the interferogram is to height change, so a trade off between height sensitivity and decorrelation must be attained. Inaccuracies in the satellite orbits reveal themselves as a phase slope across the image: clearly, the use of precise orbits will improve the phase quality. Changes in the atmosphere between the two SAR images have a detrimental affect on the interferometric phase since these differences will propagate through into the interferogram. This is particularly important for DInSAR and is discussed further in Subsection 2.4.2.

2.4.2 DInSAR basics

DInSAR is a technique that looks at differences that have occurred in the phase between SAR images. Gabriel et. al. (1989) first demonstrated DInSAR using spaceborne SAR and showed that measurements of surface change could be made at the centimetre level. Following this, in the 1990s DInSAR was successfully demonstrated in studying glacier motion (Goldstein et. al. 1993), earthquakes (Massonnet et. al. 1993; Zebker et. al. 1994), volcanoes (Massonnet et. al. 1995), landslides (Fruneau et. al. 1996) and subsidence (Massonnet et. al. 1997).

There are two broad methods of DInSAR: two-pass and multi-pass. Two-pass DInSAR, as the name suggests, involves two SAR images and a DEM. An

interferogram is formed from two SAR images which span the event of interest, for example an earthquake. The DEM is used to remove the phase relating to topography from the interferogram to leave the differential phase (Massonnet et. al. 1993); however, any errors present in the phase of the interferogram or in the DEM will be passed through into the differential phase.

The most common form of multiple-pass DInSAR involves three SAR images (and is hence called three-pass). From these three SAR images, two interferograms are formed such that they share a common master image (Gabriel et. al. 1989). The SAR images are selected such that one interferogram spans the event of interest, known as the deformation interferogram, whilst the other interferogram is formed from the two images either after or before the event, and known as the topographic interferogram (assumed to be a good model for the topography). Both interferograms are flattened with respect to an ellipsoid model and the topographic interferogram is then unwrapped. The topographic phase is then scaled by the ratio of the perpendicular baselines and subtracted from the deformation interferogram (Zebker et. al. 1994) as follows

$$\phi_{diff} = \phi_{defo} - \frac{B\perp_{defo}}{B\perp_{topo}}\phi_{topo} \qquad \text{[Equation 2.6]}$$

where ϕ_{diff} is the differential phase, ϕ_{defo} the deformation interferogram phase, ϕ_{topo} the topographic interferogram phase, $B\perp_{defo}$ the perpendicular baseline of the deformation interferogram and $B\perp_{topo}$ the perpendicular baseline of the topographic interferogram. Again, any errors present in the respective phases of the two interferograms will be passed into the differential phase. Furthermore, since the interferograms have been flattened with respect to an ellipsoid model, there is likely to be an erroneous phase slope in the differential phase, due to the altitude difference between the ellipsoid and the topography, but this can be removed a-posteriori with the use of distributed ground control.

As with InSAR, DInSAR results can be improved or optimised by using the best configuration available. When using two-pass DInSAR, a better result is obtained by using a more accurate DEM and if the interferogram phase is clean of temporal and geometric decorrelation noise. Whereas, when using three-pass DInSAR, the relative size of the baselines can have a great effect as is clear from Equation 2.6.

Apart from these factors, the limitations of DInSAR are mainly due to the quality of the input data as any noise in the interferometric phase will be propagated through into the differential phase. In general, the largest source of error will be the atmosphere, which can often swamp the phase that is being investigated. For three-pass DInSAR this is worse because there are two interferograms, and therefore two atmospheric phase errors; whereas for two-pass DInSAR there is only one atmospheric phase error but there is the additional error due to the DEM.

2.4.3 PSI processing methods

Ferretti et. al. (1999) demonstrated a new technique of DInSAR that utilised the whole back catalogue of ERS SAR images for a specific region. This technique was referred to as the 'Permanent Scatterers Technique' (Ferretti et. al. 2001). Rather than using every image pixel, this technique only selects certain pixels based upon their phase stability throughout the time evolution of the images; such pixels being termed Permanent Scatterers. In the real world these pixels relate to stable, reflective objects such as bare rock, buildings, bridges, lamp posts etc., which makes this technique ideal for monitoring in urban areas. The terms Persistent Scatterer and Permanent Scatterer can be interchanged as they generally mean the same thing, but Permanent Scatterer tends to be used when related to Ferretti's technique, so throughout this Technical Report the term Persistent Scatterer (PS) will be used to describe phase stable pixels and the term Persistent Scatterer Interferometry (PSI) to describe the technique.

PSI has been successfully used to identify urban subsidence (Ferretti et. al. 2000), progressive and seasonal ground deformation (Colesanti et. al. 2003a), landslide and tectonic motions (Colesanti et. al. 2003b) and volcanic deformation (Hooper et. al. 2004).

There are a few different methods for PSI being applied and developed at this time. The most prominent of these are:

- Permanent Scatterers Technique (Ferretti et. al. 2001);
- 'Small Baseline Subset' (SBAS) (Beradino et. al. 2002);
- 'Interferometric Point Target Analysis' (IPTA) (Werner et. al. 2003);
- 'Stable Point Network' (SPINUA) (Bovenga et. al. 2004).
- 'Coherent Pixel Technique' (Dominguez et. al. 2005);
- 'Spatio-Temporal Unwrapping Network' (STUN) (Kampes and Nico 2005);

Even though these are six distinct methods, the aims of each method are generally the same and can be summarised as follows. Interferograms are formed from the stack of SAR images, which are then flattened using a DEM to give the differential phase. Candidate PS points are then identified by some means and used in a joint spatial and temporal analysis to identify an atmospheric phase screen for each interferogram. After removing this atmospheric phase screen from the interferograms, an estimate of the deformation and error in the DEM for PS points can then be made by examining both the temporal evolution and the geometric baseline variation of each pixel.

When creating the differential phase, a two-pass method is used. To reduce the amount of data, the differential phase not relating to the candidate PS points is discarded. The differential phase for a PS point is then given by

$$\partial\phi = \phi_{atm} + \phi_{orb} + \phi_{defo} + \phi_{DEM} + \phi_n \qquad \text{[Equation 2.7]}$$

where $\partial\phi$ is the differential phase and $\phi_{atm}, \phi_{orb}, \phi_{defo}, \phi_{DEM}, \phi_n$ are phase terms due to atmosphere, orbit errors, deformation, DEM errors and noise respectively. The phase of interest is ϕ_{defo} whereas the other components can

be considered as unwanted noise, which need to be removed. ϕ_{atm}, ϕ_{orb} are spatially correlated. Depending on the method these are either not separated, so that the atmospheric phase screen effectively solves for their combine effect, or an algorithm is used to remove ϕ_{orb}, so that the atmospheric phase screen only solves for ϕ_{atm}. ϕ_{DEM} is correlated up the stack in terms of the geometric baseline and is modelled in the PSI processing. ϕ_n is then the spatially and temporally random noise component, due mainly to geometric and temporal decorrelation, which should be small by definition for a PS point. Based on this information, through an iterative algorithm it is then possible to estimate the phase components.

Ultimately, PSI provides a measure of the movement of a PS point relative to a fixed PS point, termed the 'reference scatterer', in the direction from the PS point on the Earth's surface to the satellite (i.e. along the line-of-sight to the satellite).

In comparison to conventional DInSAR, PSI is a technique which overcomes the problem that atmospheric perturbations cause in DInSAR. However, it is reliant on a DEM, requires large quantities of data (i.e. at least 30 SAR images) and has a larger computational processing time. In practice, the reliance on a DEM is not such a restraint since Shuttle Radar Topography Mission (SRTM) data was made available, but DEM errors must be modelled out in the PSI processing chain. The many SAR images required and the computational burden clearly have cost implications, but these are not restrictive and only become a problem if the area to be studied has no archived SAR data, in which case PSI cannot be used until sufficient data has been collected (e.g. using ENVISAT takes approximately 3 years to collect 30 images). Conversely, if archived data is available for an area then PSI can 'go back in time', as far as 1991. In this respect, PSI is particularly suited to monitoring slow, long term deformations such as changes in land level.

More details on the specific PSI method used in the regional study detailed in this Technical Report are given in Section 6.1.

2.4.4 PS point time series analysis

Applying one of the PSI methods introduced in the previous subsection, through PSI processing, the movement of a PS point relative to a reference scatterer, along the line-of-sight to the satellite, can be described as a time series, as shown in Figure 2.15. In this figure, the estimates are shown as blue dots, at intervals of every 35 days, depending on satellite availability, and the best fit linear trend is shown by the black line.

From the best fit linear trend shown in Figure 2.15, estimates of the velocity of the PS point, both along the line-of-sight to the satellite and in the vertical (with some assumptions) can be inferred.

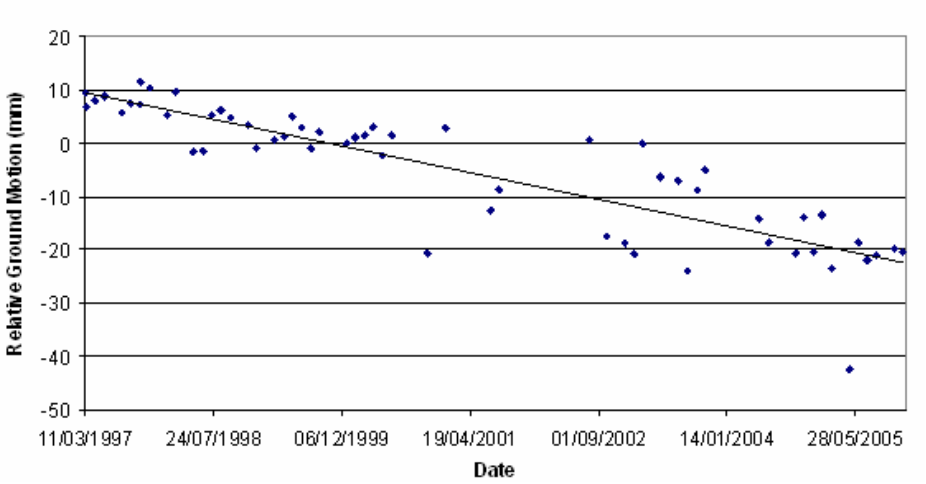

Figure 2.15 Example PS point time series

In urban areas, PSI processing can identify thousands of PS points per square kilometre. Using these it is then possible to produce maps of changes in ground level. An example of such a map is given as Figure 2.16, where each PS point has been colour coded, depending on the velocity of the point along the line-of-sight to the satellite, with yellow/red indicating subsidence of up to 5mm/yr, green indicating 'stability' and turquoise/blue indicating uplift of up to 5mm/yr.

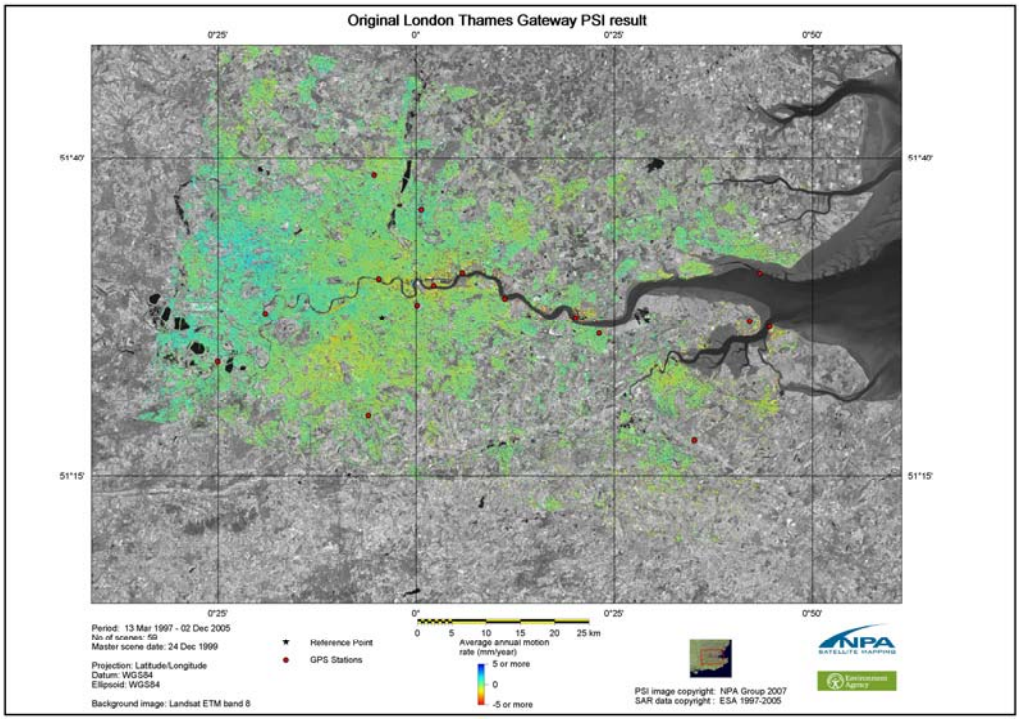

Figure 2.16 Example PSI analysis map

More details on the specific PSI processing and PS point time series analysis used in the regional study detailed in this Technical Report are given in Section 6.1.

3. Background to the national study

In 1990, 1995 and 2001, the Intergovernmental Panel on Climate Change (IPCC) reviewed the published evidence on the influence of global warming on sea levels, e.g. Church et. al. (2001). They found that global sea level had risen by 10 to 20cm over the past century, with predictions indicating further rises of the order of up to a metre by 2100. Recent studies of 20th century sea level from combined tide gauge and satellite altimetry measurements showed a globally averaged rise in sea level of 1.7 to 1.8mm/yr over the past few decades (Church et. al. 2004; Holgate and Woodworth 2004; White et. al. 2005, Church and White 2006). As stated in Section 2.1, "it is generally accepted that a high quality tide gauge record can enable the secular change of sea level to be estimated with an acceptable level of uncertainty if 30 to 50 years or more of data are used (Woodworth et. al. 1999)." However, to measure the climate related component of changes in sea level using a tide gauge, the rate of any changes in land level at the specific tide gauge must be accounted for.

In this chapter, published changes in sea level from British tide gauges are reviewed along with published changes in the land level of Great Britain. The chapter then goes on to describe the GPS and AG data sets which have been acquired, as part of the national study detailed in this Technical Report, in order to obtain site-specific, direct estimates of current changes in land level that will enable a tide gauge to be better used for studying the climate related component of changes in sea level.

3.1 Published changes in sea level from British tide gauges

As implied in the introduction to this chapter, much of the evidence for changes in sea level for the past few decades/past century came from measurements obtained at tide gauges, which measure MSL with respect to a TGBM. For Great Britain, a set of estimates of changes in sea level for a number of tide gauges in the British Isles for the period up to 1996 was published as Woodworth et. al. (1999). Following this, it is also possible to obtain updated estimates of changes in sea level from the PSMSL.

3.1.1 Changes in sea level for the period up to 1996

Woodworth et. al. (1999) analysed the Revised Local Reference (RLR) data held in the PSMSL database for a number of tide gauges in the British Isles; the RLR data set being a time series of annual MSL values for tide gauges where a full history of the connections between the tide gauge contact point, the RLR (used as reference for the MSL measurements) and a TGBM exists, to ensure the continuity of MSL time series when multiple tide gauge sensors and/or locations have been used over a number of decades. The changes in sea level obtained for a selection of the tide gauges analysed by Woodworth et. al. (1999) is given in Table 3.1.

Table 3.1 Estimates of changes in sea level for selected British tide gauges for the period up to 1996 (Woodworth et. al. 1999)

Tide gauge	Period of RLR data used	Number of complete years of RLR data used	Change in annual MSL and uncertainty (mm/yr)
Lerwick	1957-1996	35	-1.09 ± 0.40
Aberdeen	1932-1996	48	+0.67 ± 0.20
North Shields	1901-1996	77	+1.86 ± 0.15
Liverpool	1959-1983	19	+2.58 ± 0.88
Lowestoft	1956-1995	36	+1.81 ± 0.48
Sheerness	1901-1996	51	+2.14 ± 0.15
Portsmouth	1962-1996	28	+1.45 ± 0.60
Newlyn	1916-1996	80	+1.69 ± 0.12

From Table 3.1, it is clear that, with the exception of Lerwick tide gauge on Shetland, the British tide gauges all show a rise in sea level over the past few decades/past century, with a range of values from 0.67mm/yr at Aberdeen tide gauge in East Scotland to 2.58mm/yr at Liverpool tide gauge in the North-West of England; Lerwick is exceptional as the tide gauge measurements here suggest a fall in sea level of 1.09mm/yr. Here it is important to note that none of these estimates have been 'corrected' for changes in land level.

3.1.2 Changes in sea level for the period up to 2005

As stated at the start of Section 3.1, it is also possible to obtain updated estimates of changes in sea level from the PSMSL. Table 3.2 replicates Table 3.1 and presents revised estimates of changes in sea level for the period up to 2004 (PSMSL 2005).

Table 3.2 Estimates of changes in sea level for selected British tide gauges for the period up to 2004 (PSMSL 2005)

Tide gauge	Period of RLR data used	Number of complete years of RLR data used	Change in annual MSL and uncertainty (mm/yr)
Lerwick	1957-2004	37	-0.79 ± 0.36
Aberdeen	1932-2004	55	+0.86 ± 0.15
North Shields	1897-2004	86	+1.85 ± 0.12
Liverpool	1858-1983	77	+1.03 ± 0.15
Lowestoft	1956-2004	42	+2.49 ± 0.37
Sheerness	1834-2004	75	+1.64 ± 0.09
Portsmouth	1962-2003	33	+1.82 ± 0.45
Newlyn	1916-2004	87	+1.69 ± 0.11

When compared to Table 3.1, it should be noted that the revised estimates for Lerwick, Aberdeen, Lowestoft, Portsmouth and Newlyn tide gauges are based on the inclusion of new RLR data for the period from 1997 to 2003 or 2004; whereas for North Shields, Liverpool and Sheerness tide gauges the revised estimates are based on the inclusion of new RLR data for the period from 1997 to 2004 plus historical RLR data which move the start dates of the MSL time series for these three tide gauges back from 1901 to 1897, from 1959 to 1858 and from 1901 to 1834 respectively.

As with Table 3.1, with the exception of Lerwick tide gauge on Shetland, the British tide gauges all show a rise in sea level over the past few decades/past century, with a range of values from 0.86mm/yr at Aberdeen tide gauge in East Scotland to 2.49mm/yr at Lowestoft tide gauge on the East coast of England; Lerwick is exceptional as the tide gauge measurements still suggest a fall in sea level, of 0.79mm/yr.

Comparing Tables 3.1 and 3.2, however, it can be seen that the additional RLR data has had a varying effect on the estimates of changes in sea level, depending on both the period of RLR data used and the number of complete years of RLR data used:

- For North Shields tide gauge in the North-East of England and Newlyn tide gauge near to Land's end in South-West England, which now have MSL time series comprising of 86 and 87 complete years of RLR data instead of 77 and 80 years respectively, there is effectively no difference in the estimates of changes in sea level.
- For Lerwick tide gauge on Shetland, Aberdeen tide gauge in East Scotland, Lowestoft tide gauge on the East coast of England and Portsmouth tide gauge on the South coast of England, which now have MSL time series comprising of 37, 55, 42 and 33 complete years of RLR data instead of 35, 48, 36 and 28 years respectively, the estimates of changes in sea level have all increased, by 0.30, 0.19, 0.68 and 0.37mm/yr respectively.
- For Liverpool tide gauge in the North-West of England, which now has a MSL time series comprising of 77 instead of 19 complete years of RLR data and going back to 1858 not 1959, the estimate of change in sea level has reduced by 1.55mm/yr, from a rise of 2.58mm/yr to a rise of only 1.03mm/yr.
- For Sheerness tide gauge on the Thames Estuary to the East of London, which now has a MSL time series comprising of 75 instead of 51 complete years of RLR data and going back to 1834 not 1901, the estimate of change in sea level has reduced by 0.50mm/yr, from a rise of 2.14mm/yr to a rise of only 1.64mm/yr.

From Tables 3.1 and 3.2, it is clear that the uncertainties associated with the estimates of changes in sea level for the eight tide gauges considered are consistent with the statement made in Woodworth et. al. (1999) that "one needs typically 30 years of data in order to determine a secular trend with a standard error of the order of 0.5mm/yr and 50 years for an error of 0.3mm/yr." However, the evidence presented in this section also highlights that estimates of changes in sea level can still vary by up to 0.7mm/yr as MSL time series are extended forward within the range of 30 to 50 complete years of RLR data; whereas there appears to be little effect when MSL time series are extended within the range of approximately 80 to 90 complete years of RLR data. Considering the MSL time series for Sheerness tide gauge, there is a clear decrease in the change in sea level when the historical RLR data is included (the same occurs at Liverpool tide gauge but this should be treated with caution as the original MSL time series only consisted of 19 complete years of RLR data) which clearly supports the idea of a rise in sea level during the 20th century which was not present during the 19th century.

The values presented in Table 3.2 are taken forward and used in Section 5.4, where estimates of changes in sea level (decoupled from changes in land level based on CGPS and AG) are presented as part of the deliverables from the national study detailed in this Technical Report.

3.2 Published changes in the land level of Great Britain

As stated in the introduction to this chapter, to measure the climate related component of changes in sea level using a tide gauge, the rate of any changes in land level at the specific tide gauge must be accounted for. In some parts of the world it is possible to make this correction based purely on models of glacial isostatic adjustment (GIA), where this is the dominant source of change in land level, e.g. in Canada and Fennoscandia. However, such models do not necessarily account for all of the changes in land level occurring, and for Great Britain, alternative estimates based on geological studies have been presented.

In this section, a brief review of published changes in the land level of Great Britain is given, with particular emphasis on models of GIA which have often been used for 'correcting' tide gauge records in studies of changes in global sea level, and the geological studies of Shennan, as these have been used in studies of changes in sea level (decoupled from changes in land level) for the British Isles, e.g. Woodworth et. al. (1999), and have been used by the United Kingdom Climate Impacts Programme (UKCIP) (Hulme et. al. 2002).

3.2.1 Models of Glacial Isostatic Adjustment

Models of GIA consider the changes in glaciation and deglaciation (notably of the Laurentide, Fennoscandian and Scottish ice sheets) that have occurred over the past 32,000 years (as an ice model), along with assumptions about the Earth's response to these events (as a visco-elastic Earth model) in order to calculate estimates of current changes in land level. When used in studies of changes in sea level (decoupled from changes in land level) these are then assumed to represent the changes in land level that have occurred at a tide gauge for the past few decades/past century and will continue to occur at a tide gauge for the next few decades.

Two such models of GIA are those published by Lambeck and Johnston (1995) and Peltier (2001), respectively. Figure 3.1 presents a map of estimates of changes in land level for the British Isles inferred from the GIA model of Peltier (2001); in essence the contours have been inferred from the site-specific estimates given by Peltier (2001) for the 44 tide gauges in the British Isles, which form the national tide gauge network as part of the NTSLF, and 10 tide gauges in Northern France.

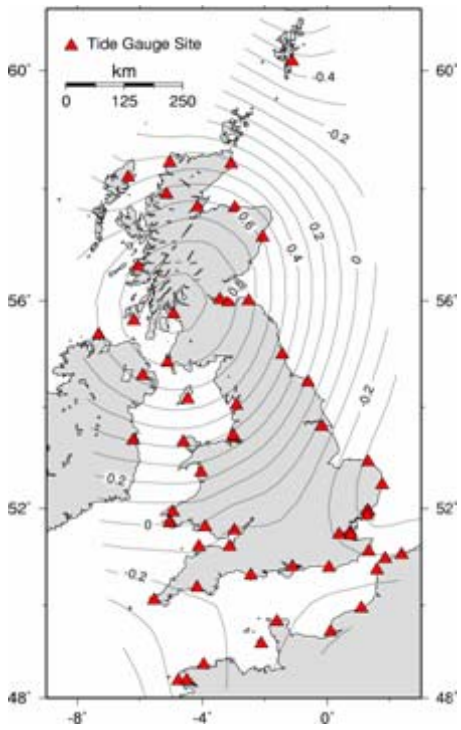

Figure 3.1 Map of estimates of changes in land level for the British Isles inferred from the GIA model of Peltier (2001)

As Figure 3.1 shows, the general pattern of expected changes in land level in Great Britain is one of uplift in Scotland and Northern England, subsidence on Shetland, and subsidence in Central and Southern England, East Anglia and Wales: the GIA model of Peltier (2001) showing a maximum uplift of 1.0mm/yr in Western Scotland and a maximum subsidence of 0.4mm/yr in East Anglia and 0.6mm/yr on Shetland. Other GIA models exhibit a similar patter of uplift and subsidence, but with varying magnitudes depending on the ice model and the visco-elastic Earth model assumed, as shown in Table 3.3 which presents estimates of changes in land level from the two GIA models mentioned previously for a selection of British tide gauges.

Table 3.3 Estimates of changes in land level for selected British tide gauges based on two GIA models (Lambeck and Johnston 1995, Peltier 2001)

Tide gauge	Changes in land level (mm/yr) based on the GIA model of Lambeck and Johnston (1995)	Changes in land level (mm/yr) based on the GIA model of Peltier (2001)
Lerwick	-1.8	-0.5
Aberdeen	0.0	+0.6
North Shields	0.0	+0.4
Liverpool	-0.3	+0.4
Lowestoft	-0.5	-0.4
Sheerness	-0.5	-0.2
Portsmouth	-0.5	-0.1
Newlyn	-1.0	-0.3

From Table 3.3, it is clear that where the GIA model of Peltier (2001) suggests subsidence, the GIA model of Lambeck and Johnston (1995) also suggests subsidence, but to a greater extent, e.g. Lerwick tide gauge on Shetland has a subsidence of 1.8mm/yr as oppose to 0.5 mm/yr, and Newlyn tide gauge near to Land's End in the South-West of England has a subsidence of 1.0mm/yr as oppose to 0.3mm/yr. This negative 'systematic offset' of the Lambeck and Johnston (1995) values from the Peltier (2001) values persists, such that where the GIA model of Peltier (2001) suggests uplift the GIA model of Lambeck and Johnston (1995) does not, e.g. Aberdeen tide gauge in East Scotland and North Shields tide gauge in the North-East of England have no uplift as oppose to uplifts of 0.6 and 0.4mm/yr respectively, and Liverpool tide gauge in the North-West of England is even subsiding by 0.3mm/yr as oppose to uplifting at 0.4mm/yr. Here it is import to note that none of this discussion is an attempt to say which of the GIA models is 'more correct', rather to point out the discrepancies that exist when comparing different GIA models due to the complexity of the modelling process and the assumptions made about glaciation and deglaciation and the Earth's elastic response to this.

3.2.2 Geological studies

In these studies, geological evidence of changes in land level that have occurred since the Last Glacial Maximum (LGM), i.e. over the past 16,000 years, are used to calculate estimates of current changes in land level. As with the models of GIA, when used in studies of changes in sea level (decoupled from changes in land level) these are then assumed to represent the changes in land level that have occurred at a tide gauge for the past few decades/past century and will continue to occur at a tide gauge for the next few decades.

In this respect, Great Britain is rather fortunate in having a detailed database of more than 1,250 radiocarbon dated samples which can be used to form sea level index points that constrain relative sea levels around Great Britain over the past 16,000 years and enable estimates of changes in land level to be made. Such estimates have been published as Shennan (1989) and Shennan and Horton (2002). Figure 3.2 presents a map of estimates of changes in land level for Great Britain, reproduced from Shennan and Horton (2002).

As Figure 3.2 shows, in sympathy with the GIA models, the geological studies also suggest that the general pattern of changes in land level in Great Britain is one of uplift in Scotland and Northern England and subsidence in Central and Southern England, East Anglia and Wales: Shennan and Horton (2002) showing a maximum uplift of 2.0mm/yr in Western Scotland and a maximum subsidence of 1.2mm/yr in South-West England.

Figure 3.2 Map of estimates of changes in land level for Great Britain based on geological studies (Shennan and Horton 2002)

Table 3.4 expands on Table 3.3 given in the previous subsection and presents estimates of changes in land level from the two GIA models and from the geological studies for the same selection of British tide gauges.

Table 3.4 Estimates of changes in land level for selected British tide gauges based on two GIA models (Lambeck and Johnston 1995, Peltier 2001) and geological studies (Shennan and Horton 2002)

Tide gauge	Changes in land level (mm/yr) based on the GIA model of Lambeck and Johnston (1995)	Changes in land level (mm/yr) based on the GIA model of Peltier (2001)	Changes in land level (mm/yr) based on the geological studies of Shennan and Horton (2002)
Lerwick	-1.8	-0.5	N/A
Aberdeen	0.0	+0.6	+0.7
North Shields	0.0	+0.4	+0.2
Liverpool	-0.3	+0.4	-0.2
Lowestoft	-0.5	-0.4	-0.6
Sheerness	-0.5	-0.2	-0.7
Portsmouth	-0.5	-0.1	-0.6
Newlyn	-1.0	-0.3	-1.1

From Table 3.4, it is clear that the geological studies are in closer agreement with the GIA model of Lambeck and Johnston (1995) at five of the seven tide gauges where it is possible to make a comparison, the only exceptions being Aberdeen tide gauge in East Scotland where the geological studies suggest uplift of 0.7mm/yr, which is more consistent with the 0.6mm/yr from the GIA model of Peltier (2001), and North Shields tide gauge in the North-East of England where the value from the geological studies sits between the values from the two GIA models; regrettably there are no estimates based on

geological studies for Lerwick tide gauge on Shetland which exhibits the biggest discrepancy between the two GIA models.

To re-iterate what was said at the end of the previous subsection, none of this discussion is an attempt to say whether either one of the GIA models or the geological studies are more correct, rather to point out the discrepancies that exist when comparing the different sources of evidence for changes in land level in Great Britain. At this point, however, it is interesting to note that since the publication of the GIA models of Lambeck and Johnston (1995), Peltier (2001) and others, several publications have investigated the discrepancies between the models and the geological studies for Great Britain in the context of testing GIA modelling and ice sheet reconstructions, namely Peltier et. al. (2002), Shennan et. al. (2002, 2006a, 2006b).

The values presented in Table 3.4 are taken forward and used in Section 5.3, in comparison with the estimates of changes in land level based on CGPS and AG, produced as part of the deliverables from the national study detailed in this Technical Report.

3.3 The GPS data set

As implied in the introduction to this chapter, GPS has the potential to obtain site-specific, direct estimates of current changes in land level that will enable a tide gauge to be better used for studying the climate related component of changes in sea level.

In this section, the GPS data set which has been acquired, as part of the national study detailed in this Technical Report, is presented. The section starts with an overview of early GPS measurements made at British tide gauges, then provides details on the establishment of CGPS stations at tide gauges and other locations in Great Britain, before giving the specifics of the GPS data set used in the national study.

3.3.1 Early GPS measurements at British tide gauges

The development of GPS techniques for monitoring changes in land level at British tide gauges has been on-going at IESSG and POL since 1990, based on research funded by both Defra and the Environment Agency. This research and development was initially based on the use of near-annual, EGPS campaigns with measurements made over 5 days for observation sessions of 8 to 24 hours per day, at a network of EGPS stations established close to 17 of the 44 tide gauges which form the national tide gauge network as part of the NTSLF. Since 1996, the research and development has focused on the establishment of CGPS stations, which are capable of providing 24 hour observation sessions on 365 days per year and, therefore, enable much more precise and accurate measurements of changes in land level. In the period from 1996 to 2002, as the network of CGPS stations was slowly expanding, some further measurements were carried out at tide gauges which were not

equipped with a CGPS station, based on EGPS campaigns or what was termed quasi-continuous GPS (QCGPS), where measurements were made over 24 hour observation sessions for one month per year, when site conditions would allow the establishment of a QCGPS station.

Through the latest research, and similar research carried out by other scientists on an international scale, the advantages of QCGPS over EGPS, but more so, the advantages of CGPS over both QCGPS and EGPS became more and more evident, so that it is now generally accepted that the precision and accuracy demands of trying to use GPS on a national or larger scale (to obtain site-specific, direct estimates of current changes in land level that will enable a tide gauge to be better used for studying the climate related component of changes in sea level) can only be met through the use of CGPS; this being the basis for the national study detailed in this Technical Report.

For studies of horizontal motion (as GPS does not just measure changes in land level but changes in three-dimensions) on a 'small to medium' (100x100 to 500x500km) regional scale and studies of vertical motion on a 'small' (100x100km) regional scale, it is generally accepted that networks of QCGPS or EGPS stations can still be used, but only as a densification of a network of CGPS stations within the region and in the knowledge that this will not enable as high precision or accuracy as using CGPS but will enable more dense networks to be monitored; this being the basis for the use of EGPS stations in the Thames Region, as detailed in Section 4.4.

3.3.2 CGPS stations at tide gauges and other locations in Great Britain

During the period from 1997 to 2005, IESSG and POL established CGPS stations at ten of the 44 tide gauges which form the national tide gauge network as part of the NTSLF. In chronological order, these were established at Sheerness, Newlyn, Aberdeen, Liverpool, Lowestoft, North Shields, Portsmouth, Lerwick, Stornoway and Dover tide gauges. All of these so-called 'CGPS@TG stations' were established such that the GPS receivers (all dual frequency) are housed in the same building as the tide gauge equipment and the GPS antennas (all Dorne Margolin choke ring antennas) are mounted on monuments, sited as close as possible to the tide gauge, i.e. within a few meters of the tide gauge itself; to fulfil the requirement to obtain site-specific, direct estimates of changes in land level.

The first CGPS@TG station in Britain, and one of the first few in the world, was established at Sheerness tide gauge on the Thames Estuary to the East of London in March 1997. For this station, the monument is located on the concrete slab roof of the tide gauge building, which is a single storey brick building on a jetty with piled foundations, and the monument consists of a 0.16m high stainless steel bracket, which is fixed to the concrete roof of the tide gauge building.

Following the establishment of the CGPS@TG station at Sheerness, two further stations were established in September 1998, one at Aberdeen tide gauge in

East Scotland and one at Newlyn tide gauge near to Land's end in South-West England. These both use IESSG-designed carbon fibre/stainless steel monuments, but in different aspects. In the case of Aberdeen tide gauge, the monument is located adjacent to the tide gauge building, which is on a concrete quay, with piled foundations, and the monument consists of a 4m high carbon fibre pipe mounted on a steel plate, which is fixed to the concrete quay. In the case of Newlyn tide gauge, the monument is located on the observation platform of a steel lighthouse adjacent to the tide gauge building, which is located at the end of a stone pier, founded on the Sandstone bedrock, and the monument consists of a 3m high carbon fibre pipe mounted on a steel plate, which is fixed to the observation platform.

The next two CGPS@TG stations to be established were at Liverpool tide gauge in the North-West of England and Lowestoft tide gauge on the East coast of England. These were established in February 1999 and both use site-specific, specially designed monuments. In the case of Liverpool tide gauge, the monument is located on a 5m high concrete pillar which forms part of a wind-break and is about 5m from the tide gauge building, which is on a stone pier with piled foundations, and the monument consists of a 0.07m high stainless steel pipe mounted on a stainless steel plate, which is fixed to the concrete pillar. In the case of Lowestoft tide gauge, the monument is located on the side wall of a two storey brick office building, adjacent to the tide gauge building, so that the antenna is raised above the roof, and the monument consists of a 0.8m carbon fibre pipe mounted on a steel bracket, which is fixed to the side wall.

In May 2001, a GPS receiver and antenna were installed at North Shields tide gauge in the North-East of England to establish a CGPS@TG station, using a monument which had first been installed by the University of Newcastle-upon-Tyne in March 1998 but effectively only used for QCGPS measurements made from June to August 1998, in August and December 1999, and from February to October 2000. In this case, the monument is located in the tide gauge building, which is on a concrete quay, with piled foundations, and the monument consists of a 4m high aluminium pole, which is fixed to the concrete quay and passes through the roof of the tide gauge building.

Then in September 2001, a CGPS@TG station was established at Portsmouth tide gauge on the South coast of England. For this station, the monument is mounted on the North end wall of a single storey brick building, which houses the tide gauge equipment, so that the antenna is raised above the roof apex, and the monument consists of a stainless steel bracket with a 1.5m high stainless steel pole.

The last three CGPS@TG stations to be established were at Lerwick tide gauge on Shetland, Stornoway tide gauge on the Western Isles and Dover tide gauge on the South-East coast of England. These three were established in August, September and November 2005 respectively, and all three have IESSG-designed carbon fibre/stainless steel monuments, similar to those installed at Aberdeen and Newlyn, but in aspects more similar to Aberdeen than Newlyn. In the case of Lerwick tide gauge, the monument is located adjacent to the tide

gauge building, which is on a stone pier/breakwater, built in 1913, and the monument consists of a 3m high carbon fibre pipe mounted on a steel plate, which is fixed to a concrete plinth on top of the pier/breakwater stone wall. In the case of Stornoway tide gauge, the monument is located about 20m from the tide gauge building, on No 2 Wharf, and the monument consists of a 2m high carbon fibre pipe mounted on a steel plate, which is fixed to the concrete of the Wharf. Lastly, in the case of Dover tide gauge, the monument is located about 15m from the tide gauge building, on the Prince of Wales Pier, and the monument consists of a 2m high carbon fibre pipe mounted on a steel plate, which is fixed to the stone wall of the pier.

A summary of the details for the CGPS@TG stations, including the 4-character station ID, the exact start date of operation and the GPS equipment currently in place are given in Table 3.5.

Table 3.5 Summary details for the British CGPS@TG stations

Tide gauge	4-character station ID	Start date of operation (yyyy-mm-dd)	Current GPS receiver type	Current GPS antenna type
Lerwick	LWTG	2005-08-19	Ashtech UZ-12	ASH701945C_M SNOW
Stornoway	SWTG	2005-09-02	Ashtech UZ-12	ASH701945C_M SNOW
Aberdeen	ABER	1998-09-18	Ashtech Z-XII3	ASH700936F_C SNOW
North Shields	NSTG	2001-05-15	Ashtech Z-XII3	ASH700936B_M SNOW
Liverpool	LIVE	1999-02-04	Ashtech Z-XII3	ASH700936D_M SNOW
Lowestoft	LOWE	1999-02-13	Ashtech Z-XII3	ASH700936F_C SNOW
Sheerness	SHEE	1997-03-27	Trimble 4000 SSI	TRM29659.00 NONE
Dover	DVTG	2005-11-24	Ashtech UZ-12	ASH701945C_M SNOW
Portsmouth	PMTG	2001-09-25	Ashtech UZ-12	ASH701945C_M SNOW
Newlyn	NEWL	1998-09-30	Ashtech Z-XII3	ASH700936D_M SNOW

Over the period from 1997 to 2005, whilst these CGPS@TG stations were being established, several other CGPS stations were established in Great Britain. Along with the ten CGPS@TG stations, the data from all of these 'non-TG CGPS stations' in the British Isles is archived by the NERC British Isles GPS archive Facility (BIGF), which is operated by IESSG. BIGF separates the stations within its archive into 'scientific stations' and 'active stations', the former having been established for specific scientific applications and the latter being those established by the Ordnance Survey of Great Britain and Ordnance Survey of Northern Ireland for more general surveying use. Clearly, in view of the published changes in the land level of Great Britain given in the previous section, estimates of changes in land level from any suitable CGPS stations can still be used in comparisons with models of GIA and geological studies. They are also of potential great use in assessing whether the estimates for changes in land level at the CGPS@TG stations are consistent with estimates for

changes in land level (a few tens of kilometres) on solid rock inland. To perform these roles, the non-TG CGPS stations should ideally fulfil two criteria: to have been operational for as long as possible, preferably more than 4.5 years, and be founded on solid rock or a 'stable structure' connected to solid rock.

There are ten scientific stations in BIGF which definitely meet both of these criteria, two of which are part of the IGS, namely Herstmonceux (HERS) and Morpeth (MORP), and others of which were established by the IESSG: for the Environment Agency, namely Barking Barrier (BARK); for the Met Office, namely Aberystwyth (ABYW), Camborne (CAMB), Dunkeswell (DUNK), Hurn (HURN), Lerwick (LERW) and Pershore (PERS); and for themselves, namely IESSG in Nottingham (IESG).

There are then two scientific stations in BIGF which definitely meet the second criteria but have not been operational for more than 4.5 years: one is part of the IGS, namely Herstmonceux (HERT), and the other of was established by the IESSG for the Met Office, namely Hemsby (HEMS).

There are then two scientific stations in BIGF which meet the first criteria but cannot be guaranteed to meet the second criteria: one is part of the IGS, namely National Physical Laboratory in Teddington (NPLD), and one was established by the IESSG for the Environment Agency, namely Sunbury Yard (SUNB).

There are then three scientific stations in BIGF which do not meet the first criteria and cannot be guaranteed to meet the second criteria, namely Cardington (CARD), Rutherford Appleton Laboratory in Oxfordshire (RAL1) and South Uist (UIST) established by the Met Office.

In addition to these 17 BIGF scientific stations, there are several active stations in BIGF which have been operational since 2000, but none of which can be guaranteed to meet the second criteria as they were established by the Ordnance Survey of Great Britain to act as reference stations for centimetric accuracy land surveying and not long-term monitoring of changes in land level of millimetres per year. Despite this, they can provide a series of non-TG CGPS stations running along the 'spine' of Great Britain, which densifies the sparser network that is formed from the CGPS@TG stations and the BIGF scientific stations only. From North to South, the 16 active stations considered were Thurso (THUR), Inverness (INVE), Mallaig (MALG), Edinburgh (EDIN), Glasgow (GLAS), Newcastle (NEWC), Carlisle (CARL), Isle of Man North (IOMN), Isle of Man South (IOMS), Blackpool (BLAK), Leeds (LEED), Daresbury (DARE), Kings Lynn (KING), Droitwich (DROI), Vauxhall in West London (LOND) and Southampton (OSHQ).

A map showing the CGPS stations considered in the national study detailed in this Technical Report is given as Figure 3.3.

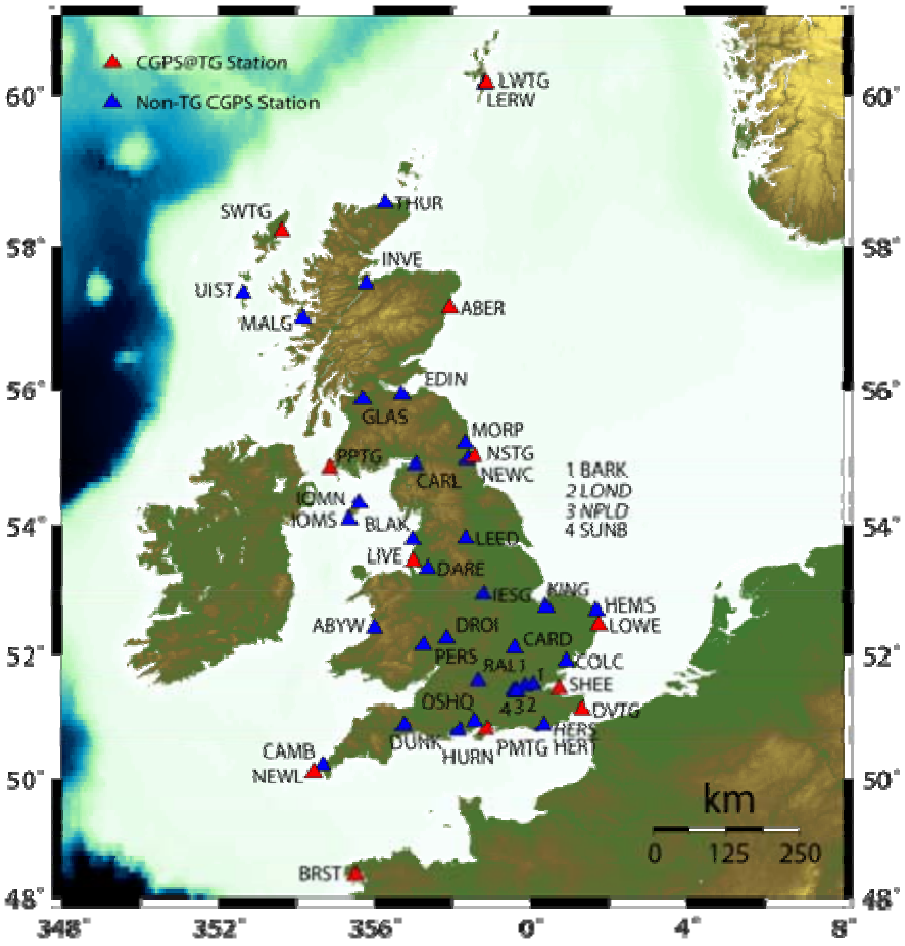

Figure 3.3 Map showing the CGPS stations in Great Britain and Northern France considered in the national study

In summary, therefore, a total of 44 CGPS stations in Great Britain and Northern France were considered in the national study detailed in this Technical Report: ten CGPS@TG stations in Great Britain, one CGPS@TG station in Northern France and 33 non-TG CGPS stations in Great Britain.

3.3.3 CGPS data used in the national study

For the national study, all archived data for the 44 CGPS stations identified in the previous subsection were collated for the period from the start of operation of the CGPS station to 31 December 2005. For each station these data consist of daily Receiver INdependent EXchange format (RINEX) observation data files and IGS-style log files (detailing any changes in the equipment at the site). To enable high accuracy positioning and GPS data processing in the manner described in Section 2.2, similar data for IGS stations on both a European and global scale were also collated.

A summary of the data availability for the CGPS stations is given in Table 3.6, which lists the stations in alphabetical order according to their 4-character station ID, and highlights the CGPS@TG stations.

Table 3.6 Data availability for the CGPS stations in Great Britain and Northern France used in the national study

Station name	4 character station ID	Start date of archived data (yyyy-mm-dd)	Approximate coordinate time series length for the period from the start of archived data to 2005-12-31 (years)	Approximate coordinate time series length for the period from 2000-01-01 to 2005-12-31 (years)
Aberdeen TG	ABER	1998-09-18	7.3	6.0
Aberystwyth	ABYW	1998-04-09	7.7	6.0
Barking Barrier	BARK	1997-04-25	8.7	6.0
Blackpool	BLAK	2002-01-02	4.0	4.0
Brest TG	BRST	1999-01-01	7.0	6.0
Camborne	CAMB	1998-04-09	7.7	6.0
Cardington	CARD	2003-01-12	3.0	3.0
Carlisle	CARL	2000-04-12	5.7	5.7
Daresbury	DARE	2000-04-10	5.7	5.7
Droitwich	DROI	2000-01-04	6.0	6.0
Dunkeswell	DUNK	2000-02-05	5.9	5.9
Dover TG	DVTG	2005-11-24	0.1	0.1
Edinburgh	EDIN	2000-03-16	5.8	5.8
Glasgow	GLAS	2000-03-15	5.8	5.8
Hemsby[1]	HEMS	1998-04-10	2.8	2.8
Herstmonceux	HERS	1997-04-27	8.7	6.0
Herstmonceux	HERT	2003-03-18	2.8	2.8
Hurn	HURN	2000-09-13	5.3	5.3
IESSG/Nott'm	IESG	1997-04-27	8.7	6.0
Inverness	INVE	2000-01-02	6.0	6.0
Isle of Man N	IOMN	2001-03-21	4.8	4.8
Isle of Man S	IOMS	2001-03-20	4.8	4.8
Kings Lynn	KING	2000-01-02	6.0	6.0
Leeds	LEED	2000-01-02	6.0	6.0
Lerwick	LERW	1998-04-18	7.7	6.0
Liverpool TG	LIVE	1999-02-04	6.9	6.9
Vauxhall/London	LOND	2000-01-02	6.0	6.0
Lowestoft TG	LOWE	1999-02-13	6.9	6.0
Lerwick TG	LWTG	2005-08-19	0.3	0.3
Mallaig	MALG	2002-02-04	3.9	3.9
Morpeth	MORP	1997-04-27	8.7	6.0
Newcastle	NEWC	2000-01-02	6.0	6.0
Newlyn TG	NEWL	1998-09-30	7.3	6.0
NPL/Teddington	NPLD	2000-08-15	5.4	5.4
N. Shields TG	NSTG	1998-06-29	7.5	6.0
Southampton	OSHQ	2000-01-02	6.0	6.0
Pershore	PERS	2001-05-09	4.6	4.6
Portsmouth TG	PMTG	2001-09-25	4.3	4.3
RAL/Oxfordshire	RAL1	2003-03-13	2.8	2.8
Sheerness TG	SHEE	1997-03-27	8.7	6.0
Sunbury Yard	SUNB	1997-04-09	8.7	6.0
Stornoway TG	SWTG	2005-09-02	0.3	0.3
Thurso	THUR	2000-05-09	5.6	5.6
South Uist	UIST	2005-01-21	0.9	0.9

[1] Hemsby (HEMS) ceased operation on 2001-01-26.

Table 3.6 gives the exact start date of archived data for each station and the approximate coordinate time series length when considering the period from the start of archived data up to 31 December 2005 and when considering the period from 1 January 2000 to 31 December 2005, which relate to the different data processing strategies and the results presented in Section 5.1.

At this stage, the significance of the non-TG CGPS station LERW must be mentioned. As stated previously, this is one of the ten scientific stations in BIGF which definitely meet the two criteria of having been operational for more than 4.5 years and being founded on solid rock or a stable structure connected to solid rock. LERW is about 5km from the CGPS@TG station LWTG and the Lerwick tide gauge on Shetland, but LWTG only has 0.3 years of data as oppose to the 7.7 years of LERW. As such, LERW has been used in the national study to compute an estimate for the changes in land level at the Lerwick tide gauge, on the assumption that the tide gauge, which is on a stone pier/breakwater, built in 1913, is well founded and therefore experiencing the same changes in land level as the solid rock on Shetland about 5km away. Clearly, the reliance on such an assumption is something that we have avoided as far as possible when establishing the CGPS@TG stations, where the GPS antennas are mounted on monuments, sited as close as possible to the tide gauge, i.e. within a few meters of the tide gauge itself; to fulfil the requirement to obtain site-specific, direct estimates of the changes in land level. However, considering the anomaly of Lerwick tide gauge being the only one in the British Isles which suggests a fall in sea level (of 0.79 or 1.09mm/yr), and the fact that this is contrary to the GIA model predictions of subsidence of Shetland (of 0.5 or 1.8mm/yr), it was considered very important to use LERW in the manner described above, at least until sufficient data is acquired for LWTG.

The data set described in this subsection and summarised in Table 3.6 was taken forward and used in Section 5.1, where estimates of changes in land level based on CGPS are presented as part of the deliverables from the national study detailed in this Technical Report.

3.4 The AG data set

As implied in the introduction to this chapter, AG has the potential to be used to obtain site-specific, direct estimates of current changes in land level that will enable a tide gauge to be better used for studying the climate related component of changes in sea level.

POL began to make AG measurements near the tide gauges at Newlyn and Aberdeen in 1995 and at Lerwick in 1996 (Williams et. al. 2001). All of the measurements made to date have been obtained with the FG5 absolute gravimeter instrument owned by POL (FG5-103). FG5-103 is also regularly inter-compared with other instruments in Europe and the USA in inter-comparison experiments.

In this section, the AG data set which has been acquired, as part of the national study detailed in this Technical Report, is detailed. The section starts with

details of the inter-comparison results then provides details on the establishment of three AG stations close to tide gauges in Great Britain, before giving the specifics of the AG data set used in the national study.

3.4.1 Inter-comparison results

When using AG for monitoring changes in land level it is important to ensure that the absolute gravimeter instrument being used continues to give results with a precision and accuracy commensurate with the highest international standards. The FG5 absolute gravimeter instrument owned by POL (FG5-103) has, therefore, been regularly compared with other absolute gravimeter instruments from around the world at fundamental gravity sites around the world. FG5-103 has been subject to inter-comparisons in 1997, 1999, 2001 and 2003. In 1997, inter-comparisons were made at Table Mountain Geophysical Observatory in the USA (TMGO), POL in the UK, Bad Homburg in Germany, and as part of the Intercomparison of Absolute Gravimeters (ICAG) experiment organised by the Bureau International des Poids et Mesures in Paris, France, every four years (Williams et. al. 2001). Further intercomparisons have since been made at TMGO in 1999 and 2003, as part of the ICAG2001 experiment and in 2003 at Walferdange in Luxembourg.

Figure 3.4 presents a summary of the results from all of the inter-comparisons involving FG5-103.

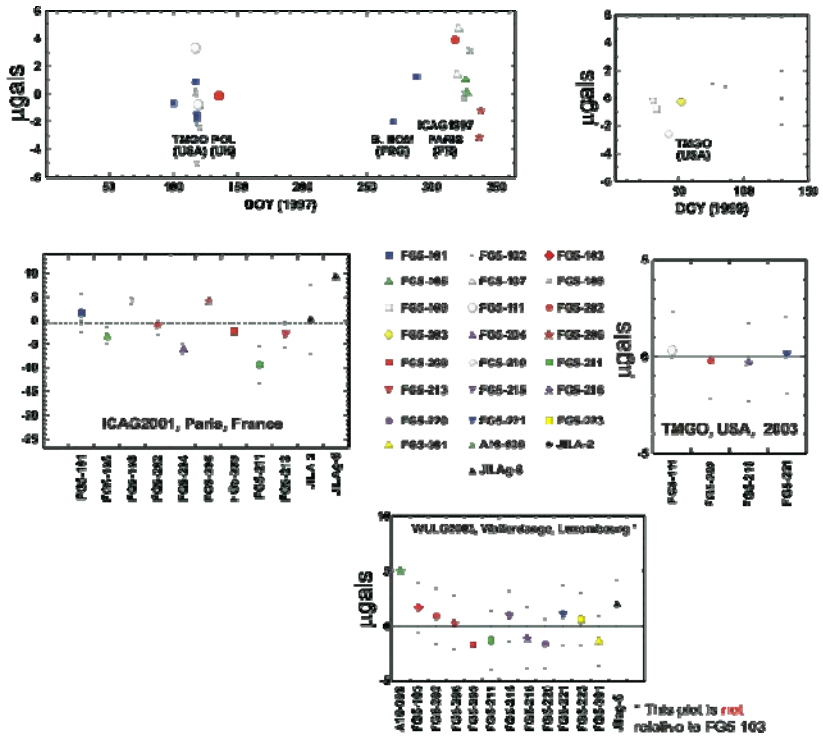

Figure 3.4 Results of the inter-comparison of the POL absolute gravimeter instrument FG5-103 with other instruments

In Figure 3.4, the first four sets of results are shown as values relative to FG5-103 and the last set of results as individual values relative to a mean. Before considering the individual results it is perhaps worth noting that a total of 22 FG5 absolute gravimeter instruments have taken part in the experiments over the period from 1997 to 2003, which is indicative of the sort of number of instruments in use throughout the world.

Considering Figure 3.4 in more detail it can be seen that in all of the experiments, the error bars are typically of the order of 1 to 2μgal and FG5-103 was shown to be in agreement with other FG5 absolute gravimeter instruments at the 1 to 2μgal level.

3.4.2 AG stations at tide gauges in Great Britain

As stated in the introduction to this section, POL began to make AG measurements near the tide gauges at Newlyn and Aberdeen in 1995 and at Lerwick in 1996 (Williams et. al. 2001). Considering the nature of AG measurements, it was decided to focus on three tide gauges and these three were selected based on: their geographical distribution; their representation of the expected changes in land level due to GIA, i.e. subsidence at Newlyn tide gauge near to Land's end in South-West England, uplift or no movement at Aberdeen in East Scotland and subsidence at Lerwick tide gauge on Shetland. Other things considered were: the fact that Newlyn and Lerwick tide gauges contribute to the Global Sea Level Observing System (GLOSS) coordinated by the Intergovernmental Oceanographic Commission (IOC); and Newlyn and Aberdeen both having long, high quality MSL time series (Williams et. al. 2001).

Considering each of the three tide gauges, a detailed reconnaissance was carried out in order to identify potential sites for the establishment of an AG station suitable for monitoring long term changes in land level. In this respect, the principle was for the AG station to be housed inside a building (to have a stable environment with no winds), which would ideally remain in place and unchanged over a long period of time, and be founded on solid rock (for both stability and to be representative of the changes in land level for the surrounding area). Furthermore, the AG station could not be too close to the coast, and certainly not at the tide gauge as for the CGPS@TG stations, as it would be near-impossible to model the direct mass attraction effect of the ocean tides.

Following the reconnaissance, suitable sites were identified for the AG stations and Figure 3.5 shows the location of the three AG stations and their relationship to the nearby tide gauge and CGPS stations.

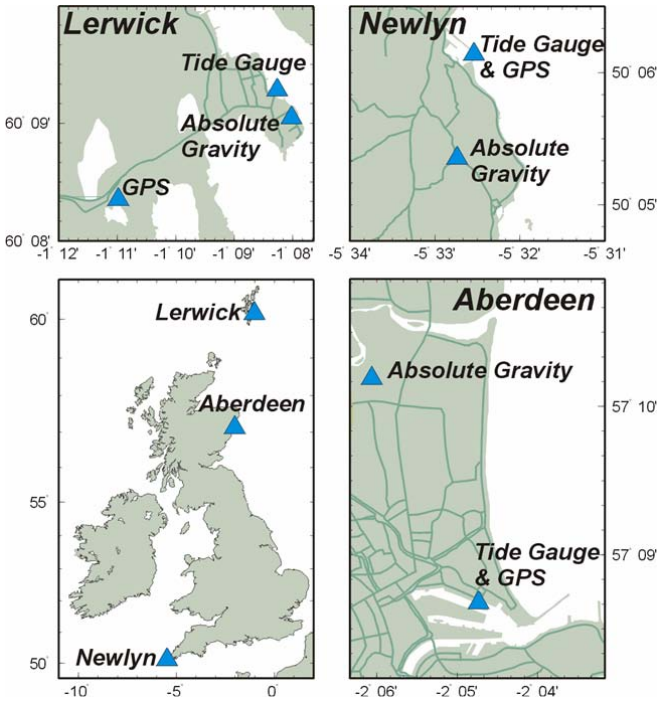

Figure 3.5 Map showing the AG stations in Great Britain considered in the national study

Lerwick AG station is located in the basement of a school, about 0.5km from the tide gauge and the CGPS@TG station LWTG and 5km from the non-TG CGPS station LERW; Aberdeen AG station is located in a church, about 3.2km from the tide gauge and the CGPS@TG station ABER; and Newlyn AG station is located in the church at Paul about 1.5km from the tide gauge and the CGPS@TG station NEWL.

3.4.3 AG data used in the national study

Since the FG5 absolute gravimeter instrument produces one complete set of drops per hour, with a value of absolute gravity obtained every 10 seconds, it is common practice to measure absolute gravity over a few hours or one day in order to compute a mean based on a large number of drops. The procedure adopted for the national study was to make near-annual, episodic AG measurements, with each set of measurements being carried out over at least three days, typically three to four days, and the absolute gravimeter instrument being carefully set up again at the start of each day. This not only produced significantly more data for a given 'field trip', but also allows a comparison of the standard deviations of the hourly means for each day with the variability from day to day, to enable an assessment of the noise in the measurements at each epoch of measurement (Williams et. al. 2001).

A summary of the data availability for the AG stations is given in Table 3.7.

Table 3.7 Data availability for the AG stations in Great Britain used in the national study

Station name	Start date of archived data (yyyy-mm)	End date of archived data (yyyy-mm)	Number of episodic AG measurements	Approximate absolute gravity time series length for the period of archived data (years)
Lerwick	1996-09	2006-08	10	9.9
Aberdeen	1995-05	2006-08	13	11.3
Newlyn	1995-10	2006-09	12	10.9

Table 3.7 gives the start and end date of archived data for each station, and the approximate absolute gravity time series length along with the number of near-annual episodic AG measurements made at each station. In this respect it can be noted that there were no measurements at Lerwick in 1997, there were two sets of measurements at Aberdeen in 1995, and there were no measurements at Newlyn in 1996 and 1999 but two sets of measurements in both 2000 and 2006.

The data set described in this subsection and summarised in Table 3.7 was taken forward and used in Section 5.2, where estimates of changes in land level based on AG are presented as part of the deliverables from the national study detailed in this Technical Report.

4. Background to the regional study

The Thames Region is linked into the national study through the CGPS@TG station SHEE at Sheerness tide gauge and the non-TG CGPS stations BARK and SUNB, at Barking Barrier and Sunbury Yard, all of which were initially established in 1997 through an EA/NERC CONNECT B project (Bingley et. al. 1999). This project also included the establishment of a number of EGPS stations in the Thames Region, to form a monitoring network of CGPS and EGPS stations designed by IESSG and BGS considering both the geodetic requirements and the geological setting of the Thames Region. Although Bingley et. al. (1999) published the initial results from this project, these only really served to confirm that no significant centimetric changes in land level were taking place in the Thames Region, apart from in areas where London Clay was at the surface, in which case, seasonal shrink-swell of the order of centimetres was observed. The relatively short GPS coordinate time series available through the EA/NERC CONNECT B project and the constraints imposed by the limited density of the monitoring network of CGPS and EGPS stations, encouraged EA to consider how best to extend this initial work in order to provide information to support planning for flood risk management for the Thames Estuary and River Thames, and led to the regional study detailed in this Technical Report.

In this chapter, published changes in sea level from Thames tide gauges are reviewed along with the geological setting of the Thames Region. The chapter then goes on to describe the tide gauge, GPS, PSI and geoscience data sets which have been acquired, as part of the regional study detailed in this Technical Report, in order to obtain direct estimates of current changes in land and sea levels for the Thames Region, the Thames Estuary and River Thames.

4.1 Published changes in sea level from Thames tide gauges

As implied in the introduction to Chapter 3, much of the evidence for changes in sea level for the past few decades/past century came from measurements obtained at tide gauges, which measure MSL with respect to a TGBM. As detailed in Section 3.1, a set of estimates of changes in sea level for a number of tide gauges in the British Isles for the period up to 1996 was published as Woodworth et. al. (1999). In terms of the Thames Estuary and River Thames, this included estimates for Sheerness, Southend, Tilbury and Tower Pier tide gauges, which were also considered in Woodworth and Jarvis (1991). However, these were by no means the first studies of the level of the Thames Estuary and River Thames.

Archaeological evidence indicates that the River Thames was not tidal in Roman times and occupation levels in London were at least 2 m below current high water level (Muir Wood 1990). Today the River Thames is tidal, as far upstream as Teddington, and over the last two centuries there has been an increased tidal range caused by a decrease in tidal friction in the Thames Estuary and River Thames. The removal of the Old London Bridge in 1830, which had always acted as a partial barrage, and the extensive dredging of the

River Thames, carried out in conjunction with the expansion of the London docks in the late 19th century, led to an increase in the tidal range from 4.6m in 1799 to 6.3 m in 1877 (Redman 1877, Muir Wood 1990). In a more recent study, Siggers et. al. (2006) reported that morphological changes in the Thames Estuary over the last century have led to an increase in the tidal range from Tower Pier upstream to Richmond, with mean spring tide range under low fluvial conditions predicted to have increased by up to 1.1m at Richmond.

In terms of tide gauges, a detailed examination of trends in the data from Southend and Tower Pier tide gauges was made by Rossiter (1969a, 1969b) using records of annual MHW, MLW, MHWI and MLWI for the period from 1934 to 1966 provided by PLA. A further examination of trends in the data from Southend, Tilbury, North Woolwich, Tower Pier, Chelsea and Richmond tide gauges for the period from 1931 to 1969 was made by Bowen (1972), with the inclusion of nodal modulation and mean river flow terms in the regression analysis. Following such studies made at that time, in 1978, the Thames tidal defences, including the Thames Barrier, were constructed to upgrade the protection of London and low-lying areas of Essex and Kent from flooding.

4.1.1 Changes in tidal parameters for the periods up to 1966 and 1969

A summary of the results of the regression analyses of Rossiter (1969a, 1969b) and Bowen (1972) are given in Tables 4.1 and 4.2.

Table 4.1 Estimates of changes in tidal parameters for Thames tide gauges for the period from 1934 to 1966 (Rossiter 1969a, 1969b)

Tide gauge	**Change in annual MHW and uncertainty (cm/cen)**	**Change in annual MLW and uncertainty (cm/cen)**	**Change in annual MTL and uncertainty (cm/cen)**	**Change in annual MTA and uncertainty (cm/cen)**
Southend	+36.3 ± 7.6	+24.9 ± 7.9	+31.1 ± 4.6	+5.2 ± 6.1
Tower Pier	+77.5 ± 11.6	+9.2 ± 8.9	+43.4 ± 8.2	+34.5 ± 7.0
Tide gauge	**Change in annual MHWI and uncertainty (mins/cen)**	**Change in annual MLWI and uncertainty (mins/cen)**	**Change in annual MI and uncertainty (mins/cen)**	**Change in annual MD and uncertainty (mins/cen)**
Southend	+0.2 ± 3.4	-4.4 ± 5.7	-1.9 ± 4.2	-4.6 ± 5.7
Tower Pier	-6.4 ± 4.7	-25.1 ± 5.6	-15.8 ± 5.0	-18.7 ± 4.0

As expected, considering the similar periods of data used by both Rossiter (1969a, 1969b) and Bowen (1972), the results for changes in annual MHW and annual MLW are in very good agreement for the Southend and Tower Pier tide gauges. The main observation from these results is that the difference between MHW and MLW at Southend and Tilbury tide gauges has increased by approximately 10cm/century (or 1mm/yr); whereas at Tower Pier tide gauge this difference has increased by 64 to 68cm/century (or 6.4 to 6.8mm/yr).

Table 4.2 Estimates of changes in tidal parameters for Thames tide gauges for the period from 1931 to 1969 (Bowen 1972)

Tide gauge	**Change in annual MHW and uncertainty (cm/cen)**	**Change in annual MLW and uncertainty (cm/cen)**		
Southend	+35.1 ± 4.3	+25.0 ± 4.6		
Tilbury	+38.1 ± 5.8	+27.7 ± 17.4		
Tower Pier	+68.0 ± 4.9	+4.3 ± 4.0		
Tide gauge	**Change in annual MHWS and uncertainty (cm/cen)**	**Change in annual MLWS and uncertainty (cm/cen)**	**Change in annual MTLS and uncertainty (cm/cen)**	**Change in annual MAS and uncertainty (cm/cen)**
Tower Pier	+75.8 ± 6.1	+2.4 ± 5.5	+41.1 ± 4.6	+38.7 ± 3.4
Tide gauge	**Change in annual MHWN and uncertainty (cm/cen)**	**Change in annual MLWN and uncertainty (cm/cen)**	**Change in annual MTLN and uncertainty (cm/cen)**	**Change in annual MAN and uncertainty (cm/cen)**
Tower Pier	+65.1 ± 6.4	+3.4 ± 4.3	+36.0 ± 4.3	+32.6 ± 3.4

The values of changes in annual MTL for Southend and Tower Pier tide gauges given by Rossiter (1969a, 1969b) are somewhat larger than the values of changes in annual MSL cited in Section 3.1 for a selection of British tide gauges at 31.1 and 43.4cm/century (or 3.11 and 4.34mm/yr) as oppose to 6.7 to 25.8cm/century (or 0.67 to 2.58mm/yr). However, considering the 33 year period used by Rossiter (1969a, 1969b) it is clearly possible that these values could be biased by up to 1mm/yr (see Subsection 3.1.1). Furthermore, it can be said that annual MTL can differ from the corresponding value of annual MSL by as much as the amplitude of the harmonic constant M_4, which can be up to 15cm in the Thames, which could also contribute to the difference in the corresponding trends.

The values presented in Tables 4.1 and 4.2 are taken forward and used in comparisons in Section 6.5, where new estimates of changes in tidal parameters are presented as part of the deliverables from the regional study detailed in this Technical Report.

4.1.2 Changes in sea level for the periods up to 1996 and 2005

A summary of the estimates of changes in sea level for a number of Thames tide gauges for the period up to 1996 (Woodworth et. al. 1999) and 2005 (PSMSL 2005) is given in Tables 4.3 and 4.4.

Table 4.3 Estimates of changes in sea level for Thames tide gauges for the period up to 1996 (Woodworth et. al. 1999)

Tide gauge	**Period of RLR data used**	**Number of complete years of RLR data used**	**Change in annual MSL and uncertainty (mm/yr)**
Sheerness	1901-1996	51	+2.14 ± 0.15
Southend	1933-1983	44	+1.22 ± 0.24
Tilbury	1961-1983	22	+1.58 ± 0.91

Table 4.4 Estimates of changes in sea level for Thames tide gauges for the period up to 2004 (PSMSL 2005)

Tide gauge	Period of RLR data used	Number of complete years of RLR data used	Change in annual MSL and uncertainty (mm/yr)
Sheerness	1834-2004	75	+1.64 ± 0.09
Southend	1933-1983	44	+1.22 ± 0.24
Tilbury	1961-1983	22	+1.58 ± 0.91

When comparing Tables 4.3 and 4.4, it should be noted that the revised estimates for Sheerness tide gauge are based on the inclusion of new RLR data for the period from 1997 to 2004 plus historical RLR data which move the start date of the MSL time series for this tide gauge back from 1901 to 1834; whereas the estimates for the Southend and Tilbury tide gauges are the same in both tables as no additional RLR data from these has been archived by the PSMSL since 1983.

From Tables 4.3 and 4.4, it is clear that the values for the Thames tide gauges are fairly consistent with the values for other British tide gauges, as given in Tables 3.1 and 3.2, in that they all show a rise in sea level over the past few decades/past century, with a range of values from 1.22mm/yr at Southend tide gauge to 1.64 or 2.14mm/yr at Sheerness tide gauge, with uncertainties of between 0.15 and 0.91mm/yr depending on the data used."

The values presented in Tables 4.3 and 4.4 are taken forward and used in comparisons in Section 6.5, where new estimates of changes in sea level are presented as part of the deliverables from the regional study detailed in this Technical Report.

4.2 The geological setting of the Thames Region

The geological setting of the Thames region was reviewed in Bingley et. al. (1999), and described more fully by Ellison et al. (2004). For the purposes of this Technical Report, the summary of potential rates of changes in land level in the Thames Region given as Table 1 in Bingley et. al. (1999) is re-presented in this section as Table 4.5.

The summary information given in Table 4.5 was based on a review of the geological processes operating in and around the region and their implications for current changes in land level. As stated in Bingley et. al. (1999): "Some of the processes involve displacement of the Earth's crust, others involve bulk volume changes with a largely vertical expression, yet others directly change the ground level by accretion or erosion. The processes operate within different time frames and over different geographical areas. Those leading to the displacement of the Earth's crust can be divided into tectonic and isostatic which in some instances are related. The bulk volume changes that may lead to ground level changes are of two contrasting types: hydrogeological, resulting from changes in the water table under Greater London, and geotechnical, concerning the behaviour of various deposits in response to natural and man-induced changes in soil geotechnical properties."

Table 4.5 Summary of potential rates of changes in land level in the Thames Region (Bingley et. al. 1999)

Cause	Effect	Potential rate of current changes in land level
Tectonic processes	Relatively uniform uplift with regional tilt and/or flexure [of the London basin]	+0.7 to +0.9mm/yr
Isostatic processes	Subsidence due to collapse of forebulge	negligible ?
Hydrogeological	Ground uplift due to rising groundwater	negligible ?
Geotechnical considerations	Natural compaction: lowering of areas underlain by alluvial clays and peats	-0.2 to -0.5 mm/yr ?
	Man-made compaction due to loading	-300 mm in 1 year -800 mm over 5 years
	Movement of ground where London Clay is at or close to the surface	up to 50 mm [seasonally]

Comparing the information given in Table 4.5 with the information given in Section 3.2, as part of the background to the national study, it is clear that:

- there is a slight discrepancy between the 'negligible ?' current changes in land level due to isostatic processes presented in Table 4.5 and the values of -0.2 or -0.5mm/yr for Sheerness tide gauge presented in Tables 3.3 and 3.4 based on the GIA models of Peltier (2001) and Lambeck and Johnston (1995) respectively.
- when considering Table 4.5, the two points in the Thames Region on Figure 3.2, which have values of -0.7 and -0.9mm/yr based on the geological studies of Shennan and Horton (2002), are most likely being affected by a combination of isostatic processes and natural compaction and not tectonic processes, based on their location.

The first point is of interest as it underlines the fact that Table 4.5 is not cast-in-stone and that the question marks and terms 'negligible ?' are there for a reason and reflect the difficulty in preparing such a general table. The second point further reinforces this and underlines the importance of considering the local geology when making interpretations of changes in land level; which is considered further in Section 4.4 when presenting the GPS data set and in Section 6.3 when analysing the combined GPS, AG and PSI results.

4.3 The tide gauge data set

The tide gauge data set used as part of the regional study detailed in this Technical Report comprised of all available and useful digital historical tide gauge records for the Thames Estuary and River Thames. These data were retrieved from various archives, and then quality controlled and validated, if necessary. Quality control and validation was carried out on data available from digital records for 1928-2003, already held by POL, and also on data available from digital records for 1988-2003 that were supplied by EA and PLA.

Quality control and validation of data was carried out by POL, using the POL graphical display program EDTEVA. EDTEVA is the principal program within the Tidal data, Editing, Visualisation and Analysis (TEVA) package. It is an interactive program which makes easy the graphical inspection and editing of tide gauge data. It allows the inter-comparison of the data and tidal predictions from several tide gauges so that records considered doubtful can be flagged and spikes corrected. In this respect, it was helpful that high quality data for the tide gauge at Sheerness, which is one of the 44 which form the national tide gauge network as part of the NTSLF, could be used as a reference.

4.3.1 POL held data

Quality controlled tide gauge data for Sheerness, for the period from 1952 onwards, was retrieved from BODC. This data is at hourly intervals up to 1992 and at 15 minute intervals thereafter. Furthermore, from 1993 onwards, two tide gauge devices have recorded at Sheerness, one providing a 'backup' for the principal channel to minimise gaps in the record. Raw tide gauge data for Richmond, Tower Pier, North Woolwich, Tilbury, Southend and Coryton were also subjected to quality control and validation as part of the regional study. A graphic illustration of the validated POL data is given in Figure 4.1.

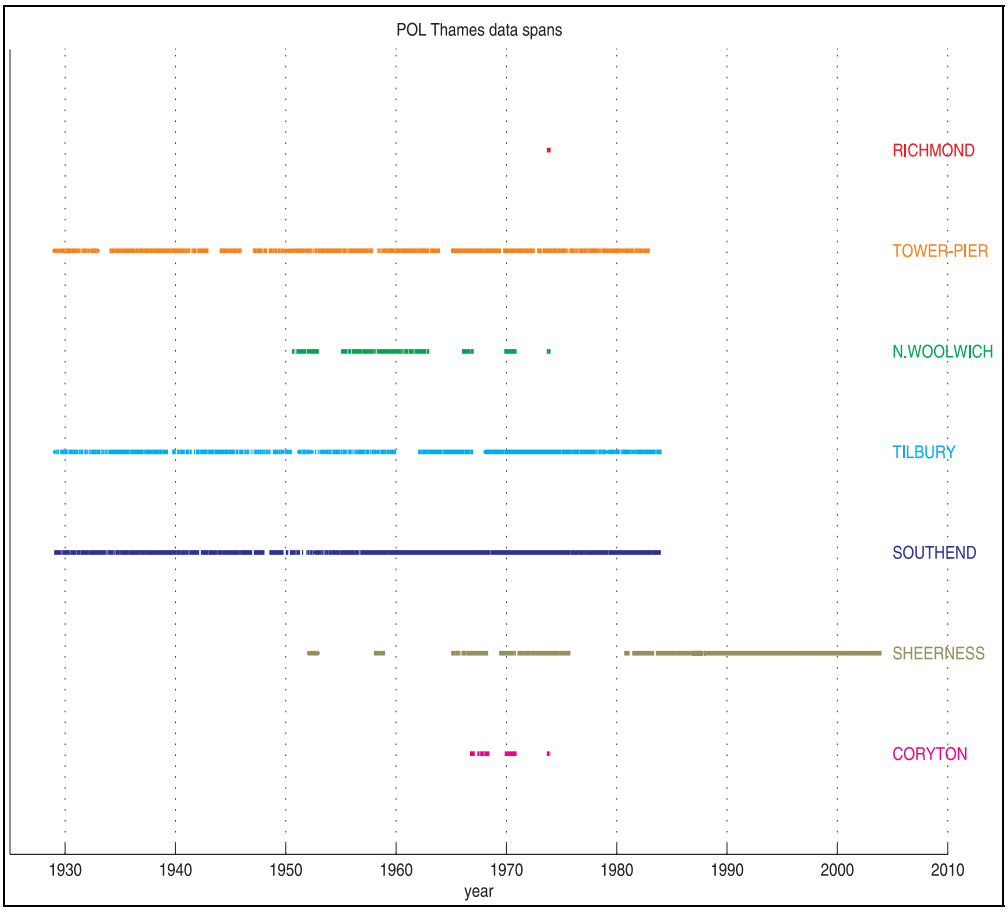

Figure 4.1 Validated POL data for tide gauges on the Thames Estuary and River Thames used in the regional study

As can be seen from Figure 4.1, the data held at POL is primarily data for the period from 1929 to 1982/3 for Tower Pier, Tilbury and Southend tide gauges on the Thames Estuary and River Thames, with data for the periods: 1951 to 1975 for North Woolwich tide gauge; 1952 to 2003 for Sheerness tide gauge; and 1966 to 1973 for Coryton tide gauge.

4.3.2 EA supplied data

To complement the data held by POL, data was provided to POL by EA on a CD containing all of the digital data that was available from 1988 to 2003 for ten tide gauges on the Thames Estuary and River Thames: Richmond, Chelsea, Westminster, Tower Pier, Charlton, Silvertown, Erith, Tilbury, Southend and Sheerness. Data for the majority of the tide gauges actually commenced in 1989 with the exception of Tower Pier, Charlton, Erith and Southend which commenced in 1988.

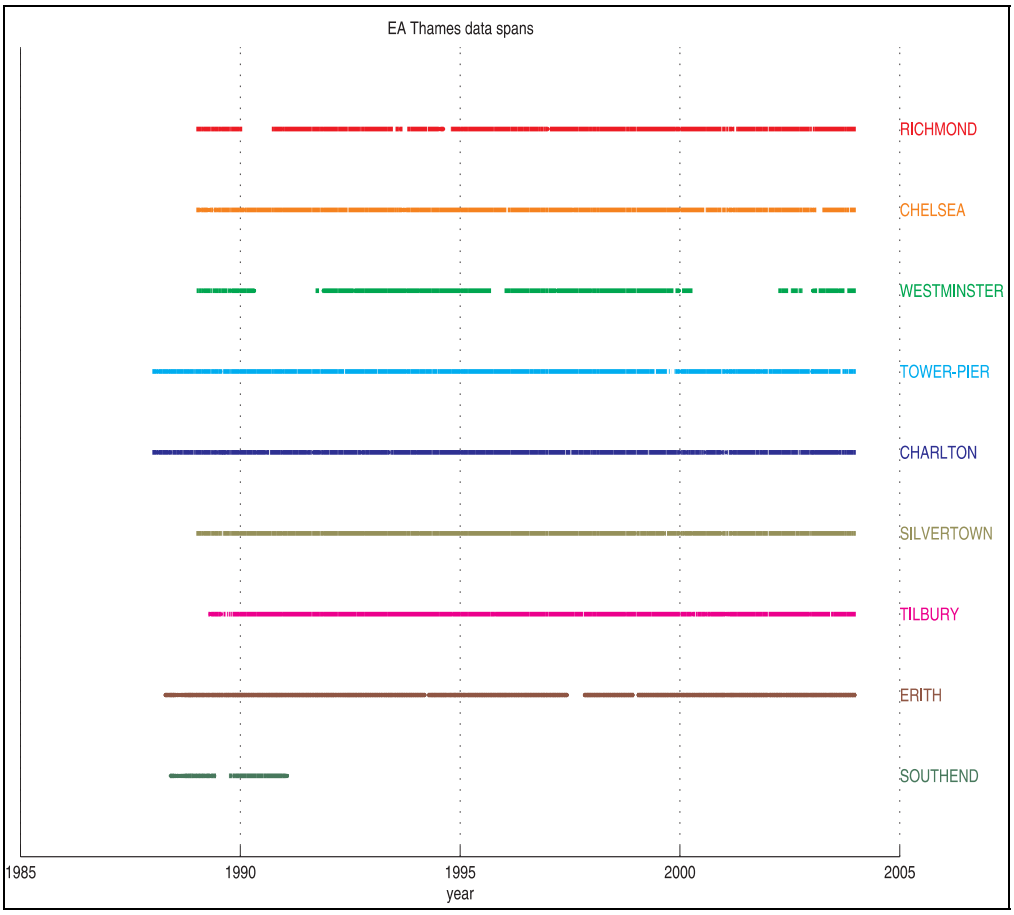

Figure 4.2 Validated EA data for tide gauges on the Thames Estuary and River Thames used in the regional study

To reduce the number of small gaps (two or less hours) of missing data, such gaps were first filled by interpolation, where possible, before using EDTEVA. This was not possible at Erith because the tide gauge dries out at low water on spring tides. Data for Southend tide gauge for the period from 1994 to 2003 was available from both EA and PLA gauges. On inspection, the PLA tide

gauge data was judged to be of a better quality so the only EA data for Southend that has been quality controlled and validated was that from 1988 to 1993. Furthermore, as data for Sheerness was already available from the tide gauge which is part of the national tide gauge network, the EA tide gauge data was only used to fill any gaps in the POL tide gauge data. A graphic illustration of the validated EA data is given in Figure 4.2.

4.3.3 PLA supplied data

Digital data from PLA tide gauges for the period from 1994 to 2003 was provided to POL for four tide gauges on the Thames Estuary and River Thames: Southend, Coryton, Margate and Walton.

As with the EA data, to reduce the number of small gaps (of two hours or less) of missing data, such gaps were first filled by interpolation, where possible, before using EDTEVA. Data from Southend and Coryton has been quality controlled and validated. Considerable further work would have been required for the validation of the Margate and Walton data and, as they were not specified in the contract, these have not been reviewed. A graphic illustration of the validated and non-validated PLA data is given in Figure 4.3.

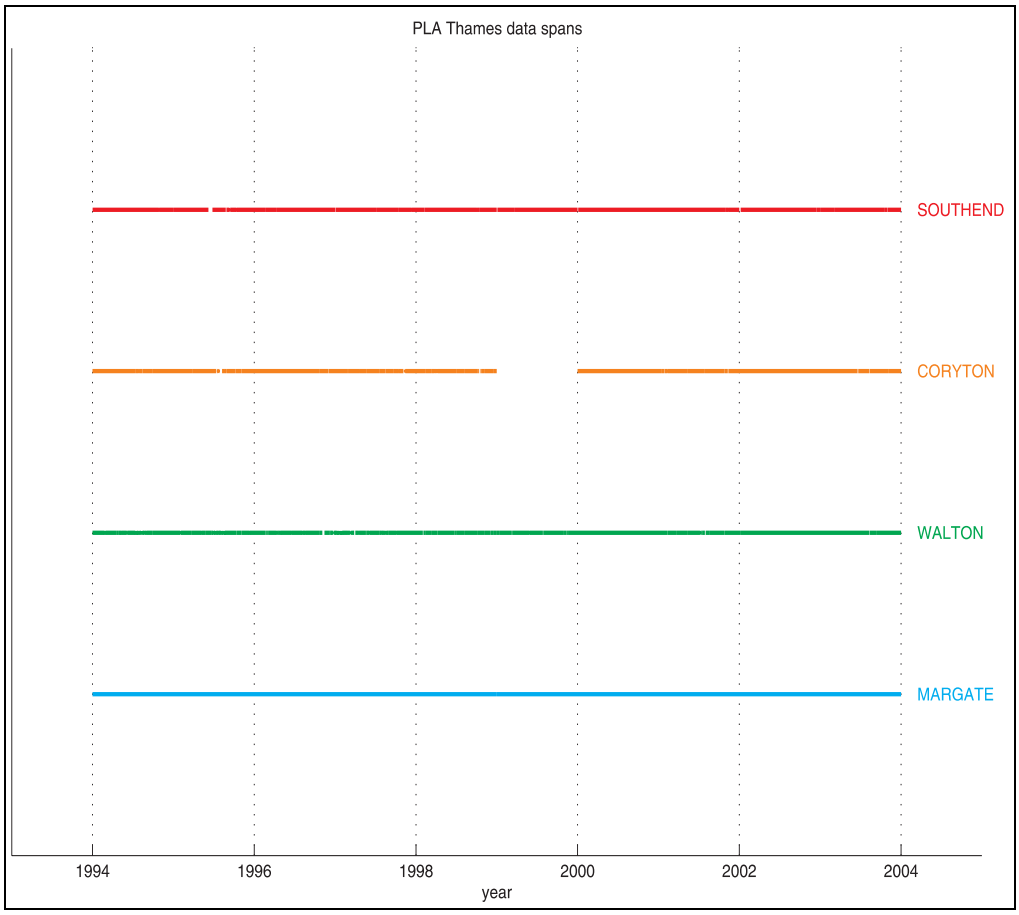

Figure 4.3 Validated and non-validated PLA data for tide gauges on the Thames Estuary and River Thames used in the regional study

4.3.4 The combined data set

The POL, EA and PLA tide gauge data described in the previous three subsections has been used to create a combined data set of quality controlled tide gauge data for the Thames Estuary and River Thames, as illustrated in Figure 4.4.

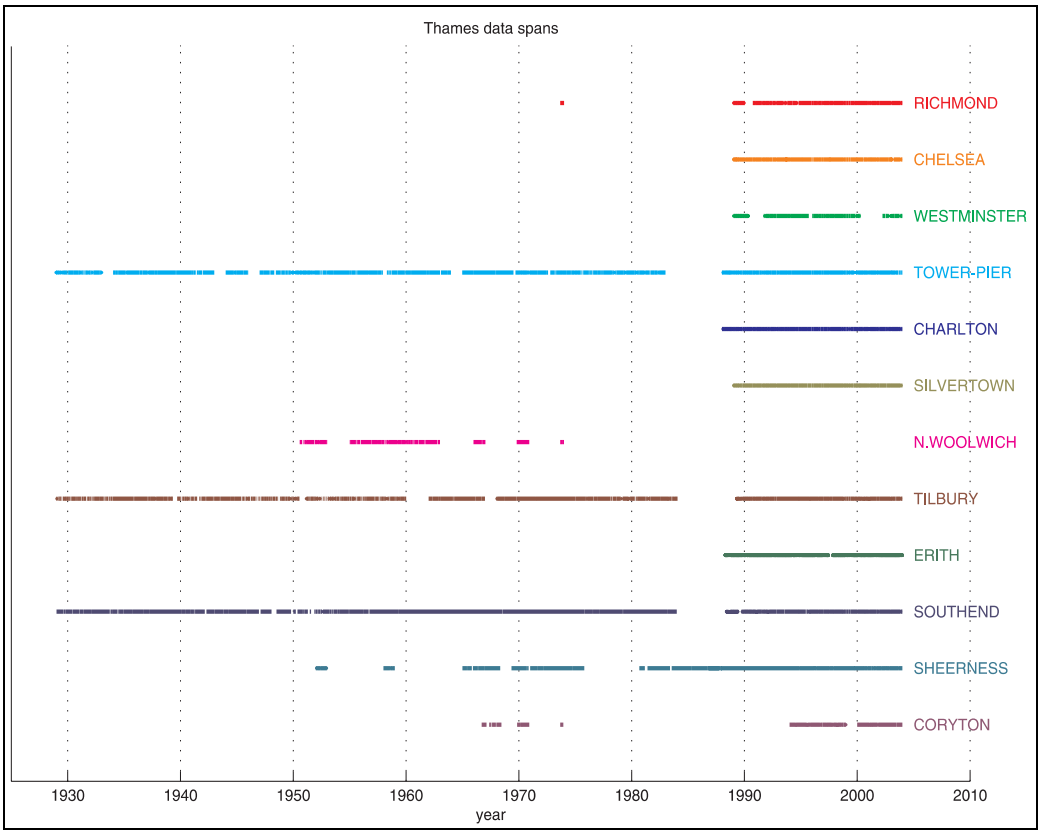

Figure 4.4 Validated data from POL, EA and PLA for tide gauges on the Thames Estuary and River Thames used in the regional study

The precise data spans for each tide gauge in the combined data set are detailed in the Project Record. Considering all of the data that has been quality controlled and validated, Appendix A summarises the amount of valid, interpolated, rejected and missing data available for the 12 tide gauges in the combined data set: Richmond, Chelsea, Westminster, Tower Pier, Charlton, Silvertown, North Woolwich, Erith, Tilbury, Southend, Sheerness and Coryton. Here it should be noted that the y-axes on these graphs differ, depending on the level of rejected or missing data, and the x-axes on these graphs differ, depending on the timespan of the data available.

When validating the data recorded after the installation of the Thames Barrier it was apparent that at times of closure, along with the expected reduction in high water heights, there was also an increase in low water heights. Figure 4.5 shows an example of the effect at Tower Pier tide gauge, following the closures of the Thames Barrier on 11-16 December 2000. From Figure 4.5, it can clearly be seen that the residual difference between the observed and predicted levels can oscillate for several days with a range of 1 to 2 metres. Such an effect will

clearly influence the estimates of any mean tidal parameters and, of course, limits the maximum height of the extreme level event.

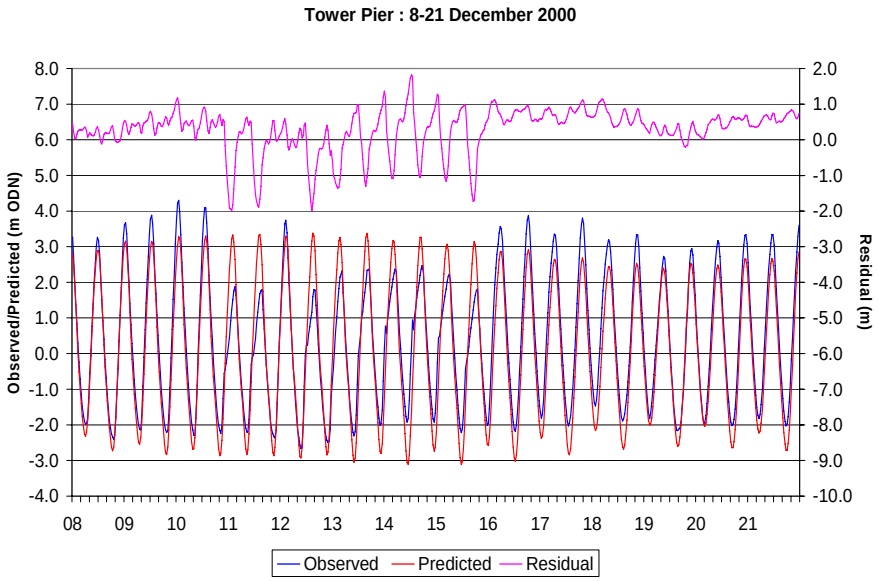

Figure 4.5 Residual surge at Tower Pier tide gauge following the operation of the Thames Barrier

Here it is important to note that although these effects were observed, and there have been many closures of the Thames Barrier during the period of observations considered, none of the affected data has been removed from the combined data set as, although there will be an affect on the monthly means, there will be less of an effect on the annual means and even less on any linear trends of changes in tidal parameters determined from several years of data. Of course, in the future, as the data period after the construction of the Thames Barrier is extended, it may be possible through further analysis to carry out more research into the effects of closures of the Thames Barrier at Tower Pier, but this would require more data and is beyond the scope of this study.

The combined data set of quality controlled tide gauge data has been taken forward and used in Section 6.5, where new estimates of changes in sea level and other tidal parameters are presented as part of the deliverables from the regional study detailed in this Technical Report.

4.4 The GPS data set

As stated in the introduction to this chapter, “the Thames Region is linked into the national study through the CGPS@TG station SHEE, at Sheerness tide gauge, and the non-TG CGPS stations BARK and SUNB, at Barking Barrier and Sunbury Yard, all of which were initially established in 1997 through an EA/NERC CONNECT B project (Bingley et. al. 1999).” Also stated in the introduction to this chapter was the fact that “this project also included the establishment of a number of EGPS stations in the Thames Region, to form a monitoring network of CGPS and EGPS stations which was designed by IESSG

and BGS considering both the geodetic requirements and the geological setting of the Thames Region."

In this section, the GPS data set which has been acquired, as part of the regional study detailed in this Technical Report, is described. The section starts with an overview of the establishment of the original monitoring network in the Thames Region and the early GPS measurements made for the period from 1997 to 1999, then provides details of the monitoring network of CGPS and EGPS stations used in the regional study, before giving the specifics of the GPS data set used in the regional study.

4.4.1 The original monitoring network of CGPS and EGPS stations in the Thames Region

The original monitoring network of CGPS and EGPS stations in the Thames Region was designed both to: provide estimates of changes in sea level (decoupled from changes in land level) at tide gauges on the Thames Estuary and River Thames; and determine the scale and trend of regional, sub-regional and local geological movements resulting from the processes summarised in Table 4.5. The geological input also aimed to ensure that the foundation conditions for all of the stations in the network were fully understood in terms of their suitability for long term geodetic monitoring.

In the earliest, desk study phase of the project a number of potential sites for the CGPS and EGPS stations were identified. During the period from April to August 1996, all of the proposed sites were visited in a series of field reconnaissances to confirm the site geology, check the condition and suitability of any existing monuments and check the suitability for GPS observations. Several of the proposed sites were discounted as a result of these visits. In addition, some compromises had to be made, particularly in the central and north-eastern part of the region where 'stable bedrock' is absent and the geology is predominantly London Clay. In these areas, the EGPS stations intended to be 'stable' were sited, wherever possible, on gravel deposits overlying the London Clay to mask its tendency to shrink-swell behaviour.

Following the field reconnaissances, the original monitoring network was designed comprising one CGPS@TG station, two non-TG CGPS stations, six 'EGPS@TG stations', eight 'regional monitoring EGPS stations' and eight 'local monitoring EGPS stations'. These are shown in Figure 4.6, which is duplicated from Figure 3 in Bingley et. al. (1999), and in which the CGPS stations are termed reference (COGR) stations, and in Table 4.6, which is an edited version of Table 2 given in Bingley et. al. (1999). In this table it is important to note that some of the stations have more than one role and are, therefore, listed twice.

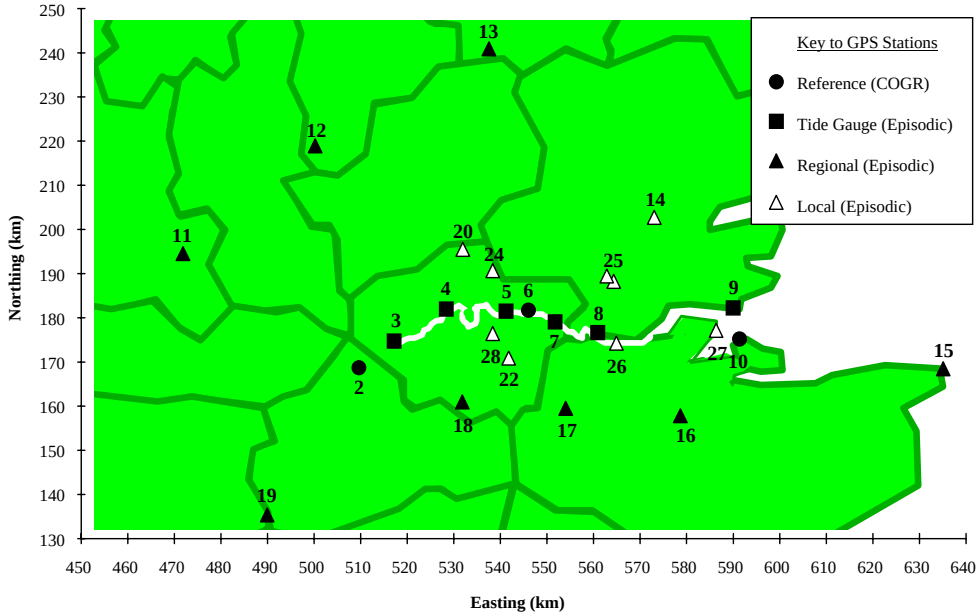

Figure 4.6 Schematic diagram of the original monitoring network of GPS stations in the Thames Region (Bingley et. al. 1999)

Table 4.6 Summary of geological considerations for the original monitoring network of GPS stations in the Thames Region (Bingley et. al. 1999)

Station role	Station name	Sta. ID	Sta. No.	Station geology	
				Formation	Lithology
CGPS	Sunbury Yard	SUNB	2	Alluvium	clay, silt, peat
	Barking Barrier	BARK	6	Upper Chalk	chalk
	Sheerness TG	SHEE	10	Alluvium ?	clay, silt, peat
Changes in sea level	Richmond TG	RICH	3	Alluvium ?	clay, silt, peat
	Tower Pier TG	TOPR	4	Alluvium ?	clay, silt, peat
	Silvertown TG	SILV	5	Upper Chalk	chalk
	Erith TG	ERIT	7	Upper Chalk	chalk
	Tilbury TG	TILB	8	Alluvium ?	clay, silt, peat
	Southend TG	SOPR	9	Alluvium ?	clay, silt, peat
	Sheerness TG	SHEE	10	Alluvium ?	clay, silt, peat
London basin tectonic activity	Shirburn Hill	SHHL	11	Upper Chalk	chalk
	Dunstable Downs	DUDO	12	Upper Chalk	chalk
	Heath Farm	HEFM	13	Upper Chalk	chalk
	Isle of Thanet	IOTH	15	Upper Chalk	chalk
	Thurnham	THUR	16	Upper Chalk	chalk
	Rowdow Hill	ROHL	17	Upper Chalk	chalk
	Riddlesdown	RIDD	18	Upper Chalk	chalk
	Hindhead	HIND	19	Hythe Beds	mainly sand
Greenwich Fault	Sundridge Park GC	SPGC	22	Thanet Formation	sand
	Greenwich Park	GRPK	28	Blackheath Beds	sand and gravel
Aquifer recharge	Bush Hill Park GC	BPGC	20	River Terrace	sand and gravel
	Mill Plane	MIPL	24	River Terrace	sand and gravel
Alluvial compaction	Tilbury TG	TILB	8	Alluvium ?	clay, silt, peat
	Southend TG	SOPR	9	Alluvium ?	clay, silt, peat
	Sheerness TG	SHEE	10	Alluvium ?	clay, silt, peat
	Gravesend Gr Sch	GGSC	26	Upper Chalk	chalk
	Grain	GRAI	27	River Terrace	sand and gravel
Shrink-swell	Mascalls	MASC	14	Claygate Beds	clay, sand
	Dunton Hills	DUHL	25	London Clay	clay

Of the 25 stations in the original monitoring network, nine were identified at sites with existing monuments considered acceptable for this project. This included one Ordnance Survey Fundamental Bench Mark, six Ordnance Survey triangulation pillars and two Ordnance Survey Surface Blocks. The other sixteen required new monuments to be installed. This included customised brackets on existing structures for the three CGPS stations, brass survey markers in existing concrete structures for the six EGPS@TG stations and Berntsen Survey Monuments (BSMs) for the other seven EGPS stations. During the period from July 1996 to February 1997 the preparations for the measurements were then completed through the establishment of the three CGPS stations, and the establishment of the EGPS stations, where necessary.

From March 1997 to July 1999, measurements were then made at the CGPS and EGPS stations. In order to detect, or mitigate, the effects of seasonal variations in land level, the schedule for the measurements was arranged so that each EGPS station was observed for one day, four times per year, on a three monthly basis. This placed some constraints on the measurements, and in order to allow sufficient time for travel between stations, the observation session length used was nine hours, from 0900 UT to 1800 UT (where UT is Universal Time). For the measurements, either a Trimble 4000 SSI or Ashtech Z-XII3 GPS receiver (both dual frequency) complete with a Dorne Margolin choke ring antenna were used. Most of the EGPS stations (numbers 3, 4, 5, 7, 11, 12, 13, 14, 15, 16, 17, 18, 19 and 25) were observed using a single 'roving' GPS receiver; whereas for some pairs of EGPS stations, that were only a few kilometres apart, namely station numbers 8 & 26, 9 & 27, 20 & 24, and 22 & 28, these were observed using two roving GPS receivers, to simultaneously record data at both stations on the same day. This resulted in each station having been observed at nine different epochs, at approximately three month intervals over a 2.25 year period. Although Bingley et. al. (1999) published the initial results from this data set, as far as the regional study detailed in this Technical Report is concerned, the most important thing is that the RINEX format observation data from these early EGPS measurements was archived in a standard manner, along with the CGPS data, for future re-processing and re-analysis.

4.4.2 The monitoring network of CGPS and EGPS stations used in the regional study

Prior to the start of the regional study, in early 2003, EA funded a sub-project for IESSG (through EA Contract Number 12396) to revisit the EGPS stations in the Thames Region and assess their suitability for continued use in the regional study and beyond.

For the regional study, IESSG proposed that a sub-set of 17 of the 25 stations used in the EA/NERC CONNECT B project should continue to be monitored through high accuracy positioning using GPS. This network of 17 stations was more focused on the Thames Estuary and River Thames and included all three CGPS stations, which had continued to operate uninterrupted over the time period between the end of the EA/NERC CONNECT B project and early 2003,

and 14 of the 22 EGPS stations. The locations of the proposed stations are shown in Figure 4.7.

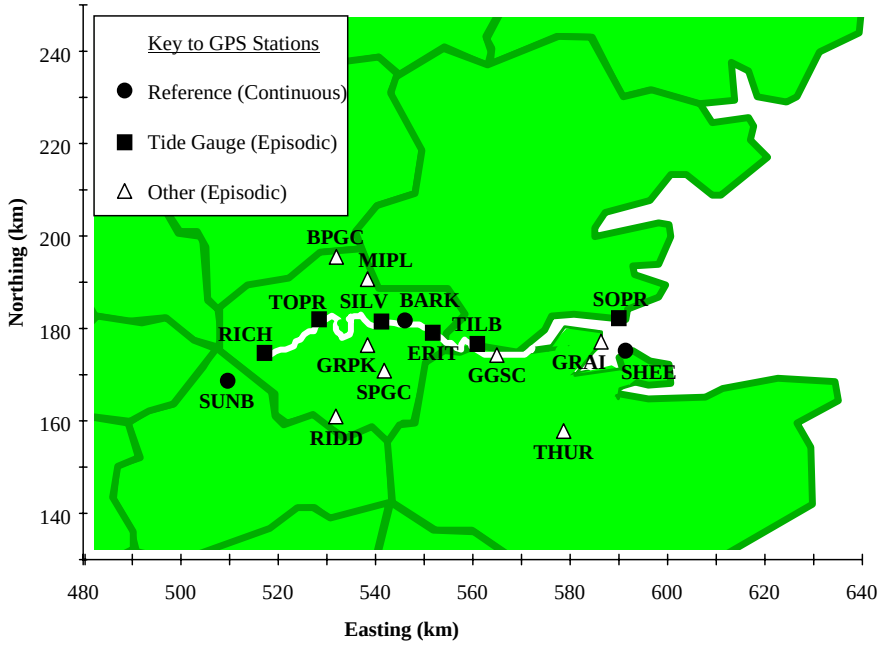

Figure 4.7 Schematic diagram of the proposed monitoring network of GPS stations to be used in the regional study

The 2003 sub-project essentially comprised three tasks, namely:

- Re-establish contact with landowners, where the existing 14 EGPS stations are located and investigate any changes which may affect the usability of any site.
- Carry out a set of nine-hour observations at each of the 14 EGPS stations, process and analyse the new data, re-analyse the archived data from the original set of nine episodic measurements and produce preliminary ITRF2000 coordinate time series for the combined data sets.
- Report to EA on
  - the condition and usability of each GPS station [and EA benchmark (EABM)], together with costed requirements for remedial actions.
  - any gross movements of the stations that may have occurred since the completion of the EA/NERC CONNECT B project.

In December 2002 and early January 2003, contact was re-established with the landowners for the 14 EGPS stations. Permission was sought to carry out a reconnaissance at each of the sites and, subject to the outcome of this, to carry out a further set of measurements at each of the EGPS stations.

The objective of the reconnaissance was to investigate any changes which may affect the usability of any of the stations. During the site visits, consideration was given to any factors that may have caused a disturbance to the station monument and any changes to the surrounding area that may affect the quality of the GPS signals. A summary of the reconnaissance is given in Table 4.7, in the form of brief comments on each of the 14 EGPS stations.

Table 4.7 Details of the 2003 reconnaissance of the 14 EGPS stations proposed for use in the regional study

Station name	4 char station ID	Comments on the condition and usability of the station
Richmond TG	RICH	At Richmond Lock, the EABM installed in 1990 and the GPS station installed in 1996 were both still in place, with no visible signs of disturbance. The only changes to the surrounding area were the growth of trees to the North-East of the GPS station.
Tower Pier TG	TOPR	At Tower Pier, the EABM installed in 1997 was still in place, with no visible signs of disturbance. However, the GPS station installed in 1996 had been destroyed during the re-construction of the river wall at the Tower of London.
Silvertown TG	SILV	The EABM installed in 1990 was not inspected as access to the Tate & Lyle Sugar Refinery was not arranged in advance. The GPS station installed in the Thames Barrier North Bank Compound in 1996 was still in place, with no visible signs of disturbance. Furthermore, no changes to the area surrounding the GPS station were observed.
Erith TG	ERIT	The EABM installed in 1990 is not currently accessible following the re-development of the pier at Erith in 1998. The EABM may still exist and only be covered by block paving, however, the block paving was not disturbed. The GPS station installed in 1996 was still in place, with no visible signs of disturbance. Furthermore, there were no changes to the surrounding area since the re-development of the pier.
Tilbury TG	TILB	At Tilbury Docks, the EABM installed in 1990 and the GPS station installed in 1996 were both still in place, with no visible signs of disturbance and no changes to the surrounding area observed.
Southend TG	SOPR	At Southend Pier major changes had taken place since 1999. Firstly, the EABM installed in 1990 had been destroyed during the installation of a security fence. The GPS station installed in 1996 was still in place, although its coordinates may have been affected by major re-construction work that is currently being carried out on the pier extension. During our site visit we witnessed a platform mounted crane being stabilised by driving the legs of the platform into the alluvium. The combined effect of the construction work on the pier extension and the platform mounted crane may have affected the absolute position of the pier extension, whose foundations are also piled into the alluvium.
Thurnham	THUR	At Thurnham, the GPS station installed in 1996 was still in place, with no visible signs of disturbance or changes to the surrounding area.
Riddlesdown	RIDD	At Riddlesdown Park, the GPS station was still in place, with no visible signs of disturbance and no apparent changes to the surrounding area.
Bush Hill	BPGC	At Bush Hill Park Golf Course, the GPS station installed in 1996 was still in place, with no visible signs of disturbance. The only changes to the surrounding area were the continued growth around the station.
Sundridge	SPGC	At Sundridge Park Golf Course, the GPS station installed in 1996 had been damaged and disturbed during major re-landscaping of the former practice area to create an artificial pond. As a result the GPS station was considered to have been effectively destroyed and unusable.
Mill Plane	MIPL	At Mill Plane, the GPS station installed in 1996 was still in place, with no visible signs of disturbance and no apparent changes to the surrounding area.
Gravesend	GGSC	At Gravesend Grammar School, the GPS station installed in 1996 was still in place, with no visible signs of disturbance and no apparent changes to the surrounding area.
Grain	GRAI	At Grain, the GPS station was still in place, with no visible signs of disturbance and no apparent changes to the surrounding area.
Greenwich Park	GRPK	At Greenwich Park, the GPS station installed in 1996 was still in place, with no visible signs of disturbance and no apparent changes to the surrounding area.

To supplement Tables 4.6 and 4.7, BGS and IESSG compiled the information given in Table 4.8, which describes the 'monument' (BSM or supporting structure) for the GPS station and considers elements of local geology which can be expected to influence the stability of the GPS station in a local context.

Table 4.8 Summary of local geological considerations for the CGPS and EGPS stations in the Thames Region used in the regional study

Station name	4 char station ID	'Monument'	Surface geology	Foundation geology	Stability factor
Barking Barrier	BARK	On West Tower of Barking Barrier	Alluvium / Tidal flat deposits	Chalk	'Stable'
Sheerness TG	SHEE	Adjacent to tide gauge, on a jetty	Alluvium / Tidal flat deposits	Terrace gravel?	Compressible Alluvium?
Sunbury Yard	SUNB	On a two-storey building	Alluvium	Alluvium	Compressible Alluvium
Bush Hill	BPGC	BSM, installed to a depth of ~3.8m	Terrace gravel	Terrace gravel	'Stable'
Erith TG	ERIT	Close to tide gauge, on a pier	Alluvium / Tidal flat deposits	Terrace gravel / Chalk	'Stable'
Gravesend	GGSC	BSM, installed to a depth of ~5.0m	Thanet Sand Formation	Chalk	'Stable'
Grain	GRAI	Ordnance Survey surface block	Terrace gravel	Terrace gravel	London Clay shrink-swell?
Greenwich Park	GRPK	BSM, installed to a depth of ~2.0m	Harwich Formation	Harwich Formation	'Stable'
Mill Plane	MIPL	BSM, installed to a depth of ~4.1m	Terrace gravel	London Clay	London Clay shrink-swell?
Richmond TG	RICH	On Richmond Lock, adjacent to tide gauge	Alluvium	Terrace gravel	'Stable'
Riddlesdown	RIDD	Ordnance Survey surface block	Chalk	Chalk	'Stable'
Silvertown TG	SILV	On Thames Barrier sea wall	Made ground / alluvium	Chalk	'Stable'
Southend TG	SOPR	On Southend Pier, close to tide gauge	Tidal flat deposits	Terrace gravel / London Clay	'Stable'
Thurnham	THUR	On open ground on the North Downs	Chalk	Chalk	'Stable'
Tilbury TG	TILB	Adjacent to tide gauge in Tilbury Docks	Made ground / Alluvium	Made ground / Alluvium	Compressible Alluvium
Tower Pier TG	TOPR	On sea wall within Tower of London	Made ground / Alluvium	Made ground / Alluvium	Compressible Alluvium

In Table 4.8, it should be noted that ‘stable’ means stable in a local context, i.e. these stations are still subject to regional instability.

As a result of the 2003 reconnaissance, 12 of the 14 EGPS stations were accepted for use in the regional study and more long term monitoring, such that the map of stations selected for use in the regional study is given in Figure 4.8.

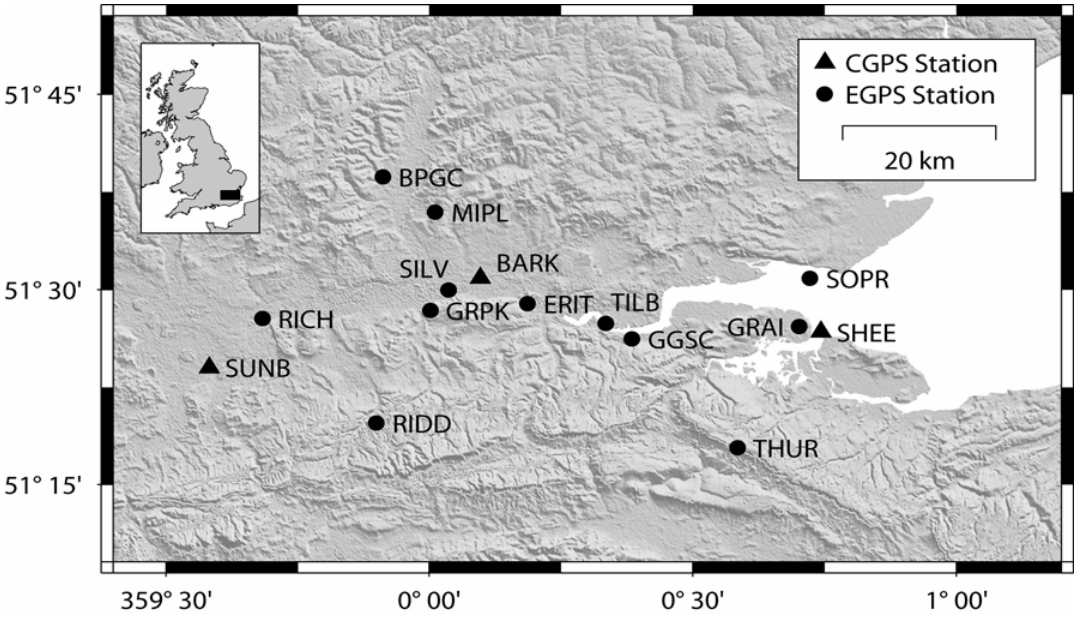

Figure 4.8 Map showing the CGPS and EGPS stations in the Thames Region considered in the regional study

In the context of the second task of the 2003 sub-project, a set of 8-hour observation sessions were made at each of the 12 EGPS stations in February 2003, and these new data were processed and analysed along with a re-analysis of the archived data from the original set of nine EGPS measurements. Based on this processing and analysis, the report to EA contained the following conclusions relating to whether any gross movements of the stations may have occurred since the completion of the EA/NERC CONNECT B project:

- 11 of the 12 EGPS stations do not appear to have experienced any significant movements and high quality GPS observations are still possible at these stations.
- At Southend Pier, the GPS station (SOPR) appears to have risen by 5cm since the completion of the EA/NERC CONNECT B project, which may be due to the effects of the major re-construction work that is currently being carried out on the pier extension, but it is not possible to make any conclusions on this until more episodic GPS measurements are made.

The RINEX format observation data from the February 2003 EGPS measurements were then archived in a standard manner, along with the data from the earlier EGPS measurements and the corresponding CGPS data, for future re-processing and re-analysis.

Following this, as part of the regional study, from July 2004 to December 2005, six further sets of EGPS measurements were made at the 12 EGPS stations.

These were again based on 8-hour observation sessions and comprised one in July 2004 and then one approximately every two months from March to December 2005 inclusive (March, May, July, October and December 2005). For the measurements, the stations were observed as pairs of EGPS stations (RIDD & RICH, GRPK & SILV, MIPL & BPGC, GGSC & TILB, GRAI & SOPR, and ERIT & THUR) using two roving GPS receivers (two Ashtech Z-XII3 dual-frequency GPS receivers complete with Dorne Margolin choke ring antennas) to simultaneously record data at both stations on the same day. The RINEX format observation data from these EGPS measurements were then archived in a standard manner, along with the data from the earlier EGPS measurements and the corresponding CGPS data, for processing and analysis and future re-processing and re-analysis, if required.

4.4.3 GPS data used in the regional study

For the regional study, all archived data for the three CGPS stations, the 12 EGPS stations identified in the previous subsection, and the EGPS@TG station at Tower Pier tide gauge were collated for the period from the start of operation of the CGPS stations to 31 December 2005. For each CGPS station these data consist of daily RINEX observation data files and IGS-style log files (detailing any changes in the equipment at the site) and for each EGPS station these data consist of episodic RINEX observation data files and field booking sheets (detailing the equipment used at each site and the antenna height from the survey marker to the antenna reference point for each set up).

A summary of the data availability for the CGPS and EGPS stations is given in Tables 4.9 and 4.10, which list the stations in alphabetical order according to their 4-character station ID, and highlight the CGPS@TG and EGPS@TG stations.

Table 4.9 Data availability for the CGPS stations in the Thames Region used in the regional study

Station name	4 char station ID	Start and end date of archived data (yyyy-mm-dd to yyyy-mm-dd)		Approximate coordinate time series length for the period of archived data (years)
Barking Barrier	BARK	1997-04-25 to 2005-12-31		8.7
Sheerness TG	SHEE	1997-03-27 to 2005-12-31		8.7
Sunbury Yard	SUNB	1997-04-09 to 2005-12-31		8.7

Tables 4.9 and 4.10 give the exact start and end date of archived data for each station and the approximate coordinate time series length when considering the period from the start of archived data up to 31 December 2005 for the CGPS stations and when considering the period from the start to end of archived data for the EGPS stations.

Table 4.10 Data availability for the EGPS stations in the Thames Region used in the regional study

Station name	4 char station ID	Start and end date of archived data (yyyy-mm-dd to yyyy-mm-dd)	No. of EGPS meas.	Approximate coordinate time series length for the period of archived data (years)
Bush Hill	BPGC	1997-06-23 to 2005-12-08	16	8.5
Erith TG	ERIT	1997-05-22 to 2005-12-15	16	8.5
Gravesend	GGSC	1997-06-27 to 2005-12-13	16	8.5
Grain	GRAI	1997-06-26 to 2005-12-14	16	8.5
Greenwich Park	GRPK	1997-06-24 to 2005-12-07	16	8.5
Mill Plane	MIPL	1997-06-23 to 2005-12-08	16	8.5
Richmond TG	RICH	1997-04-29 to 2005-12-06	16	8.6
Riddlesdown	RIDD	1997-04-30 to 2005-12-06	16	8.6
Silvertown TG	SILV	1997-05-21 to 2005-12-07	16	8.5
Southend TG	SOPR	1997-06-26 to 2005-12-14	15	8.5
Thurnham	THUR	1997-06-25 to 2005-12-15	16	8.5
Tilbury TG	TILB	1997-06-27 to 2005-12-13	16	8.5
Tower Pier TG	TOPR	1997-05-08 to 1999-04-29	9	2.0

The data set described in this subsection and summarised in Tables 4.9 and 4.10 was taken forward and used in Section 6.2, where estimates of changes in land level based on EGPS are presented as part of the deliverables from the regional study detailed in this Technical Report.

4.5 The PSI data set

As stated in the introduction to this chapter, “the relatively short GPS coordinate time series available through the EA/NERC CONNECT B project and the constraints imposed by the limited density of the monitoring network of CGPS and EGPS stations, encouraged EA to consider how best to extend this initial work in order to provide information to support planning for flood risk management for the Thames Estuary and River Thames.”

In addition to extending the coordinate time series for the three CGPS stations and 12 EGPS stations, as detailed in Section 4.1, the other method of ‘extending the initial work’ in order to provide information to support planning for flood risk management for the Thames Estuary and River Thames was through the use of PSI. The intention being to process and analyse all archived SAR data, for the period from March 1997 to December 2005, for an area of interest (AOI) within the Thames Region, using the PSI technique.

The AOI was agreed as being approximately 95x55km (5,323km^2 to be precise), centred on the Thames Estuary and River Thames and encompassing all of the CGPS and EGPS stations. The 100x100km footprint for the descending SAR scene (yellow square) and the 95x55km AOI (red rectangle) that formed the basis of the PSI data set considered in the regional study are shown in Figure 4.9.

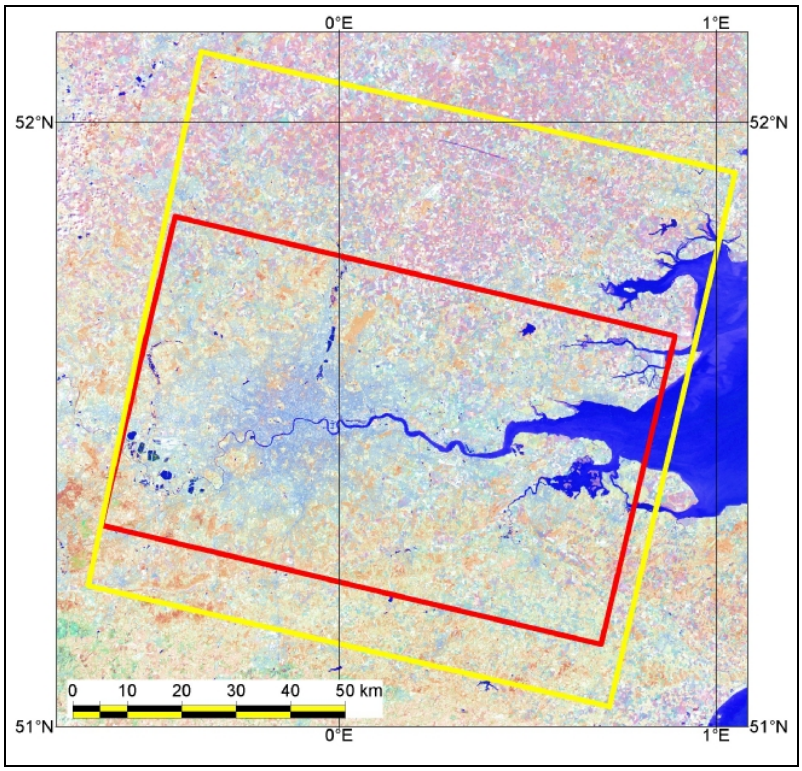

Figure 4.9 Map of the 100x100km ERS footprint and the 95x55km AOI that formed the basis of the PSI data set considered in the regional study

Based on this AOI, 82 descending ERS and ENVISAT SAR scenes (Track 51, Frame 2565) spanning nearly nine years (March 1997 to December 2005) were acquired by NPA for processing and analysis. This effectively equated to all useable ERS SAR data from March 1997 to December 2005 and all useable ENVISAT ASAR data from December 2002 to December 2005 for the AOI.

A list of the 82 scenes is given in Table 4.10 along with statistics on their perpendicular baseline and temporal separation with respect to a master image (against which all measurements are relative to in the PSI processing), which is highlighted in red. The scenes that were found to be unprocessable are shaded and the ENVISAT scene highlighted in blue is the scene used for the ERS/ENVISAT integration, which does not form part of the final results.

Table 4.11 shows that out of 82 scenes, 60 (73%) could be processed successfully. The 22 that were not processed were either due to: high Doppler Centroid values making them unsuitable for full PSI processing; poor ERS-2 data after February 2000 (the pointing control of ERS-2 was compromised from February 2000 when one gyro failed on the satellite and since then some scenes need to be discarded due to reduced pointing accuracy); or, in the case of ENVISAT, scenes which did not cover the entire AOI.

Table 4.11 Summary of the ERS and ENVISAT data used in the PSI processing and analysis for the regional study

Sat	Date	Perpendic-ular Baseline (m)	Temp-oral sep-aration (days)	Sat	Date	Perpendic-ular Baseline (m)	Temp-oral sep-aration (days)
ERS-1	19970313	270.23	-1016	ERS-2	20010706	554.70	560
ERS-2	19970314	141.63	-1015	ERS-2	20010810	1172.48	595
ERS-2	19970418	614.16	-980	ERS-2	20011019		
ERS-2	19970523	-68.11	-945	ERS-2	20011228	-1087.43	735
ERS-2	19970627	-101.49	-910	ERS-2	20020517		
ERS-2	19970801	5.24	-875	ERS-2	20020726	186.06	945
ERS-2	19970905	512.15	-840	ERS-2	20021004	286.81	1015
ERS-1	19971009	152.31	-806	ERS-2	20021213	-516.28	1085
ERS-2	19971010	353.76	-805	ERS-2	20030117	2.60	1120
ERS-2	19971114	29.44	-770	ERS-2	20030221	296.28	1155
ERS-2	19971219	-90.78	-735	ERS-2	20030502	-49.66	1225
ERS-2	19980123	-222.44	-700	ERS-2	20030606		
ERS-2	19980227	-899.43	-665	ERS-2	20030711	-396.05	1295
ERS-2	19980508	592.25	-595	ERS-2	20030815	394.50	1330
ERS-2	19980612	903.92	-560	ERS-2	20030919	882.96	1365
ERS-2	19980717	-712.37	-525	ERS-2	20031024	354.44	1400
ERS-2	19980821	-525.37	-490	ERS-2	20031128	-1365.32	1435
ERS-2	19980925	455.85	-455	ERS-2	20040206		
ERS-2	19981204	-412.32	-385	ERS-2	20040416		
ERS-2	19990108	-1016.41	-350	ERS-2	20040625	125.25	1645
ERS-2	19990319	27.86	-280	ERS-2	20040730		
ERS-2	19990423	71.60	-245	ENVISAT	20021213	620.21	1085
ERS-2	19990528	543.21	-210	ENVISAT	20030502	1294.85	1225
ERS-2	19990702	212.31	-175	ENVISAT	20030606	-859.95	1260
ERS-2	19990806	489.19	-140	ENVISAT	20030815	-731.43	1330
ERS-2	19990910	-646.37	-105	ENVISAT	20031024	764.14	1400
ERS-2	19991224	0	0	ENVISAT	20040102	560.82	1470
ERS-1	20000127	-146.86	34	ENVISAT	20040416	-17.39	1575
ERS-2	20000128	-4.36	35	ENVISAT	20040521	158.36	1610
ERS-2	20000303	-589.27	70	ENVISAT	20040730	216.83	1680
ERS-2	20000407	-95.10	105	ENVISAT	20041008	34.86	1750
ERS-2	20000512	1039.62	140	ENVISAT	20041112	-607.04	1785
ERS-2	20000616	-279.68	175	ENVISAT	20041217	59.08	1820
ERS-2	20000721			ENVISAT	20050121	-318.22	1855
ERS-2	20000825			ENVISAT	20050225	-8.53	1890
ERS-2	20001103	-34.51	315	ENVISAT	20050506	474.03	1960
ERS-2	20001208			ENVISAT	20050610	-142.50	1995
ERS-2	20010112	208.39	385	ENVISAT	20050715	739.70	2030
ERS-2	20010323			ENVISAT	20050819	318.26	2065
ERS-2	20010427			ENVISAT	20051028	402.02	2135
ERS-2	20010601			ENVISAT	20051202	-54.24	2170

The data set described in this section and summarised in Table 4.11 was taken forward and used in Sections 6.1 and 6.3, where estimates of changes in land level based on PSI are presented as part of the deliverables from the regional study detailed in this Technical Report.

4.6 The geoscience data sets

Section 4.2 gave an introduction to the geological setting of the Thames Region and, in Section 4.4, the geological information considered during the establishment and continued use of the CGPS and EGPS stations in the Thames Region was discussed.

Unlike GPS, it is clear from Section 2.4 that PS points are not selected in advance but are identified as part of the PSI processing and their exact location and nature are not known. However, this is countered by the fact that for the regional study, the changes in land level would be based on a relatively small number of CGPS and EGPS stations (16 in total) and a massive number of PS points (several hundred thousand for the AOI).

Considering the geological setting and the various processes that affect changes in land level in the Thames Region along with the anticipated spatial density of the PS points within the AOI, specific geoscience data sets were used by BGS to enable the geological interpretation of any changes in land level, as part of the regional study detailed in this Technical Report. These data sets include digital geological and geohazard maps, data on the thickness of Holocene deposits and of peat, regional groundwater level data and geophysical data, and are described in this section.

4.6.1 Digital geological maps and geohazard data

DiGMapGB50 is a digital geological map based on the published BGS 1:50,000 scale geological map sheets. For DiGMapGB50, the geological information shown on the paper maps has been digitised under five themes, each of which can be displayed individually or in combination with other themes. These are:

1. Bedrock formations (pre-Quaternary deposits).
2. Superficial deposits (Quaternary-aged deposits).
3. Artificially modified ground (mainly worked ground, made ground or infilled ground).
4. Mass movement deposits (landslide deposits).
5. Geological lines (mainly faults).

Geohazard data from GeoSure are derived geological datasets, prepared by BGS, based largely on ArcMap9.1 Geographical Information System (GIS) analysis of DiGMapGB50, in combination with other datasets such as a high-precision digital terrain model (DTM) and known physical properties of individual formations or deposits. They help predict local susceptibility to ground movement as a consequence of six major natural geological hazards:

- Shrink-swell clays - the propensity of clay-rich subsoils to change volume with changes in moisture content;
- Compressible ground - the propensity of the ground to undergo a volume reduction under load;
- Collapsible ground - the possible presence of metastable soil structures associated with ‘brickearth’ deposits, liable to abrupt collapse under load when water-saturated;

- Dissolution - the propensity for subsidence associated with water-soluble rocks (limestones, gypsum, halite). In this region, the hazard is associated only with the Chalk;
- Running sand - the propensity for water-saturated sand to flow into boreholes or excavations;
- Slope stability - the propensity for landslip formation.

4.6.2 3-D Models of Holocene and Peat thickness

BGS used two 3-D models of Holocene thickness for the Thames Region, which can be referred to as 1997 and 2006. Both models represent the thickness of Holocene (late Quaternary) deposits (comprising alluvium, peat, tidal flat deposits, etc.) in parts of London, the Thames Estuary and River Thames. The 1997 model is derived from part of the 'geological database', created by BGS as part of the EA/NERC CONNECT B project (Bingley et. al. 1999). The model represents the difference in height between the base of the Holocene (as modelled in three dimensions using borehole records) and the land surface, or sea level. The 2006 model was created for a project within the current BGS strategic programme. In contrast to the 1997 model, it represents the difference in height between the base of the Holocene as modelled in three dimensions using borehole records (a different set to that used previously) and either the land surface or the river bed.

Holocene deposits tend to compress, either under their own weight (natural consolidation) or under a superimposed load (typically either made ground, built structures, or flood water). Peat is by far the most compressible material found in Holocene deposits. For the regional study, data for the thickness of peat present in the Thames alluvium were extracted from borehole records. For this, two sets of records were used: those encoded as part of the EA/NERC CONNECT B project (which form another part of the geological database), and those held within the BGS corporate database 'Borehole Geology' up to 15 August 2006. Some of the data appears in both datasets, so they were combined.

4.6.3 Regional groundwater level data

When water is extracted from the ground (for public water supply, for example), the ground surface tends to subside as the water table falls. If the water table recovers, then some uplift of the ground surface can be expected, but only by up to about 10% of the subsidence (Freeze and Cherry 1979).

Since 1991, EA has published an annual report on changing groundwater levels in the Chalk-Thanet Sand aquifer in the central London basin. Each report includes a contour map showing groundwater levels for January of the year of the report, derived from observations in water boreholes, together with a short discussion of the observed changes. Figure 4.10 presents an example of a map for January 1997, which has contours at 10 metre intervals and where the dark stipple indicates outcrop of Palaeogene deposits older than the London

Clay and the Chalk crops out in the areas to the north-west and south-east of the stippled areas

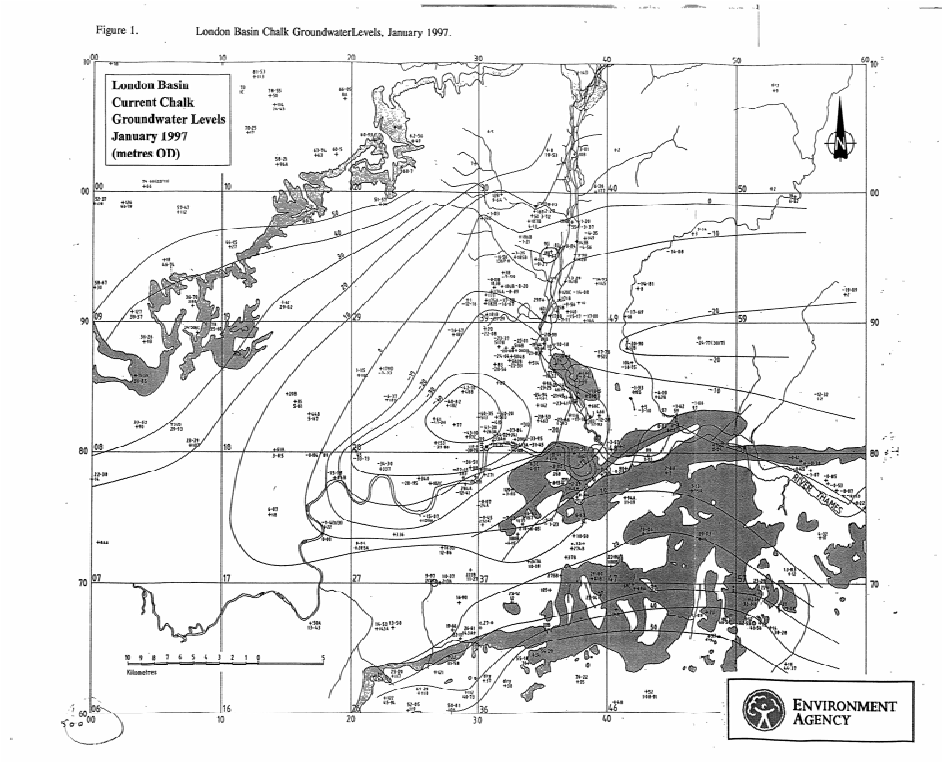

Figure 4.10 Example of an EA groundwater level map for the London Basin: January 1997

For the regional study, the EA maps for January 2006 and January 1997 were each obtained as a digital grid, and the older data was subtracted from the younger. The resultant grid thus represents the overall change in groundwater level during a period approximately corresponding to the period of the GPS and PSI data sets. Here it should be noted that this data does not take account of minor aquifers in the superficial deposits; however, it is felt that the variations of groundwater level within these minor aquifers are likely to show little, if any, net change over the period of the project.

4.6.4 Geophysical data

Data from regional aeromagnetic surveys and regional gravity surveys were processed in a variety of standard ways to investigate possible relationships between changes in land level and deep-seated geological structures. Variations in these two geophysical datasets in the London area relate to geological formations occurring beneath the Chalk Group, mostly of Palaeozoic or Proterozoic age. The gravity and magnetic anomaly maps of the London area show small departures from the expected value of the Earth's gravity and magnetic field (anomalies) caused by variations in the density and magnetisation of rocks within the crust. They can be used in conjunction with borehole and seismic information to determine the concealed geological

structure beneath London. Most of the gravity and magnetic material provided for this study was derived from Busby et al. (2006).

Gravity data are displayed as Bouguer gravity anomaly maps which incorporate a Bouguer correction that allows for the gravitational attraction of the rocks between the observation point at the surface, and sea-level. The Bouguer correction removes the gravitational effect due to topography in areas of high relief and leaves the gravity anomaly due to geological structure.

Magnetic maps are typically shown as Total Field magnetic anomaly and Reduced to Pole anomaly. The latter is the Total Field anomaly converted to the field that would be observed at the magnetic pole (vertical field). This has the advantage of simplifying the anomaly pattern and adjusting the location of the peak anomaly to lie immediately over the source. However, if remnant magnetisation is present some distortion will occur.

Several standard techniques are used to enhance regional geophysical data, as follows:

- ***Upward continuation*:** The primary gravity and magnetic data are further processed to enhance geophysical anomalies associated with near surface rocks and separate these from those associated with deeper sources. This process can be achieved by the method of upward-continuation, which transforms the observed field to the field that would appear at some greater height. As the height increases so the response from narrow and shallow bodies diminishes, thus clarifying the response from deeper bodies and structure.
- ***Residual anomaly*:** By subtracting the upward continued field from the observed field a series of residual anomaly maps can be produced. These can be considered as depth slices, and reflect the presence of bodies and structures, progressively deeper into the ground.
- ***Vertical derivatives:*** The vertical gradient enhances the high frequencies at the expense of the low ones. This improves the resolution of near surface features, particularly where anomalies from adjacent bodies or bodies at different depths are overlapping.
- ***Horizontal gradient*:** This enhances the response from near surface features and produces anomaly peaks along the edges of wide bodies.

The enhanced gravity and magnetic images are typically shown as colour-shaded relief images that show anomaly amplitudes as colour and anomaly gradients as relief. Linear or arcuate features are generally attributed to faulting or fold structures whilst circular anomalies are generally associated with igneous intrusions or small local sedimentary basins.

Figure 4.11 shows a colour shaded relief image of the regional gravity field with the AOI of the PSI data set superimposed (as a red rectangle). The gravity field is displayed as a variable density residual Bouguer anomaly map where the gravity field has been upward continued to 10 km and then removed from the primary field to emphasise the near surface structure. Red represents a gravity ‘high’ (mass of underlying rock is greater than average) and blue represents a gravity ‘low’ (mass of underlying rock is less than average).

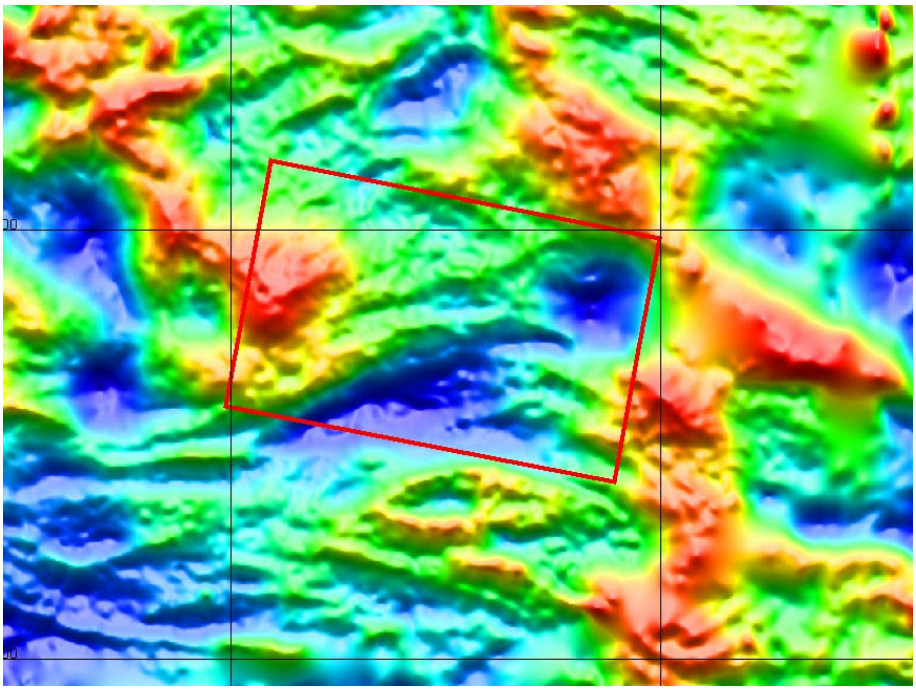

Figure 4.11 Regional gravity field with the AOI of the PSI data set superimposed

4.6.5 Other information used in the regional study

For the regional study, existing interpretations of near-surface and buried geological structures, published in the London Memoir (Ellison et. al. 2004) or the London and Thames Valley Regional Guide (Sumbler 1996), were scanned and geo-registered so that they, too, could be directly compared with the other datasets within the GIS.

In addition to the geoscience datasets, the following datasets were also compiled for reference and location purposes: Ordnance Survey topographical maps at 1:250,000; 1:50,000 and 1:10,000 scale; 'historical' 1:10,560 scale Ordnance Survey topographic maps, of various dates between about 1870 and 1950.

All of the geoscience data sets described in this section were taken forward and used in Section 6.4, where the estimates of changes in land level based on a combination of AG, GPS and PSI are subject to geological interpretations, as part of the deliverables from the regional study detailed in this Technical Report.

5 Results of the national study

As stated in the Chapter 1 of this Technical Report, “for the national study, CGPS stations have been established at ten tide gauges around the coast of Great Britain and AG measurements have been made at three of these.” A background to the national study was given in Chapter 3, including details on published changes in sea level from British tide gauges, published changes in the land level of Great Britain, and the GPS and AG data sets used. The results of the national study are now presented in this chapter, firstly as the independent results from CGPS and AG, then as the results from combining the two techniques and lastly as the estimates of changes in land and sea levels computed on a national scale.

5.1 GPS results

In this section, the independent results from using GPS on a national scale are presented. The section starts with details of the specific CGPS data processing strategies and CGPS coordinate time series analysis strategies employed, then the CGPS coordinate time series and vertical station velocity estimates are presented.

5.1.1 CGPS data processing strategies

For the national study, daily RINEX observation data from British and IGS CGPS stations were processed to produce daily coordinate estimates (latitude, longitude and ellipsoidal height) using two different strategies.

In both strategies, the following common options relating to the mitigation of systematic errors were employed:

- the IGS final products, including satellite coordinates, satellite clocks and Earth orientation parameters, were used to mitigate satellite-related systematic errors.
- the final solution was based on the ionospherically free observable, to mitigate the atmospheric-related systematic errors from the ionosphere.
- the final solution included a standard tropospheric model and the inclusion of zenith delay parameters as additional unknowns, to mitigate the atmospheric-related systematic errors from the troposphere.
- the IGS_01.pcv relative receiver-antenna PCV models (i.e. assuming zero PCVs for the Dorne-Margolin choke ring receiver-antennas employed) were used, to mitigate the station-related systematic errors from this effect.
- corrections for solid Earth tides were applied based on the IERS 2000 standards, to mitigate the station-related systematic errors from this loading process.
- corrections for ocean tide loading were applied based on the IERS 2000 standards and coefficients from the FES99 ocean tide loading model, made available by the International Association of Geodesy (IAG), to mitigate the station-related systematic errors from this loading process.

The main difference between the two strategies was, therefore, in the observation equations used and the reference frame definition employed.

In the first strategy, the IESSG's GPS Analysis Software version 2.4 (GAS2.4) (Stewart et. al. 2002) was used to produce a series of daily DD RNSs, i.e. 'Double Difference Regional Network Solutions', for the period from March 1997 to December 2005. In this case, the reference frame definition was effected through the inclusion of four European IGS CGPS stations, with 'well-determined' station coordinates and velocities in the ITRF2000, as reference stations, namely: Kootwijk in the Netherlands, which has a CGPS stations co-located with an SLR station; Onsala in Sweden, which has a CGPS station co-located with a VLBI station; Villafranca in Spain, which has a CGPS station co-located with a VLBI station; and Wettzell in Germany, which has a CGPS station co-located with both an SLR and a VLBI station. With the processing carried out on a daily basis, the known coordinates of the four European IGS CGPS stations were computed at the mid-epoch of each day from their published ITRF2000 station coordinates and velocities; hence, the coordinates of the British CGPS stations were also estimated in the ITRF2000 at the mid-epoch of each day.

In the second strategy, the IESSG's iGNSS processing tools (Orliac et. al. 2006) were used to run Bernese software version 5.0 (BSW5.0) (Hugentobler et. al. 2006) and produce a series of daily PPP GTSs, i.e. 'Precise Point Positioning Globally Transformed Solutions', for the period from January 2000 to December 2005 (Teferle et. al. 2007). In this case, the reference frame definition was effected by using the 99 IGS CGPS stations which were included in IGb00, the IGS realisation of ITRF2000, as reference stations when computing the transformation parameters. With the processing carried out on a daily basis, the known coordinates of the 99 IGS CGPS stations were computed at the mid-epoch of each day from their published ITRF2000 station coordinates and velocities; hence, the coordinates of the British CGPS stations were also estimated in the ITRF2000 at the mid-epoch of each day.

5.1.2 CGPS coordinate time series analysis strategies

As stated in Subsection 2.2.3, "coordinate time series are a data set of changes in coordinates with respect to time." For the national study, the outputs from both CGPS data processing strategies can be used to form coordinate time series, based on the ITRF2000 coordinates (latitude, longitude and ellipsoidal height) estimated at the mid-epoch of each day, for each of the British CGPS stations. These raw coordinate time series have then been subjected to a regional filtering, to remove any periodic signals which are common across the region, resulting in a total of four coordinate time series for each station:

- Unfiltered coordinate time series based on a GAS2.4 DD RNS.
- Filtered coordinate time series based on a GAS2.4 DD RNS.
- Unfiltered coordinate time series based on a BSW5.0 PPP GTS.
- Filtered coordinate time series based on a BSW5.0 PPP GTS.

As we are primarily interested in the vertical station velocities and their uncertainties when considering changes in land level, the four height time series for each station have been analysed using IESSG's CTSAna tools to run POL's CATS software (Williams 2003), which employs Maximum-Likelihood estimation (MLE) to compute a linear trend, periodic signals, coordinate offset magnitudes and stochastic noise parameters in a single process (Williams et. al. 2004). Based on experience, a white plus flicker noise (WN+FN) model, as oppose to a white plus power-law noise model (WN+PLN), was assumed in all four cases.

5.1.3 CGPS coordinate time series and estimates of vertical station velocity

For each of the 44 CGPS stations listed in Table 3.6 in Subsection 3.3.3 of Chapter 3, up to five coordinate time series are presented and considered in this subsection. The first are based on CGPS data for the period up to the end of 2004, as presented in Bingley et. al. (2006), and the other four are based on CGPS data for the period up to the end of 2005, as detailed in Subsection 5.1.2. A summary of these five solutions is presented in Table 5.1.

Table 5.1 Summary of the CGPS solutions for the national study

Solution	Data period	Software and strategy	TRF	Spatial filtering	Noise model
1	< 11/04	GAS2.4 DD RNS	ITRF2000	Unfiltered	WN+PLN
2	< 12/05	GAS2.4 DD RNS	ITRF2000	Unfiltered	WN+FN
3	< 12/05	GAS2.4 DD RNS	ITRF2000	Filtered	WN+FN
4	< 12/05	BSW5.0 PPP GTS	ITRF2000	Unfiltered	WN+FN
5	< 12/05	BSW5.0 PPP GTS	ITRF2000	Filtered	WN+FN

The CGPS coordinate time series for all 44 stations are included in the Project Record as both text files of changes in three-dimensional coordinates and graphics of the height time series. In this Technical Report, the height time series from the five solutions, for the ten CGPS@TG stations in Great Britain and the non-TG CGPS station at LERW on Shetland, are presented graphically in Appendix B.

As described in Subsection 2.2.4, the CGPS height time series plots show the changes in height from day to day as green dots, any coordinate offsets accounted for as dashed vertical lines and the best fit linear plus periodic trend as a blue line. Statistics relating to the coordinate time series analysis are also given on the height time series plots in terms of the RMS difference between the individual height estimates and the best fit trend and the estimates of vertical station velocity with their corresponding uncertainty. At this stage it must be made clear that the estimates of vertical station velocity for the three most recently established CGPS@TG stations, DVTG at Dover tide gauge on the South-East coast of England, LWTG at Lerwick tide gauge on Shetland and SWTG at Stornoway tide gauge on the Western Isles, are nonsensical due to their extremely short time series of 0.1, 0.3 and 0.3 years respectively; however their RMS values are of use. Their height time series are shown in Appendix B for completeness but also to highlight that the RMS values of 4 to 5mm for DVTG, 5 to 6mm for LWTG and 5 to 8mm for SWTG are consistent with those

obtained for the other CGPS@TG stations with longer time series and are an indication that the data quality from these three newly established CGPS@TG stations is of the required, high level.

The discussions in the remainder of this section are focused on the other seven CGPS@TG stations in Great Britain and the non-TG CGPS station at LERW, all of which have time series of at least 6 years in length, with the exception of PMTG at Portsmouth tide gauge on the South coast of England, but this still has a time series length of 4.3 years.

The height time series for a selection of three of these eight CGPS stations, namely LERW, which is about 5km from the tide gauge at Lerwick on Shetland, SHEE, which is at the Sheerness tide gauge on the Thames Estuary, East of London, and NEWL which is at the Newlyn tide gauge near to Land's End in the South-West of England, are re-presented in this section as Figure 5.1.

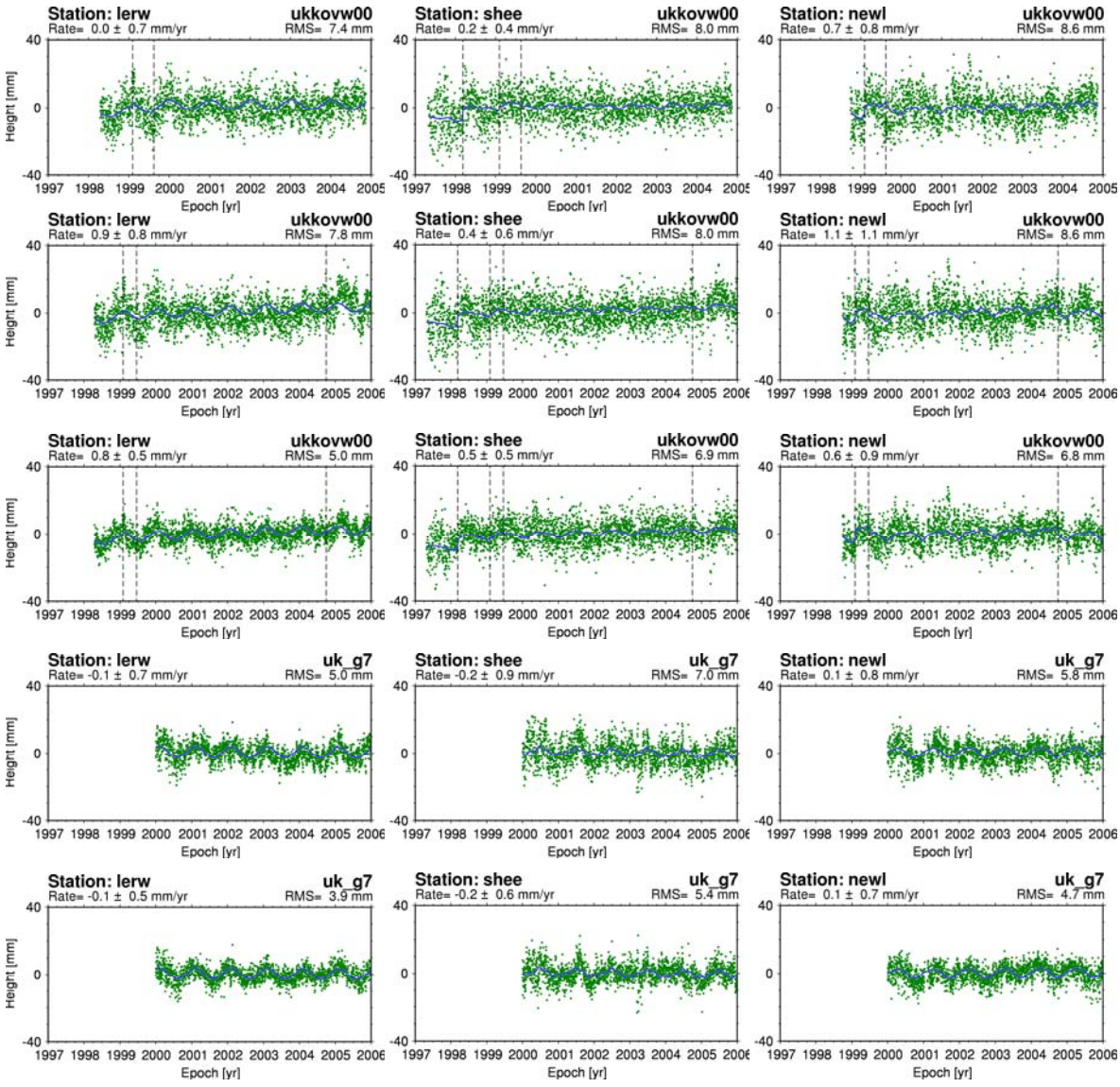

Figure 5.1 CGPS height time series from Solutions 1, 2, 3, 4 and 5 for a selection of three CGPS stations in the national study

Several points can be made regarding Figure 5.1:

- The uncertainties in the CGPS estimates of vertical station velocity are at the level of 0.5 to 1.0mm/yr for these time series, which are between 6 and 8.7 years in length.
- A comparison of Solutions 2 and 3 shows the effect of spatial filtering with the RMS values for LERW, SHEE and NEWL reducing from 7.8 to 5.0, 8.0 to 6.9 and 8.6 to 6.8mm respectively and the uncertainties for the vertical station velocity estimates reducing from 0.8 to 0.5, 0.6 to 0.5 and 1.1 to 0.9mm/yr respectively. A similar effect being apparent between Solutions 4 and 5 with the RMS values reducing by 5.0 to 3.9, 7.0 to 5.4 and 5.8 to 4.7mm respectively and the uncertainties for the vertical station velocity estimates reducing from 0.7 to 0.5, 0.9 to 0.6 and 0.8 to 0.7mm/yr respectively.
- A comparison of Solutions 1 and 2 shows the effect of extending the CGPS height time series by 13 months, i.e. from 6.6 to 7.7 years for LERW, from 7.6 to 8.7 years for SHEE and from 6.2 to 7.3 years for NEWL. Here it can be seen that the estimates of vertical station velocity are changed systematically by approximately +0.9, +0.2 and +0.4mm/yr for LERW, SHEE and NEWL respectively.
- A comparison of Solutions 2 and 4 or 3 and 5, show a further systematic offset between the use of GAS2.4 DD RNS and BSW5.0 PPP GTS, with the estimates of vertical station velocity based on GAS2.4 DD RNS being more positive than the estimates based on BSW5.0 PPP GTS by about 0.5 to 1.0mm/yr.

The RMS values for the CGPS height time series, and the CGPS estimates of vertical station velocities and their uncertainties, from Solutions 2, 3, 4 and 5 for the seven CGPS@TG stations in Great Britain and the non-TG CGPS station at LERW, are summarised in Tables 5.2 and 5.3.

Table 5.2 RMS values for the CGPS height time series from Solutions 2, 3, 4 and 5 for a selection of eight CGPS stations in the national study

Station name	4 char station ID	CGPS height time series RMS value			
		GAS2.4 DD RNS		BSW5.0 PPP GTS	
		Solution 2 (mm)	Solution 3 (mm)	Solution 4 (mm)	Solution 5 (mm)
Lerwick	LERW	7.8	5.0	5.0	3.9
Aberdeen TG	ABER	8.8	7.7	5.6	4.0
N. Shields TG	NSTG	14.5	14.1	7.5	6.1
Liverpool TG	LIVE	6.7	4.8	5.4	3.8
Lowestoft TG	LOWE	6.3	5.6	5.3	3.8
Sheerness TG	SHEE	8.0	6.9	7.0	5.4
Portsmouth TG	PMTG	6.6	5.6	4.4	3.0
Newlyn TG	NEWL	8.6	6.8	5.8	4.7

From an inspection of Table 5.3 it is clear that the uncertainties for Solutions 2 and 4 range from 0.60 to 1.12mm/yr. These are consistent with an analysis of 99 global IGS stations based on BSW5.0 PPP GTS and two other solutions from international standard software/processing strategies (GAMIT/GLOBK GNS DD and GIPSY PPP GTS) presented by Teferle et. al. (2007), from where it can be inferred that a time series length of 10 to 13 years is typically required to obtain an uncertainty of 0.5mm/yr and 20 to 25 years for 0.3mm/yr.

Table 5.3 CGPS estimates of vertical station velocities and uncertainties from Solutions 2, 3, 4 and 5 for a selection of eight CGPS stations in the national study

Station name	4 char station ID	CGPS vertical station velocity and uncertainty			
		GAS2.4 DD RNS		BSW5.0 PPP GTS	
		Solution 2 (mm/yr)	Solution 3 (mm/yr)	Solution 4 (mm/yr)	Solution 5 (mm/yr)
Lerwick	LERW	+0.89 ± 0.80	+0.77 ± 0.50	-0.10 ± 0.71	-0.09 ± 0.50
Aberdeen TG	ABER	+1.63 ± 0.65	+1.27 ± 0.32	-0.88 ± 1.00	-0.28 ± 0.44
N. Shields TG	NSTG	+0.55 ± 0.95	+0.07 ± 0.82	+0.11 ± 1.12	+0.30 ± 0.48
Liverpool TG	LIVE	+0.06 ± 0.89	+1.09 ± 0.31	+0.84 ± 1.07	+1.07 ± 0.37
Lowestoft TG	LOWE	+0.05 ± 0.61	-0.01 ± 0.50	-0.57 ± 0.70	-0.61 ± 0.33
Sheerness TG	SHEE	+0.43 ± 0.60	+0.53 ± 0.50	-0.22 ± 0.93	-0.21 ± 0.63
Portsmouth TG	PMTG	+0.67 ± 0.97	+0.48 ± 0.70	-0.56 ± 0.93	-0.59 ± 0.41
Newlyn TG	NEWL	+1.06 ± 1.11	+0.61 ± 0.91	+0.13 ± 0.83	+0.13 ± 0.66

Considering the results presented in Tables 5.2 and 5.3 along with the height time series plots given in Appendix B, it is clear that there are issues with three of the eight stations which are apparent through either a visual inspection of the CGPS height time series or the RMS values. Looking at each of the three stations in turn:

- In the case of ABER, a visual inspection of the time series shows that the data up to some point in 2001 was noisy, so much so that this data was not useable in Solutions 4 and 5, which are based on BSW5.0 PPP GTS. This noise was due to radio frequency interference at the site, as reported by Teferle et. al. (2003), and as a result of this, Solutions 4 and 5 for ABER (highlighted in grey in Table 5.3) are considered to be unreliable.
- In the case of NSTG, a visual inspection of the time series shows that Solutions 2 and 3, which are based on GAS2.4 DD RNS, are much noisier than Solutions 4 and 5, which are based on BSW5.0 PPP GTS. This is reflected in the RMS values given in Table 5.2 which are 14.5 and 14.1mm for Solutions 2 and 3, and 7.5 and 6.1mm for Solutions 4 and 5; however, in this case, Solutions 2 and 3 are still considered to be reliable, but less reliable than Solutions 4 and 5.
- In the case of LIVE, the RMS values given in Table 5.2 show that Solutions 2, 3, 4 and 5 are similar in terms of noise. The issue at this station relates to the gap in the time series from mid-2003 to early 2005, which was caused by rejecting data in order to avoid potentially erroneous results due to gradual, salt-water corrosion of the GPS antenna over this time period. In this case, the visual inspection reveals something different in that there is clearly more of a discontinuity over the gap in Solutions 2 and 3, which are based on GAS2.4 DD RNS, as oppose to Solutions 4 and 5, which are based on BSW5.0 PPP GTS. As a result of this, Solutions 2 and 3 for LIVE (highlighted in grey in Table 5.3) are considered to be unreliable.

Taking the reliable estimates given in Table 5.3, it is possible to compute differences between the CGPS estimates of vertical station velocities from GAS2.4 DD RNS and BSW5.0 PPP GTS and to compute the CGPS vertical station velocities in a relative sense. These are presented in Table 5.4.

Table 5.4 Comparison of the CGPS estimates of vertical station velocities from Solutions 2, 3, 4 and 5 for a selection of eight CGPS stations in the national study

Station name	4 char station ID	CGPS vertical station velocity			
		Differences between GAS2.4 DD RNS and BSW PPP GTS		Relative to one CGPS station	
		Solution 2 minus Solution 4 (mm/yr)	Solution 3 minus Solution 5 (mm/yr)	Solution 3 relative to ABER (mm/yr)	Solution 3 relative to LOWE (mm/yr)
Lerwick	LERW	+0.99	+0.86	-0.74	+0.77
Aberdeen TG	ABER			-	+1.28
N. Shields TG	NSTG	+0.43	-0.23	-1.20	+0.08
Liverpool TG	LIVE				
Lowestoft TG	LOWE	+0.62	+0.60	-1.58	-
Sheerness TG	SHEE	+0.65	+0.75	-1.20	+0.54
Portsmouth TG	PMTG	+1.23	+1.07	-0.97	+0.49
Newlyn TG	NEWL	+0.94	+0.49	-0.57	+0.62

Considering the five longest, homogeneous time series (LERW, LOWE, SHEE, PMTG and NEWL), the mean offset (and corresponding standard deviation) between the CGPS estimates of vertical station velocity from the two software/processing strategies are 0.89 ± 0.25mm/yr between Solutions 2 and 4, and 0.75 ± 0.23mm/yr between Solutions 3 and 5. Expanding on the discussion following Figure 5.1, the results given in Table 5.4 confirm the systematic nature of the offset between the use of GAS2.4 DD RNS and BSW5.0 PPP GTS, with the estimates of vertical station velocity based on GAS2.4 RNS DD being more positive than the estimates based on BSW5.0 PPP GTS by about 0.5 to 1.0mm/yr.

In a relative sense, however, the results from GAS2.4 DD RNS do exhibit the expected patterns of subsidence at all stations with respect to the uplifting station at Aberdeen tide gauge, and patterns of uplift at all stations with respect to the subsiding station at Lowestoft tide gauge. This is also the case if such values are computed based on Solution 2. Furthermore, patterns of uplift at all stations with respect to the subsiding station at Lowestoft tide gauge are also seen if such values are computed based on Solutions 4 or 5, using the results given in given in Table 5.3 based on BSW5.0 PPP GTS.

Based on the results presented in this subsection, therefore, it can be concluded that parallel processing with DD and PPP is essential in order to make the best use of stations that have data of varying quality, i.e. the ‘better’ solutions for ABER were 2 and 3 (GAS2.4 DD RNS) whereas the ‘better’ solutions for NSTG and LIVE were 4 and 5 (BSW5.0 PPP GTS). It can also be concluded that, at this demanding, high level of accuracy, an independent measure of vertical station velocities is essential, in order to assess the systematic offsets apparent between different software/processing strategies, hence the use of AG, the results of which are given in the next section.

5.2 AG results

In this section, the independent results from using AG on a national scale are presented. The section starts with details of the specific AG data processing strategy and absolute gravity time series analysis strategy employed, then the absolute gravity time series and vertical station velocity estimates are presented.

5.2.1 AG data processing strategy

As stated in Subsection 3.4.3, "the procedure adopted for the national study was to make near-annual, episodic AG measurements, with each set of measurements being carried out over at least three days, typically three to four days, and the absolute gravimeter instrument being carefully set up again at the start of each day."

Data from each day were processed separately, with corrections made for solid-earth tides, ocean-loading effects, atmospheric pressure, polar motion and comparator response. From this it was possible to compute one mean value per day and then a weighted mean for the epoch, or just one mean value for the epoch. The uncertainty being the root sum square of the instrument uncertainty estimate (1 to 2μgal) and the statistical error ($\sigma / \sqrt{N}$ where σ is the drop to drop standard deviation and *N* is the number of drops).

5.2.2 Absolute gravity time series analysis strategy

The absolute gravity values for each epoch were then used to form time series for each AG station. A best fit linear trend was then used to obtain an estimate of the change of absolute gravity and its uncertainty, from which the equivalent vertical station velocity and uncertainty were inferred, through applying a conversion factor of -2μgal/cm or -5mm/μgal, consistent with the Bouger model described in Subsection 2.3.1.

5.2.3 Absolute gravity time series and AG estimates of vertical station velocity

For each of the three AG stations listed in Table 3.7 in Subsection 3.4.3, two absolute gravity time series are presented and considered in this subsection. The first (Solution A) are based on AG data for the period up to September 2004, as presented in Bingley et. al. (2006), and the others (Solution B) are based on AG data for the period up to September 2006. For both solutions, the AG data was processed using POL in-house developed software.

The absolute gravity time series for all three AG stations are included in the Project Record as both text files of changes in absolute gravity and graphics of the absolute gravity time series. In this Technical Report, the absolute gravity time series from the two solutions, for the three AG stations in Great Britain are

presented as Figures 5.2 and 5.3. As described in Subsection 2.3.4, the AG estimates of absolute gravity for a station are shown as red dots, at approximately annual intervals, and the plots also show the best fit linear trend in the absolute gravity estimates (as a blue line).

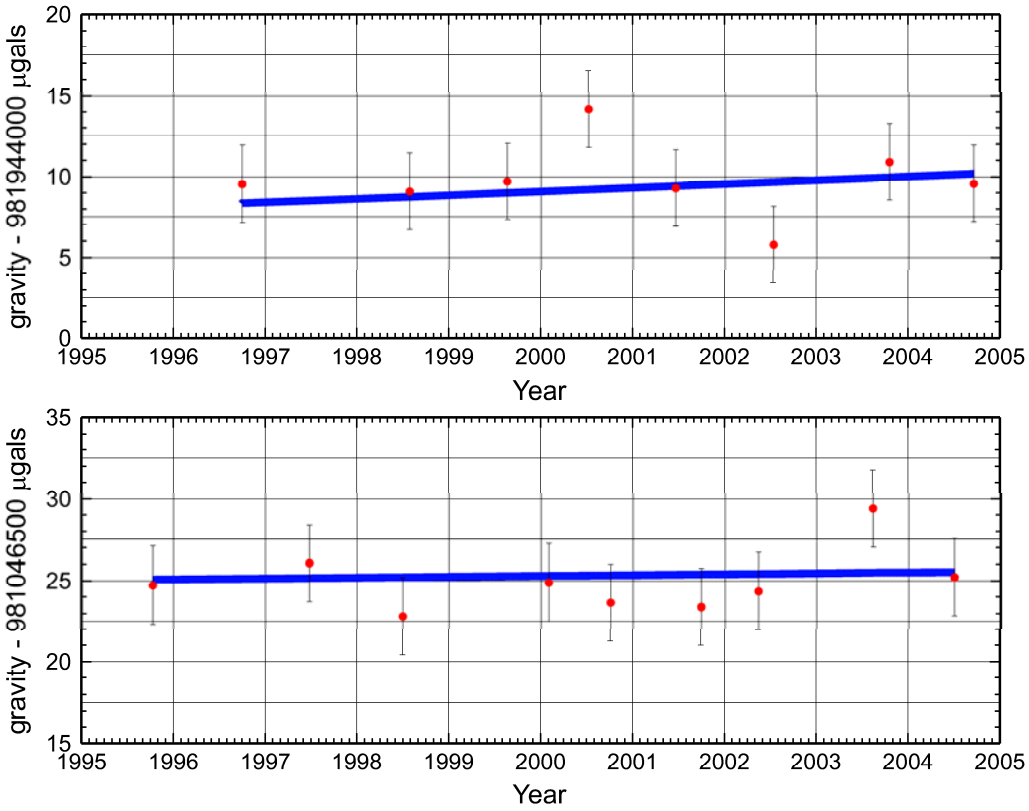

Figure 5.2 Absolute gravity time series from Solution A for Lerwick (top) and Newlyn (bottom) AG stations used in the national study

A visual inspection of Figures 5.2 and 5.3 shows that there appears to be a positive change in absolute gravity at both Lerwick and Newlyn AG stations, which would equate to a negative vertical station velocity, and a negative change in absolute gravity at Aberdeen AG station, which would equate to a positive vertical station velocity. In the case of the AG station in Aberdeen, however, the absolute gravity time series is clearly, significantly different in character to the time series for the other two AG stations: it shows a change in absolute gravity which is six to nine times greater than that observed at the other two AG stations and the data for the period up to September 2004 appears to exhibit a bi-modal distribution, as illustrated by the red and green dots. At this stage, therefore, any estimate of a change in absolute gravity or vertical station velocity based on the current AG station in Aberdeen must be treated with extreme caution.

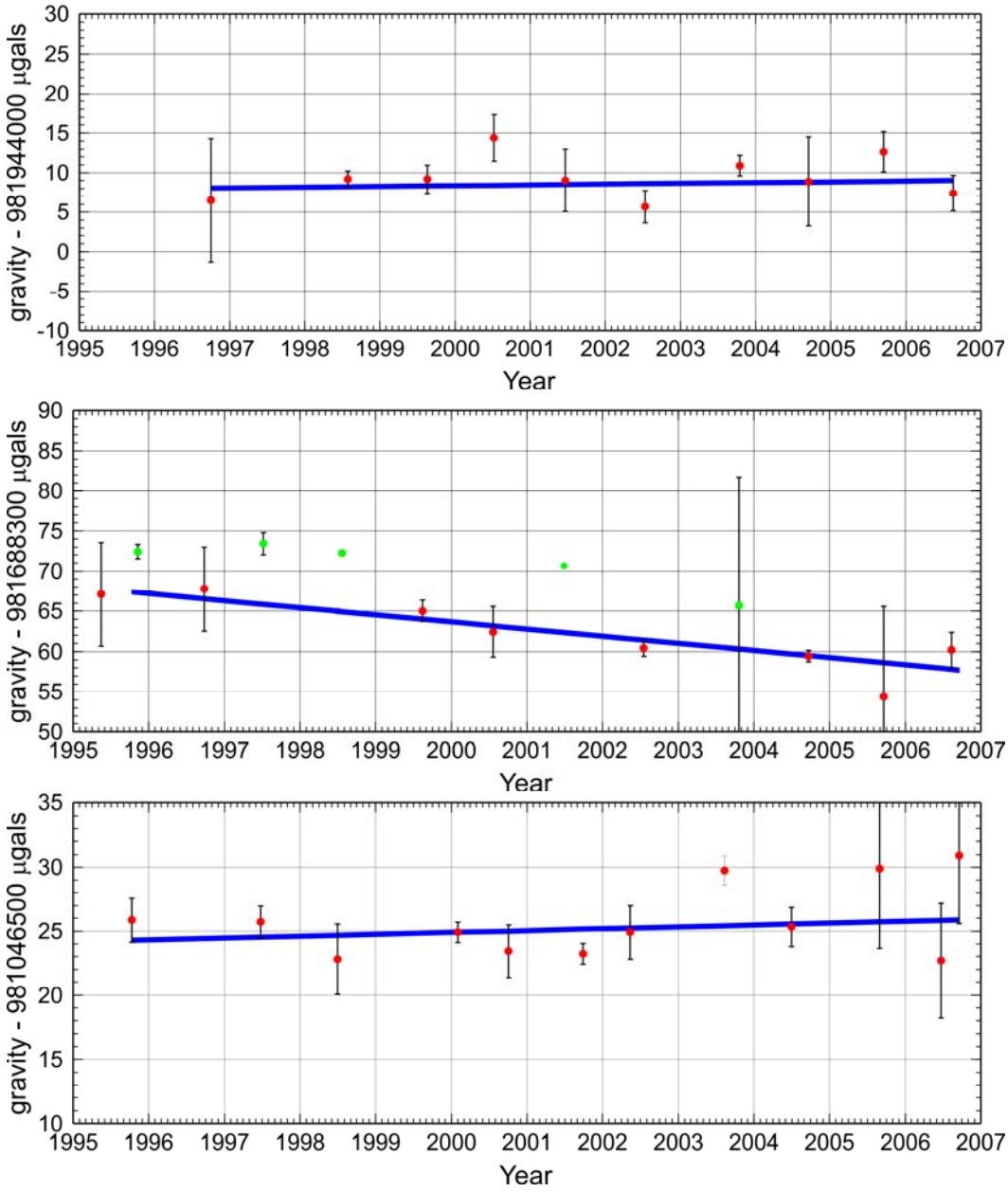

Figure 5.3 Absolute gravity time series for Solution B for Lerwick (top), Aberdeen (middle) and Newlyn (bottom) AG stations used in the national study

The estimates of vertical station velocities and their uncertainties, from both solutions for the two reliable AG stations in Great Britain are summarised in Table 5.5, which confirms that both stations have negative vertical station velocities and presents their magnitudes as being of the order of 0.5 to 1.1mm/yr.

Table 5.5 Estimates of changes in absolute gravity and AG vertical station velocities, and their uncertainties, from Solutions A and B for two AG stations in the national study

Station name	AG change in absolute gravity and uncertainty		AG vertical station velocity and uncertainty	
	Solution A (μgal/yr)	Solution B (μgal/yr)	Solution A (mm/yr)	Solution B (mm/yr)
Lerwick	+0.2 ± 0.2	+0.10 ± 0.19	-1.1 ± 1.1	-0.49 ± 0.96
Newlyn	+0.1 ± 0.2	+0.14 ± 0.14	-0.5 ± 0.9	-0.74 ± 0.72

Considering Figures 5.2 and 5.3 along with Table 5.5, two points of interest can be made:

- The uncertainties in the AG estimates of vertical station velocity are at the level of 0.7 to 1.0mm/yr for the Solution B time series, which are between 9.9 and 10.9 years in length.
- A comparison of Solutions A and B shows the effect of extending the absolute gravity time series by approximately 2 years, i.e. from 8.0 to 9.9 years for Lerwick, from 8.8 to 10.9 years for Newlyn. Here it can be seen that the estimates of vertical station velocity are changed by approximately +0.6mm/yr for Lerwick and -0.2mm/yr for Newlyn respectively.

5.3 Combined AG and GPS results

In this section, we compare the CGPS and AG estimates of vertical station velocities with each other and with other independent evidence of changes in land level for Great Britain, and then present a strategy for combining the current CGPS and AG estimates of vertical station velocities to enable estimates for the changes in land and sea levels around the coast of Britain.

5.3.1 Comparison of CGPS and AG estimates of vertical station velocities

Based on AG Solution B, presented in Table 5.5 in Subsection 5.2.3, and CGPS Solutions 2, 3, 4 and 5, presented in Table 5.3 in Subsection 5.1.3, a comparison between the CGPS and AG vertical station velocities can be made for stations close to Lerwick tide gauge on Shetland and close to or at the Newlyn tide gauge near to Land's End in the South-West of England. The results of this comparison are given in Table 5.6.

Table 5.6 Comparison of CGPS and AG estimates of vertical station velocities from the national study

Station name	4 char station ID	CGPS minus AG difference in vertical station velocity			
		GAS2.4 DD RNS		BSW5.0 PPP GTS	
		Solution 2 (mm/yr)	Solution 3 (mm/yr)	Solution 4 (mm/yr)	Solution 5 (mm/yr)
Lerwick	LERW	+1.38	+1.26	+0.39	+0.40
Newlyn TG	NEWL	+1.80	+1.35	+0.87	+0.87
Weighted Mean		+1.52	+1.27	+0.59	+0.56
Standard Deviation		±0.30	±0.07	±0.34	±0.33

As stated in Subsection 5.1.3, “when considering the five longest, homogeneous CGPS height time series, the mean offset (and corresponding standard deviation) between the CGPS estimates of vertical station velocity from the two software/processing strategies were 0.89 ± 0.25mm/yr between Solutions 2 and 4, and 0.75 ± 0.23mm/yr between Solutions 3 and 5, with the estimates of vertical station velocity based on GAS2.4 RNS DD being more positive than the estimates based on BSW5.0 PPP GTS.” When considering AG, the weighted mean offset (and corresponding standard deviation) suggest that all of the CGPS estimates of vertical station velocity are systematically offset from the estimates based on AG: those based on GAS2.4 RNS DD being more positive by 1.27 or 1.52mm/yr and those based on BSW5.0 PPP GTS being more positive by 0.56 or 0.59mm/yr.

5.3.2 Comparison of CGPS and AG estimates of vertical station velocities with other independent evidence

At this stage of the discussions it is quite correct to ask the question of which is the more correct: AG or CGPS? Before attempting to answer this question, it is worth considering the uncertainties in the estimates of vertical station velocity presented thus far, which show that CGPS and AG are in agreement within the 1-sigma uncertainties given in Tables 5.3 and 5.5, in Subsections 5.1.3 and 5.2.3 respectively, e.g. in the worst case for Newlyn tide gauge, the CGPS estimate from Solution 2 is +1.06 ± 1.11mm/yr, or between -0.05 and +2.17mm/yr at the 1-sigma level, and the AG estimate from Solution B is -0.74 ± 0.72mm/yr, or between -1.46 and -0.02mm/yr at the 1-sigma level.

Nevertheless, to explore this question further, in this subsection we: consider the stability, in a local and regional context, of the AG and CGPS@TG stations for Newlyn tide gauge; compare the AG and CGPS estimates of vertical station velocity with the published changes in the land level of Great Britain; consider other published evidence on CGPS estimates of vertical station velocity at this demanding, high level of accuracy; compare the CGPS estimates of vertical station velocity for the IGS station HERS with the ITRF2000 published vertical station velocity for Herstmonceux, on the South Coast of England, which is based on a combination of CGPS and SLR as part of the realisation of ITRF2000.

Stability of the AG and CGPS@TG stations for Newlyn tide gauge

The CGPS@TG station NEWL is founded on the pier at Newlyn tide gauge near to Land’s End in the South-West of England. The stability, in a local and regional context, of NEWL could have an impact on the nature of the apparent systematic offset between the CGPS estimate of vertical station velocity and the AG estimate, which is for the AG station located in the church at Paul about 1.5km away.

The MSL records from the Newlyn tide gauge for the period 1915-21 were used to define Ordnance Datum Newlyn (ODN) and the Tidal Observatory has remained in the same location since that time. The primary tide gauge

benchmark (PTGBM) at Newlyn is a bolt, adjacent to the stilling well, inside the Tidal Observatory. The PTGBM was first connected to the primary levelling network in 1915 and was last verified by precise levelling (line G001) in 1990. The TGBM network is effectively formed from seven benchmarks, comprising the PTGBM, two benchmarks on the pier, two benchmarks in the village and two fundamental benchmarks (FBMs), located at Tolcarne, about 900 m to the North-West of the PTGBM and at Paul, about 1.4 km South-West of the PTGBM. The FBMs are founded on 'solid rock', whereas all of the other inland benchmarks are Ordnance Survey flush brackets set into walls. The TGBM network was first connected to the PTGBM in 1952 and last verified by precise levelling (line G001) in 1990. The results of the repeated precise levelling surveys showed no significant changes (i.e. less than 0.1 mm) in height within the TGBM network over the period from 1952 to 1990, which suggests that the pier on which the tide gauge and the CGPS@TG station are located did not experience any uplift or subsidence relative to any of the benchmarks, including the two FBMs founded on solid rock, and is stable in a local context.

A further confirmation of this can be obtained for a regional context by considering the vertical station velocities estimated for NEWL along with the vertical station velocities estimated for the non-TG CGPS station CAMB, which is at Camborne about 20km away and founded on solid rock. In this respect, it can be reported that the CGPS estimates of vertical station velocity for CAMB were +0.79 ± 0.75 and +0.54 ± 0.44mm/yr for Solutions 2 and 3 respectively, which agree with the estimates for NEWL (given in Table 5.3 in Subsection 5.1.3) of +1.06 ± 1.11 and +0.61 ± 0.91mm/yr to within 0.27 and 0.07mm/yr.

Considering these two different sets of results, therefore, it can be concluded that the apparent systematic offsets of +1.80, +1.35, +0.87 and +0.87mm/yr (given in Table 5.6 of Subsection 5.3.1) between the CGPS and AG estimates of vertical station velocity for Newlyn are not due to relative movements between the CGPS@TG station NEWL founded on the pier adjacent to Newlyn tide gauge and the AG station founded on solid rock in the church at Paul, some 1.5km away. Unfortunately, a similar assessment cannot be carried out for the CGPS and AG stations at Lerwick on Shetland as similar data to that presented for Newlyn is not available.

Comparisons with published evidence for changes in land level in Great Britain

The nature of the apparent systematic offset between the CGPS and AG estimates of vertical station velocity can be further investigated through a comparison with the published evidence for changes in land in level in Great Britain, presented in Section 3.2.

Considering AG, the vertical station velocities for Newlyn and Lerwick for Solution B were presented in Table 5.5 in Subsection 5.2.3 as -0.49 ± 0.96mm/yr and -0.74 ± 0.72mm/yr respectively. A comparison of these with the values presented in Table 3.4 in Subsection 3.2.2 shows that the AG estimate of vertical station velocity for Lerwick is in agreement with the value of -0.5mm/yr from the GIA model of Peltier (2001), and the AG estimate of vertical

station velocity for Newlyn is somewhere in between the values from the GIA model of Peltier (2001) at -0.3mm/yr and the values from the GIA model of Lambeck and Johnston (1995) of -1.0mm/yr and the geological studies of Shennan and Horton (2002) of -1.1mm/yr.

Considering CGPS, the comparisons are presented as Figures 5.4 and 5.5 for Solutions 2 and 3, and Solutions 4 and 5 respectively, where each figure consists of a series of four plots, which show the vertical land movement (VLM) estimates, i.e. estimates of changes in land level, from the CGPS estimates of vertical station velocity (shown in red on all four plots) in comparison with estimates from:

- Geological studies, using the values given in Table 3.4 in Subsection 3.2.2 which are based on Shennan and Horton (2002), and a value for Brest from Woodworth et. al. (1999); shown in blue on the top plots.
- Models of GIA, using values also given in Table 3.4 in Subsection 3.2.2, and shown on the bottom plots with Lambeck and Johnston (1995) in green and Peltier (2001) in blue.

A visual inspection of Figure 5.4 clearly shows that, in most cases, the CGPS estimates of vertical station velocity from GAS2.4 DD RNS are more positive than the published evidence for changes in land level. A visual inspection of Figure 5.5 shows that with the systematic offset between the GAS2.4 DD RNS and BSW5.0 PPP GTS effectively removed, the GPS estimates of vertical station velocity are more in sympathy with the published changes in land level.

To assess whether there are any systematic offsets between the different CGPS solutions and the published changes in land level, a comparison between the reliable (as discussed in Subsection 5.1.3) CGPS vertical station velocities for stations in Great Britain and the published changes in land level is given in Tables 5.7, 5.8 and 5.9.

Tables 5.7, 5.8 and 5.9 appear to confirm what is apparent from a visual inspection of Figures 5.4 and 5.5, especially as the tables only consider the reliable CGPS estimates of vertical station velocity. The results showing that the mean and standard deviation of the differences between the CGPS estimates of vertical station velocity and the published changes in land level are:

- +1.37 ± 0.80mm/yr, +0.83 ± 0.47mm/yr and +1.08 ± 0.63mm/yr for Solution 2, based on GAS2.4 DD RNS.
- +1.15 ± 0.80mm/yr, +0.60 ± 0.49mm/yr and +0.84 ± 0.64mm/yr for Solution 3, also based on GAS2.4 DD RNS.
- +0.60 ± 0.71mm/yr, +0.05 ± 0.37mm/yr and +0.45 ± 0.56mm/yr for Solution 4, based on BSW5.0 PPP GTS.
- +0.66 ± 0.74mm/yr, +0.10 ± 0.41mm/yr and +0.52 ± 0.60mm/yr for Solution 5, also based on BSW5.0 PPP GTS.

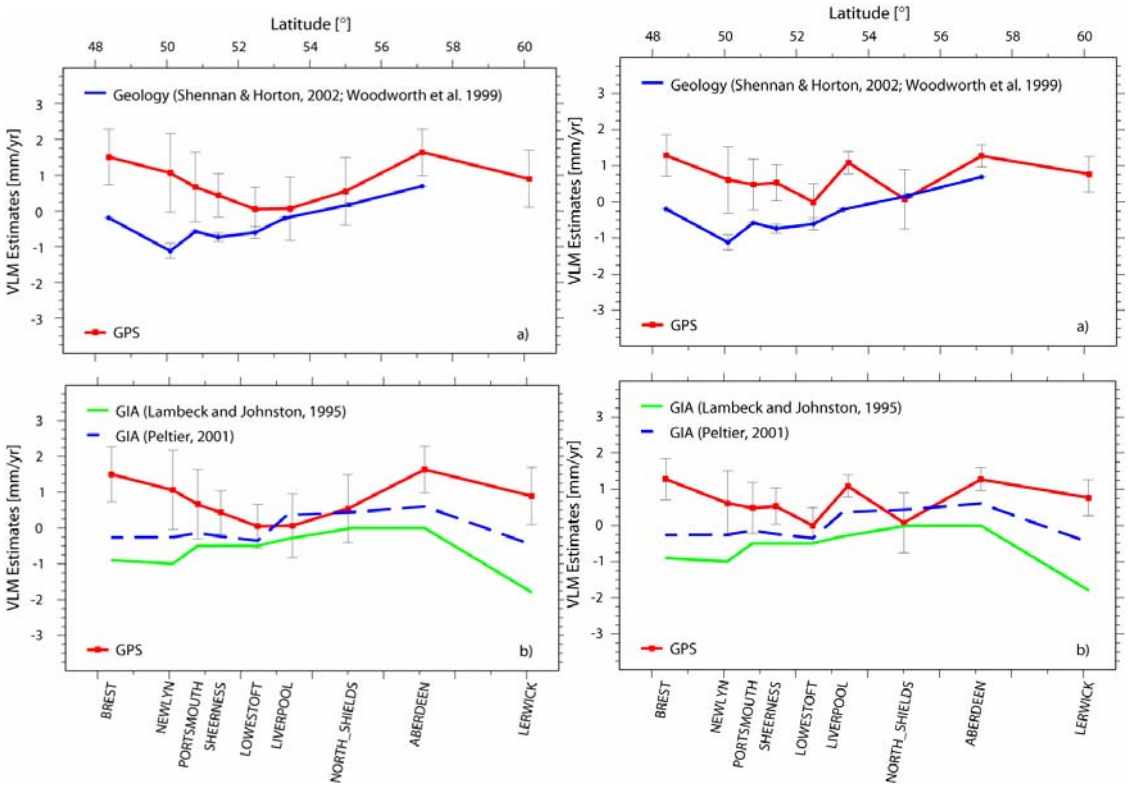

Figure 5.4 CGPS estimates of vertical station velocities from Solutions 2 (left) and 3 (right) compared to published evidence for changes in the land level of Great Britain

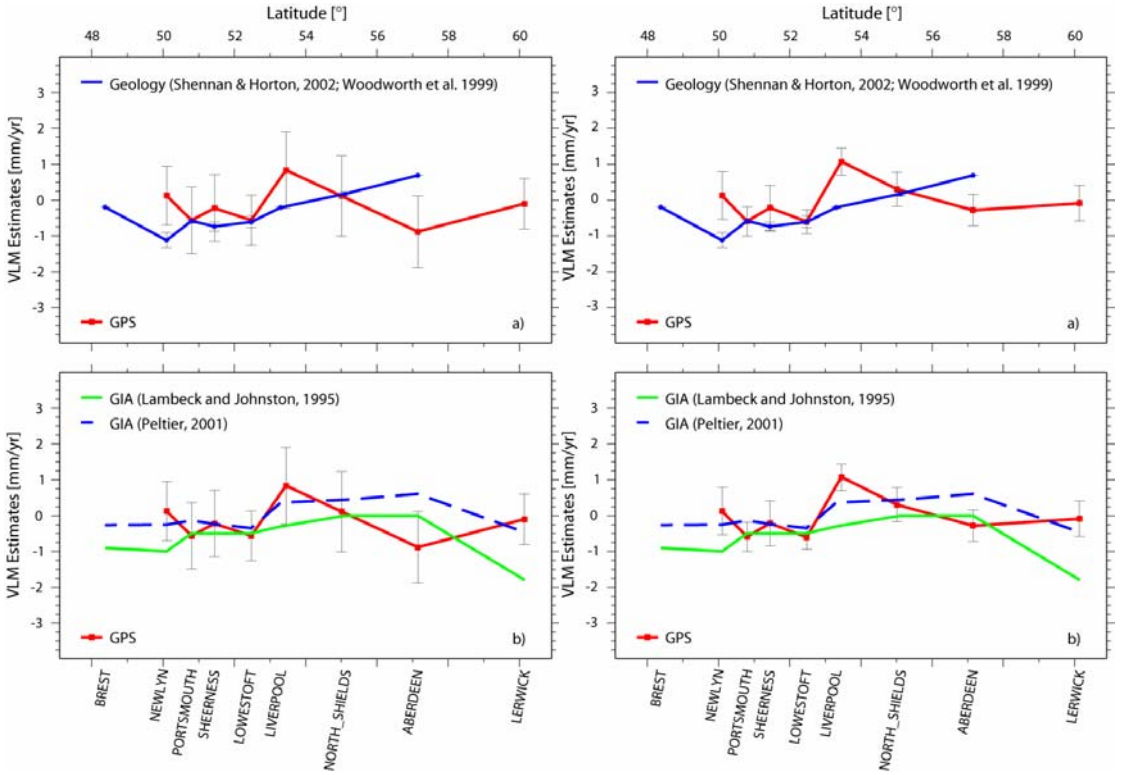

Figure 5.5 CGPS estimates of vertical station velocities from Solutions 4 (left) and 5 (right) compared to published evidence for changes in the land level of Great Britain

Table 5.7 Comparison of CGPS estimates of vertical station velocities from the national study and published changes in land level based on the GIA model of Lambeck and Johnston (1995)

Station name	4 char station ID	CGPS minus GIA difference in vertical station velocity			
		GAS2.4 DD RNS		BSW5.0 PPP GTS	
		Solution 2 (mm/yr)	Solution 3 (mm/yr)	Solution 4 (mm/yr)	Solution 5 (mm/yr)
Lerwick	LERW	+2.69	+2.57	+1.70	+1.71
Aberdeen TG	ABER	+1.63	+1.27		
N. Shields TG	NSTG	+0.55	+0.07	+0.11	+0.30
Liverpool TG	LIVE			+1.14	+1.37
Lowestoft TG	LOWE	+0.55	+0.49	-0.07	-0.11
Sheerness TG	SHEE	+0.93	+1.03	+0.28	+0.29
Portsmouth TG	PMTG	+1.17	+0.98	-0.06	-0.09
Newlyn TG	NEWL	+2.06	+1.61	+1.13	+1.13
Mean		+1.37	+1.15	+0.60	+0.66
Standard Deviation		±0.80	±0.80	±0.71	±0.74

Table 5.8 Comparison of CGPS estimates of vertical station velocities from the national study and published changes in land level based on the GIA model of Peltier (2001)

Station name	4 char station ID	CGPS minus GIA difference in vertical station velocity			
		GAS2.4 DD RNS		BSW5.0 PPP GTS	
		Solution 2 (mm/yr)	Solution 3 (mm/yr)	Solution 4 (mm/yr)	Solution 5 (mm/yr)
Lerwick	LERW	+1.39	+1.27	+0.40	+0.41
Aberdeen TG	ABER	+1.03	+0.67		
N. Shields TG	NSTG	+0.15	-0.33	-0.29	-0.10
Liverpool TG	LIVE			+0.44	+0.67
Lowestoft TG	LOWE	+0.45	+0.39	-0.17	-0.21
Sheerness TG	SHEE	+0.63	+0.73	-0.02	-0.01
Portsmouth TG	PMTG	+0.77	+0.58	-0.46	-0.49
Newlyn TG	NEWL	+1.36	+0.91	+0.43	+0.43
Mean		+0.83	+0.60	+0.05	+0.10
Standard Deviation		±0.47	±0.49	±0.37	±0.41

Table 5.9 Comparison of CGPS estimates of vertical station velocities from the national study and published changes in land level based on geological studies (Shennan and Horton 2002)

Station name	4 char station ID	CGPS minus GEOL difference in vertical station velocity			
		GAS2.4 DD RNS		BSW5.0 PPP GTS	
		Solution 2 (mm/yr)	Solution 3 (mm/yr)	Solution 4 (mm/yr)	Solution 5 (mm/yr)
Lerwick	LERW				
Aberdeen TG	ABER	+0.93	+0.57		
N. Shields TG	NSTG	+0.35	-0.13	-0.09	+0.10
Liverpool TG	LIVE			+1.04	+1.27
Lowestoft TG	LOWE	+0.65	+0.59	+0.03	-0.01
Sheerness TG	SHEE	+1.13	+1.23	+0.48	+0.49
Portsmouth TG	PMTG	+1.27	+1.08	+0.04	+0.01
Newlyn TG	NEWL	+2.16	+1.71	+1.23	+1.23
Mean		+1.08	+0.84	+0.45	+0.52
Standard Deviation		±0.63	±0.64	±0.56	±0.60

Before considering these results any further, it is worth considering that six of the 12 differences could be considered as zero, within the 1-sigma uncertainties given in Tables 5.7, 5.8 and 5.9, and all could be considered zero at the 2-sigma level. Furthermore, it is clear that CGPS Solutions 4 and 5 are in good agreement with the GIA model of Peltier (2001). Apart from this one GIA model, the other mean offsets are of the same sign and of a similar magnitude to the systematic offset between the CGPS and AG estimates of vertical station velocity: those based on GAS2.4 DD RNS being more positive than AG by 1.27 or 1.52mm/yr and those based on BSW5.0 PPP GTS being more positive than AG by 0.56 or 0.59mm/yr.

At this stage, therefore, considering all of the published evidence for changes in land level, and the fact that 80% of the differences presented in Tables 5.7, 5.8 and 5.9 are positive, it is reasonable to conclude that the CGPS, and not the AG, estimates of vertical station velocity are systematically offset from the published changes in land level, with the CGPS estimates of vertical station velocity being more positive than the published changes in land level.

Other published evidence on CGPS vertical station velocities

To investigate this further, we can consider other published evidence on CGPS estimates of vertical station velocity at this demanding, high level of accuracy. In this respect, several authors have reported systematic offsets when comparing CGPS estimates of vertical station velocity to independent evidence:

- Prawirodirdjo and Bock (2004) compared CGPS estimates of vertical station velocity, based on another international standard software/processing strategies (GAMIT/GLOBK GNS DD), with estimates from a GIA model and reported an offset of +1.1mm/yr for sites in North America and +1.7mm/yr for sites in Northern Europe, with the CGPS estimates being more positive than the GIA model.
- MacMillan (2004) compared CGPS and Very Long Baseline Interferometry (VLBI) which forms a critical component of the ITRF, and found that CGPS estimates of vertical station velocity were 1.5mm/yr more positive than VLBI estimates at 22 co-located global sites.
- As part of the European Sea Level Service – Research Infrastructure project, CGPS and AG estimates of vertical station velocity at Newlyn were also compared, based on two other international standard software/processing strategies (GAMIT/GLOBK GNS DD and GIPSY-OASIS II GTS PPP) with offsets of +0.6 and +1.7 to +2.5mm/yr found, i.e. the CGPS estimates were more positive than the AG estimates.

At the moment, therefore, the general consensus in the international community is that there is a systematic bias in all ‘current’ CGPS estimates of vertical station velocity at this demanding, high level of accuracy, which is due to a combination of: the use of models for relative antenna phase centre variations, i.e. inadequate modelling of satellite and receiver antenna phase centres in a changing satellite constellation (Ge et al., 2005); the use of ITRF2000; and, in the case of GAS2.4 DD RNS, limitations in using a regional network solution (rather than a globally transformed solution), for which we have already shown a systematic offset of 0.75 or 0.89mm/yr. At this point it should be noted that

the use of models for relative antenna phase centre variations and the use of ITRF2000 is inherent in all of the CGPS estimates of vertical station velocity computed for the national study detailed in this Technical Report, as these models and reference frame are what were adopted and used by the IGS to produce the IGS products and in our own processing, which was made to be consistent with the IGS processing strategy as it was during the period of the national study. In this respect, since 26 November 2006, the IGS have changed their processing strategy to include models for absolute antenna phase centre variations and the use of International Terrestrial Reference Frame 2005 (ITRF2005). This revised processing strategy is now being used by the IGS in the computation of new IGS products, and will be used by the IGS in a re-processing and re-analysis effort planned for the next three years or so, to produce revised and improved IGS products that go back in time, which will then enable re-processing and re-analysis efforts to be made on CGPS data sets such as the one used in the national study.

Comparisons at Herstmonceux IGS station

Lastly, the nature of the apparent systematic offset between the CGPS and AG estimates of vertical station velocity can be further investigated through a comparison of the CGPS estimates of vertical station velocity for the IGS station HERS with the ITRF2000 published vertical station velocity for Herstmonceux, on the South Coast of England, which is based on a combination of CGPS and SLR as part of the realisation of ITRF2000.

Due to equipment problems at the site the early CGPS data for HERS is not of a particularly high quality and the height time series require two coordinate offsets in 1998 and three coordinate offsets in 1999, in addition to one further coordinate offset in 2001. As such, the height time series from Solutions 2 and 3 (based on GAS2.4 DD RNS) are not as reliable as those from Solutions 4 and 5 (based on BSW5.0 PPP GTS), as the latter only consider data from 1 January 2000 onwards. Considering the estimates of vertical station velocity for HERS from Solutions 4 and 5, these are +0.41 ± 0.98 and +0.13 ± 0.62 respectively. The ITRF2000 published vertical station velocity for Herstmonceux was -0.64mm/yr. In comparison, the CGPS estimates based on BSW5.0 PPP GTS are, again, too positive by 1.05 or 0.77mm/yr. These offsets are of the same sign and of a similar magnitude to the systematic offset between the CGPS and AG estimates of vertical station velocity based on BSW5.0 PPP GTS and given in Table 5.6 in Subsection 5.3.1, which for Newlyn were 0.89mm/yr and which as a weighted mean for Lerwick and Newlyn were 0.56 or 0.59mm/yr.

Summary

At the end of Subsection 5.1.3, it was concluded that the CGPS estimates of vertical station velocity are systematically offset from the estimates based on AG, so at the start of this subsection, the question “which is the more correct: AG or CGPS?” was posed.

Based on other published evidence on CGPS estimates of vertical station velocity at this demanding, high level of accuracy, it was stated that “the general

consensus in the international community is that there is a systematic bias in all 'current' CGPS estimates of vertical station velocity at this demanding, high level of accuracy, which is due to a combination of: the use of models for relative antenna phase centre variations; the use of ITRF2000; and limitations in using a regional network solution (rather than a globally transformed solution)."

Accepting that there is a potential systematic bias in our CGPS estimates of vertical station velocity presented thus far, the question posed at the beginning of this subsection was further explored, in terms of our results, through: a consideration of the stability, in a local and regional context, of the AG and CGPS@TG stations for Newlyn tide gauge; a comparison of the AG and CGPS estimates of vertical station velocity with the published changes in the land level of Great Britain; a comparison of the CGPS estimates of vertical station velocity with the ITRF2000 published vertical station velocity for the IGS station HERS. From these it was concluded that the apparent systematic offsets between the CGPS and AG estimates of vertical station velocity for Newlyn are not due to relative movements between the CGPS@TG station NEWL founded on the pier adjacent to Newlyn tide gauge and the AG station founded on solid rock in the church at Paul, some 1.5km away; the CGPS, and not the AG, estimates of vertical station velocity are systematically offset from the published changes in land level, with the CGPS estimates of vertical station velocity being more positive than the published changes in land level; the CGPS estimates of vertical station velocity for HERS are systematically offset from the ITRF2000 published value, based on a combination of CGPS and SLR, with the CGPS estimates of vertical station velocity being more positive than the ITRF2000 published value. Furthermore, in the latter two 'tests' it was shown that the majority of the systematic offsets seen are of the same sign and of a similar magnitude to the systematic offset between the CGPS and AG estimates of vertical station velocity.

In our opinion, therefore, it can be concluded that the CGPS estimates of vertical station velocity presented thus far are systematically offset from the estimates based on AG, due mostly to a systematic bias in current CGPS estimates of vertical station velocity, which is apparent at this demanding, high level of accuracy.

5.3.3 AG-aligned CGPS estimates of vertical station velocities

At the start of the previous subsection (Subsection 5.3.2), the question "which is the more correct: AG or CGPS?" was posed. Following the summary at the end of that subsection, the question would perhaps be better rephrased as "considering that there is a potential systematic bias in the CGPS estimates of vertical station velocity at this demanding, high level of accuracy, how can CGPS and AG be best combined in order to provide an 'engineering solution' and obtain some estimates of changes in sea level (decoupled from changes in land level) based on the approximately 8.5 years of CGPS data and 10 or 11 years of AG data acquired to date?"

One such engineering solution was given in Teferle et. al. (2006), who presented a procedure for combining CGPS and AG estimates of vertical station velocities, based on aligning the CGPS estimates to the AG estimates using the systematic offset between them. In Table 5.6 in Subsection 5.3.2 a comparison of the CGPS and AG estimates of vertical station velocity for Newlyn and Lerwick were presented and a weighted mean offset (and corresponding standard deviation) computed to show that the CGPS estimates based on GAS2.4 DD RNS were more positive than the AG estimates by 1.52mm/yr for Solution 2 and 1.27mm/yr for Solution 3, and the CGPS estimates based on BSW5.0 PPP GTS were more positive than the AG estimates by 0.56mm/yr for Solution 4 and 0.59mm/yr for Solution 5.

Following the procedure of Teferle et. al. (2006), to compute an AG-aligned CGPS estimate of vertical station velocity, the systematic offset relating to a particular CGPS solution is basically subtracted from the CGPS estimate of vertical station velocity for a station. Through this procedure, the CGPS estimates of vertical station velocities presented in Table 5.3 in Subsection 5.1.3 are changed to the following AG-aligned CGPS estimates given in Table 5.10, which only shows the reliable estimates (based on the discussions in Subsection 5.1.3).

Table 5.10 AG-aligned CGPS estimates of vertical station velocities and uncertainties from Solutions 2, 3, 4 and 5 for a selection of eight CGPS stations in the national study

Station name	4 char station ID	AG-aligned CGPS vertical station velocity and uncertainty			
		GAS2.4 DD RNS		BSW5.0 PPP GTS	
		Solution 2 (mm/yr)	Solution 3 (mm/yr)	Solution 4 (mm/yr)	Solution 5 (mm/yr)
Lerwick	LERW	-0.63 ± 0.82	-0.50 ± 0.50	-0.69 ± 0.74	-0.65 ± 0.54
Aberdeen TG	ABER	+0.11 ± 0.68	0.00 ± 0.32		
N. Shields TG	NSTG	-0.97 ± 0.97	-1.20 ± 0.82	-0.48 ± 1.14	-0.26 ± 0.52
Liverpool TG	LIVE			+0.25 ± 1.09	+0.51 ± 0.43
Lowestoft TG	LOWE	-1.47 ± 0.64	-1.28 ± 0.50	-1.16 ± 0.73	-1.17 ± 0.40
Sheerness TG	SHEE	-1.09 ± 0.64	-0.74 ± 0.50	-0.81 ± 0.96	-0.77 ± 0.67
Portsmouth TG	PMTG	-0.85 ± 0.99	-0.79 ± 0.70	-1.15 ± 0.96	-1.15 ± 0.46
Newlyn TG	NEWL	-0.46 ± 1.13	-0.66 ± 0.91	-0.46 ± 0.86	-0.43 ± 0.70

It is clear from Table 5.10 that, when considering the five longest, homogeneous time series (LERW, LOWE, SHEE, PMTG and NEWL), the AG-aligned CGPS estimates of vertical station velocity from the four solutions are in much better agreement than the corresponding CGPS estimates of vertical station velocity. Without re-presenting Table 5.4 given in Subsection 5.1.3, it can be stated that the mean offset (and corresponding standard deviation) between the estimates of vertical station velocity from the two CGPS software/processing strategies are reduced from +0.89 ± 0.25mm/yr between Solutions 2 and 4, and +0.75 ± 0.23mm/yr between Solutions 3 and 5, when considering the CGPS estimates, to -0.04 ± 0.25mm/yr between Solutions 2 and 4, and +0.04 ± 0.23mm/yr between Solutions 3 and 5, when considering the AG-aligned CGPS estimates.

From Table 5.10, the reliable AG-aligned CGPS estimates of vertical station velocities for stations in Great Britain show a general pattern in which there are

negative vertical station velocities for the CGPS stations in England (with the exception of CGPS@TG station LIVE at Liverpool tide gauge in North-West England) and the CGPS station LERW close to Lerwick on Shetland, and a zero or slightly positive vertical station velocity for the CGPS@TG station ABER at the Aberdeen tide gauge in East Scotland. Expanding on this, it is possible to supplement the comparisons given in Tables 5.7, 5.8 and 5.9 in Subsection 5.3.2, with comparisons between the 'reliable' AG-aligned CGPS estimates of vertical station velocities for stations in Great Britain and the published changes in land level. These are presented in Tables 5.11, 5.12 and 5.13.

Table 5.11 Comparison of AG-aligned CGPS estimates of vertical station velocities from the national study and published changes in land level based on the GIA model of Lambeck and Johnston (1995)

Station name	4 char station ID	AG-aligned CGPS minus GIA difference in vertical station velocity			
		GAS2.4 DD RNS		BSW5.0 PPP GTS	
		Solution 2 (mm/yr)	Solution 3 (mm/yr)	Solution 4 (mm/yr)	Solution 5 (mm/yr)
Lerwick	LERW	+1.17	+1.30	+1.11	+1.15
Aberdeen TG	ABER	+0.11	0.00		
N. Shields TG	NSTG	-0.97	-1.20	-0.48	-0.26
Liverpool TG	LIVE			+0.55	+0.81
Lowestoft TG	LOWE	-0.97	-0.78	-0.66	-0.67
Sheerness TG	SHEE	-0.59	-0.24	-0.31	-0.27
Portsmouth TG	PMTG	-0.35	-0.29	-0.65	-0.65
Newlyn TG	NEWL	+0.54	+0.34	+0.54	+0.57
Mean		-0.15	-0.12	+0.01	+0.10
Standard Deviation		±0.80	±0.80	±0.71	±0.74

Table 5.12 Comparison of AG-aligned CGPS estimates of vertical station velocities from the national study and published changes in land level based on the GIA model of Peltier (2001)

Station name	4 char station ID	AG-aligned CGPS minus GIA difference in vertical station velocity			
		GAS2.4 DD RNS		BSW5.0 PPP GTS	
		Solution 2 (mm/yr)	Solution 3 (mm/yr)	Solution 4 (mm/yr)	Solution 5 (mm/yr)
Lerwick	LERW	-0.13	0.00	-0.19	-0.15
Aberdeen TG	ABER	-0.49	-0.60		
N. Shields TG	NSTG	-1.37	-1.60	-0.88	-0.66
Liverpool TG	LIVE			-0.15	+0.11
Lowestoft TG	LOWE	-1.07	-0.88	-0.76	-0.77
Sheerness TG	SHEE	-0.89	-0.54	-0.61	-0.57
Portsmouth TG	PMTG	-0.75	-0.69	-1.05	-1.05
Newlyn TG	NEWL	-0.16	-0.36	-0.16	-0.13
Mean		-0.69	-0.67	-0.54	-0.46
Standard Deviation		±0.47	±0.49	±0.37	±0.41

Table 5.13 Comparison of AG-aligned CGPS estimates of vertical station velocities from the national study and published changes in land level based on geological studies (Shennan and Horton 2002)

Station name	4 char station ID	AG-aligned CGPS minus GEOL difference in vertical station velocity			
		GAS2.4 DD RNS		BSW5.0 PPP GTS	
		Solution 2 (mm/yr)	Solution 3 (mm/yr)	Solution 4 (mm/yr)	Solution 5 (mm/yr)
Lerwick	LERW				
Aberdeen TG	ABER	-0.59	-0.70		
N. Shields TG	NSTG	-1.17	-1.40	-0.68	-0.46
Liverpool TG	LIVE			0.45	0.71
Lowestoft TG	LOWE	-0.87	-0.68	-0.56	-0.57
Sheerness TG	SHEE	-0.39	-0.04	-0.11	-0.07
Portsmouth TG	PMTG	-0.25	-0.19	-0.55	-0.55
Newlyn TG	NEWL	+0.64	+0.44	+0.64	+0.67
Mean		-0.44	-0.43	-0.14	-0.04
Standard Deviation		±0.63	±0.64	±0.56	±0.60

From Tables 5.11, 5.12 and 5.13, the mean and standard deviation of the differences between the AG-aligned CGPS estimates of vertical station velocity and the published changes in land level are:

- -0.15 ± 0.80mm/yr, -0.12 ± 0.80mm/yr, +0.01 ± 0.71mm/yr and +0.10 ± 0.74mm/yr when the four solutions are compared to the published changes in land level based on the GIA model of Lambeck and Johnston (1995).
- -0.69 ± 0.47mm/yr, -0.67 ± 0.49mm/yr, -0.54 ± 0.37mm/yr and -0.46 ± 0.41mm/yr when the four solutions are compared to the published changes in land level based on the GIA model of Peltier (2001).
- -0.44 ± 0.63mm/yr, -0.43 ± 0.64mm/yr, -0.14 ± 0.56mm/yr and -0.04 ± 0.60mm/yr when the four solutions are compared to the published changes in land level based on geological studies (Shennan and Horton 2002).

Unlike the consideration of the CGPS estimates of vertical station velocity where only six of the 12 mean differences could be considered zero within the 1-sigma uncertainties, it is clear that when considering the AG-aligned CGPS estimates of vertical station velocity, all 12 of the differences could be considered zero at the 1-sigma level. However, considering all of the individual values given in Tables 5.11, 5.12 and 5.13, it is also clear that the best general agreements for all stations are with the published changes in land level based on the geological studies of Shennan and Horton (2002).

At this stage it is worth noting that we should not necessarily expect perfect agreement between the last decade, as represented by the AG-aligned CGPS estimates of vertical station velocities, and the last 10,000 years, as represented by the published changes in land level based on GIA models and geological studies. Nevertheless, it can be seen that for all four CGPS solutions, the AG-aligned CGPS estimates of vertical station velocity are generally more negative than both Peltier (2001) and Shennan and Horton (2002) for all stations; with the principle exception of the CGPS@TG station NEWL, at Newlyn tide gauge near to Land's End in South-West England, which has AG-aligned CGPS estimates of vertical station velocity which are

consistently less negative than the published change in land level from Shennan and Horton (2002).

This aside, it is reasonable to conclude that the AG-aligned CGPS estimates of vertical station velocity are not systematically offset from the published changes in land level, unlike the CGPS estimates of vertical station velocity which were found to be systematically more positive than the published changes in land level (see Subsection 5.3.2). Hence, the AG-alignment procedure carried out provides an 'engineering solution' from which we can obtain some estimates of changes in sea level (decoupled from changes in land level) based on the approximately 8.5 years of CGPS data and 10 or 11 years of AG data acquired to date, and answer the rephrased question posed at the start of this subsection.

5.4 Estimated changes in land and sea levels for Great Britain

In this section, the AG-aligned CGPS estimates of vertical station velocities are considered to represent changes in land level and these are then combined with changes in sea level in order to compute an estimate for the average change in sea level (decoupled from changes in land level) around the coast of Britain over the past few decades/past century. The changes in land level are then taken forward and combined with future predictions of changes in global sea level to provide an assessment of future changes in relative sea level (i.e. referenced to the local land).

5.4.1 Past changes in land and sea levels

Figures 5.6 and 5.7 show the negative of the 'emergence / subsidence (E/S) rate', which are the AG-aligned CGPS estimates of vertical station velocity given in Tables 5.10 in Subsection 5.3.3, plotted against the 'MSL trends' for the past few decades/past century, which are the changes in sea level given in Table 3.2 of Subsection 3.1.2, based on PSMSL (2005) supplemented with a value for Brest tide gauge in Northern France, based on Woodworth et. al. (1999). The figures are presented in this manner so as to give a positive correlation between the different parameters, and to be consistent with similar plots given in Woodworth et. al. (1999), which used the published changes in land level based on the geological studies of Shennan (1989).

When considering Figure 5.6 it is worth noting that this includes all eight of the CGPS stations listed in Table 5.10 plus the CGPS@TG station BRST at Brest tide gauge in Northern France, i.e. the CGPS@TG station LIVE at Liverpool tide gauge in North-West England is excluded from Solutions 2 and 3 in Table 5.10 but included in Figure 5.6. Similarly, when considering Figure 5.7 it is worth noting that this includes all eight of the CGPS stations listed in Table 5.10, i.e. the CGPS@TG station ABER at Aberdeen tide gauge in East Scotland is excluded from Solutions 4 and 5 in Table 5.10 but included in Figure 5.7.

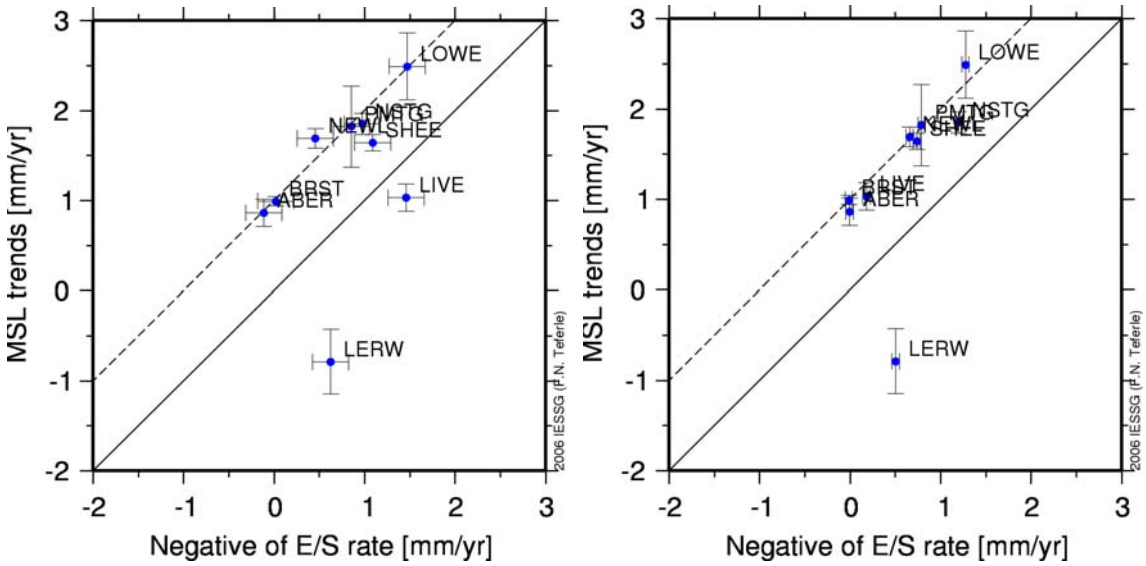

Figure 5.6 Changes in land and sea levels around the coast of Great Britain and Northern France based on AG-aligned CGPS estimates of vertical station velocities from Solution 2 (left) and Solution 3 (right) in the national study

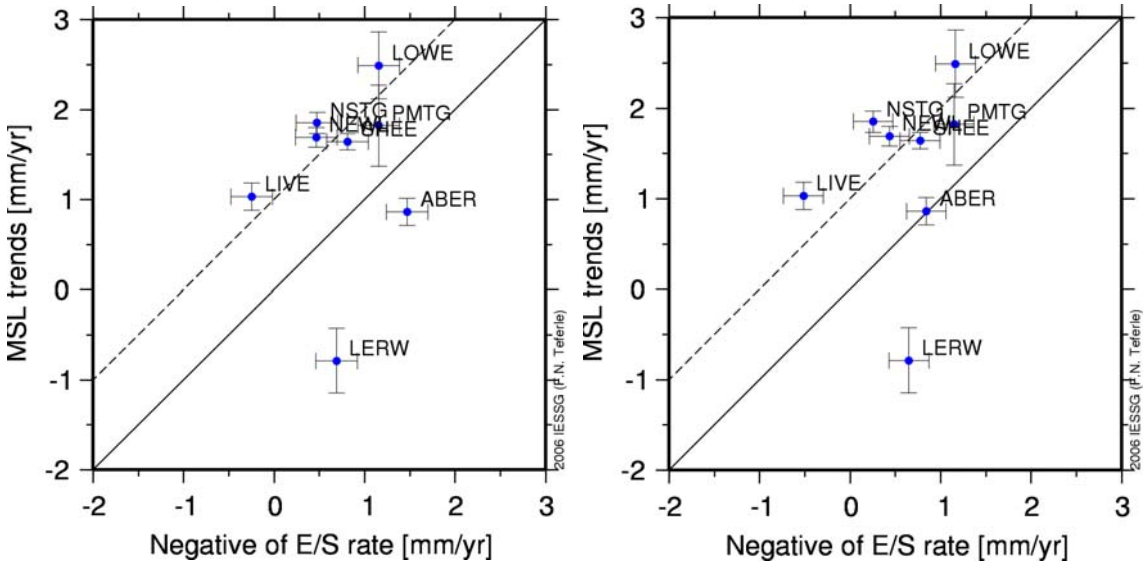

Figure 5.7 Changes in land and sea levels around the coast of Great Britain and Northern France based on AG-aligned CGPS estimates of vertical station velocities from Solution 4 (left) and Solution 5 (right) in the national study

In terms of changes in sea level, just considering the vertical spread of the points in Figures 5.6 and 5.7, these plots graphically present the values given in Table 3.2 of Subsection 3.1.2 and show that, with the exception of Lerwick tide gauge on Shetland, the British tide gauges all show a rise in sea level over the past few decades/past century, with a range of values from 0.86mm/yr at Aberdeen tide gauge in East Scotland to 2.49mm/yr at Lowestoft tide gauge on the East coast of England; Lerwick being exceptional as the tide gauge measurements suggest a fall in sea level, of 0.79mm/yr.

In terms of changes in land level, just considering the horizontal spread of the points in Figures 5.6 and 5.7, and ignoring LIVE in Figure 5.6 and ABER in Figure 5.7, these plots visually confirm the results given in Table 5.10 as showing:

- subsidence (shown by a value greater than zero for the negative of E/S rate) at the non-TG CGPS station LERW, close to Lerwick on Shetland.
- subsidence (shown by a value greater than zero for the negative of E/S rate) at most of the CGPS@TG stations in England: namely NSTG, at North Shields tide gauge in the North-East of England; LOWE, at Lowestoft tide gauge on the East coast of England; SHEE, at Sheerness tide gauge on the Thames Estuary to the East of London; PMTG, at Portsmouth tide gauge on the South coast of England; and NEWL, at Newlyn tide gauge near to Land's End in the South-West of England.
- slight uplift (shown by a value of less than zero for the negative of E/S rate) for the CGPS@TG station ABER, at Aberdeen tide gauge in East Scotland.
- stability or slight uplift (shown by a value of zero or less than zero for the negative of E/S rate) for the CGPS@TG station LIVE, at Liverpool tide gauge in the North-West of England.

In terms of an average change in sea level (decoupled from changes in land level) around the coast of Britain over the past few decades/past century, the solid diagonal line in Figures 5.6 and 5.7 would imply a zero average change; whereas the dashed diagonal line would represent an average change of 1.0mm/yr.

Ignoring LIVE in Figure 5.6 and ABER in Figure 5.7, as being unreliable estimates of changes in land level, the plots clearly show that for LERW, the fall in sea level from the tide gauge measurements is not matched by an uplift in land level from the AG-aligned CGPS estimates of vertical station velocity. In other words, this would seem to suggest that the Lerwick tide gauge measurements are an anomaly specific to this tide gauge, which is worthy of further investigation.

From Figure 5.6, excluding LERW and LIVE, an average sea level rise (decoupled from changes in land level) of 0.9 ± 0.2mm/yr is obtained for both Solution 2 and 3; with a clear agreement between NEWL and BRST, i.e. the changes in land level from the AG-aligned CGPS vertical station velocities clearly account for the 0.7mm/yr difference in the change in sea level obtained from the two sets of tide gauge measurements alone.

From Figure 5.7, excluding ABER and LERW, an average sea level rise (decoupled from changes in land level) of 1.1 ± 0.3mm/yr is obtained for Solution 4 and 1.2 ± 0.8mm/yr is obtained for Solution 5. These are slightly greater than those from Solutions 2 and 3, and all four estimates of average sea level rise (decoupled from changes in land level) are slightly less than the value of 1.3 ± 0.3mm/yr given in Bingley et. al. (2006); based on CGPS and AG data for the period up to the end of 2004 only.

All of these estimates of average sea level rise (decoupled from changes in land level) compare well with previously published estimates such as: Woodworth et

al. (1999), who computed a value of 1.0 mm/yr using changes in sea level based on the annual MSL time series for the period from ~1900-1999 for Aberdeen, Liverpool, Newlyn, North Shields and Sheerness tide gauges, and changes in land level based on the geological studies of Shennan (1989); and Holgate and Woodworth (2004), who computed a value of 1.5 mm/yr, but which specifically considered changes in sea level based on decadal MSL time series for the more recent period from 1948-2002, for tide gauges in the British Isles and along the North Sea coast in Northern Europe, and changes in land level based on a GIA model of Peltier (2001).

Possibly more interesting than this, in view of the AG-alignment procedure used in the national study, are the recent results of Wöppelmann et al. (2007). These are based on a global study of data from CGPS@TG stations and non-TG stations within 10km of a tide gauge. This study used changes in sea level based on annual MSL time series, in a similar way to Woodworth et. al. (1999), but with changes in land level based on CGPS estimates of vertical station velocity. Furthermore, as this study was carried out as part of the IGS Tide Gauge Benchmark Monitoring (TIGA) Project, the CGPS estimates of vertical station velocity were based on a GAMIT Double Difference (DD) Global Network Solution (GNS) in which absolute antenna phase centre variation (PCV) models were used along with a pre-released version of the ITRF2005; effectively a test of something similar to the new IGS data processing strategy. From this study, Woppelmann et. al. (2007) computed a 'best estimate' of global average sea level rise over the past few decades/past century of 1.3 ± 0.3mm/yr; within which were individual estimates of the change in sea level (decoupled from change in land level) at both Aberdeen and Newlyn tide gauges of +0.7 mm/yr.

In conclusion, therefore, our 'best estimates' for the average change in sea level (decoupled from changes in land level) around the coast of Britain over the past few decades/past century of +0.9 to 1.2mm/yr is slightly higher than the Woodworth et al. (1999) value of +1.0 mm/yr and slightly higher than the Wöppelmann et al. (2007) value of +0.7 mm/yr; but all within agreement, really, when considering the uncertainties in the CGPS and AG estimates at the present time. Apart from this, it is comforting that the AG-alignment procedure appears to have led to AG-aligned CGPS estimates of vertical station velocities that are comparable with CGPS estimates of vertical station velocity which are based on something similar to the new IGS data processing strategy.

5.4.2 Future changes in land and sea levels

The changes in land level, used in the previous subsection to look at changes in sea level (decoupled from changes in land level) for the past few decades/past century, can also be combined with future predictions of changes in global sea level to provide an assessment of future changes in relative sea level (with respect to the land) or 'net sea level change'.

In this regard, the UKCIP has previously calculated regional net sea level change estimates for Great Britain, using predictions of future changes in global

sea level and changes in land level based on geological studies. In the UKCIP02 Scientific Report (Hulme et. al. 2002), the predictions of future changes in global sea level were based on (Church et. al. 2001), part of the Third Assessment Report of the IPCC, and the changes in land level were based on Shennan (1989). Since then, these have been updated in November 2005 and August 2006 with the changes in land level based on Shennan and Horton (2002).

An extract from Table 2 from the August 2006 UKCIP update is re-presented below as Table 5.14, which presents the net sea level change (relative to 1961-1990) for Scotland and for some of the administrative regions of England; these being selected and ordered to coincide with the list of CGPS@TG stations used in the national study. In this respect it should be noted that UKCIP does not provide any estimates for Shetland due to the unavailability of information on changes in land level for this region in Shennan and Horton (2002).

Table 5.14 UKCIP updated rates of net sea level change (relative to 1961-1990) for Great Britain, computed from changes in land level based on Shennan and Horton (2002) and the full range of global sea level changes estimated by the Third Assessment Report of the IPCC (UKCIP 2006)

Region	Change in land level (mm/yr)	Net sea level change relative to 1961-1990 (cm)					
		Low Emissions 'Low' IPCC Estimate			High Emissions 'High' IPCC Estimate		
		2020s	2050s	2080s	2020s	2050s	2080s
Scotland	+0.8	0	+1	0	+10	+30	+60
NE England	+0.2	+3	+5	+6	+13	+34	+66
NW England	+0.6	+1	+2	+3	+11	+31	+63
East of England	-0.8	+8	+13	+17	+18	+42	+77
London	-0.8	+8	+13	+17	+18	+42	+77
SE England	-0.5	+6	+11	+14	+16	+40	+74
SW England	-1.0	+9	+15	+20	+19	+44	+80

Table 5.15 presents an alternative to Table 5.14, with the changes in land level based on Shennan and Horton (2002) replaced by the changes in land level based on the 'most reliable' AG-aligned CGPS estimates of vertical station velocity from the national study; these being estimates from Solution 2 for the CGPS@TG stations ABER, LOWE, SHEE, PMTG and NEWL and estimates from Solution 4 for CGPS@TG stations NSTG and LIVE.

Table 5.16 then gives the differences in the values of net sea level change calculated in Tables 5.14 and 5.15.

Table 5.15 UKCIP-style rates of net sea level change (relative to 1961-1990) for Great Britain, computed from changes in land level based on the AG-aligned CGPS estimates of vertical station velocity from the national study and the full range of global sea level changes estimated by the Third Assessment Report of the IPCC

Station name	4 char sta ID	Change in land level (mm/yr)	Net sea level change relative to 1961-1990 (cm)					
			Low Emissions 'Low' IPCC Estimate			High Emissions 'High' IPCC Estimate		
			2020s	2050s	2080s	2020s	2050s	2080s
Aberdeen TG	ABER	+0.11	+3	+6	+8	+13	+35	+68
N. Shields TG	NSTG	-0.48	+6	+11	+14	+16	+40	+74
Liverpool TG	LIVE	+0.25	+3	+5	+6	+13	+34	+66
Lowestoft TG	LOWE	-1.47	+11	+19	+25	+21	+48	+85
Sheerness TG	SHEE	-1.09	+9	+16	+21	+19	+45	+81
Portsmouth TG	PMTG	-0.85	+8	+14	+18	+18	+43	+78
Newlyn TG	NEWL	-0.46	+6	+11	+14	+16	+40	+74

Table 5.16 Difference in UKCIP-style rates of net sea level change (relative to 1961-1990) for Great Britain, depending on whether the changes in land level are based on Shennan and Horton (2002) or the AG-aligned CGPS estimates of vertical station velocity from the national study

Station name	4 char sta ID	Diff. in change in land level (mm/yr)	Difference in net sea level change relative to 1961-1990 (cm)					
			Low Emissions 'Low' IPCC Estimate			High Emissions 'High' IPCC Estimate		
			2020s	2050s	2080s	2020s	2050s	2080s
Aberdeen TG	ABER	-0.69	+3	+5	+8	+3	+5	+8
N. Shields TG	NSTG	-0.68	+3	+6	+8	+3	+6	+8
Liverpool TG	LIVE	-0.35	+2	+3	+3	+2	+3	+3
Lowestoft TG	LOWE	-0.67	+3	+6	+8	+3	+6	+8
Sheerness TG	SHEE	-0.29	+1	+3	+4	+1	+3	+4
Portsmouth TG	PMTG	-0.35	+2	+3	+4	+2	+3	+4
Newlyn TG	NEWL	+0.54	-3	-4	-6	-3	-4	-6

When viewed in this manner, it is clear that the overall effect of replacing the changes in land level based on Shennan and Horton (2002) with changes in land level based on the AG-aligned CGPS estimates of vertical station velocity from the national study is that the net sea level change is increased by a few centimetres in all cases except when considering CGPS@TG station NEWL at Newlyn tide gauge near to Land's End in South-West England where the effect is a decrease of a few centimetres. This is obviously a function of the fact that, with the principle exception of the CGPS@TG station NEWL, the AG-aligned CGPS estimates of vertical station velocity are consistently more negative than the published change in land level from Shennan and Horton (2002), as previously concluded in Subsection 5.3.3.

When considering the predicted changes in global sea level by the 2080s for the high emissions scenario, as these are significantly greater than the changes in land level, such increases or decreases are at the 5 to 13% level of the values given in Table 5.14. However, when considering the same scenario for the 2050s and 2020s, their effect is increased to 7 to 18% and 6 to 30% respectively. Furthermore, when considering the predicted changes in global

sea level for the low emissions scenario, the increases and decreases shown in Table 5.16 have an effect of between 13 and 200%.

Based on this comparison, it can be concluded that, just as there is a wide range of estimates for changes in global sea level from the various IPCC emissions scenarios, subtle differences in estimates of changes in land level at the sub-millimetre per year level can have a significant impact on the net sea level change, particularly when considering the next few decades.

6. Results of the regional study

As stated in the Chapter 1 of this Technical Report, “for the regional study, CGPS and EGPS data from a network of stations in the Thames Region and SAR data for hundreds of thousands of PS points in the Thames Region have been analysed and the changes in land level interpreted using various geoscience data sets.” A background to the regional study was given in Chapter 4, including details on published changes in sea level from Thames tide gauges, the geological setting of the Thames Region, and the tide gauge, GPS, PSI and geoscience data sets used. The results of the regional study are now presented in this chapter, firstly as the independent results from PSI and GPS, then as the results from combining the two techniques, along with AG. After this, the results of geological presentations are given, followed by a summary of the tide gauge results, which all lead to an estimate of the change in sea level (decoupled from changes in land level) along the Thames Estuary and River Thames over the past few decades/past century.

6.1 PSI results

In this section, the independent results from using PSI in the Thames Region are presented. The section starts with details of the specific PSI processing strategy and PS point time series analysis strategy employed, then the PS point time series and line-of-sight velocity estimates are presented.

6.1.1 PSI processing strategy

Details of various PSI processing methods were given in Subsection 2.4.3. For the regional study detailed in this Technical Report, the IPTA, or ‘Interferometric Point Target Analysis’ method , as developed by GAMMA Remote Sensing, Switzerland (Werner et. al. 2003), was used by NPA. As stated in Subsection 2.4.3, “PSI provides a measure of the movement of a PS point relative to a fixed PS point, termed the reference scatterer, in the direction from the PS point on the Earth’s surface to the satellite (i.e. along the line-of-sight to the satellite).”

In the regional study, the output from IPTA was used to create a database of information for each PS point identified, which includes:

- a numeric CODE;
- approximate EASTING and NORTHING coordinates, which are based on geo-referencing accurate to about 15 to 50m and can be presented in Ordnance Survey of Great Britain (OSGB) 1936 National Grid (OSGB36NG);
- approximate HEIGHT above ODN, relative to the assumed height for the reference scatterer;
- the change in satellite-point range at each epoch.

6.1.2 PS point time series analysis strategy

As stated in Subsection 2.4.4, “through PSI processing, the movement of a PS point relative to a reference scatterer, along the line-of-sight to the satellite, can be described as a time series.” Such time series are effectively the changes in satellite-point range considered with respect to time, values of which are included in the database output from IPTA for every PS point identified.

Fitting a best fit linear trend to such time series it is then possible to obtain an estimate of the velocity of a PS point, along the line-of-sight to the satellite, and some measure of uncertainty, as a standard deviation of the epochal satellite-point ranges. These parameters are also output from IPTA and given in the database of information for each PS point identified as:

- VEL, the estimated velocity along the line-of-sight to the satellite;
- ST_DEV, the standard deviation of the epochal satellite-point ranges.

Although IPTA does not give an estimate of the velocity uncertainty, it is possible to obtain an estimate for this based on the standard deviation, using a similar approach to that applied for EGPS estimates of station velocities, and following Equation 2.1 given in Subsection 2.2.4.

6.1.3 PS point time series and PSI estimates of line-of-sight velocity

From the PSI processing, a total of approximately 950,000 PS points across the AOI of 5,323km^2 were identified, which is equivalent to a mean density of approximately 179 PS points per km^2. Time series for 60 epochs between March 1997 and December 2005 were obtained for each one of these PS points, based on a master scene of 24 December 1999. These time series are included in the Project Record as part of a database file. In this Technical Report, an example time series for one of these PS points is given as Figure 6.1, which is a replication of Figure 2.15 given in Subsection 2.4.4, and shows the movement of this PS point relative to the reference scatterer, along the line-of-sight to the satellite, with the 60 estimates shown as blue dots, and the best fit linear trend shown by the black line.

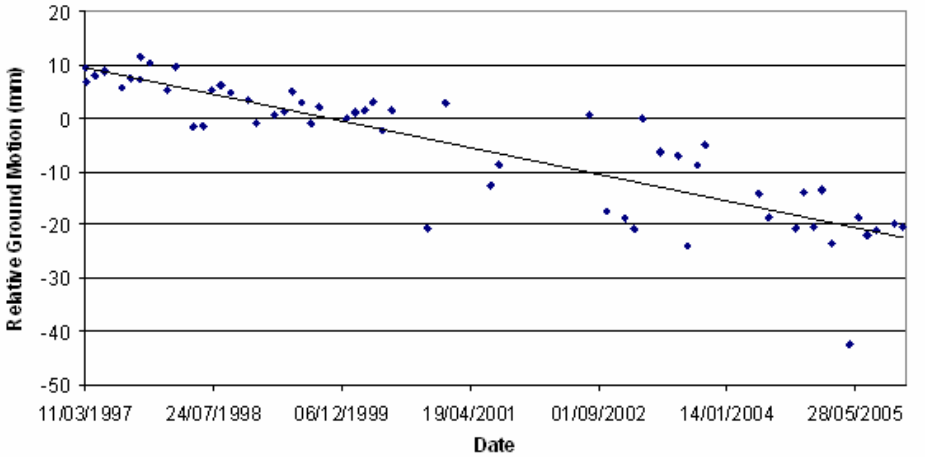

Figure 6.1 Example PS point time series output from the regional study

A summary of the PS point line-of-sight velocities is then given in Table 6.1, in which the velocities have been separated into five 'bins' and the total number of points within each bin is given.

Table 6.1 PS point line-of-sight velocities from the regional study classified into five bins

Line-of-sight velocity bin (mm/yr)		Number of PS points in the bin	% of PS points in the bin
From	To		
-19.96	-3.5	3,174	0.33
-3.5	-1.5	44,375	4.67
-1.5	+1.5	879,840	92.53
+1.5	+3.5	22,938	2.41
+3.5	+11.55	563	0.06

As can be seen from Table 6.1, relative to the reference scatterer, about 93% of all PS points in the AOI have a line-of-sight velocity of within 1.5mm/yr, while 5% have a negative line-of-sight velocity of more than -1.5mm/yr and about 2% have a positive line-of-sight velocity of more than +1.5mm/yr. Considering the whole database, the average line-of-sight velocity for the AOI, relative to the reference scatterer, is -0.14mm/yr with a standard deviation of ±0.89mm/yr which, in turn, would suggest that 95% of the PS points have a line-of-sight velocity within a range from -1.92 to +1.64mm/yr.

On querying the database, it was found that 93% of the PS points have a standard deviation of between 2 and 5mm, with 70% having a standard deviation of between 2 and 4 mm. Considering Equation 2.1 given in Subsection 2.2.4, it is possible to use these ranges of standard deviation to estimate representative values for the uncertainties in the PS point line-of-sight velocities based on a total time span of 8.7 years (from March 1997 to December 2005), and a mean time interval of 0.145 years (as 60 epochs over 8.7 years). In this case, the standard deviations of 2, 3, 4 and 5mm become uncertainties in the line-of-sight velocities of ±0.10, 0.15, 0.20 and 0.25mm/yr.

Figure 6.2 presents the PSI analysis map for the regional study, where the location of the reference scatterer is marked by a black star and the monitoring network of CGPS and EGPS stations, described in Subsection 4.4.2, are marked as red dots. In this figure, each PS point has been colour coded, depending on the velocity of the point along the line-of-sight to the satellite, on a scale of +5mm/yr to -5mm/yr ranging from blue, turquoise, green, yellow, red, where green is around zero.

In terms of coverage, from Figure 6.2, it can be seen that the majority of PS points fall into the urban centre of London, with the measurement density reducing for rural areas towards the East and the edges of the defined AOI, which are mainly vegetated areas with a lack of scatterers to form sufficient PS points. In terms of the CGPS and EGPS stations, with the exception of the EGPS@TG station SOPR at Southend tide gauge and the EGPS station GRAI on the Isle of Grain, all other stations have some PS points in close proximity.

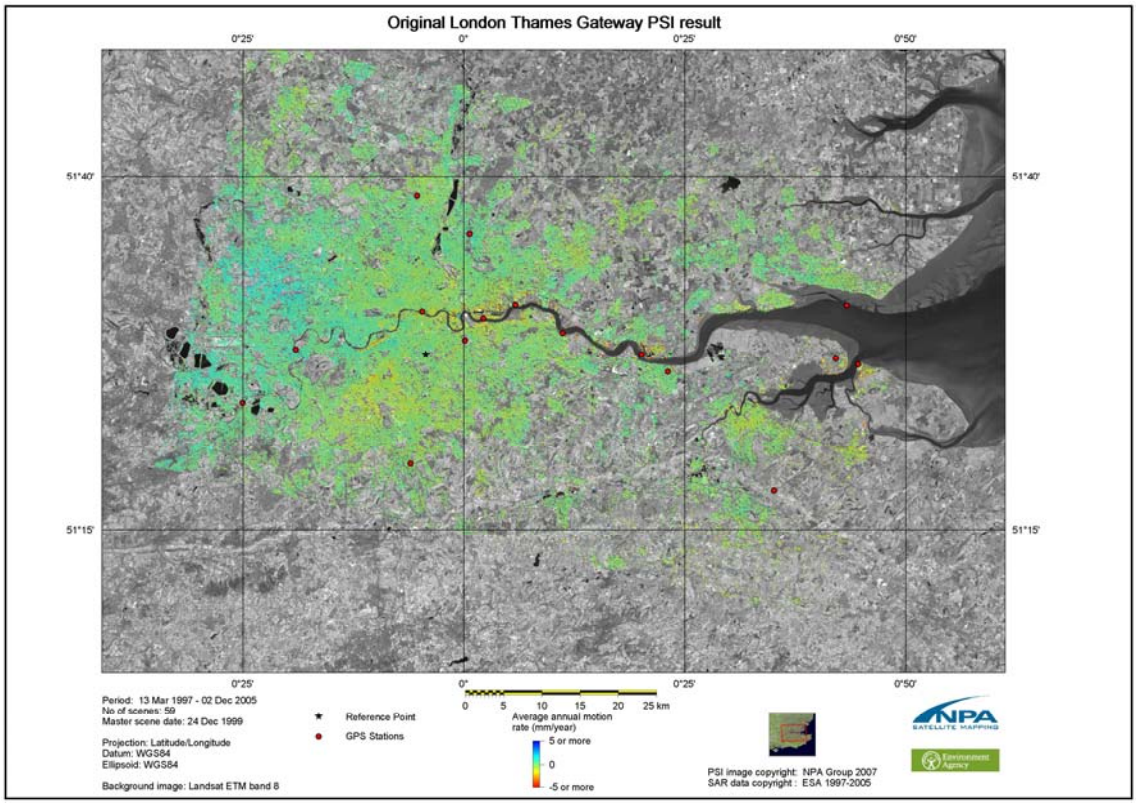

Figure 6.2 PSI analysis map showing the line-of-sight velocities for the 950,000 PS points in the regional study

In terms of line-of-sight velocities, Figure 6.2 effectively confirms the results given in Table 6.1, with the predominance of green being consistent with the statistic that 93% of all PS points over the AOI have a line-of-sight velocity of within 1.5mm/yr, with respect to the reference scatterer. Apart from these there is: a concentration of turquoise (slightly more positive line-of-sight velocities) to the West and North-West of the Thames Region; concentrations of yellow (slightly more negative line-of-sight velocities) along the River Thames and to the South of the River Thames in Central London; and a clear, linear feature in red (significantly more negative line-of-sight velocities) relating to the subsidence around the Jubilee Line extension and the Battersea area. These 'anomalies' are discussed in more detail in Section 6.4 as part of the geological interpretations carried out for the regional study.

6.2 GPS results

In this section, the independent results from using GPS in the Thames Region are presented. The section starts with details of the specific EGPS data processing strategies and EGPS coordinate time series analysis strategies employed, then the CGPS and EGPS coordinate time series and vertical station velocity estimates are presented.

6.2.1 EGPS data processing strategies

For the regional study, epochal RINEX format observation data from Thames region EGPS stations were processed, along with corresponding data from the CGPS stations, to produce epochal coordinate estimates (latitude, longitude and ellipsoidal height) using two different strategies.

The only difference between the two strategies was in the reference frame definition employed. For the regional study, this was effected through the inclusion of the three CGPS stations in the Thames Region, namely: Barking Barrier, Sheerness tide gauge and Sunbury Yard, as reference stations. In the first strategy, these three CGPS stations were constrained based on their station coordinates and velocities in ITRF2000, as computed in Solution 2 from the national study; hence, the coordinates of the Thames region EGPS stations were also estimated in the ITRF2000 at the epoch of their observation. Whereas, in the second strategy, the three CGPS stations were constrained to their station coordinates given in the European Terrestrial Reference System 1989 (ETRS89) at epoch 1989.0, as published through BIGF; hence, the coordinates of the Thames region EGPS stations were also estimated in the ETRS89 at epoch 1989.0.

Apart from this, in both strategies, to maintain consistency with the processing for the national study, the following common options relating to the mitigation of systematic errors were employed:

- the IGS final products, including satellite coordinates, satellite clocks and Earth orientation parameters, were used to mitigate satellite-related systematic errors.
- the final solution was based on the ionospherically free observable, to mitigate the atmospheric-related systematic errors from the ionosphere.
- the final solution included a standard tropospheric model and the inclusion of zenith delay parameters as additional unknowns, to mitigate the atmospheric-related systematic errors from the troposphere.
- the IGS_01.pcv relative receiver-antenna PCV models (i.e. assuming zero PCVs for the Dorne-Margolin choke ring receiver-antennas employed) were used, to mitigate the station-related systematic errors from this effect.
- corrections for solid Earth tides were applied based on the IERS 2000 standards, to mitigate the station-related systematic errors from this loading process.
- corrections for ocean tide loading were applied based on the IERS 2000 standards and coefficients from the FES99 ocean tide loading model, made available through the IAG, to mitigate the station-related systematic errors from this loading process.

Furthermore, in both strategies, the processing was based on a series of epochal GAS2.4 DD RNSs, i.e. ‘Double Difference Regional Network Solutions’, for the period from March 1997 to December 2005.

6.2.2 EGPS coordinate time series analysis strategies

As stated in Subsection 2.2.3, “coordinate time series are a data set of changes in coordinates with respect to time.” For the regional study, the outputs from the first EGPS data processing strategy can be used to form coordinate time series, based on the ITRF2000 coordinates (latitude, longitude and ellipsoidal height) estimated at the epoch of observation, for each of the Thames region EGPS stations.

Here it should be noted that, due to their nature, the outputs from the second EGPS data processing strategy were not used to form coordinate time series but were simply used to obtain average ETRS89 e1989.0 coordinates for each of the Thames region EGPS stations. These are given in the Project Record along with the corresponding OSGB36NG coordinates and heights above ODN, based on Ordnance Survey Transformation 2002 (OSTN02) and Ordnance Survey Geoid Model 2002 (OSGM02), and new heights above ODN for the tide gauge benchmarks at each of the tide gauges used in the regional study.

As we are primarily interested in the vertical station velocities and their uncertainties when considering changes in land level, the ITRF2000 height time series for each station were analysed using MS-Excel software to obtain a best fit linear trend, from which estimates of vertical station velocity were inferred. A white noise (random error) only model was then assumed in order to compute the standard deviation of the individual height estimates, from which an estimate of the velocity uncertainty was obtained using Equation 2.1 given in Subsection 2.2.4.

6.2.3 CGPS and EGPS coordinate time series and estimates of vertical station velocity

The CGPS coordinate time series for the three CGPS stations in the Thames Region are included in the Project Record as both text files of changes in three-dimensional coordinates and graphics of the height time series and the EGPS coordinate time series for the EGPS stations in the Thames Region are included in the Project Record as MS-Excel files (containing worksheets and charts). In this Technical Report, the height time series for the three CGPS stations in the Thames Region, based on Solution 2 from the national study are presented graphically in Appendix C, and the height time series for the 13 EGPS stations in the Thames Region, based on the first EGPS data processing strategy, are presented graphically in Appendix D.

As described in Subsection 2.2.4, the CGPS height time series plots show the changes in height from day to day as green dots, any coordinate offsets accounted for as dashed vertical lines and the best fit linear plus periodic trend as a blue line; whereas the EGPS height time series plots show the change in height from epoch to epoch as red dots, and the best fit linear trend as a black line.

The height time series for the three CGPS stations, namely BARK, which is on the Barking Barrier in the centre of the Thames Region, SHEE, which is at the Sheerness tide gauge on the Thames Estuary, East of London, and SUNB, which is at the Environment Agency's Sunbury yard to the West of London, are re-presented in this section as Figure 6.3.

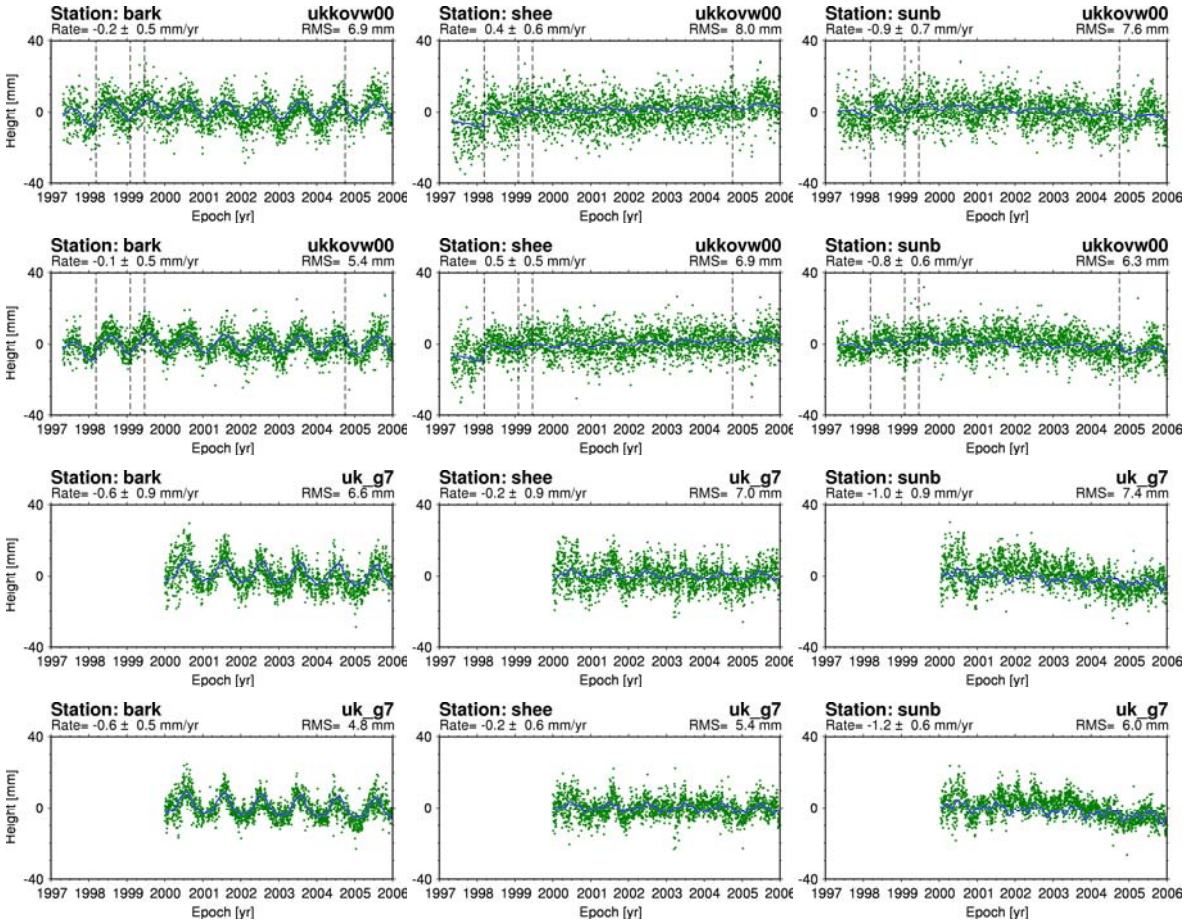

Figure 6.3 CGPS height time series from Solutions 2, 3, 4 and 5 for the three CGPS stations in the regional study

As with the national study (see Section 5.1.3), Figure 6.3 shows that: the uncertainties in the CGPS estimates of vertical station velocity are at the level of 0.5 to 1.0mm/yr for these time series, which are all 8.7 years in length; a comparison of Solutions 2 and 3 or 4 and 5 shows the effect of spatial filtering with the RMS values reducing; a comparison of Solutions 2 and 4 or 3 and 5, show the systematic offset between the use of GAS2.4 DD RNS and BSW5.0 PPP GTS, with the estimates of vertical station velocity based on GAS2.4 DD RNS being more positive than the estimates based on BSW5.0 PPP GTS. Apart from this, there is a clear annual signal in the CGPS height time series for BARK, which appears to have a maxima in the summer and a minima in the winter, and is most likely related to thermal expansion of the 40m concrete structure which forms the West Tower of the Barking Barrier and on which the GPS antenna is located. Here it is important to note that, along with other less visible but statistically significant periodic signals in the time series, this will

have been modelled as part of the MLE and should not have an effect on the vertical station velocity for this station.

The RMS values for the CGPS height time series, and the CGPS estimates of vertical station velocities and their uncertainties, from Solutions 2, 3, 4 and 5 for the three CGPS stations in the Thames Region are summarised in Tables 6.2 and 6.3.

Table 6.2 RMS values for the CGPS height time series from Solutions 2, 3, 4 and 5 for the three CGPS stations in the regional study

Station name	4 char station ID	CGPS height time series RMS value			
		GAS2.4 DD RNS		BSW5.0 PPP GTS	
		Solution 2 (mm)	Solution 3 (mm)	Solution 4 (mm)	Solution 5 (mm)
Barking Barrier	BARK	6.9	5.4	6.6	4.8
Sheerness TG	SHEE	8.0	6.9	7.0	5.4
Sunbury Yard	SUNB	7.6	6.3	7.4	6.0

Table 6.3 CGPS estimates of vertical station velocities and uncertainties from Solutions 2, 3, 4 and 5 for the three CGPS stations in the regional study

Station name	4 char station ID	CGPS vertical station velocity and uncertainty			
		GAS2.4 DD RNS		BSW5.0 PPP GTS	
		Solution 2 (mm/yr)	Solution 3 (mm/yr)	Solution 4 (mm/yr)	Solution 5 (mm/yr)
Barking Barrier	BARK	-0.21 ± 0.54	-0.12 ± 0.46	-0.59 ± 0.89	-0.64 ± 0.50
Sheerness TG	SHEE	+0.43 ± 0.60	+0.53 ± 0.50	-0.22 ± 0.93	-0.21 ± 0.63
Sunbury Yard	SUNB	-0.92 ± 0.67	-0.83 ± 0.60	-1.04 ± 0.92	-1.16 ± 0.63

Considering the results presented in Tables 6.2 and 6.3 it is clear that BARK and SUNB are of a similar high quality to SHEE and to the other five CGPS stations considered to have reliable estimates of vertical station velocity in the national study (see Subsection 5.1.3). Considering the CGPS vertical station velocities in a relative sense it can be seen that the estimates for SHEE are more positive than the estimates for BARK by 0.64, 0.65, 0.37 and 0.43mm/yr and that the estimates for SUNB are more negative than the estimates for BARK by 0.71, 0.71, 0.45 and 0.52mm/yr. Based on these levels of agreement and uncertainty, the three CGPS stations were considered to have 'well-determined' station coordinates and velocities, and those computed in Solution 2 were used in the production of the EGPS station coordinate time series for the Thames Region, as detailed in Subsections 6.2.1 and 6.2.2.

The height time series for the 13 EGPS stations in the Thames Region, based on the first EGPS data processing strategy, are presented graphically in Appendix D. An example time series for one of these EGPS stations, Silvertown TG (SILV) in the Thames Barrier North Bank Compound, is given as Figure 6.4, with the epochal height estimates shown as red dots and the best fit linear trend shown by the black line.

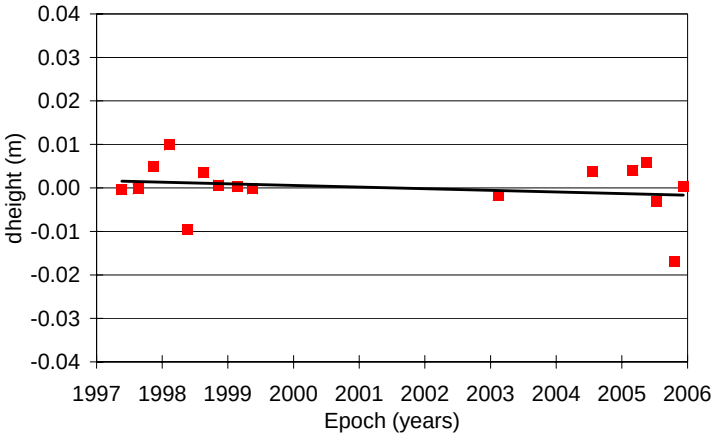

Figure 6.4 Example EGPS height time series output from the regional study

The standard deviation values for the EGPS height time series are summarised in Table 6.4, which presents the statistics for the two separate periods of EGPS measurements (1997/1999 and 2003/2005) and for the complete period (1997/2005) for the 13 EGPS stations.

Table 6.4 Standard deviation values for the EGPS height time series for the 13 EGPS stations in the regional study

Station name	4 char. station ID	Number of acceptable epochal solutions			Height standard deviation (mm)		
		1997 / 1999	2003 / 2005	1997 / 2005	1997 / 1999	2003 / 2005	1997 / 2005
Bush Hill	BPGC	8	6	14	10.4	11.7	11.2
Erith TG	ERIT	9	7	16	13.8	7.4	11.6
Gravesend	GGSC	9	7	16	9.4	7.9	8.9
Grain	GRAI	9	7	16	8.4	16.7	16.7
Greenwich Park	GRPK	9	7	16	2.8	6.6	4.7
Mill Plane	MIPL	9	7	16	9.2	7.3	8.8
Richmond TG	RICH	9	7	16	9.4	10.5	9.6
Riddlesdown	RIDD	9	7	16	10.9	6.4	9.0
Silvertown TG	SILV	9	7	16	5.2	7.7	6.3
Southend TG	SOPR	8	6	14	7.6	16.0	12.5
Thurnham	THUR	9	7	16	10.1	6.8	8.8
Tilbury TG	TILB	9	3	12	8.8	2.2	7.5
Tower Pier TG	TOPR	9	N/A	N/A	6.4	N/A	N/A

A few issues are highlighted (with grey shading) in Table 6.4:

- For BPGC, two epochal solutions were rejected as statistical outliers;
- For GRAI, the increased standard deviation values for 2003/2005 is due to the station being affected by local subsidence due to quarrying activity which started to the North of the site in late 2003;
- For SOPR, the increased standard deviation values for 2003/2005 are due to the station being affected by local subsidence during and following the engineering works on the pier in 2003, and the reduced number of solutions for 1997/1999 and 2003/2005 due to inaccessibility of the pier (the latter being due to a fire on the pier in September 2005);
- For TILB, the reduced number of solutions for 2003/2005 is due to problems with data quality at this station, since mid-2005.

- For TOPR, there were no solutions for 2003/2005 due to the station being destroyed some time between 1999 and 2003

Leaving these issues aside, the general pattern is of overall standard deviations of between 8 and 12mm, with the exception of GRPK and SILV which have even better values of 5 to 6mm. These are generally at a level that is similar or slightly higher than the 'equivalent' RMS values for the CGPS height time series presented in Table 5.2 in Subsection 5.1.3; which can be attributed to the shorter (9 as oppose to 24 hour) observation sessions used, countered by the scale of the monitoring network of CGPS and EGPS stations in the Thames Region being much smaller than the scale of the equivalent monitoring network of CGPS and IGS stations used in the national study.

The homogeneity of each EGPS height time series can be further assessed by comparing the estimate of vertical station velocity based on a best fit linear trend for the complete period with a 'nominal' vertical station velocity computed from the difference between the mean height for the 1997/1999 EGPS measurements and the mean height for the 2003/2005 EGPS measurements, divided by the nominal time period. The results of this assessment are presented in Table 6.5, which also includes estimates of the vertical station velocity uncertainty based on Equation 2.1 given in Subsection 2.2.4, and using the standard deviation values from Table 6.4 along with a total time span of 8.7 years (from March 1997 to December 2005), and a mean time interval of 0.544 years (as 16 epochs over 8.7 years).

Table 6.5 Vertical station velocity comparison for the EGPS height time series for the 13 EGPS stations in the regional study

Station name	4 char. station ID	Difference (2003/2005 minus 1997/1999) in mean height (mm)	Difference (linear minus nominal) in vertical station velocity (mm/yr)	Vertical station velocity uncertainty (mm/yr)
Bush Hill	BPGC	7.9	0.01	1.02
Erith TG	ERIT	-6.6	-0.10	1.06
Gravesend	GGSC	-5.1	-0.07	0.81
Grain	GRAI	-22.1	-0.24	1.52
Greenwich Park	GRPK	-1.7	-0.09	0.43
Mill Plane	MIPL	-6.5	0.01	0.80
Richmond TG	RICH	-1.7	-0.10	0.87
Riddlesdown	RIDD	1.2	-0.24	0.82
Silvertown TG	SILV	-2.1	-0.06	0.57
Southend TG	SOPR	-9.7	0.12	1.13
Thurnham	THUR	-4.0	-0.19	0.80
Tilbury TG	TILB	0.4	0.31	0.69
Tower Pier TG	TOPR	N/A	N/A	N/A

From Table 6.5, it can be seen that the maximum difference between the two velocity estimates is 0.31mm/yr and, when considering all stations, the mean difference is -0.05 ± 0.16mm/yr. This test confirms that the two different periods of EGPS measurements do form homogeneous EGPS height time series. The final column in Table 6.5, however, shows that the relatively small number of measurements, when compared to the 60 epochs obtained from PSI, leads to

uncertainties in any vertical station velocity estimates at the ±0.43 to 1.06mm/yr level rather than the 0.10 to 0.25mm/yr level of PSI.

6.2.4 AG-aligned CGPS and EGPS estimates of vertical station velocity

As the EGPS estimates of vertical station velocity were effectively constrained by the CGPS estimates of vertical station velocity for the three CGPS stations in the Thames Region, namely Barking Barrier (BARK), Sheerness tide gauge (SHEE) and Sunbury Yard (SUNB), their absolute values will be affected by the same issues as those considered in the national study. It follows, therefore, that the best, current estimates for the vertical station velocities of the CGPS and EGPS stations in the Thames Region can be obtained by using the same AG-alignment procedure as that used in the national study.

The AG-aligned CGPS and EGPS vertical station velocities and their uncertainties, for the three CGPS stations and 12 of the 13 EGPS stations in the Thames Region are summarised in Table 6.6.

Table 6.6 AG-aligned CGPS and EGPS estimates of vertical station velocities and uncertainties for the three CGPS stations and the 13 EGPS stations in the regional study

Station name	4 char station ID	AG-aligned CGPS vertical station velocity and uncertainty (mm/yr)	Station name	4 char station ID	AG-aligned EGPS vertical station velocity and uncertainty (mm/yr)
Barking Barrier	BARK	-1.73 ± 0.58	Bush Hill	BPGC	-0.26 ± 1.02
Sheerness TG	SHEE	-1.09 ± 0.64	Erith TG	ERIT	-2.50 ± 1.06
Sunbury Yard	SUNB	-2.44 ± 0.70	Gravesend	GGSC	-2.26 ± 0.81
			Grain	GRAI	-5.00 ± 1.52
			Greenwich Park	GRPK	-1.77 ± 0.43
			Mill Plane	MIPL	-2.38 ± 0.80
			Richmond TG	RICH	-1.77 ± 0.87
			Riddlesdown	RIDD	-1.48 ± 0.82
			Silvertown TG	SILV	-1.79 ± 0.57
			Southend TG	SOPR	-2.76 ± 1.13
			Thurnham	THUR	-2.21 ± 0.80
			Tilbury TG	TILB	-1.04 ± 0.69
			Tower Pier TG	TOPR	N/A

The highlighted (with grey shading) results in Table 6.6 are stations which are not suitable for long-term studies of changes in land level for various reasons:

- For BPGC, from experience in making EGPS measurements at this station, it is now considered that this station is affected by very local ground movement, which may be linked to shrink/swell or ‘waterlogging of the monument’;
- For GRAI, the station has definitely been affected by local subsidence due to quarrying activity which started to the North of the site in late 2003;
- For SOPR, the station has definitely been affected by local subsidence during and following the engineering works on the pier in 2003;
- For TOPR, the station was destroyed some time between 1999 and 2003.

For the other stations, the results given in Table 6.6 show a general pattern of negative vertical station velocities in the range from -1.04 to -2.50mm/yr, with the average vertical station velocity for the 12 reliable CGPS/EGPS stations being -1.87mm/yr with a standard deviation of ±0.50mm/yr.

6.3 Combined AG, GPS and PSI results

PSI produces estimates of velocity for dense networks of PS points in urban environments, with no requirements to go 'into the field', however, for studies of long term changes in ground level:

- the PSI estimates presented in Section 6.1 are given with respect to a reference scatterer, i.e. they are relative;
- unlike GPS and AG, which directly measure vertical station velocities, the PSI estimates presented in Section 6.1 are velocities of the PS points along the line-of-sight to the satellite;
- unlike GPS and AG, where monitoring is carried out with reference to a physical, survey marker, the physical nature of PS points is largely unknown, e.g. is it a lamppost, a building or natural bedrock?

For the purposes of comparing the GPS and PSI results and for the geological interpretations to be carried out as part of the regional study, the objective was to create estimates of velocity for the dense network of PS points that were effectively estimates of changes in ground level in the 'AGGPS TRF' realised through the national study. This was carried out in three stages: firstly a classification of the PS points close to the CGPS/EGPS stations, followed by the calculation of a 'shift' to convert the line-of-sight velocities given with respect to the reference scatterer to AGGPS-aligned PSI estimates of vertical velocities for the PS points, followed by the application of this shift to all PS points in the database output from IPTA.

6.3.1 Classification of PS points close to the CGPS/EGPS stations

In order to rigorously compare the estimates of vertical station velocity for the CGPS and EGPS stations (obtained in Section 6.2) with the estimates of line-of-sight velocity (obtained in Section 6.1) for PS points close to the CGPS/EGPS stations, it was necessary to consider whether the local geological conditions at the PS points are the same as the local geological conditions at the specific CGPS/EGPS station. This was effected by considering the locations of the PS points on aerial photographs and BGS large scale geological maps; although it is not possible to identify the exact location and, therefore, the physical nature of a PS point, due to the spatial resolution of the radar images making the identification of the 'dominant scatterer' inside a resolution cell ambiguous.

To achieve this, all PS points within an area of 400x400m centred on each CGPS/EGPS station, were extracted from the database output from IPTA. The PS points within 300m plan distance of the CGPS/EGPS station were then classified into five categories and colour coded, as detailed in Table 6.7, where the final column was a special category based on local knowledge of the site.

Table 6.7 Classification criteria for the PS points close to CGPS/EGPS stations used in the regional study

Classification colour code	Plan distance from PS point to CGPS/EGPS station	PS point considered to have the same local geological conditions as CGPS/EGPS station?	PS point considered to most likely represent the velocity of the CGPS/EGPS station?
blue	100-300m	No	-
bold blue	100-300m	Yes	-
green	< 100m	No	-
bold green	< 100m	Yes	-
bold red	< 100m	Yes	Yes

The number of PS points, within each classification colour code, close to each CGPS/EGPS station are presented in Table 6.8, in which the 'best PS points' for each station are indicated by grey shading.

Table 6.8 The number of PS points close to each CGPS/EGPS station in the regional study, based on the classification criteria

Station name	**4 char. station ID**	**Classification colour code**				
		blue	**bold blue**	green	**bold green**	**bold red**
Barking Barrier	BARK	4			9	2
Sheerness TG	SHEE	9			8	
Sunbury Yard	SUNB	22	26	3	8	3
Station name	**4 char. station ID**	**Classification colour code**				
		blue	**bold blue**	green	**bold green**	**bold red**
Bush Hill	BPGC	2	11			
Erith TG	ERIT	1				
Gravesend	GGSC	9	8	4	2	1
Grain	GRAI					
Greenwich Park	GRPK		1		2	
Mill Plane	MIPL		22		1	
Richmond TG	RICH	5	1		1	1
Riddlesdown	RIDD		18			5
Silvertown TG	SILV	7	5		1	3
Southend TG	SOPR					
Thurnham	THUR	1	3			
Tilbury TG	TILB	3	3			
Tower Pier TG	TOPR	49	4	8		1

Considering Table 6.8, it is clear that Barking Barrier (BARK), Sunbury Yard (SUNB), Riddlesdown (RIDD) and Silvertown TG (SILV) are the only CGPS/EGPS stations with more than one PS point coded as bold red, i.e. being less than 100m in distance from; considered to have the same local geological conditions as; and considered to most likely represent the velocity of, the CGPS/EGPS station.

6.3.2 AGGPS-aligned PSI estimates of vertical velocity

For the calculation of a shift to convert the line-of-sight velocities given with respect to the reference scatterer to AGGPS-aligned vertical velocities for PS points, it was decided to use EGPS station RIDD, as this was founded directly on Chalk and had the most PS points coded as bold red, i.e. also founded directly on Chalk, within 100m of the EGPS station and considered unlikely to experience differential movements due to local geological conditions.

To calculate the shift, the line-of-sight velocities for the five best PS points close to RIDD were first converted to vertical velocities on the assumption that all of the velocity is due to changes in land level, i.e. there is no relative horizontal movement between the reference scatterer and the PS point. This was effected by accounting for the zenith angle of the satellite (approximately 23 degrees), which changed the velocity values by about 10%. Then, the average vertical velocity was calculated based on the five best PS points for that station, and found to be -0.82mm/yr with a standard deviation of ±0.57mm/yr. This was compared to the AG-aligned EGPS estimate of vertical station velocity of -1.48 ± 0.82 mm/yr and a shift of -0.66mm/yr calculated. As a check on this alignment procedure, average AGGPS-aligned PSI estimates of vertical velocity for the PS points close to each CGPS/EGPS station, as identified in Table 6.8, were calculated and compared to the AG-aligned CGPS and EGPS estimates of vertical station velocity, as presented in Table 6.6. The results of this test are presented in Table 6.9, in which the uncertainty on the average AGGPS-aligned PSI estimates of vertical velocity is based on the standard deviation of the individual velocities where more than one PS point was available.

Table 6.9 AG-aligned CGPS and EGPS estimates of vertical station velocities and uncertainties compared to average AGGPS-aligned PSI estimates of vertical velocity for PS points close to each of the three CGPS stations and the 13 EGPS stations in the regional study

Station name	4 char station ID	AG-aligned CGPS/EGPS vertical station velocity and uncertainty (mm/yr)	Average AGGPS-aligned PSI vertical velocity and uncertainty (mm/yr)	Difference (mm/yr)
Barking Barrier	BARK	-1.73 ± 0.58	-1.53 ± 0.34	+0.20
Sheerness TG	SHEE	-1.09 ± 0.64	-1.01 ± 0.94	+0.08
Sunbury Yard	SUNB	-2.44 ± 0.70	-2.13 ± 0.35	+0.31
Bush Hill	BPGC	-0.26 ± 1.02	-0.13 ± 0.47	+0.13
Erith TG	ERIT	-2.50 ± 1.06	-2.64 ± N/A	-0.14
Gravesend	GGSC	-2.26 ± 0.81	-1.37 ± N/A	+0.89
Grain	GRAI	-5.00 ± 1.52	N/A	N/A
Greenwich Park	GRPK	-1.77 ± 0.43	-1.64 ± 1.67	+0.13
Mill Plane	MIPL	-2.38 ± 0.80	-1.29 ± N/A	+1.09
Richmond TG	RICH	-1.77 ± 0.87	-1.22 ± N/A	+0.55
Riddlesdown	RIDD	-1.48 ± 0.82	-1.48 ± 0.57	0.00
Silvertown TG	SILV	-1.79 ± 0.57	-1.24 ± 0.17	+0.55
Southend TG	SOPR	-2.76 ± 1.13	N/A	N/A
Thurnham	THUR	-2.21 ± 0.80	-2.27 ± 0.29	-0.06
Tilbury TG	TILB	-1.04 ± 0.69	-0.86 ± 0.33	+0.18
Tower Pier TG	TOPR	N/A	-0.42 ± N/A	N/A

When considering the 12 difference values calculated in Table 6.9, the differences between the average AGGPS-aligned PSI estimates of vertical velocity for the PS points close to each CGPS/EGPS station and the AG-aligned CGPS and EGPS estimates of vertical station velocity has a range from -0.14 to +1.09 mm/yr and a mean of +0.33mm/yr, with a standard deviation of ±0.37mm/yr, when careful consideration is given to the classification and selection of the PS points to consider.

Further considering the results in Table 6.9, as there would appear to be no degradation in the difference values with increasing distance from RIDD this can be taken as a confirmation that the application of a single, constant shift was adequate to effectively convert the PSI results from relative to absolute.

Based on this, for every PS point in the database output from IPTA, an AGGPS-aligned PSI estimate of vertical velocity was calculated by converting from line-of-sight to vertical and then applying a shift of -0.66mm/yr. These are considered further in the geological interpretations in Section 6.4; however, the overall effect is summarised in Table 6.10, which is an update on Table 6.1, and presents a summary of the AGGPS-aligned PSI estimates of vertical velocity for the PS points, in which the velocities have been separated into six bins and the total number of points within each bin is given.

Table 6.10 AGGPS-aligned PSI estimates of vertical velocity for PS points in the regional study classified into six bins

Vertical velocity bin (mm/yr)		Number of PS points in the bin	% of PS points in the bin
From	To		
-19.96	-3.5	7,836	0.82
-3.5	-1.5	182,151	19.17
-1.5	0.0	598,538	62.98
0.0	+1.5	154,299	16.24
+1.5	+3.5	7,183	0.76
+3.5	+11.55	368	0.04

As can be seen from Table 6.10, in an absolute sense, about 83% of all PS points in the AOI have a negative AGGPS-aligned vertical velocity, with 63% having a negative velocity of within 0 to -1.5mm/yr. Considering the whole database, the average vertical velocity for the AOI is -0.80mm/yr with a standard deviation of ±0.89mm/yr which, in turn, would suggest that 95% of the PS points have a vertical velocity within a range from -2.58 to +0.98mm/yr.

Figure 6.5 presents the AGGPS-aligned PSI analysis map for the regional study, where the location of the reference scatterer is marked by a black star and the monitoring network of CGPS and EGPS stations, described in Subsection 4.4.2, are marked as red dots. As with Figure 6.2 in Subsection 6.1.3, in this figure, each PS point has been colour coded, depending on the vertical velocity of the point, on a scale of +5mm/yr to -5mm/yr ranging from blue, turquoise, green, yellow, red, where green is around zero.

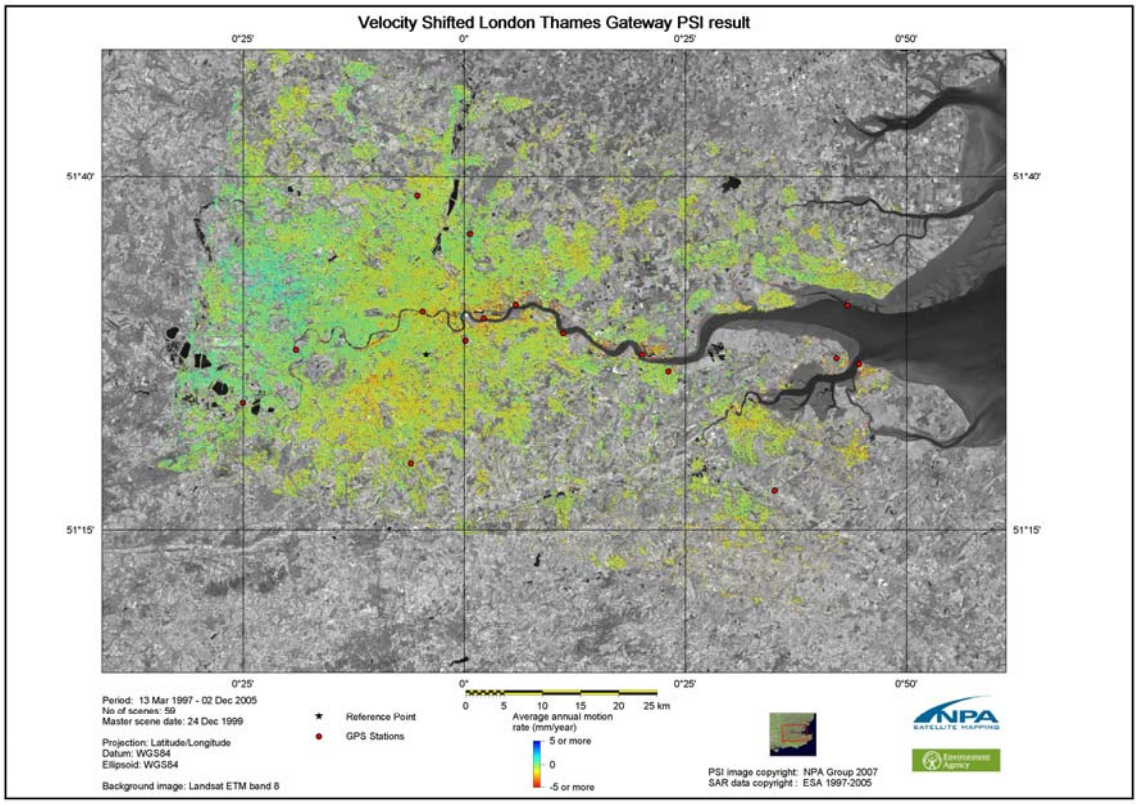

Figure 6.5 AGGPS-aligned PSI analysis map showing the vertical velocities for the 950,000 PS points in the regional study

Figure 6.5 effectively confirms the results given in Table 6.10, with the predominance of yellow being consistent with the statistic that 63% of all PS points over the AOI have an AGGPS-aligned vertical velocity of within 0 to -1.5mm/yr. Apart from these there is: a concentration of turquoise (positive vertical velocities) to the West and North-West of the Thames Region; concentrations of yellow/red (negative vertical velocities) along the River Thames and to the South of the River Thames in Central London; and a clear, linear feature in red (significantly more negative velocities) relating to the subsidence around the Jubilee Line extension and the Battersea area. These 'anomalies' are discussed in more detail in Section 6.4 as part of the geological interpretations carried out for the regional study.

6.4 Geological interpretations

As stated in Section 4.6, considering the geological setting and the various processes that affect changes in land level in the Thames Region along with the anticipated spatial density of the PS points within the AOI, specific geoscience data sets were used by BGS to enable the interpretation of any changes in land level, as part of the regional study detailed in this Technical Report. These data sets include digital geological maps and geohazard data, 3-D models of Holocene and Peat thickness, regional groundwater level data and geophysical data, as described in Subsections 4.6.1 to 4.6.5 inclusive.

6.4.1 Initial interpretations, domains and general domains

As stated in Subsection 6.3.2, an AGGPS-aligned PSI estimate of vertical velocity was calculated for every PS point in the database output from IPTA, which also includes approximate (15 to 50m) coordinates for each PS point presented in OSGB36NG.
The geological interpretations were based on a comparison of the AGGPS-aligned PSI estimates with the geoscience data sets, within the ArcMap 9.1 GIS. Clearly, to compare all 950,000 or so PS points individually was not feasible so an approach was adopted whereby the AGGPS-aligned PSI estimates of vertical velocity were initially plotted by BGS in several ways within the GIS:

- As various scatter plots, with values grouped into different classes (some with a selected range of data, e.g. all values between +1 and –1 mm/year, hidden); and coloured in different ways.
- As various smoothed grids (some with a selected range of data hidden) based on average values within an array of 50m cells, using IDW (Inverse Distance Weighting) over a radius of 250m or 'nearest neighbour' criteria.

These plots showed that the average changes in land level for the 8.7 year period considered (March 1997 to December 2005) were far from being evenly distributed, with some areas having mainly undergone uplift, some areas having mainly undergone subsidence and some areas presenting a 'stippled effect' where PS points indicating uplift and subsidence were approximately balanced. In order to simplify the process of interpretation and also to help ensure that the AGGPS-aligned PSI estimates of vertical velocity were interpreted in a reasonably consistent manner, a variety of these plots were inspected to identify 'domains' of approximately uniform, average AGGPS-aligned PSI estimates of vertical velocity, and to note lineaments within the data distribution. This is analogous to processes employed in the geological interpretation of satellite images.

In this respect, although different plots tended to enhance different aspects of the distribution of velocity estimates, a reasonably consistent pattern emerged and domain boundaries could be defined. Here it should be emphasised that the delineation/identification of the domains and lineaments was, except very locally, undertaken without reference to the geoscience datasets. In a few places, the domain boundaries were subsequently modified when considering some specific features at larger scales (e.g. 1:50,000), but this was not done systematically.

The resultant domains are shown in Figure 6.6. As described, these domains were identified based on a qualitative, visual inspection of graphic data plots; however, once defined, they were substantiated by compiling statistics for each domain using the GIS. These statistics are presented in Table 6.11 which shows the number of PS points within each domain along with the average AGGPS-aligned PSI estimates of vertical velocity for that domain, its standard deviation and the minimum and maximum values within.

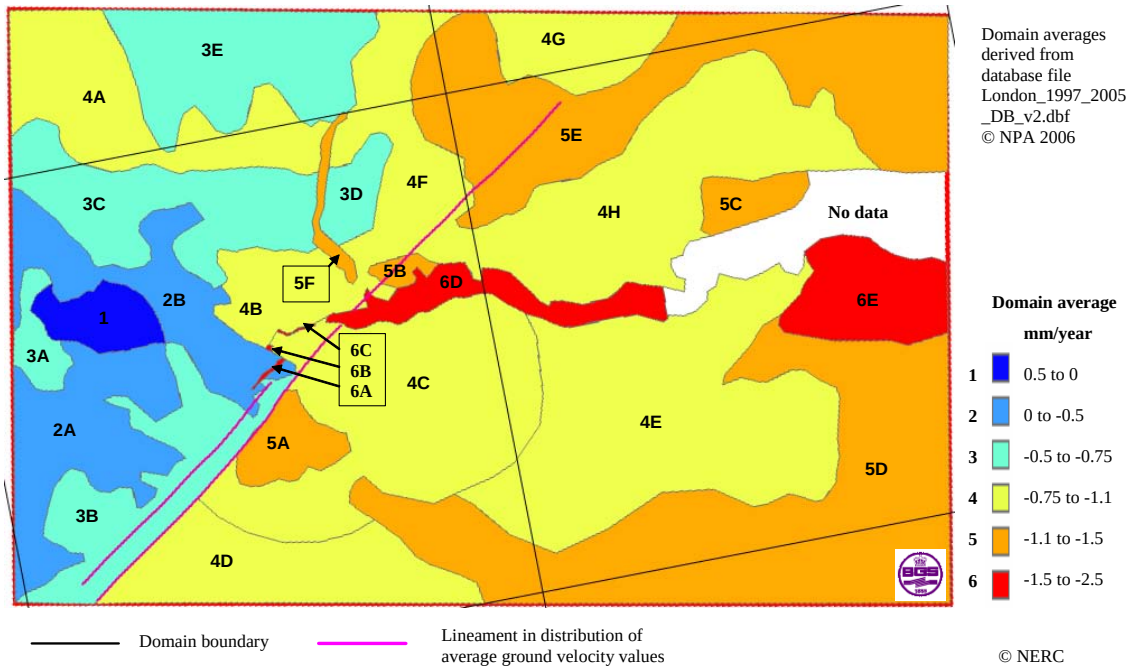

Figure 6.6 Domains of approximately uniform, average AGGPS-aligned PSI estimates of vertical velocity identified in the regional study

Table 6.11 Summary statistics for PS points within each domain identified in the regional study

Domain	Number of PS points	AGGPS-aligned PSI estimates of vertical velocity (mm/yr)			
		Average	Standard Deviation	Minimum	Maximum
1	23,632	+0.34	±0.83	-7.51	+9.16
2A	66,802	-0.11	±0.82	-10.51	+6.11
2B	79,863	-0.34	±0.86	-10.67	+10.91
3A	10,304	-0.55	±0.83	-9.06	+4.78
3B	59,741	-0.61	±0.80	-12.96	+6.44
3C	81,264	-0.68	±0.80	-12.89	+11.89
3D	18,893	-0.53	±0.81	-12.24	+10.34
3E	27,166	-0.59	±0.86	-11.75	+9.74
4A	36,318	-1.02	±0.82	-11.89	+6.53
4B, 4F, 4H	163,667	-0.86	±0.84	-15.02	+11.37
4C	171,691	-1.06	±0.81	-13.78	+9.74
4D	26,180	-0.98	±0.84	-14.80	+8.47
4E	52,884	-0.86	±0.88	-15.35	+10.37
4G	2,963	-1.04	±0.90	-12.74	+3.31
5A	31,955	-1.55	±0.83	-16.68	+8.63
5B	6,271	-1.18	±0.84	-6.45	+3.85
5C	5,441	-1.31	±1.07	-10.75	+3.35
5D	34,844	-1.49	±0.91	-20.59	+4.52
5E	28,991	-1.23	±0.83	-10.34	+8.61
5F	3,398	-1.30	±0.95	-5.59	+5.27
6A	1,066	-2.06	±1.34	-6.93	+2.50
6B	272	-2.43	±0.87	-5.10	-0.22
6C	655	-2.25	±1.56	-9.33	+1.27
6D	14,090	-1.99	±1.87	-22.34	+6.58
6E	3,322	-2.05	±1.64	-15.23	+4.34

As illustrated in Figure 6.6 and Table 6.11, the domains of approximately uniform, average AGGPS-aligned PSI estimates of vertical velocity were ranked

from 1 to 6, with individual areas within each rank given suffix letters to assist reference. From the figure and table, the following comments can be made:

- Domain 1 has a positive average vertical velocity, indicating that it has probably experienced uplift, in general;
- Domains 4, 5 and 6 have a negative average vertical velocity and mainly negative vertical velocities, indicating that they have experienced subsidence, in general;
- Domains 2 and 3 also have a negative average vertical velocity, indicating that on the whole these domains have also undergone subsidence, but these domains are of intermediate and mixed character, with some parts having undergone subsidence and some uplift.

Here it should be stated that these are general comments as, considering the uncertainties in the AG, CGPS, EGPS and PSI results presented thus far, it is not really possible to make any conclusions regarding velocities of less than 0.5 mm/yr magnitude. With this in mind, therefore, it is possible that Domain 1 could be uplifting more, while Domain 2 is slightly uplifting and Domain 3 is stable, or that Domain 1 could be stable or slightly subsiding while Domains 2 and 3 are definitely subsiding. Nevertheless, the occurrence of net uplift in Domain 1 is supported by some aspects of the local Quaternary geology, as noted in Subsection 6.4.2.

As the analysis for the geological interpretations proceeded, it became apparent that some of the smaller domains are probably controlled by processes acting locally and at relatively shallow levels (i.e. within 100m of the surface). If these domains are disregarded, then a more generalised pattern of average AGGPS-aligned PSI estimates of vertical velocity can be discerned, as shown in Figure 6.7, in which the domains identified in Figure 6.6 are overlain by five general domains, denoted Gi to Gv and separated by the purple lines.

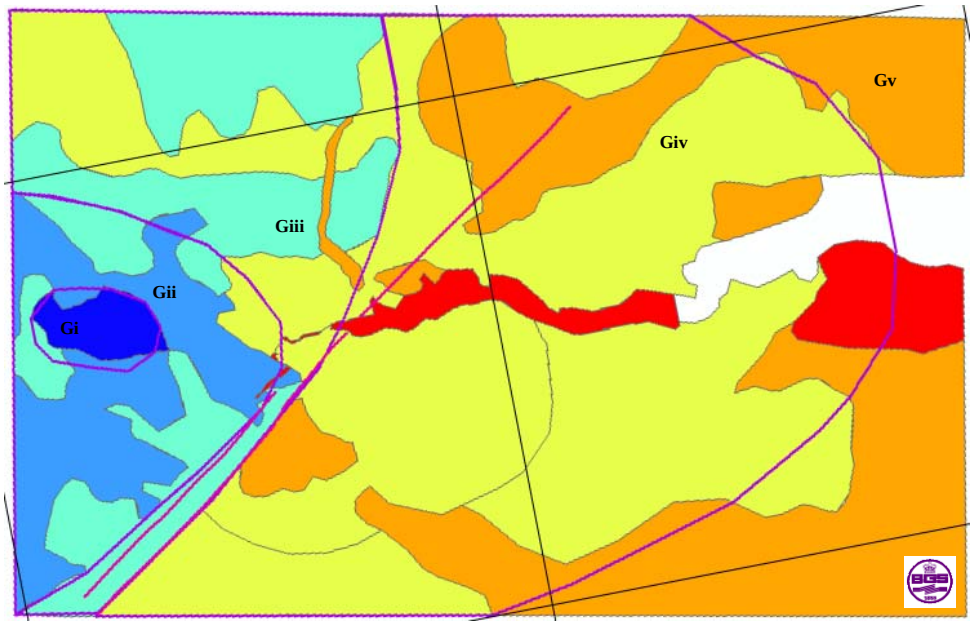

Figure 6.7 General domains of approximately uniform, average AGGPS-aligned PSI estimates of vertical velocity identified in the regional study

In Figure 6.7, the velocities are presumed to approximate to a more regional pattern of changes in land level, in which Domain Gi appears to be undergoing uplift, on the whole, Domains Giv and Gv appear to be subsiding, and Domains Gii and Giii could be experiencing slight subsidence, or neither subsidence nor uplift. Interestingly, this generalised pattern of average AGGPS-aligned PSI estimates of vertical velocity bears little apparent relation to 'near-surface' geology but, as discussed in Subsection 6.4.2, can be correlated with elements of the deeper geological structure.

6.4.2 Results of comparisons with geoscience datasets

For the more detailed geological interpretations, both the domain maps of uniform, average AGGPS-aligned PSI estimates of vertical velocity presented in the previous subsection and, at larger scales, the AGGPS-aligned PSI estimates of vertical velocity for individual PS points were systematically compared with the various geoscience datasets described in Subsections 4.6.1 to 4.6.5 inclusive by BGS. Comparison was undertaken visually on a 19" VDU, using the GIS to display selected datasets at various scales (between about 1:420,000 and 1:20,000), as appropriate.

Not all of the geoscience datasets showed any correlation with the AGGPS-aligned PSI estimates of vertical velocity, and some apparent variations in velocity could not be attributed to known geological variation. Indeed, in some cases, no correlation was to be expected. For example, although running sand, dissolution, collapsible deposits and slope stability (natural geohazards assessed by the GeoSure themes, see Subsection 4.6.1) can cause significant subsidence, the ground movements tend to be very localised. Separately, although shrink-swell behaviour of clays can also give rise to significant changes in land level (up to about 50mm would be usual) over quite wide areas, the movement is reversible and can be observed to follow seasonal variations in precipitation (Bingley et. al. 1999), so no systematic change in land level due to this phenomenon would necessarily be expected over 8.7 years worth of seasonal cycles; it might be, however, that some of the local heterogeneity in the AGGPS-aligned PSI estimates of vertical velocity for individual PS points reflects local variations in land level due to shrink-swell. Furthermore, some of the geoscience datasets could not be fully evaluated because of there being too few relevant PS points, e.g. landslide deposits tend not to be built on, hence very few PS points coincide with mapped landslides.

The remainder of the discussion in this subsection, therefore, deals only with the geoscience datasets which showed positive correlations with the domains and generalised domains of uniform, average AGGPS-aligned PSI estimates of vertical velocity. In this respect, some degree of correlation was found with the following five phenomena:

- Distribution of compressible ground;
- Fall in groundwater level in the Chalk-Thanet Sand aquifer;
- Faulting within the Wimbledon to Greenwich tectonic zone;
- Geological basement structures;
- Artificially modified ground.

In each case, either Figure 6.6 or Figure 6.7 given in the previous subsection are re-presented to aid the discussions.

Distribution of compressible ground

Compressible deposits are susceptible to either local or regional subsidence, due either to self-loading or imposed loading. Two types of compressible deposits are recognised in the London area: Holocene deposits, which occur alongside rivers and estuaries, and 'made ground', which can include poorly consolidated landfill, for example. Holocene deposits can also undergo significant shrinkage through desiccation of the topmost few metres of sediment. This tends to occur in areas where Holocene deposits have been protected from flood and is not significantly reversible.

Where Holocene deposits are most extensive and generally thick, there is a clear correlation between areas prone to subsidence and compressible ground. Domains 5F, 6D, 5C and 6E coincide with extensive areas of Holocene deposits in the valleys of the Lea, Thames and Medway (other extensive areas of Holocene deposits have few coincident PS points). Here it is important to note that Domains 6A, 6B and 6C, and Domains 5A and 5B do not coincide with occurrences of Holocene deposits (see discussions on fall in groundwater level and artificially modified ground, below).

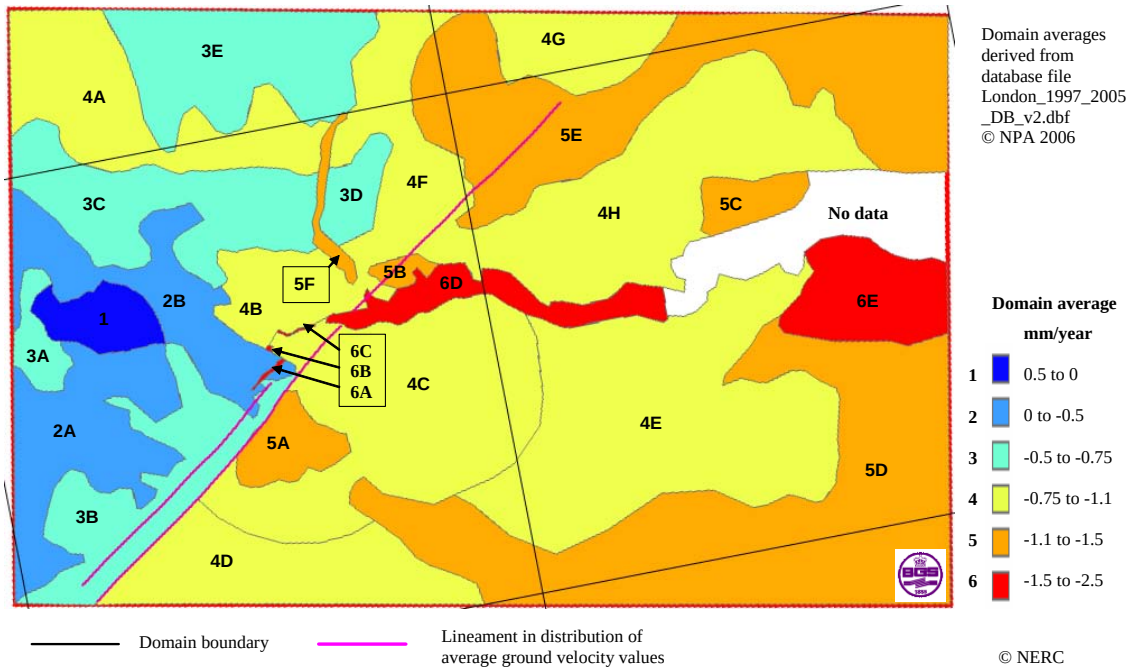

Figure 6.6 (re-presented) Domains of approximately uniform, average AGGPS-aligned PSI estimates of vertical velocity identified in the regional study

The distribution of PS points within the area of the two 3-D models of Holocene thickness (see Subsection 4.6.2) is very uneven, with their density tending to be least where the Holocene sequence is thickest. However, where the Holocene is in the range of up to 20m thick, there seems to be no correlation between sediment thickness and the amount of subsidence based on velocity values.

Conversely, in the upper parts of river catchments, including the River Thames upstream of Tower Bridge, where alluvium can be expected to be less than 5m thick, in general, areas of Holocene deposits show essentially the same range and distribution of velocity values as in surrounding areas.

Most of the data points for peat thickness lie in areas where PS points are relatively sparse. Where concentrations of the two datasets coincide, then no clear correlation between peat thickness and average velocity can be seen. For example, the general rate of subsidence is less in the Erith Marshes than in the West Thurrock Marshes, and around Tilbury, although the range of thickness of peat is similar in each area. Conversely, in the Thames Haven area, just west of Canvey Island, the rate of subsidence appears similar to that of West Thurrock, but the peat is generally thinner.

Where PS points coincide with potentially compressible made ground or infilled ground, no consistent contrast in average velocity can be seen, compared with adjacent areas. There are some areas of apparent average uplift (up to about 1mm/year) or relatively slight subsidence within the Thames Holocene deposits. These anomalous areas occur where there is extensive building on areas of made ground and may be attributed to the alluvium (and overlying made ground) reaching its effective limit of compression, or the presence of deep piles rendering the building not susceptible to compression of the alluvium.

Fall in groundwater level in the Chalk-Thanet Sand aquifer

As described in Subsection 4.6.3, for the regional study, the EA groundwater level maps for January 2006 and January 1997 were each obtained as a digital grid, and the older data was subtracted from the younger. The resultant grid, representing the overall change in groundwater level during a period approximately corresponding to the period of the GPS and PSI data sets, was then compared with the domains of uniform, average AGGPS-aligned PSI estimates of vertical velocity.

The most striking correlation occurs in the Merton area of south-west London, where groundwater levels have been lowered by at least 30m since 1995, as a consequence of abstraction at public water supply boreholes. The largest negative anomaly is centred close to the Merton Abbey public water supply well, one of a number of sites in this part of the London area where water is abstracted from the Chalk at depths in excess of 70m. Depression of the water table in this area can be seen in the record of an observation borehole at Springfield Hospital, about 2.3 km north of Merton Abbey well (Environment Agency 2005). The area of depressed groundwater level around Merton coincides with Domain 5A, as illustrated in Figure E1 in Appendix E. No other explanation for the existence of this domain has been identified.

The north-west edge of Domain 5A is coincident with the Wimbledon Fault (see below). The north-west edge of the area of lowered groundwater is aligned with the same structure, and with the major lineaments in average velocity distribution shown on Figure 6.6, although the low resolution of the groundwater level data does not necessarily reveal the true extent of the cone of depression

around this pumping station. Nevertheless, it appears that fractures parallel to the Wimbledon Fault are exerting some control on groundwater movement.

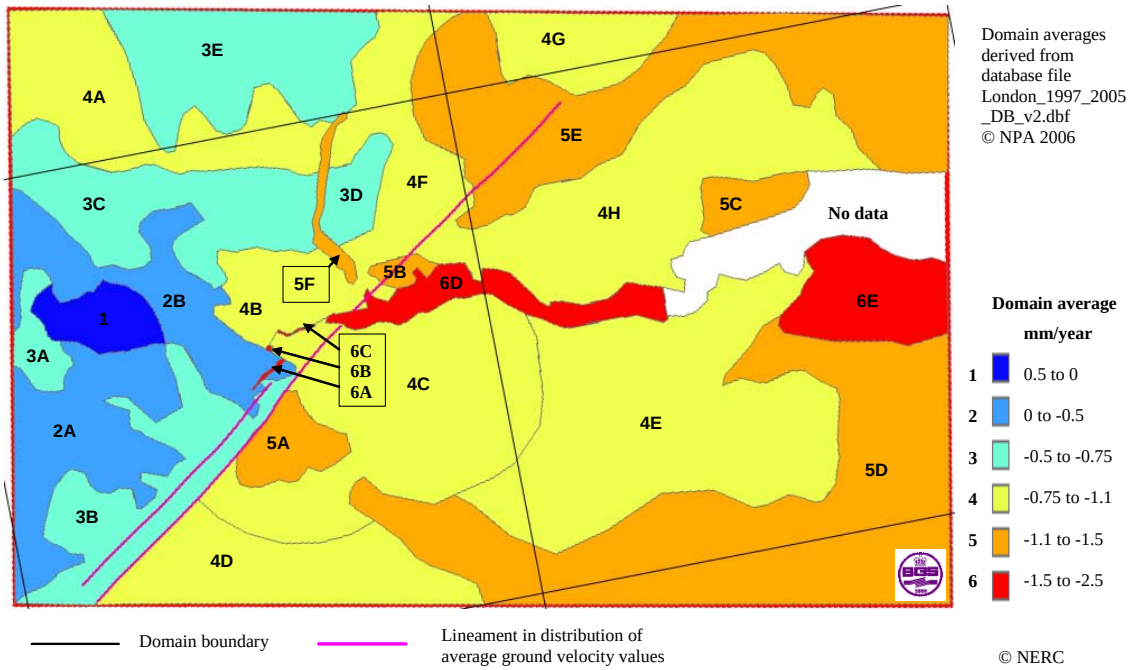

Figure 6.6 (re-presented) Domains of approximately uniform, average AGGPS-aligned PSI estimates of vertical velocity identified in the regional study

A smaller anomaly, to the north-east of Merton, coincides with the Honor Oak pumping station. This also extracts water from the Chalk aquifer at a depth of about 70m. No subsidence closely associated with Honor Oak can be discerned in the AGGPS-aligned PSI estimates of vertical velocity. However, some ill-defined areas of subsidence in Domain 4C might be related to groundwater abstraction, particularly where the aquifer is deeply covered by younger deposits.

Large-scale dewatering of the Thanet Sand Formation associated with the construction of the Channel Tunnel Rail Link took place between Stratford and East Ham during 2001- 2004. The net groundwater lowering of between 5 and 10 m in this area is partly associated with this operation and partly with groundwater abstraction for public water supply. Domain 5B, in which negative velocity is somewhat greater than in adjacent parts of Domain 4F (which has a similar geology) appears to coincide with part of this zone of groundwater depression. The north-westerly extent of Domain 5B is close to the major lineament in average velocity distribution, and so is likely to have been controlled by faults, in an analogous manner to that found in Domain 5A. No faults have been mapped at surface in this position but faulting in the London Clay under London is known to be significantly more extensive than mapped, and the coincidence of the portion of the velocity data lineament in Domain 5B with an abrupt lateral change in the gravity field (see below) indicates the probable presence of major faults at depth.

There is another, weaker, correlation between groundwater change and the domains north of London, where the eastern portion of Domain 4A (east of Borehamwood) extending east of the Lea Valley into the northern part of Domain 4F, corresponds to a zone in which groundwater level has dropped, relative to the levels within the adjacent Domains 3C and 3E. Note that the western portion of Domain 4A, in which groundwater levels have risen, corresponds to a region where the Chalk aquifer is unconfined (i.e. it is not covered by Palaeogene deposits) allowing more direct aquifer recharge. The groundwater levels in the unconfined Chalk declined significantly during dry weather in 1995 and 1996 but have since recovered.

Small areas of greatest net groundwater recovery (more than 15m rise), especially those in the south-west of the area, tend to coincide with areas with few PS points. This is possibly a consequence of enhanced recharge in less built-up areas, which have a smaller proportion of surface sealing. The other areas all occur at the edge of the data grid, and could reflect poor data coverage. Overall, little evidence for uplift associated with groundwater recovery can be seen.

Faulting within the Wimbledon to Greenwich tectonic zone

Linear discontinuities, trending north-east to south-west, are apparent in the distribution of the domains of uniform, average AGGPS-aligned PSI estimates of vertical velocity in Figure 6.6. The relative abruptness of the change in average velocity apparent at these lineaments suggests that they are controlled by faults at a relatively shallow level, probably at rockhead. If a change were marking a structure at a deeper level, a more diffuse change would be expected. Indeed, this may be the case in the north of the area, where the major lineament becomes less well-defined.

These lineaments are sub-parallel to the nearby *en echelon* swarm of faults which has been mapped in south-west London: principally the Wimbledon, Streatham and Greenwich faults (Ellison et. al. 2004). The Wimbledon Fault is downthrown on its south-east side; the other two are down-thrown in the opposite sense.

Part of the more extensive lineament is coincident with part of the Wimbledon Fault, and the north-west margin of Domain 5A is partly bounded by the Wimbledon Fault. As noted above, the same fault zone also appears to control the north-western extent of Domain 5B. It is also noteworthy that the width of the Thames floodplain increases markedly downstream of this major lineament, as shown by the outcrop of the Holocene deposits. This implies a sense of ‘down to the south-east’ neotectonic motion on faults parallel to the Wimbledon and Greenwich faults (‘neotectonic’ refers to earth movements on currently active faults and more generally to those post-dating the main Alpine period of mountain-building, in mid-Cainozoic times). If correct, this finding implies that additional sub-parallel faults, so far unmapped, lie north-west of the Greenwich Fault.

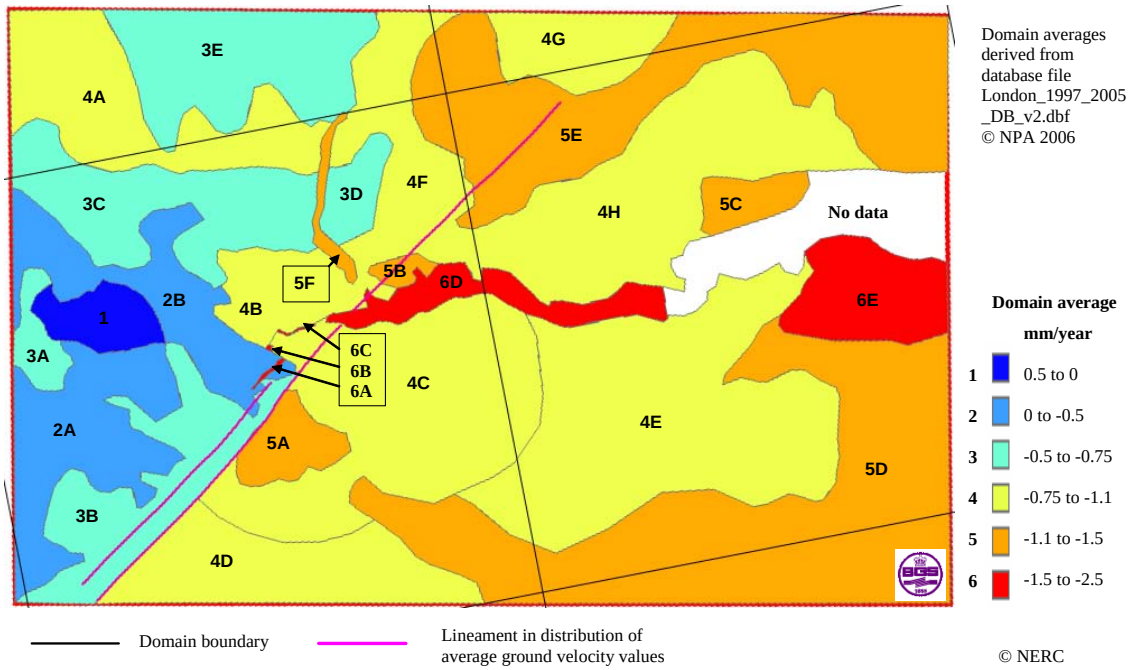

Figure 6.6 (re-presented) Domains of approximately uniform, average AGGPS-aligned PSI estimates of vertical velocity identified in the regional study

These correlations demonstrate local control of the patterns of average ground velocity by near-surface tectonic structures. They imply that some differential ground movement has been accommodated by neotectonic movement on the Wimbledon Fault, and probably also on sub-parallel, unmapped faults.

Geological basement structures

Figure E2 in Appendix E shows a colour shaded relief image of the regional gravity field with the AOI of the PSI data set superimposed (as a red rectangle). The gravity field is displayed as a variable density residual Bouguer anomaly map where the gravity field has been upward continued to 10 km and then removed from the primary field to emphasise the near surface structure. Red represents a gravity 'high' (mass of underlying rock is greater than average) and blue represents a gravity 'low' (mass of underlying rock is less than average)

Regional geophysical surveys, supported by information from seismic reflection profiles and boreholes, show that the AOI is underlain by portions of three geological terranes within the pre-Mesozoic basement. The north-western part of the area is underlain by the Midlands Microcraton, an area where Proterozoic rocks occur at relatively shallow depths, and which has been relatively tectonically stable during the Phanerozoic. Structural trends are complex. The north-eastern part of the area is underlain by a portion of a Caledonide fold belt, formed during mid-Palaeozoic times, in which the dominant structural trends are north-west to south-east. The southern part of the area includes the northern margin of a Variscan fold belt, formed in late Palaeozoic times. This terrane is represented by arcuate structural trends, oriented approximately east-west (Pharaoh et. al. 1993).

Domains Gi and Gii (see Figure 6.7) coincide with a gravity high within the Midlands Microcraton, in the west of the area, as illustrated in Figure E2 in Appendix E. There is no correlation between these domains and any feature of near-surface bedrock geology. The south-east margin of Domains Gii and Giii lie parallel to the lineament in the average velocities, to the Wimbledon Fault, and to the faulted south-east margin of the Midlands Microcraton, as illustrated in Figure E2 in Appendix E. This correlation implies that in the London area, isostatic uplift is confined within the Midlands Microcraton, with the extent of differential movement between Gii, Giii and Giv being controlled by deep-seated tectonic structures.

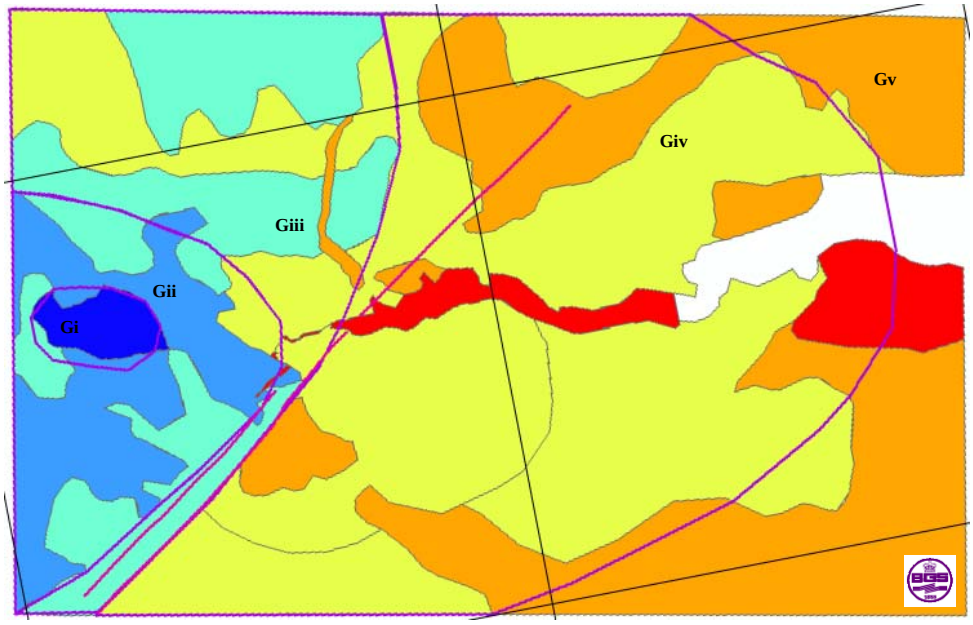

Figure 6.7 (re-presented) General domains of approximately uniform, average AGGPS-aligned PSI estimates of vertical velocity identified in the regional study

The cause of the isostatic uplift in Domain Gi (and perhaps in Gii) is not certain. The coincidence of Gi with the centre of the gravity high implies a causative relationship. The gravity high indicates the presence of relatively dense rocks, relatively close to the surface. These are likely to be of Early Palaeozoic or Proterozoic age, forming a ridge between Late Palaeozoic basins to the north-east and south-west. The presence of this ridge implies a zone of relative tectonic uplift, apparently enhanced at its south-eastern end by interaction with uplift at the faulted margin with the Devonian basin under south London. The presence of Domain Gi indicates that the tectonic structures that control the position of the ridge have in some way been reactivated at the present time.

The contrast in relative movement between Domains Gii and Giii (slight subsidence or possible slight uplift), compared with the somewhat greater rate of subsidence in Domains Giv and Gv, is possibly a consequence of net erosion during the Quaternary in the middle and upper Thames Basin (Bridgland 2006) and further to the west (Watts et. al. 2005); alternative hypotheses are noted in those papers. In this connection, it may be noted that Domain Gi has few superficial deposits. In this respect it is similar to portions of Domains 2B, 3C

and 4B, to the north, although not to Domains 2A, 3A, and 3B to the south and east, which largely coincide with river valleys.

Indeed, it should be noted that although the River Thames flows generally eastwards across the Palaeogene outcrop in the London Basin, between Windsor and Chiswick its course traces a broad loop by about 10 km southwards. The area within this loop is underlain by unusually broad outcrops of the Taplow Gravel and the Kempton Park Gravel, which form two of the lowest river terrace deposits. This relationship suggests that uplift centred on Domain Gi has occurred during deposition of these river terraces, in the later part of the Quaternary, so diverting the River Thames southwards.

The course of the River Colne also appears to be anomalous, in that it flows south-west and then south before joining the Thames. The south-westerly flowing portion follows a pre-glacial valley. However, it seems possible that the course of the southerly-flowing portion (which might be expected to flow south-eastwards, like the Colne's north-western tributaries) is in part controlled by uplift of Domain Gi.

Several other correlations between Domain boundaries and basement structures suggest that some elements of the regional changes in land level are controlled in a general way by neotectonic movement on deep-seated structures. The eastern edge of Domain Giv approximately follows the margin of the large gravity lows in the centre of the project area and the north-eastern portion of Domain Giv follows the Caledonide structural trend. Some parts of the south-eastern margin of Domain 4E coincide with basement structures highlighted by the horizontal gradient analysis, and the north-eastern margin of Domain 4H likewise follows structural elements within the Caledonide fold belt. There is also an approximate correlation between the generalised domains and the regional aeromagnetic anomalies.

Artificially modified ground

A linear zone of subsidence (Domain 6C) between London Bridge station and Green Park, previously identified by NPA, has been associated with part of the route of the Jubilee Line Extension.

A similar zone of subsidence, some several hundred metres wide, occurs in Battersea between Nine Elms and Wandsworth (Domain 6A). This has been reported to be associated with construction of a utilities tunnel for London Electricity. No evidence for local variation in the superficial deposits, that could explain this anomaly, can be discerned in local borehole records.

A small domain of localised subsidence (Domain 6B), several hundred metres across, is also centred on the Sloane Square London Underground station (District and Circle lines). However, no causative relationship has been demonstrated.

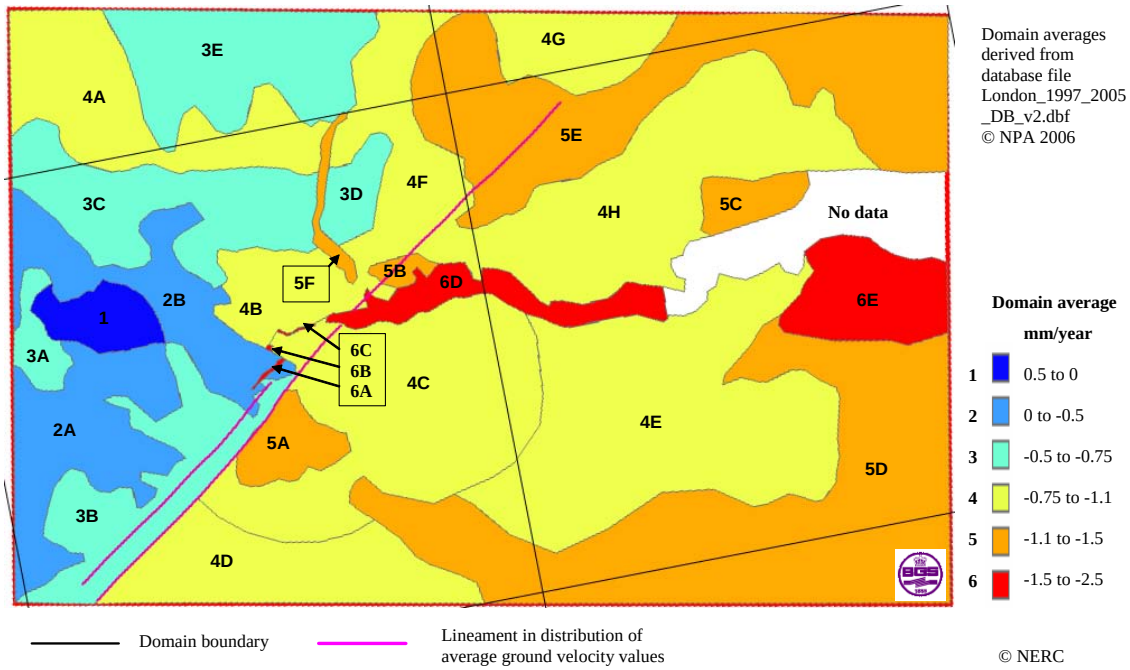

Figure 6.6 (re-presented) Domains of approximately uniform, average AGGPS-aligned PSI estimates of vertical velocity identified in the regional study

Summary

From the comparisons between the geoscience datasets and both the domain maps of uniform, average AGGPS-aligned PSI estimates of vertical velocity and, at larger scales, the AGGPS-aligned PSI estimates of vertical velocity for individual PS points, the geological interpretations for the measured changes in land level between March 1997 and December 2005 can be summarised as follows:

- Regional patterns of uplift and subsidence are controlled, to some extent, by deep-seated geological structures.
- There is also some local control by neotectonic movement on near-surface structures, such as the Wimbledon Fault.
- Parts of the AOI, north-west of the Wimbledon Fault and its lateral extensions, are prone to uplift or relatively slight subsidence: centred on a gravity 'high' within the Midlands Microcraton.
- The remainder of the AOI is prone to subsidence.
- Where Holocene deposits are extensive and thicker than about 5m, the ground is generally prone to a greater rate of subsidence than found regionally.
- Groundwater abstraction and tunnelling can cause subsidence at a similar rate to that found within areas of Holocene deposits.
- In some areas, however, where thick Holocene deposits are overlain by old made ground, subsidence due to compression currently appears to be negligible and may have ceased.

In summary, therefore, it can be concluded that the main sources of significant changes in land level for the Thames Region are:

- Regional uplift (in the west) and regional subsidence (especially in the north-east and south-east).
- Groundwater abstraction.
- Compaction of Holocene deposits.

In terms of future changes in land level, a specific comment can be made regarding each of these sources as follows:

- Regional changes in land level can be expected to continue at similar rates over thousands of years, assuming similar conditions.
- Future subsidence rates related to groundwater abstraction should be in some proportion to the rates at which the aquifer is drawn down. However, when abstraction rates reach a 'steady state' within the aquifer, with no further drawdown, then subsidence can be expected to cease, probably after a time lag in the order of one to five years. Some rebound could take place following rising groundwater levels but this is likely to be less than 10 per cent of the previous subsidence.
- Where no further natural sedimentation occurs, shrinkage of Holocene deposits due to compression can be expected to be effectively complete within tens to a few hundreds of years, depending on the thickness of the deposits, their composition and the superimposed load. Shrinkage due to desiccation of Holocene deposits that have been protected from flood can be expected to be effectively complete within some tens of years, depending on the prevailing weather and the level of the local water table. Some areas of Holocene deposits in the Thames Region have already been protected from flood for a significant proportion of this time scale and it can be concluded that within this century, such areas will no longer be subsiding to due to compression. However, formerly protected areas of Holocene deposits that become flooded, for example through managed retreat, can be expected to resume subsidence (or to continue to subside) due to increased loading by water and by newly deposited sediments.

6.5 Tide gauge results

Published changes in sea level from Thames tide gauges were presented in Section 4.1 and the combined data set of quality controlled tide gauge data compiled for the regional study was described in Section 4.3. As stated in Subsection 4.3.4, "the precise data spans for each tide gauge in the combined data set are detailed in the Project Record and Appendix A summarises the amount of valid, interpolated, rejected and missing data available for the 12 tide gauges in the combined data set: Richmond, Chelsea, Westminster, Tower Pier, Charlton, Silvertown, North Woolwich, Erith, Tilbury, Southend, Sheerness and Coryton."

In this section, details of the analysis carried out by POL and the results obtained based on the combined data set of quality controlled tide gauge data are discussed and new estimates of changes in sea level and other tidal parameters for the Thames Estuary and River Thames are presented.

6.5.1 Tidal parameter estimation methods

The tidal parameter estimation methods employed can be separated into those used for:

- MHW, MLW, MTL and MA estimation;
- MSL estimation;
- MHWS, MHWN, MLWN and MLWS estimation;
- Estimation of lunitidal intervals in stages of moon's transit;
- Estimation of time intervals between tide gauges for high and low waters in stages of moon's transit;
- Comparison between observed and predicted high and low water times and heights.

MHW, MLW, MTL and MA estimation

The method employed by POL for MHW, MLW, MTL and MA was to compute the high and low water times and heights from the tide gauge data. Equal interval heights of the sea level observations were interpolated, using a cubic spline fitted to four consecutive interval heights as an interpolation function, in order to provide the heights and times of high and low waters. All of the tide gauges on the Thames Estuary and River Thames are in areas of predominately semi-diurnal tides and there are few cases of double high or low water. Those that do occur are due to storm surge events or barrier closures and in such cases the data set was inspected using the visualisation package EDTEVA for the correct choice of event. In the case of Erith and Richmond tide gauges, which dry out at low water, only high water heights and times could be estimated. Turning point values were subsequently added together and averaged to estimate annual MHW, MLW, MTL and MA, with the proviso that an acceptable mean had to include data from at least 80% of the year, in order to avoid distortion to the mean from missing data and the seasonal cycle of these levels. This is a somewhat weaker requirement than the 90% that was used in the previous study by Amin (1983) but was chosen as a compromise so as not to lose too many annual values from most of the already very short data series.

MSL estimation

The standard POL method employed was to rate reduce the equal interval data to hourly values and then apply the Doodson X0 filter to obtain daily values of MSL. Missing values result in a missing daily value. Daily values were then averaged to monthly and annual values of MSL, with values only included if there were at least 80% of days in the month or year available.

MHWS, MHWN, MLWN and MLWS estimation

The estimation of MHWS, MHWN, MLWN and MLWS involves consideration of Mean Tidal Curves in stages of moon's transit. The method used for processing each year's data entails preparing 12 tables listing the dates and times of the moon's meridian passage: the times between 00 and 01 hrs and 12 and 13 hrs for the first table, between 01 and 02 hrs and 13 and 14 hrs for the second, and so on. Each tide is then listed in the appropriate table, first the

high water nearest to the time of the moon's transit followed by the succeeding low water. At the end of the year, each table is totalled and the mean times and levels obtained; the group of tides with the highest and lowest levels are taken as MHWS and MLWS respectively, and the group with the smallest range as MHWN and MLWN. These levels are presented in tabular form in the Project Record.

Estimation of lunitidal intervals in stages of moon's transit

The mean time of transit in each of the 12 moon's transit time bands, e.g. 00 to 01 hrs and 12 to 13 hrs, was subtracted from the mean high or low water time in the corresponding transit time band for each tide gauge. This is a way for estimating the time of high or low water related to the time of lunar transit. These intervals are also presented in tabular form in the Project Record.

Estimation of time intervals between tide gauges for high and low waters in stages of moon's transit

By subtracting the mean high or low water time in the corresponding transit time band for one tide gauge from the corresponding value for the next nearest tide gauge, an estimate of the high or low water time difference between tide gauges related to the time of lunar transit is obtained. These time intervals are also presented in tabular form in the Project Record.

Comparison between observed and predicted high and low water times and heights

The time and height differences between the observed and predicted times and heights of high and low water were computed in averaged monthly tabular format and are also presented in the Project Record.

6.5.2 Annual tidal parameter regression analysis

Following the estimation of the annual tidal parameters outlined in the previous subsection, time series of annual estimates for MHW, MLW, MTL, MSL, MA, MHWS, MHWN, MLWN, MLWS MHWI, MLWI, MI, MD, MAS, MAN, MTLS and MTLN were compiled for 12 tide gauges on the Thames Estuary and River Thames. Multiple regression analyses, using the maximum spans of data available for each tide gauge, were then carried out by POL on the annual time series of the various tidal parameters.

The annual MHW, MLW, MTL and MSL time series for all 12 tide gauges are shown in Figures F1 to F4 respectively in Appendix F, where each figure also includes the annual mean freshwater flow over Teddington Weir. From Figure F1, it can be seen that the variations in levels are coherent from tide gauge to tide gauge, with the magnitude of the variations increasing upriver; primarily due to the increasing effect of the freshwater discharge. The dependence on flow does not conceal the importance of the nodal tide of 18.6 year period which can be seen more readily in the annual MA time series shown in Figure F5 in

Appendix F. The annual MHWS, MHWN, MLWN, MLWS, MHWI, MLWI, MI and MD time series are then given as Figures F6 to F13 respectively in Appendix F; again with the annual mean freshwater flow over Teddington Weir included in all plots, except for MD.

Tide gauges with long period time series

For the four tide gauges with the longest time series (approximately 1929-2003), namely Sheerness, Southend, Tilbury and Tower Pier, the regression model chosen was the same as that used by Amin (1983) but with an additional term for mean freshwater flow at Teddington, i.e.

$$H_y = a_0 + a_1 y + a_2 \cos N'_y + a_3 \sin N'_y + a_4 \cos 2N'_y + a_5 \sin 2N'_y + a_6 \, flow_y + Z_y$$

[Equation 6.1]

where

y is the number of years elapsed from 2000 (y=0 in 2000),
a_0 is the intercept at the year 2000,
a_1 is the trend per year,
a_2,a_3 are the coefficients to determine nodal cycle modulation,
a_4,a_5 are the coefficients to determine semi nodal cycle modulation,
a_6 is the coefficient to determine modulation due to flow in year y,
N' is the negative of the longitude of the Moon's node (the nodal cycle), and
Z represents those variations in annual values which cannot be accounted for by this model and are treated as noise.

The regression fit and the linear trend for each of the tidal parameters are superimposed on each time series plot given in Figures F1 to F13.

A summary of the results of the regression analyses of Rossiter (1969a, 1969b) and Bowen (1972) were given in Tables 4.1 and 4.2 in Subsection 4.1.1. All of the regression coefficients, and their standard errors, output from the regional study for Sheerness, Southend, Tilbury and Tower Pier tide gauges are presented in Tables F1, F2 and F3 in Appendix F. Tables 6.12 and 6.13 summarise these in comparison with the published values of Rossiter (1969a, 1969b) and Bowen (1972).

Here it should be noted that comparisons using a similar span of data to that used by Rossiter (1969a, 1969b) and Bowen (1972) were carried out and are detailed in the Project Record. These comparisons were in good agreement and validated the methods applied in the regional study for estimation of the high and low water times and levels by cubic spline fitting of the interval.

Table 6.12 Estimates of changes in tidal parameters for Thames tide gauges for the period from 1934 to 1966 (Rossiter 1969a, 1969b) and for the period from 1929 to 2003 as output from the regional study

Tide gauge	Change in annual MHW and uncertainty (cm/cen)	Change in annual MLW and uncertainty (cm/cen)	Change in annual MTL and uncertainty (cm/cen)	Change in annual MTA and uncertainty (cm/cen)
For the period from 1934 to 1966 based on Rossiter (1969a, 1969b)				
Southend	+36.3 ± 7.6	+24.9 ± 7.9	+31.1 ± 4.6	+5.2 ± 6.1
Tower Pier	+77.5 ± 11.6	+9.2 ± 8.9	+43.4 ± 8.2	+34.5 ± 7.0
For the period from 1929 to 2003 as output from the regional study				
Southend	+23.2 ± 1.9	+14.2 ± 1.6	+18.7 ± 1.5	+4.4 ± 0.9
Tower Pier	+27.1 ± 3.1	+16.0 ± 2.7	+21.5 ± 1.7	+5.7 ± 2.3
Tide gauge	**Change in annual MHWI and uncertainty (mins/cen)**	**Change in annual MLWI and uncertainty (mins/cen)**	**Change in annual MI and uncertainty (mins/cen)**	**Change in annual MD and uncertainty (mins/cen)**
For the period from 1934 to 1966 based on Rossiter (1969a, 1969b)				
Southend	+0.2 ± 3.4	-4.4 ± 5.7	-1.9 ± 4.2	-4.6 ± 5.7
Tower Pier	-6.4 ± 4.7	-25.1 ± 5.6	-15.8 ± 5.0	-18.7 ± 4.0
For the period from 1929 to 2003 as output from the regional study				
Southend	0.0 ± 0.8	+5.4 ± 1.4	+2.7 ± 1.0	+5.4 ± 1.0
Tower Pier	-2.5 ± 1.1	-8.4 ± 1.7	-5.5 ± 1.3	-5.9 ± 1.4

Table 6.13 Estimates of changes in tidal parameters for Thames tide gauges for the period from 1931 to 1969 (Bowen 1972) and for the period from 1929 to 2003 as output from the regional study

Tide gauge	Change in annual MHW and uncertainty (cm/cen)	Change in annual MLW and uncertainty (cm/cen)		
For the period from 1931 to 1969 based on Bowen (1972)				
Southend	+35.1 ± 4.3	+25.0 ± 4.6		
Tilbury	+38.1 ± 5.8	+27.7 ± 17.4		
Tower Pier	+68.0 ± 4.9	+4.3 ± 4.0		
For the period from 1929 to 2003 as output from the regional study				
Southend	+23.2 ± 1.9	+14.2 ± 1.6		
Tilbury	+39.1 ± 2.1	+26.2 ± 1.9		
Tower Pier	+27.1 ± 3.1	+16.0 ± 2.7		
Tide gauge	**Change in annual MHWS and uncertainty (cm/cen)**	**Change in annual MLWS and uncertainty (cm/cen)**	**Change in annual MTLS and uncertainty (cm/cen)**	**Change in annual MAS and uncertainty (cm/cen)**
For the period from 1931 to 1969 based on Bowen (1972)				
Tower Pier	+75.8 ± 6.1	+2.4 ± 5.5	+41.1 ± 4.6	+38.7 ± 3.4
For the period from 1929 to 2003 as output from the regional study				
Tower Pier	+25.0 ± 4.2	+15.1 ± 3.2	+20.1 ± 2.2	+5.2 ± 3.0
Tide gauge	**Change in annual MHWN and uncertainty (cm/cen)**	**Change in annual MLWN and uncertainty (cm/cen)**	**Change in annual MTLN and uncertainty (cm/cen)**	**Change in annual MAN and uncertainty (cm/cen)**
For the period from 1931 to 1969 based on Bowen (1972)				
Tower Pier	+65.1 ± 6.4	+3.4 ± 4.3	+36.0 ± 4.3	+32.6 ± 3.4
For the period from 1929 to 2003 as output from the regional study				
Tower Pier	+31.8 ± 3.6	+15.1 ± 2.9	+23.4 ± 2.5	+8.3 ± 2.0

In Subsection 4.1.1, it was stated that: “as expected, considering the similar periods of data used by both Rossiter (1969a, 1969b) and Bowen (1972), the results for changes in annual MHW and annual MLW are in very good agreement for the Southend and Tower Pier tide gauges. The main observation from these results is that the difference between MHW and MLW at Southend and Tilbury tide gauges has increased by approximately 10cm/century (or 1mm/yr); whereas at Tower Pier tide gauge this difference has increased by 64 to 68cm/century (or 6.4 to 6.8mm/yr).”

Considering the outputs from the regional study presented in Tables 6.12 and 6.13, it is clear that with the use of a greater period of data (1929-2003) the difference between MHW and MLW at the Southend and Tilbury tide gauges is still an increase of approximately 10cm/century (or 1mm/yr). However, for Tower Pier the new estimates show a reduction in the change in MHW by about 41 to 50cm/century (or 4.1 to 5.0mm/yr) and an increase in the change in MLW by about 7 to 12cm/century (or 0.7 to 1.2mm/yr). The new estimates, therefore, clearly show a much more consistent change in MHW and MLW at Southend, Tilbury and Tower Pier tide gauges than that previously published by Rossiter (1969a, 1969b) and Bowen (1972).

In terms of changes in annual MSL, a summary of the estimates of changes in sea level for a number of Thames tide gauges for the period up to 1996 (Woodworth et. al. 1999) and for the period up to 2005 (PSMSL 2005) were given in Tables 4.4 and 4.5 in Subsection 4.1.2. The changes in annual MSL, and their uncertainties, output from the regional study for Sheerness, Southend, Tilbury and Tower Pier tide gauges are included in Table F1 in Appendix F and summarised in Table 6.14, in comparison with the published values of Woodworth et. al. (1999) and PSMSL (2005).

Table 6.14 Estimates of changes in sea level for Thames tide gauges for the period up to 1996 (Woodworth et. al. 1999), for the period up to 2004 (PSMSL 2005) and for the period from 1929 to 2003 as output from the regional study

Tide gauge	Period of RLR data used	Number of complete years of RLR data used	Change in annual MSL and uncertainty (mm/yr)
For the period up to 2006 based on Woodworth et. al. (1999)			
Sheerness	1901-1996	51	+2.14 ± 0.15
Southend	1933-1983	44	+1.22 ± 0.24
Tilbury	1961-1983	22	+1.58 ± 0.91
For the period up to 2004 based on PSMSL (2005)			
Sheerness	1834-2004	75	+1.64 ± 0.09
Southend	1933-1983	44	+1.22 ± 0.24
Tilbury	1961-1983	22	+1.58 ± 0.91
For the period from 1929 to 2003 as output from the regional study			
Sheerness	1952-2003	32	+1.99 ± 0.36
Southend	1933-2003	64	+1.44 ± 0.16
Tilbury	1929-2003	50	+2.89 ± 0.18
Tower Pier	1929-2003	56	+1.18 ± 0.21

When comparing the values in Table 6.14, it should be noted that the new estimate for Southend is based on the inclusion of new RLR data for the period

from 1988 to 2003, the new estimate for Tilbury is based on the inclusion of new RLR data for the period from 1988 to 2003 plus historical RLR data for the period from 1929 to 1960, and that the new estimate for Sheerness is based on the period from 1952 to 2003 only.

From Table 6.15, it is clear that the estimates from the regional study still suggest that the Thames tide gauges are fairly consistent with the values for other British tide gauges, as given in Tables 3.1 and 3.2 in Section 3.1, in that they all show a rise in sea level over the past few decades/past century, with a range of values from 1.18mm/yr at Tower Pier tide gauge to 2.89mm/yr at Tilbury tide gauge. A comment can then be made on each tide gauge, as follows:

- The regional study estimate for Sheerness tide gauge of +1.99mm/yr is clearly in between the values of +2.14 and +1.64mm/yr given in Woodworth et. al. (1999) and PSMSL (2005), which can be attributed to a combination of restricting the historical RLR data but including the most recent RLR data.
- The regional study estimate for Southend tide gauge of +1.44mm/yr is slightly higher than the previous published value of +1.22mm/yr, which can be attributed to the inclusion of the new RLR data for the period from 1988 to 2003.
- The regional study estimate for Tilbury tide gauge of +2.89mm/yr is clearly higher than the previous published value of +1.58mm/yr, but this is most likely related to the fact that the previously published value was only based on 22 years of RLR data, whereas the new value is based on 50 years.

Tide gauges with short period time series

For Coryton, Erith, Silvertown, Charlton, Westminster, Chelsea and Richmond tide gauges, the time series, mostly from 1988 to 2003, are shorter than an 18.61 year nodal cycle. The regression model chosen was again the same as that used by Amin (1983) with the additional term for mean freshwater flow at Teddington, presented as Equation 6.1. However, as the data span is less than a nodal cycle in length, the coefficients a_2, a_3, a_3 and a_4 cannot be resolved directly and they have been assumed to be the same as those for the nearest tide gauge with a longer span e.g. Tilbury's for Charlton etc.. It is the length of data and not the methodology that can cause problems. The assumption that the nodal variation parameters are the same as for the reference may not be correct, especially, once the distance to the reference tide gauge increases.

The regression coefficients, and their standard errors, for annual MHW, MLW, MTL, MSL and MA are presented in Tables F4 and F5 in Appendix F, which also includes values for the four tide gauges with long period time series, i.e. Sheerness, Southend, Tilbury and Tower Pier, but considered over the same short period, i.e. 1989 to 2003. The changes in annual MSL, and their uncertainties, are included in Table F5 in Appendix F and summarised in Table 6.15. For comparison, Table 6.15 also re-presents the changes in annual MSL given in Table 6.14 for the four tide gauges with long period time series.

Table 6.15 Estimates of changes in sea level for Thames tide gauges for the periods from 1929 to 2003 and 1988 to 2003 as output from the regional study

Tide gauge	Period of RLR data used	Number of complete years of RLR data used	Change in annual MSL and uncertainty (mm/yr)
For the period from 1929 to 2003 as output from the regional study			
Sheerness	1952-2003	32	+1.99 ± 0.36
Southend	1933-2003	64	+1.44 ± 0.16
Tilbury	1929-2003	50	+2.89 ± 0.18
Tower Pier	1929-2003	56	+1.18 ± 0.21
For the period from 1988 to 2003 as output from the regional study			
Sheerness	1988-2003	16	+3.93 ± 1.29
Southend	1988-2003	13	+1.56 ± 1.65
Tilbury	1988-2003	13	+8.16 ± 1.17
Silvertown	1988-2003	14	+6.21 ± 1.44
Charlton	1988-2003	9	+11.32 ± 2.05
Tower Pier	1988-2003	12	+4.63 ± 2.20
Westminster	1988-2003	7	+27.63 ± 6.15
Chelsea	1988-2003	12	+5.57 ± 2.85

Table 6.15 immediately highlights the problems in using such short time series through a comparison of the estimates from the short period with the estimates from the longer period for Sheerness, Southend, Tilbury and Tower Pier. For these four tide gauges, the estimates of change in annual MSL are increased by 1.94, 0.12, 5.27 and 3.45mm/yr with their corresponding uncertainties increased by 0.93, 1.49, 0.99 and 1.99mm/yr to the level of 1.17 to 2.20mm/yr, when only considering the period from 1988 to 2003. For Silvertown and Chelsea, the estimates of change in annual MSL are comparable to those of Tilbury and Tower Pier over the same short period, but none are reliable estimates of changes in sea level. For Charlton and Westminster, apart from having the least number of complete years of RLR data, these results also raise questions regarding the maintenance of these tide gauges and their usefulness for long term studies.

As a test to investigate the sensitivity of the regression coefficients and standard errors to such shorter periods of data, data for Sheerness, Southend, Tilbury and Tower Pier for 1934-48, 1949-63, 1964-78 and 1988-2003 were also analysed but, as expected, the standard errors were consistently much greater than for the long period time series (1929-2003) and there was little consistency between the 1934-48, 1949-63, 1964-78 and 1988-2003 estimated trends.

This effectively confirms that, at this stage, due to their short period time series, Coryton, Erith, Silvertown, Charlton, Westminster, Chelsea and Richmond tide gauges cannot be used in any assessment of long term changes in tidal parameters, which for the Thames Estuary and River Thames, must be based on the long period time series for Sheerness, Southend, Tilbury and Tower Pier, where decadal and nodal variations can be resolved.

6.5.3 Monthly tidal parameter regression analysis

Following the estimation of the monthly tidal parameters outlined in Subsection 6.5.1, time series of monthly estimates of MHW, MLW, MTL, MSL, MA, MHWI, MLWI, MI and MD were compiled for 12 tide gauges on the Thames Estuary and River Thames. Multiple regression analyses, using the maximum spans of data available for each tide gauge, were then carried out by POL on the monthly time series of the various tidal parameters.

The monthly MHW, MLW, MTL and MSL time series for all 12 tide gauges are shown in Figures G1 to G4 respectively in Appendix G, where each figure also includes the monthly mean freshwater flow over Teddington Weir. The monthly MA, MHWI, MLWI, MI and MD time series are then given as Figures G5 to G9 respectively in Appendix G; again with the annual mean freshwater flow over Teddington Weir included in all plots, except for MA and MD.

Tide gauges with long period time series

For Sheerness, Southend, Coryton, Tilbury, North Woolwich and Tower Pier tide gauges, the regression model chosen was the same as that used for the annual tidal parameter regression analysis (as given in Equation 6.1) but with the addition of two terms to account for the seasonal variation in the monthly data, i.e.

$$H_m = a_0 + a_1 y + a_2 \cos N'_m + a_3 \sin N'_m + a_4 \cos 2N'_m + a_5 \sin 2N'_m + a_6 \, flow_m + a_7 \cos h_m + a_8 \sin h_m + a_9 \cos 2h_m + a_{10} \sin 2h_m + Z_m$$

[Equation 6.2]

where

y is the number of years elapsed from 2000 (y=0 in 2000),
a_0 is the intercept at the year 2000,
a_1 is the trend per year,
a_2,a_3 are the coefficients to determine nodal modulation,
a_4,a_5 are the coefficients to determine semi nodal modulation,
a_6 is the coefficient to determine modulation due to flow in year y,
a_7,a_8 are the coefficients to determine annual modulation,
a_9,a_{10} are the coefficients to determine semi annual modulation
N' is the negative of the longitude of the Moon's node (the nodal cycle),
h is the mean longitude of the sun (the annual solar cycle), and
Z represents those variations in annual values which cannot be accounted for by this model and are treated as noise.

The regression fit and the linear trend for each of the tidal parameters are superimposed on each time series plot given in Figures G1 to G9. The regression coefficients and their standard errors are shown in Tables G1 and G2 in Appendix G, which also re-present the values of Rossiter (1969a, 1969b) and Bowen (1972) given in Table F1 and F2 in Appendix F, based on annual time series.

From a cursory comparison of the results from the regional study presented in Tables G1 and G2 with those presented in Tables F1 and F2 sit is clear that the tidal parameters based on monthly time series are not too different to those based on annual time series. For example, considering the changes in MSL, the estimates based on monthly time series are 0.13mm/yr less, 0.02mm/yr less, 0.09mm/yr less and 0.11mm/yr greater than those based on annual time series for Sheerness, Southend, Tilbury and Tower Pier respectively.

Apart from this, a visual inspection of Figures G1 to G9 clearly does not resolve the issues in the annual time series for Charlton and Westminster, highlighted at the end of the previous subsection, and may raise some issues relating to Tower Pier which is seemingly anomalous to other tide gauges after 1997.

6.5.4 Extreme sea levels analysis

In the analysis of extreme sea levels the simplest and most widely used method is the annual maxima method. This involves fitting the limiting generalised extreme value (GEV) distribution to the annual maxima. The r-largest GEV method (Smith 1986; Tawn 1988) was considered the most appropriate method for comparison between the 12 tide gauges on the Thames Estuary and River Thames.

Time series of the r-largest high water extremes were assembled using all the available data and extreme still water return period estimates computed. A storm length of 30 hours was assumed for this and 10 event maxima were extracted per year.

To help direct comparison between the tide gauges with only data after 1988 to those tide gauges with data before and after 1988, subsets of data were analysed as well. Full details of the return period estimates are given in the Project Record but are summarised in Figures 6.8 to 6.11, which present the return levels above ODN in 2004.

Here it should be noted that, it is usually considered only realistic to extrapolate to four times the length of the number of years of data. This means that for data sets of 15 years or less (Figures 6.10 and 6.11) any return period estimates above 50 years should be treated with caution. Furthermore, the standard errors may seem to be small but the range of observed extremes is also limited and may not represent the true population if we had sufficient years of data.

From a comparison of Figures 6.9 with Figure 6.10, it can be seen that the estimates computed from the longer data sets are significantly different to those computed from the shorter data sets at Southend and Sheerness, but not at Tilbury. Considering Tower Pier in Figures 6.9 and 6.11, the installation and operation of the barrier has clearly further distorted the estimates with pre-barrier levels no longer obtained.

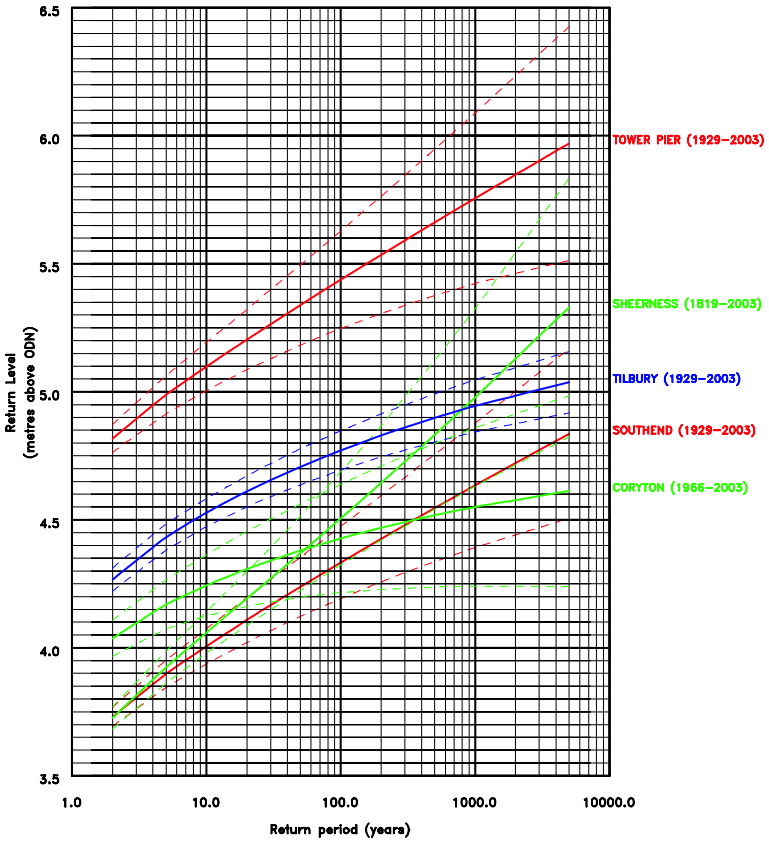

Figure 6.8 Extreme sea level estimates using maximum available (up to 2003) data spans

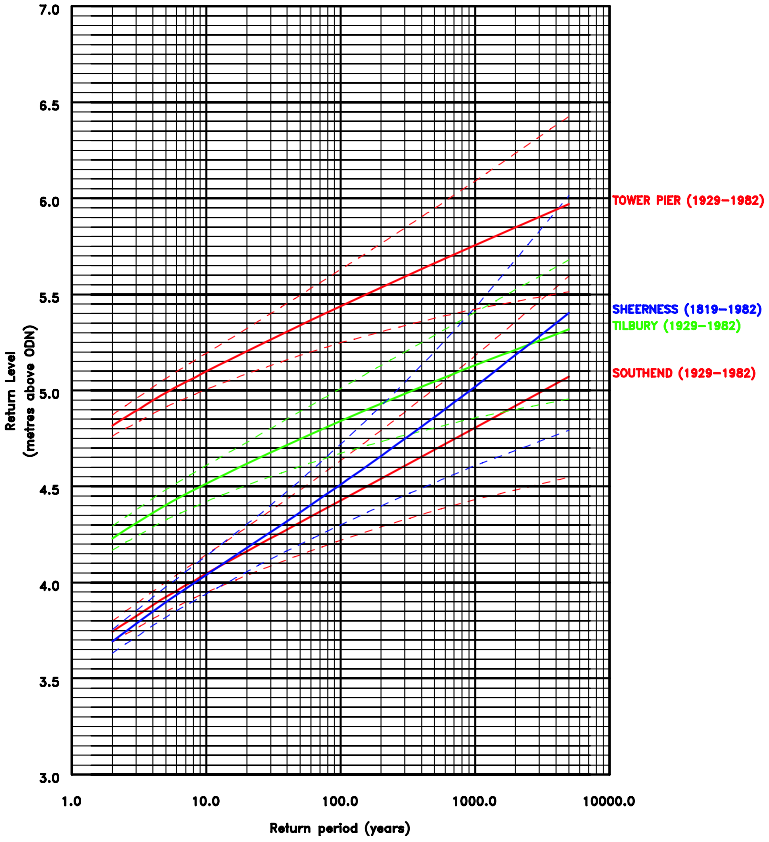

Figure 6.9 Extreme sea level estimates using maximum available pre-barrier (up to 1982) data spans

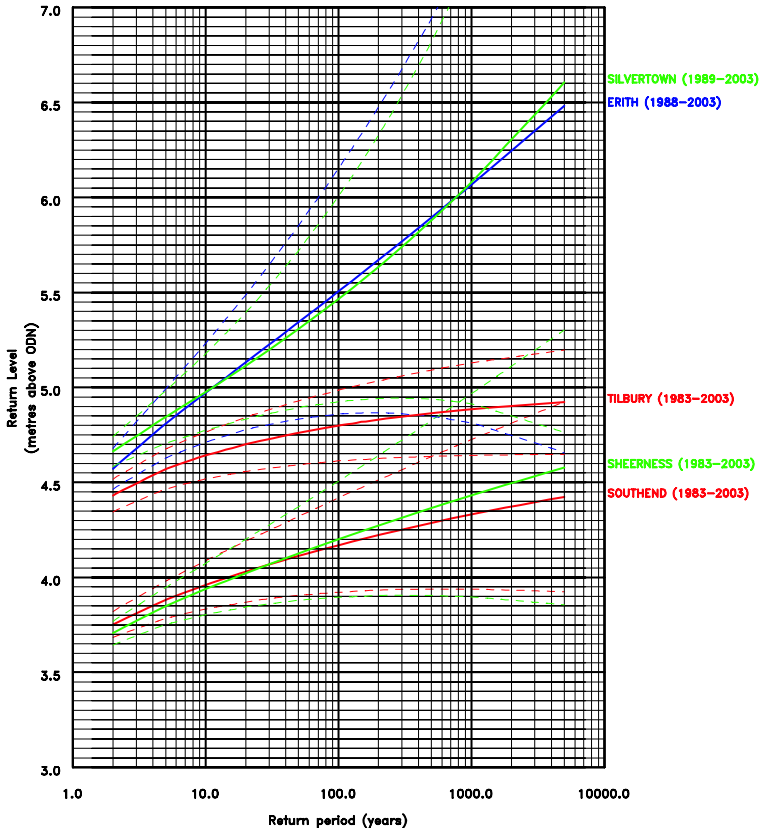

Figure 6.10 Extreme sea level estimates using maximum available post-barrier (after 1983) downstream data spans

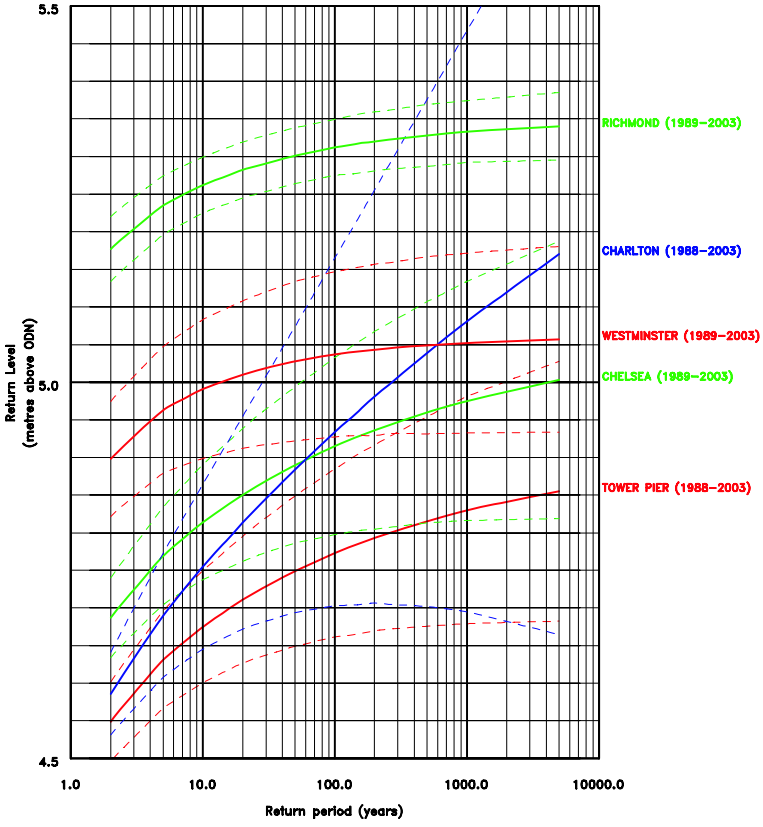

Figure 6.11 Extreme sea level estimates using maximum available post-barrier (after 1983) upstream data spans

Considering Figure 6.10 and 6.11, the estimates for Silvertown are clearly greater than those for Charlton. This is because the highest maximum level in 1993, just after a barrier closure, was some 0.4 metres higher than any other in the entire data span from 1988-2003; which looks to be genuine as the barrier was closed, and both Sheerness and Southend showed the same surge event.

Comparing Figures 6.8 and 6.9, it can be seen that the exclusion of post-barrier data for the longest records does not make much difference (a bit at Tower Pier due to 'removal' of the largest extremes by the barrier) but again it should be remembered that for the post-barrier period the effect of the larger storm events can be limited by the use of the barrier, which is more evident in Figures 6.10 and 6.11 by the flatter return periods.

6.5.5 Other analyses

An analysis of harmonic constants and estimations of extreme still water return periods were also carried out by POL, as part of the regional study. The annual amplitude and phase data for Sheerness, Southend, Coryton, Tilbury, Silvertown, Charlton, Tower Pier, Westminster and Chelsea tide gauges were analysed using regression to solve for up to 103 harmonic constants. The regression coefficients and their standard errors for the amplitude and phase of some of the major terms are given in the Project Record, and comparisons with Amin (1983) showed good agreement when considering Southend tide gauge.

6.6 Estimated changes in land and sea levels for Thames Region

The results of the national study, in terms of past changes in land and sea levels were given in Section 5.4, in which it was concluded that the average change in sea level (decoupled from changes in land level) around the coast of Britain over the past few decades/past century was +0.9 to 1.2mm/yr based on AG-aligned CGPS estimates of vertical station velocity and changes in annual MSL at seven tide gauges, including Sheerness on the Thames Estuary to the East of London.

In this section, the AG-aligned CGPS and EGPS estimates of vertical station velocity and the AGGPS-aligned PSI estimates of vertical velocities are considered to represent changes in land level and these are then combined with changes in sea level in order to compute an estimate for the average change in sea level (decoupled from changes in land level) along the Thames Estuary and River Thames. Considering the results presented in Table 6.9 in Subsection 6.3.2 as the available estimates of changes in land level and the results presented in Table 6.14 in Subsection 6.5.2 as the available estimates for changes in sea level, it is clear that an assessment of the average change in sea level (decoupled from changes in land level) along the Thames Estuary and River Thames can be made based on Sheerness, Tilbury and Tower Pier tide gauges. The results of this are given in Table 6.16.

Table 6.16 Changes in sea level (decoupled from changes in land level) along the Thames Estuary and River Thames based on AG-aligned CGPS and EGPS estimates of vertical station velocities, AGGPS-aligned PSI estimates of vertical velocity and estimates of changes in annual MSL from the regional study

Station name	4 char station ID	AG-aligned CGPS/EGPS vertical station velocity and uncertainty (mm/yr)	Average AGGPS-aligned PSI vertical velocity and uncertainty (mm/yr)	Change in annual MSL and uncertainty (mm/yr)	Change in sea level (decoupled from a change in land level) (mm/yr)	
					Based on AG-aligned CGPS/ EGPS (mm/yr)	Based on average AGGPS-aligned PSI (mm/yr)
Changes in annual MSL based on PSMSL (2005)						
Sheerness TG	SHEE	-1.09 ± 0.64	-1.01 ± 0.94	+1.64 ± 0.09	+0.55	+0.63
Tilbury TG	TILB	-1.04 ± 0.69	-0.86 ± 0.33	+1.58 ± 0.91	+0.54	+0.72
Tower Pier TG	TOPR	N/A	-0.42 ± N/A	N/A	N/A	N/A
Changes in annual MSL based on output from the regional study						
Sheerness TG	SHEE	-1.09 ± 0.64	-1.01 ± 0.94	+1.99 ± 0.36	+0.90	+0.98
Tilbury TG	TILB	-1.04 ± 0.69	-0.86 ± 0.33	+2.89 ± 0.18	+1.85	+2.03
Tower Pier TG	TOPR	N/A	-0.42 ± N/A	+1.18 ± 0.21	N/A	+0.76

From Table 6.16, considering all nine estimates of the change in sea level (decoupled from a change in land level) along the Thames Estuary and River Thames over the past few decades/past century, an average of +1.00 ± 0.56mm/yr is obtained. This is clearly consistent with the statistics from the national study, which had a full range of values of +0.9 ± 0.2mm/yr, +0.9 ± 0.2mm/yr, +1.1 ± 0.3mm/yr and +1.2 ± 0.8mm/yr. It can be concluded, therefore, that overall the changes in sea level (decoupled from changes in land level) along the Thames Estuary and River Thames are consistent with those obtained around the coast of Great Britain, i.e. they suggest that sea level has risen by 0.9 to 1.2mm/yr over the past few decades/past century.

As demonstrated in Subsections 6.4.1 and 6.4.2, when the CGPS and AG estimates of changes in land level from the national study are combined with the EGPS and PSI estimates of changes in land level from the regional study, the estimates of changes in land level for the Thames Region generally range from approximately 0.3mm/yr uplift to 2.1mm/yr subsidence and correlate with certain aspects of the geoscience datasets to explain the pattern of land movements observed on a regional scale.

When the CGPS and AG estimates of changes in land level from the national study are combined with the EGPS and PSI estimates of changes in land level from the regional study and considered along with the results of the new analysis of the tide gauge data for the Thames Estuary and River Thames, the combined effect of changes in land and sea levels is a 1.8 to 3.3mm/yr rise in sea level with respect to the land along the Thames Estuary and River Thames over the past few decades/past century. The lower figure in this range is based on a combination of a 0.9mm/yr sea level rise, as the low estimate from the national study, and a 0.9mm/yr subsidence for Domain 4E, as given in Table

6.11 in Subsection 6.4.1; whereas, the higher figure in this range is based on a combination of a 1.2mm/yr sea level rise, as the high estimate from the national study, and a 2.1mm/yr subsidence for Domain 6E, as given in Table 6.11 in Subsection 6.4.1.

In terms of the future changes in sea level component of this combined effect, Subsection 5.4.2 includes the results for Sheerness tide gauge as part of the national study. In terms of the future changes in land level component of this combined effect, some specific comments were made at the end of Subsection 6.4.2 which, in terms of the land along the Thames Estuary and River Thames, suggest that regional changes in land level can be expected to continue at similar rates over thousands of years, assuming similar conditions; whereas shrinkage of Holocene deposits due to compression depends on the thickness of the deposits, their composition and the superimposed load, and their past and future state in terms of being protected from flood.

7. Conclusions

The aims and objectives of the research work detailed in this Technical Report were stated in Chapter 1, along with the fact that the research work was carried out as a national study and a regional study.

Considering the information presented in Chapters 2, 3 and 5, the results for the national study demonstrate how:

- the combined CGPS and AG estimates of changes in land level correlate with long term geological and geophysical evidence for the 'tilt' of Great Britain, which has Scotland rising by 1 to 2 mm/yr and the South of England subsiding by up to 1.2 mm/yr.
- the combined CGPS and AG estimates of changes in land level are in general agreement with long term geological and geophysical evidence, in terms of whether there is subsidence or uplift at individual stations, although in some cases there are differences which are of the same order as the changes in land level themselves and are, therefore, significant in relation to any assumptions made regarding future changes in land level:
  - for station LERW, close to Lerwick on Shetland, the estimated subsidence of about 0.5 to 0.7mm/yr is in agreement with the geophysical evidence;
  - for station ABER, at Aberdeen tide gauge in East Scotland, the estimated slight uplift of up to 0.1mm/yr is about 0.6mm/yr less than both that of the geological and geophysical evidence;
  - for station NSTG, at North Shields tide gauge in the North-East of England, the estimated slight subsidence of 0.3 to 0.5mm/yr is contrary to the geological and geophysical evidence which suggests uplift of 0.2 to 0.4mm/yr;
  - for station LIVE, at Liverpool tide gauge in the North-West of England, the estimated slight uplift of 0.3 to 0.5mm/yr is in agreement with the geophysical evidence but contrary to the 0.2mm/yr subsidence from the geological evidence;
  - for station LOWE, at Lowestoft tide gauge on the East coast of England, the estimated subsidence of 1.2 to 1.5mm/yr is about 0.6 to 1.1mm/yr greater than the geological and geophysical evidence;
  - for station SHEE, at Sheerness tide gauge on the Thames Estuary to the East of London, the estimated subsidence of 0.7 to 1.1mm/yr is up to 0.4mm/yr greater than the geological evidence and 0.5 to 0.9mm/yr greater than the geophysical evidence;
  - for station PMTG, at Portsmouth tide gauge on the South coast of England, the estimated subsidence of 0.8 to 1.2mm/yr is 0.2 to 0.6mm/yr greater than the geological evidence and 0.7 to 1.1mm/yr greater than the geophysical evidence;
  - for station NEWL, at Newlyn tide gauge near to Land's End in the South-West of England, the estimated subsidence of 0.4 to 0.7mm/yr is 0.4 to 0.7mm/yr less than the geological evidence but only up to 0.4mm/yr less than the geophysical evidence.
- when the combined CGPS and AG estimates of changes in land level are considered along with tide gauge data, two estimates for the average change in sea level (decoupled from changes in land level) around the coast

of Great Britain over the past few decades/past century can be obtained: the first, based on CGPS and AG data for the period up to the end of 2004, suggests that sea level has risen by 1.3mm/yr, and the second, based on CGPS data for the period up to the end of 2005 and AG data for the period up to September 2006, suggests that sea level has risen by 0.9 to 1.2mm/yr, which is on the low side when compared to published studies of changes in globally averaged sea level.
- the direct estimates of changes in land level at specific tide gauges can be combined with IPCC predictions of future changes in sea level to provide an alternative UKCIP-style assessment of future changes in sea level around the coast of Great Britain.

Considering the information presented in Chapters 2, 4 and 6, the results for the regional study demonstrate how:
- when the CGPS and AG estimates of changes in land level from the national study are combined with the EGPS and PSI estimates of changes in land level from the regional study, the estimates of changes in land level for the Thames Region, which generally range from approximately 0.3mm/yr uplift to 2.1mm/yr subsidence, correlate with certain aspects of the geoscience data sets to explain the pattern of land movements observed on a regional scale.
- when the CGPS and AG estimates of changes in land level from the national study are combined with the EGPS and PSI estimates of changes in land level from the regional study and considered along with the results of a new analysis of the tide gauge data for the Thames Estuary and River Thames, the estimates for the changes in sea level (decoupled from changes in land level) along the Thames Estuary and River Thames are consistent with those obtained around the coast of Great Britain.
- when the CGPS and AG estimates of changes in land level from the national study are combined with the EGPS and PSI estimates of changes in land level from the regional study and considered along with the results of a new analysis of the tide gauge data for the Thames Estuary and River Thames, the combined effect of changes in land and sea levels is a 1.8 to 3.3mm/yr rise in sea level with respect to the land along the Thames Estuary and River Thames over the past few decades/past century.

It has been clearly demonstrated, therefore, that the aims and objectives of the research work have been met as direct estimates of current changes in land level on the scale of millimetres per year, in a stable reference frame, both at tide gauges and at other specific locations, and estimates of changes in sea level (decoupled from changes in land level) over the past few decades/past century have been obtained through a method developed to best combine the information from the three complementary monitoring techniques: GPS and AG for the national study and GPS, AG and PSI for the regional study.

The results obtained, however, also highlight that the formal uncertainties in any of the estimates are at about the 0.5 to 1.0mm/yr level, with a further 0.5 to 1.0 mm/yr of potential systematic bias being apparent in many instances, e.g. the change in the CGPS vertical station velocities when the time series were extended from approximately 7.5 to 8.5 years; the change in the AG vertical

station velocities when the time series were extended from approximately 8 or 9 to 10 or 11 years; the agreement between the combined CGPS and AG vertical station velocities and other evidence for changes in land level on a national scale; the standard deviations for the PSI average vertical station velocities, as an indication of the variation in the values obtained for a series of PS points in a relatively small area of a few hundred metres. With these in mind, the estimates presented can be used now, but do need to be treated with some caution.

In conclusion, therefore, the national and regional studies were extremely successful and have greatly improved our knowledge of changes in land and sea levels around the coast of Great Britain and along the Thames Estuary and River Thames well beyond what was known at the start of the studies in 2003. They have provided new estimates of changes in land level due to 'land tilt' and regional/local geological effects, new estimates of climate driven changes in sea level based on tide gauges and a new assessment of future sea level rise. The results are, therefore, of direct relevance to the Joint Defra/EA Flood and Coastal Erosion Risk Management R&D Programme Modelling and Risk (MAR) Theme, in providing information and knowledge to support decision making in terms of coastal flood risk management and climate change, as part of the cross cutting risk based knowledge and methods sub-theme. The results are also a direct input to the Environment Agency Thames Estuary 2100 project.

The next section gives a number of recommendations for improving the confidence we can place on the current results and for further actions relating to long term monitoring.

8. Recommendations

Throughout this Technical Report, the results obtained have served to demonstrate the capability for monitoring long term changes in land and sea levels by using a combination of three complementary monitoring techniques: CGPS and AG on a national scale and CGPS/EGPS, AG and PSI on a regional scale.

The results also highlight that the formal uncertainties in any estimates are at about the 0.5 to 1.0mm/yr level, with a further 0.5 to 1.0mm/yr of potential systematic bias being apparent in some instances.

The study has also tackled the issue of 'aligning' the CGPS to the AG to overcome the small but significant systematic bias currently present in the vertical station velocity estimates from CGPS at the demanding, high level of accuracy required.

Considering all of the above, this chapter contains a number of recommendations for either improving the confidence we can place on the current results and for further actions relating to long term monitoring.

Improving confidence in the current results

In terms of improving the confidence we can place on the current results, it is recommended that the archived CGPS data for the period from 1997 to 24 November 2006 is re-processed using the IGS's new GPS data processing strategy along with re-analysed global products (satellite orbits, clocks and Earth orientation parameters), either computed by the IGS over the next three years or computed in-house; taking into consideration the latest TRF, using absolute antenna PCV models and applying corrections for ocean tide loading.

In principle, this should remove the need for 'aligning' the CGPS to the AG and could result in CGPS coordinate time series with less coloured noise and, therefore, vertical station velocities with lower formal uncertainties. It would then result in new, more reliable, estimates for the changes in land and sea levels for both the national and regional studies.

Long term monitoring on a national scale

In terms of further actions relating to long term monitoring it is recommended that on a national scale:

- the CGPS and AG measurements, and their processing and analysis, are continued at thirteen tide gauges around the coast of Great Britain.
  - CGPS measurements at the current ten tide gauges of Sheerness, Newlyn, Aberdeen, Liverpool, Lowestoft, North Shields, Portsmouth, Lerwick, Stornoway and Dover, plus Portpatrick and two others, i.e. not necessarily Holyhead and Millport, depending on the Environment Agency's requirements; AG measurements at the three tide gauges of Newlyn, Aberdeen and Lerwick.

    - This should lead to a convergence of the vertical station velocity estimates, removing the changes currently seen when 1 or 2 more years of data are added, and will lead to lower formal uncertainties for any vertical station velocity estimates.

- the AG measurements, and their processing and analysis, are extended to three other CGPS stations in Great Britain, selected based on geological setting.
    - This will enable more comparisons between CGPS and AG vertical station velocity estimates.

- the tide gauge measurements are subjected to a refined analysis, in order to obtain revised estimates of changes in sea level at the thirteen tide gauges which have CGPS stations, considered over specific time periods rather than just taken from PSMSL.
    - This will enable a focus on changes in sea level over the past few decades rather than the past few decades/past century.

- the use of PSI measurements, and their processing and analysis, is extended, following the success of their application in the regional study, to tide gauge sites around the coast of Great Britain which have CGPS stations.
    - This will be a means for assessing the 'local stability' of the CGPS stations and provide information on how applicable the CGPS estimates of vertical station velocity are over a larger coastal area.

All of these will lead to improved estimates for the changes in sea level (decoupled from changes in land level) around the coast of Great Britain over the past few decades/past century but, perhaps more importantly, will establish the selected tide gauges as devices with increasingly concurrent sea level and land level data from where estimates for any accelerations in changes sea level can be obtained. This will enable the validation of climate change model predictions of sea level rise around Great Britain, particularly as we move into the period of increasing variance between the different IPCC scenario predictions, which will lead to a better assessment of risk and more informed decisions on planning and managing flood risk at the coast and in our estuaries.

Long term monitoring on a regional scale

In terms of further actions relating to long term monitoring it is recommended that on a regional scale:

- the CGPS and EGPS measurements, and their processing and analysis, are continued at three non-tide gauges and four other tide gauges in the Thames Region.
    - CGPS measurements at Barking and EGPS measurements at Riddlesdown and Greenwich Park; EGPS measurements at the four tide gauges of Richmond, Tower Pier, Silvertown and Tilbury.
    - This should lead to improved vertical station velocity estimates and lower formal uncertainties for any vertical station velocity estimates.

- the PSI measurements, and their processing and analysis, are continued in the Thames Region, with the introduction of PSI corner reflectors at selected CGPS and EGPS stations also considered.
  - Further measurements should lead to improved vertical velocity estimates and lower formal uncertainties for all PS points.
  - The use of corner reflectors will enable a direct estimate of changes in land level at a specific location to be obtained and remove the issues over the variations in the values obtained for PS points over relatively small areas of a few hundred metres; however, it should be recognised that their data cannot then go back in time.

- the TG analysis is extended for the Thames Estuary and River Thames.
  - This should lead to improved estimates for changes in sea level, especially considering the number of tide gauges which currently have short period time series.

Concluding remarks

The recommendations for long term monitoring on a national scale are particularly important in the context of policy needs from the sciences over the next 10 years which were set out in Defra (2004) and include the need for key long-term evidence relating to climate change and the specific requirements for monitoring, reliable regional predictions and a comprehensive understanding of the range of climate change impacts, including sea level rise.

The recommendations for long term monitoring on a regional scale aim to provide a monitoring solution for the Thames Estuary and River Thames. This would be part of an adaptive strategy for the long term planning of flood and coastal defences in that region, established as a result of the Environment Agency Thames Estuary 2100 project.

9. References

Amin, M., 1983. On perturbations of harmonic constants in the Thames Estuary. Geophysical Journal of the Royal Astronomical Society, **73**, 587-603.

Beradino, P., Fornaro, G., Lanari, R. and Sansosti, E., 2002. A new algorithm for surface deformation monitoring based on small baseline differential SAR interferograms. IEEE Transactions on Geoscience and Remote Sensing, **40**(11), 2375-2383.

Bingley, R. M., Ashkenazi, V., Penna, N. T., Booth, S. J., Ellison, R. A. and Morigi, A. N., 1999. Monitoring changes in regional ground level, using high precision GPS. Environment Agency R&D Technical Report, W210.

Bingley, R. M., Teferle, F. N., Dodson, A. H., Williams, S. D. P. and Baker, T. F., 2006. Measuring changes in ground level at tide gauges, using continuous GPS and absolute gravimetry, to improve estimates of changes in sea level around Britain. Proceedings of the 41st Defra Flood and Coastal Management conference, York, UK, July 2006, 09.4.1 to 09.4.5.

Bovenga, F., Nutricato, R., Refice, A., Guerriero, L. and Chiaradia, M. T., 2004. SPINUA: A flexible processing chain for ERS/Envisat long term interferometry. Proceedings of the 2004 Envisat and ERS Symposium (EAS SP-572), Salzburg, Austria.

Bowen, A. J., 1972. The tidal régime of the River Thames; long-term trends and their possible causes. Philosophical Transactions of the Royal Society A, **272**, 187-199.

Bridgland, D. R., 2006. The Middle and Upper Pleistocene sequence in the Lower Thames: a record of Milankovitch climatic fluctuation and early human occupation of southern Britain. Proceedings of the Geologists' Association, **117**, 281-305.

Busby, J. P., Walker, A. S. D. and Rollin, K. E., 2006. Regional geophysics of south-east England. [CD-ROM]. Version 1.0. Keyworth, Nottingham: British Geological Survey.

Church, J. A., Gregory, J. M., Huybrechts, P., Kuhn, M., Lambeck, K., Nhuan, M. T., Quin, D. and Woodworth, P. L., 2001. Changes in sea level, in Climate Change 2001: The Scientific Basis: Contribution of Working Group I to the Third Assessment Report of the Intergovernmental Panel on Climate Change, Houghton et. al. (eds.), Cambridge University Press, New York, 639-694.

Church, J. A., White, N. J., Coleman, R., Lambeck, K. and Mitrovica, J. X., 2004. Estimates of the regional distribution of sea level rise over the 1950-2000 Period. Journal of Climatology, **17**, 2609-2625.

Church, J.A. and White, N. J., 2006. A 20th century acceleration in global sea-level rise. Geophysical Research Letters, **33**, L01602, 10.1029/2005GL024826.

Colesanti, C., Ferretti, A., Novali, F., Prati, C. and Rocca, F., 2003a. SAR monitoring of progressive and seasonal ground deformation using the Permanent Scatterers Technique. IEEE Transactions on Geoscience and Remote Sensing, **41**(7), 1685-1701.

Colesanti, C., Ferretti, A., Prati, C. and Rocca, F., 2003b. Monitoring landslides and tectonic motions with the Permanent Scatterers Technique. Engineering Geology, **68**, 3-14.

Defra, 2004. Evidence and innovation: Defra's needs from the sciences over the next 10 years. Defra publication PB9227.

Dixon, T., 1991. An introduction to the Global Positioning System and some geological applications. Reviews of Geophysics, **29**, 249-276.

Dominguez, J., Romero, R., Carrasco, D., Martinez, A., Mallorqui, J. J., Blanco, P. and Navarrete, D., 2005. Advanced DInSAR based on coherent pixels: development and results using CPT technique. Proceedings of the FRINGE 2005 Workshop, Frascatti, Italy.

Ellison, R. A., Woods, M. A., Allen, D. J., Forster, A., Pharaoh, T. C. and King, C., 2004. Geology of London. Memoir of the British Geological Survey, Sheets 256 (North London), 257 (Romford), 270 (South London) and 271 (Dartford) (England and Wales).

Environment Agency. 2005. Groundwater levels in the Chalk-basal sands aquifer of the central London Basin.

Ferretti, A., Prati, C. and Rocca, F., 1999. Permanent scatterers in SAR interferometry. Proceedings of IGARSS 99, Hamburg, Germany.

Ferretti, A., Prati, C. and Rocca, F., 2000. Nonlinear subsidence rate estimation using Permanent Scatterers in Differential SAR Interferometry. IEEE Transactions on Geoscience and Remote Sensing, **38**, 2202-2212.

Ferretti, A., Prati, C. and Rocca, F., 2001. Permanent scatterers in SAR interferometry. IEEE Transactions on Geoscience and Remote Sensing, **39**(1), 8-20.

Freeze, R. A. and Cherry, J. A., 1979. Groundwater. London: Prentice-Hall.

Fruneau, B., Achache, J. and Delacourt, C., 1996. Observation and modelling of the Saint-Etienne-de-Tinée landslide using SAR interferometry. Tectonophysics, **265**, 181-190.

Gabriel, A. K., Goldstein, R. M. and Zebker, H., 1989. Mapping small elevation changes over large areas: differential radar interferometry. Journal of Geophysical Research, **94**, B7, 9183-9191.

Ge, M., Gendt, G., Dick, G., Zhang, F. P. and Reigber, C., 2005. Impact of GPS satellite antenna offsets on scale changes in global network solutions. Geophysical Research Letters, **32**, L06310, 10.1029/2004GL022224.

Goldstein, R. M., Engelhardt, H., Kamb, B. and Frolich, R. M., 1993. Satellite radar interferometry for monitoring ice sheet motion: Application to an Antarctic ice stream. Science, **262**, 1525-1530.

Hanssen, R., 2001. Radar Interferometry: Data interpretation and Error Analysis. Kluwer Academic Publishers.

Holgate, S. and Woodworth, P. L., 2004. Evidence for enhanced coastal sea level rise during the 1990s. Geophysical Research Letters, **31**, L07305, 10.1029/2004GL019626.

Hooper, A., Zebker, H., Segall, P. and Kampes, B., 2004. A new method for measuring deformation on volcanoes and other natural terrains using InSAR Persistent Scatterers. Geophysical Research Letters, **31**(23).

Hugentobler, U., Dach, R. and Fridez, P., 2006. Bernese GPS Software Version 5.0 Draft. (eds) Astronomical Institute University of Berne, pp 388.

Hulme, M., Jenkins, G. J., Lu, X., Turnpenny, J. R., Mitchell, T. D., Jones, R. G., Lowe, J., Murphy, J. M., Hassell, D., Boorman, P., McDonald, R. and Hill, S., 2002. Climate change scenarios for the United Kingdom: the UKCIP02 scientific report. Tyndall Centre for Climate Change Research, School of Environmental Sciences, University of East Anglia, Norwich, UK, 120 pp.

Kampes, B. and Usai, S., 1999. Doris: the Delft Object-oriented Radar Interferometric Software. 2nd International Symposium on Operationalization of Remote Sensing, Enschede, The Netherlands.

Kampes, B. and Nico, A., 2005. The STUN algorithm for Persistent Scatterer Interferometry. Proceedings of the FRINGE 2005 Workshop, Frascatti, Italy.

Lambeck, K. and Johnston, P. J., 1995. Land subsidence and sea-level change: Contributions from the melting of the last great ice sheets and the isostatic adjustment of the Earth. In: *Land Subsidence*, Barends, Brouwer and Schröder (eds.), Balkema, Rotterdam, 3-18.

MacMillan, D. S., 2004. Rate difference between VLBI and GPS reference frame scales. Eos Transactions, **85(47)**, AGU Fall Meeting Supplement, G21B-05.

Massonnet, D., Rossi, M., Carmona, C., Adragna, F., Peltzer, G., Feigl, K. and Rabaute, T., 1993. The Displacement field of the Landers Earthquake mapped by Radar Interferometry. Nature, **364.**

Massonnet, D., Briole, P. and Arnaud, A. 1995. Deflation of Mount Etna monitored by spaceborne radar interferometry. Nature, **375**: 567-570.

Massonnet, D., Holzer, T. and Vadon, H., 1997. Land subsidence caused by the East Mesa geothermal field, California, observed using SAR interferometry. Geophysical Research Letters, **24**(8), 901-904

Muir Wood, R., 1990. London: not waving but drowning. Terra Nova, **2(3)**, 284-291.

NTSLF, 2006. UK tide gauge network. National Tidal and Sea level Facility (NTSLF). http://www.pol.ac.uk/ntslf/networks.html.

Orliac, E. J., Teferle, F. N. and Bingley, R. M., 2006. iGNSS processing tools user manual. IESSG, University of Nottingham, Nottingham, UK.

Peltier, W. R, 2001. ICE4G (VM2) glacial isostatic adjustment corrections. In: Sea Level Rise History and Consequences. International Geophysics Series, **75**, Academic Press, San Diego, 65-96.

Peltier, W. R., Shennan, I., Drummond, R. and Horton, B. P., 2002. On the postglacial isostatic adjustment of the British Isles and the shallow viscoelastic structure of the Earth. Geophysical Journal International, **148**, 443-475.

Pharaoh, T. C., Molyneux, S. G., Merriman, R. J., Lee, M. K. and Verniers, J., 1993. The Caledonides of the Anglo-Brabant massif reviewed. Geological Magazine, **130**, 561-562.

Prawirodirdjo, L. and Bock, Y., 2004. Instantaneous global plate motion model from 12 years of continuous GPS observations. Journal of Geophysical Research, **109(8)**, B08405.

PSMSL, 2005. Table of MSL secular trends derived from PSMSL RLR data [online, last update 3 August 2005]. Permanent Service for Mean Sea Level (PSMSL). http://www.pol.ac.uk/psmsl/datainfo/rlr.trends.

Redman, J. B., 1877. The River Thames. Proceedings of the Institution of Civil Engineers, **49**, 67-157.

Rickards, L. and Kilonsky, B., 1997. Developments in sea level data management and exchange. Available at http://www.bodc.ac.uk/projects/wocedac/guides/odspaper.html, 12 pp.

Rossiter, J. R., 1969a. Tidal régime of the River Thames. Dock. Harb. Auth., **49**, 461-462.

Rossiter, J. R., 1969b. Thames flood prevention, first report of studies, Appendix 6. London: GLC.

Shennan, I., 1989. Holocene crustal movements and sea-level changes in Great Britain. Journal of Quaternary Science, **4(1)**, 77-89.

Shennan, I. and Horton, B., 2002. Holocene land- and sea-level changes in Great Britain. Journal of Quaternary Science, **17(5-6)**, 511-526.

Shennan, I., Peltier, W. R., Drummond, R. and Horton, B., 2002. Global to local scale parameters determining relative sea-level changes and the post-glacial isostatic adjustment of Great Britain. Quaternary Science Reviews, **21**, 397-408.

Shennan, I., Bradley, S. L., Milne, G. A., Brooks, A., Bassett, S. E., and Hamilton, S., 2006a. Relative sea-level changes, glacial isostatic modelling and ice-sheet reconstructions from the British Isles since the Last Glacial Maximum. Journal of Quaternary Science, **21**, 585-599, doi:510.1002/jqs.1049.

Shennan, I., Hamilton, S., Hillier, C., Hunter, A., Woodall, R., Bradley, S. L., Milne, G. A., Brooks, A. and Bassett, S. E., 2006b. Relative sea-level observations in western Scotland since the Last Glacial Maximum for testing models of glacial isostatic land movements and ice-sheet reconstructions. Journal of Quaternary Science, **21**, 601-613, doi:510.1002/jqs.1048.

Siggers, G., Spearman, J., Littlewood, M. and Donovan, B., 2006. One hundred years of morphological change in the Thames Estuary: impacts on tide levels and implications for flood risk management to 2100. Proceedings of the 41st Defra Flood and Coastal Management conference, York, UK, July 2006, 04.1.1 to 04.1.12.

Smith, R. L. 1986. Extreme value analysis based on the r largest annual events. Journal of Hydrology, **86**, 27-43.

Sumbler, M. G., 1996. British regional geology: London and the Thames Valley (Fourth). London: HMSO for the British Geological Survey.

Stewart, M. P., Ffoulkes-Jones, G. H., Ochieng, W. Y., Shardlow, P. J., Penna, N. T. and Bingley, R. M., 2002. GAS: GPS Analysis Software version 2.4 user manual. IESSG, University of Nottingham, Nottingham, UK.

Tawn, J. A. 1988. An extreme value theory model for dependent observations. Journal of Hydrology, **101**, 227-250.

Teferle, F. N., Bingley, R. M., Dodson, A. H., Apostilidis, P. and Staton, G., 2003. RF interference and multipath effects at continuous GPS installations for long-term monitoring of tide gauges in UK harbours. Proceedings of the 16th Technical Meeting of the Satellite Division of the Institute of Navigation (ION-GPS 2003), Portland, Oregon, USA.

Teferle, F. N., Bingley, R. M., Williams, S. D. P, Baker, T. F. and Dodson, A. H., 2006. Using continuous GPS and absolute gravity to separate vertical land movements and changes in sea level at tide gauges in the UK. Philosophical Transactions of the Royal Society Series A: Mathematical, Physical, and Engineering Sciences, **364**, 10.1098/rsta.2006.1746, pp 971-930.

Teferle, F. N., Orliac, E. J. and Bingley, R. M., 2007. An assessment of Bernese GPS software precise point positioning using IGS final products for global site velocities. GPS solutions, 10.10007/s10291-006-0051-7.

UKCIP, 2006. Update to estimates of net sea-level change for Britain [online, updated in August 2006]. UK Climate Impacts Programme (UKCIP). http://www.ukcip.org.uk/resources/publications/pub_dets.asp?ID=80.

Warren, M., 2007. The development of a 3-pass persistent scatterer algorithm using the integer ambiguity search method. PhD Thesis (submitted), University of Nottingham.

Watts, A. B., McKerrow, W. S. and Richards, K., 2005. Localised Quaternary uplift of south-central England. Journal of the Geological Society, London, **162**, 13-24.

Werner, C., Wegmuller, U., Strozzi, T. and Weismann, A., 2003. Interferometric Point Target Analysis for deformation mapping. Proceedings of IGARSS 03, Toulouse, France.

White, N. J., Church, J. A. and Gregory, J. M., 2005. Coastal and global averaged sea level rise for 1950 to 2000. Geophysical Research Letters, **32**, L01601, 10.1029/2004GL021391.

Williams, S.D.P., Baker, T.F. and Jeffries, G., 2001. Absolute gravity measurements at UK tide gauges. Geophysical Research Letters, **28(12)**, 2317-2320, 10.1029/2000GL012438.

Williams, S. D. P., 2003. The effect of coloured noise on the uncertainties of rates estimated from geodetic time series. Journal of Geodesy, **76(9-10)**, 483-494.

Williams, S. D. P., Bock, Y., Fang, P., Jamason, P., Nikolaidis, R. M., Prawirodirdjo, L., Miller, M., and Johnson, D. J., 2004. Error analysis of continuous GPS position time series. Journal of Geophysical Research, **109(B3)**, B03412, 10.1029/2003JB002741.

Woodworth, P. L. and Jarvis, J., 1991. A feasibility study of the use of short historical and short modern tide gauge records to investigate long term sea level changes in the British Isles. Proudman Oceanographic Laboratory Internal Document No. 23.

Woodworth, P. L., Tsimplis, M. N., Flather, R. A. and Shennan, I., 1999. A review of the trends observed in British Isles mean sea level data measured by tide gauges. Geophysical Journal International, **136**, 651-670.

Woppelmann, G., Martin Miguez, B., Bouin, M-N. and Altamimi, Z., 2007. Geocentric sea-level trend estimates from GPS analyses at relevant tide gauges world-wide. Global and Planetary Change (in press).

Zebker, H., Rosen, P. A., Goldstein, R. M., Gabriel, A. and Werner, C. 1994. On the derivation of coseismic displacment fields using differential radar interferometry: the Landers earthquake. Journal of Geophysical Research, **99**, 19617–19643.

Appendix A: Validated data statistics for the quality controlled tide gauge data in the Thames Estuary and River Thames combined data set

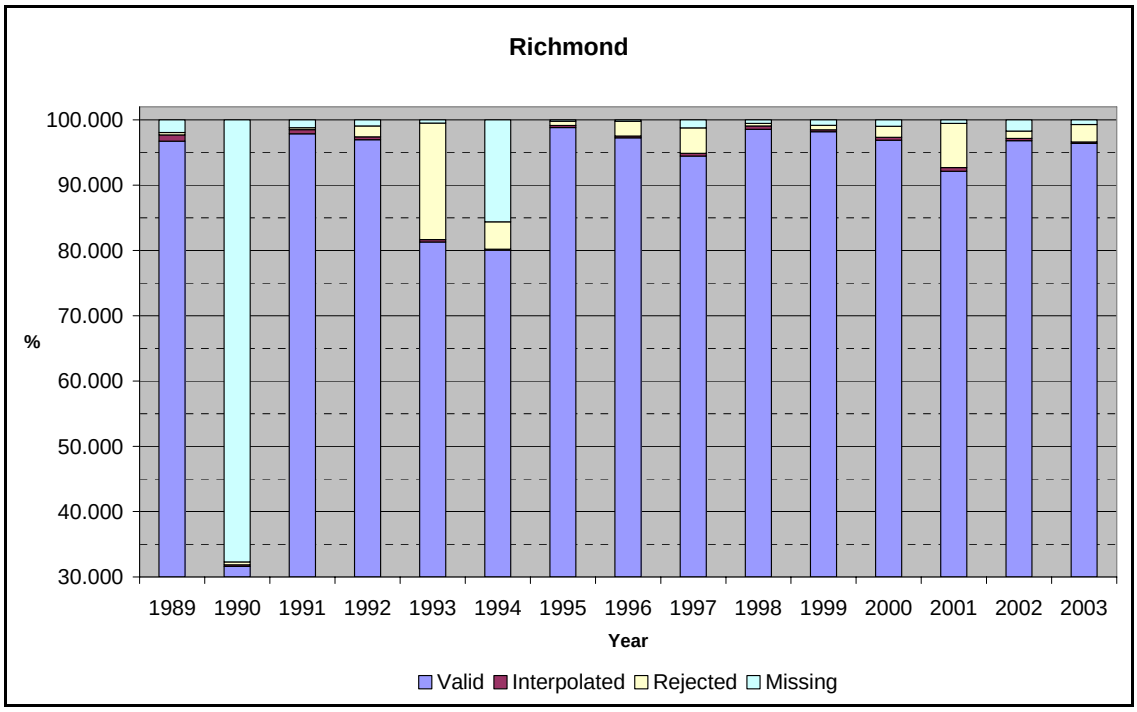

Figure A1 Validated data statistics for Richmond tide gauge for the period from 1989 to 2003

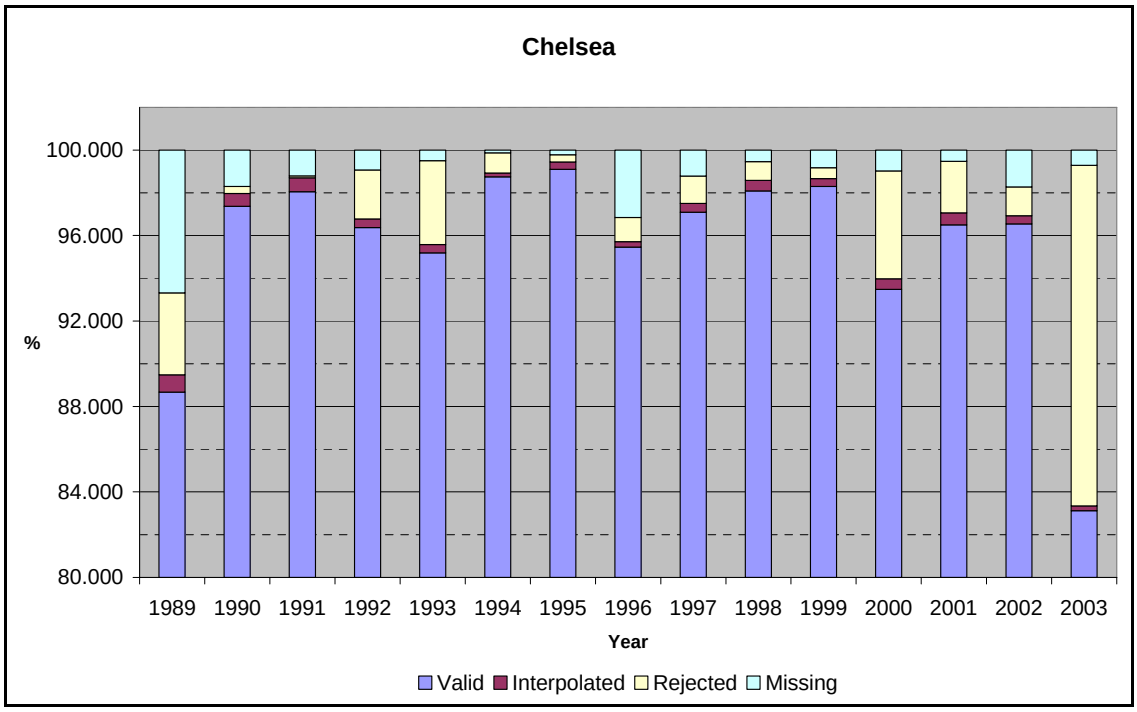

Figure A2 Validated data statistics for Chelsea tide gauge for the period from 1989 to 2003

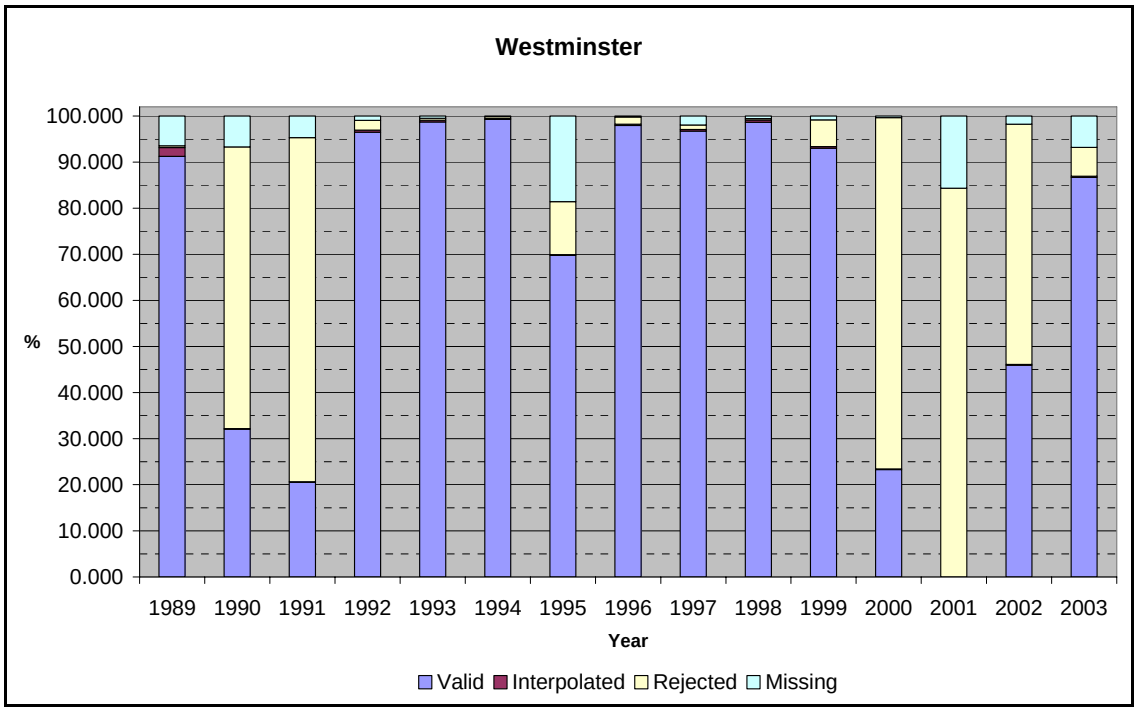

Figure A3 Validated data statistics for Westminster tide gauge for the period from 1989 to 2003

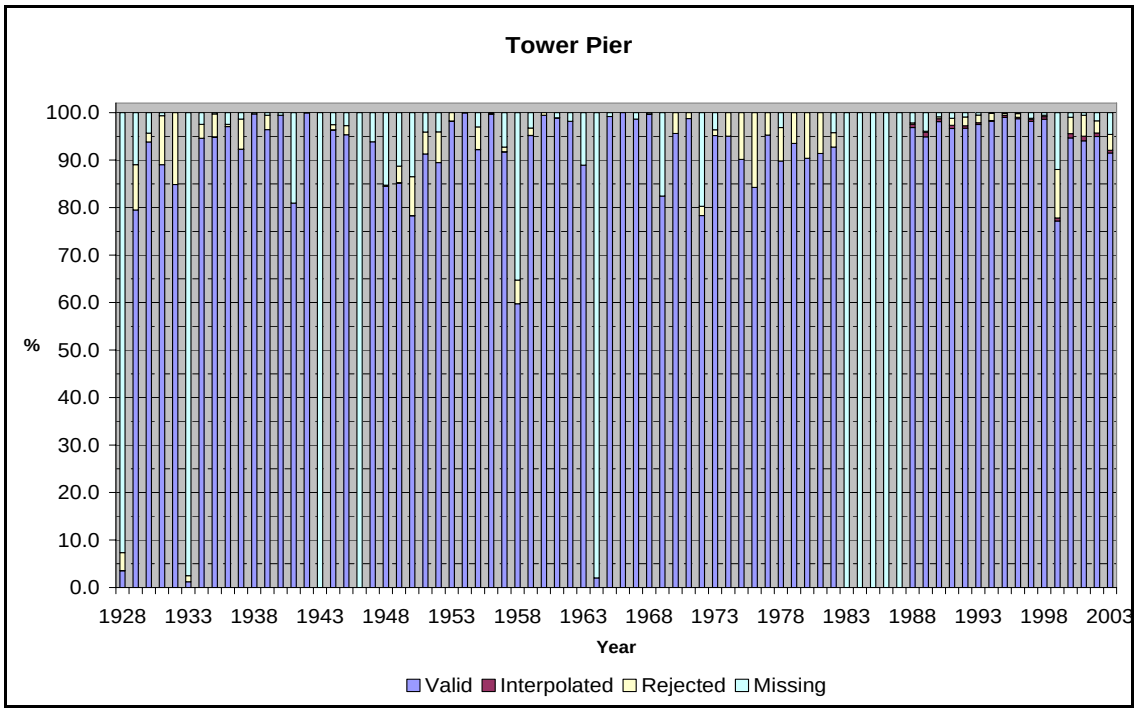

Figure A4 Validated data statistics for Tower Pier tide gauge for the period from 1928 to 2003

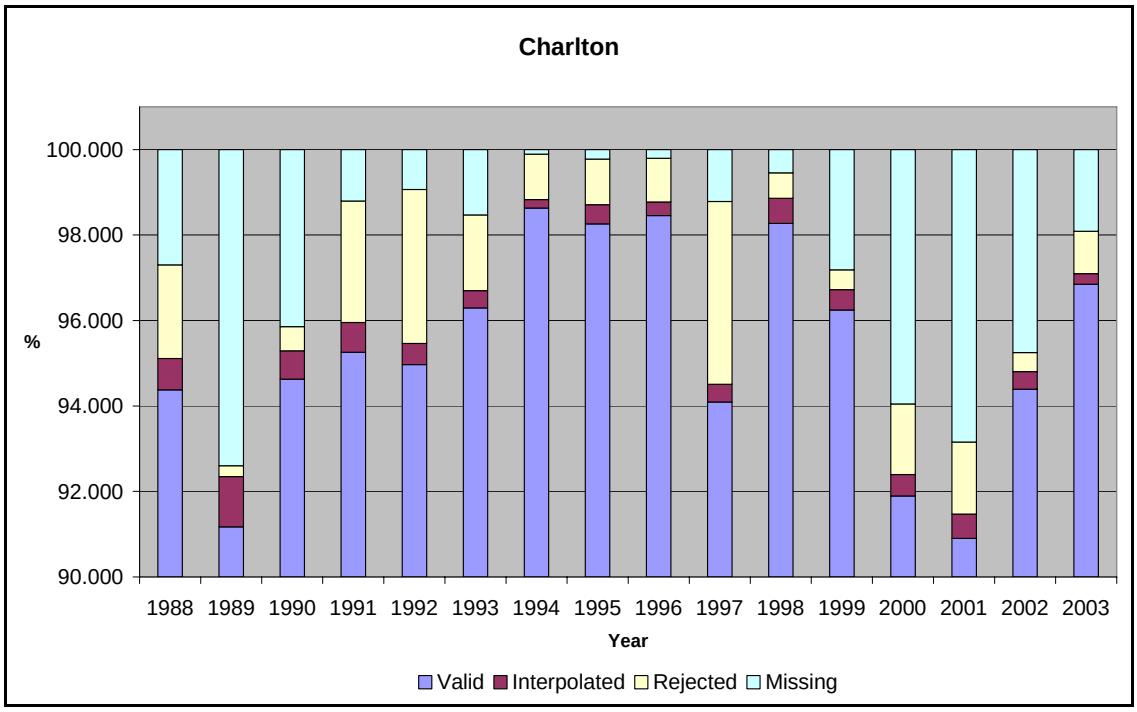

Figure A5 Validated data statistics for Charlton tide gauge for the period from 1989 to 2003

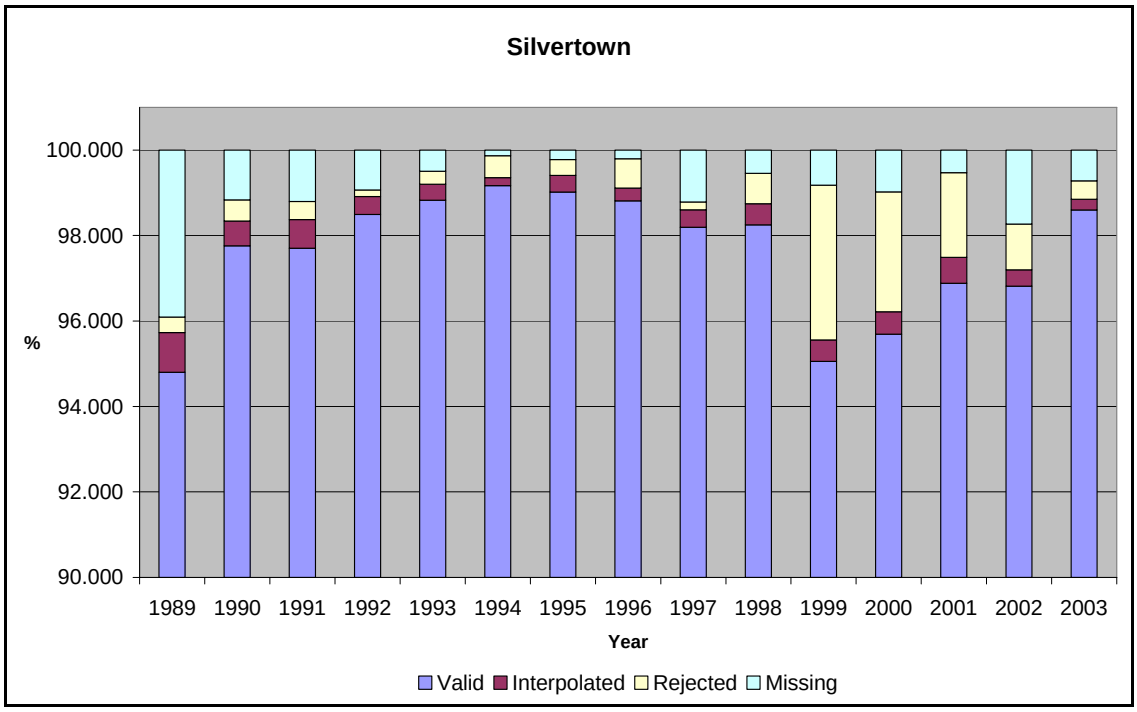

Figure A6 Validated data statistics for Silvertown tide gauge for the period from 1989 to 2003

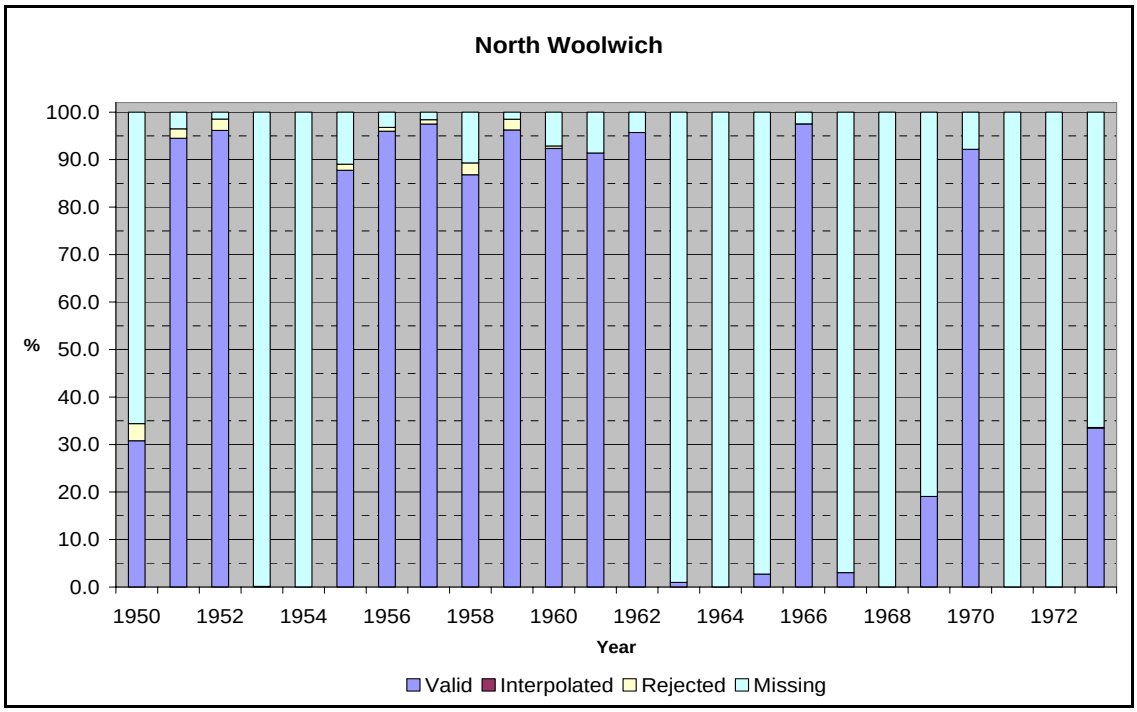

Figure A7 Validated data statistics for North Woolwich tide gauge for the period from 1950 to 1973

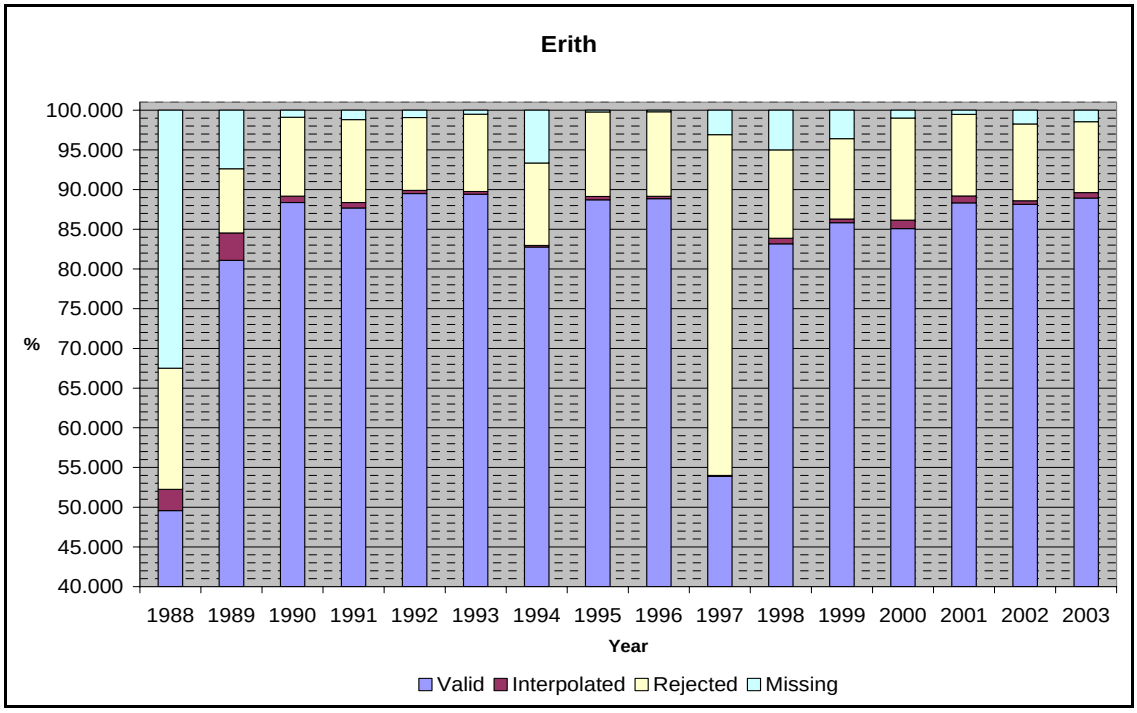

Figure A8 Validated data statistics for Erith tide gauge for the period from 1988 to 2003

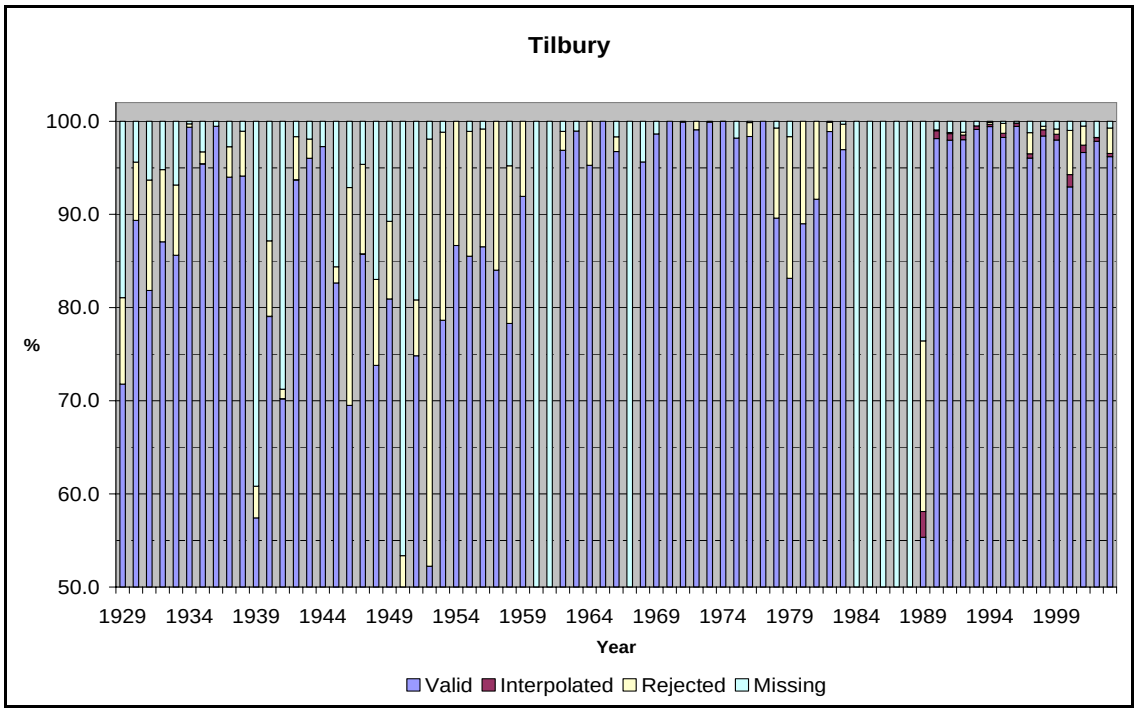

Figure A9 Validated data statistics for Tilbury tide gauge for the period from 1929 to 2003

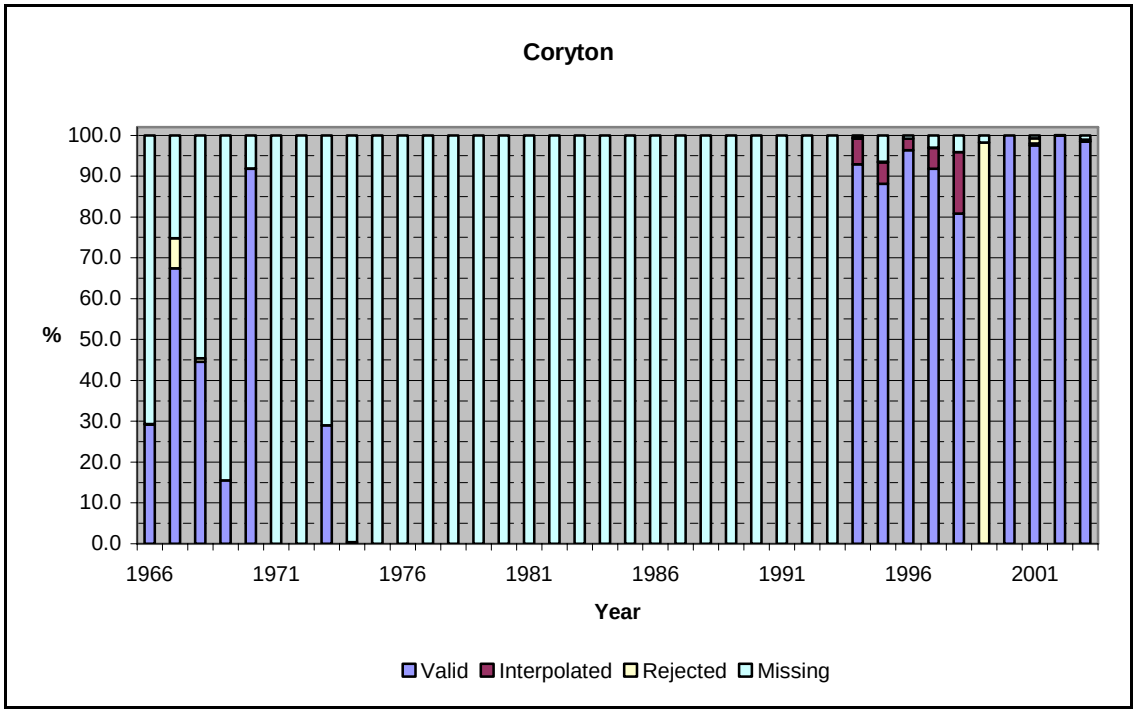

Figure A10 Validated data statistics for Coryton tide gauge for the period from 1966 to 2003

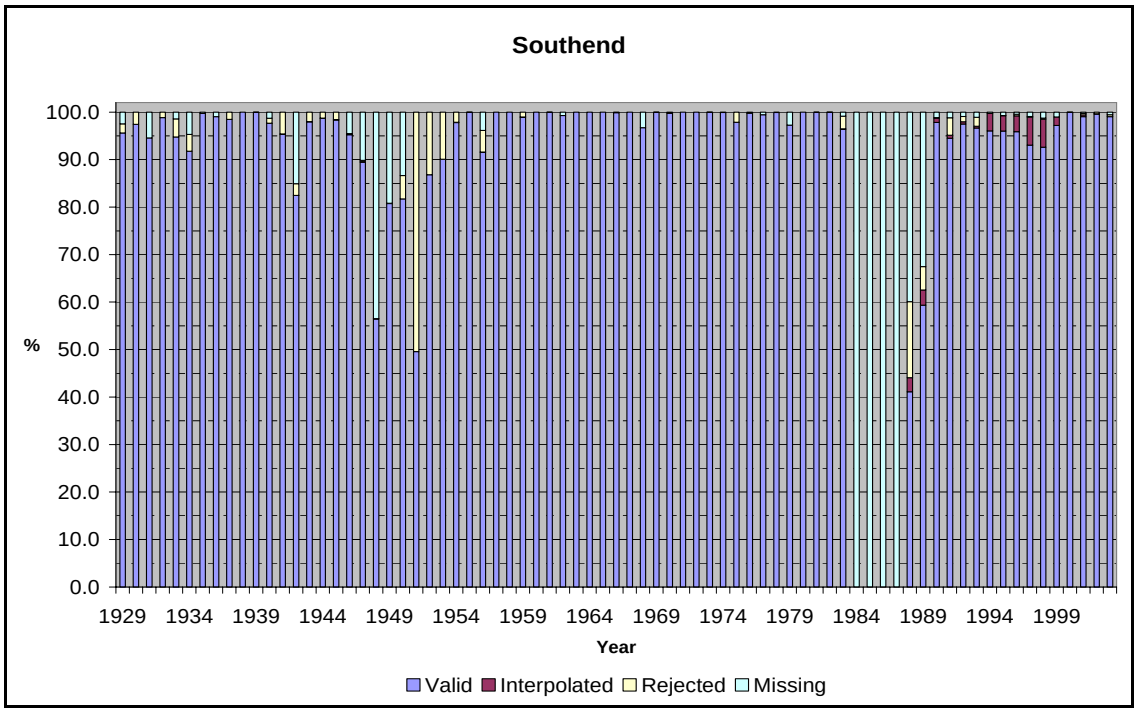

Figure A11 Validated data statistics for Southend tide gauge for the period from 1929 to 2003

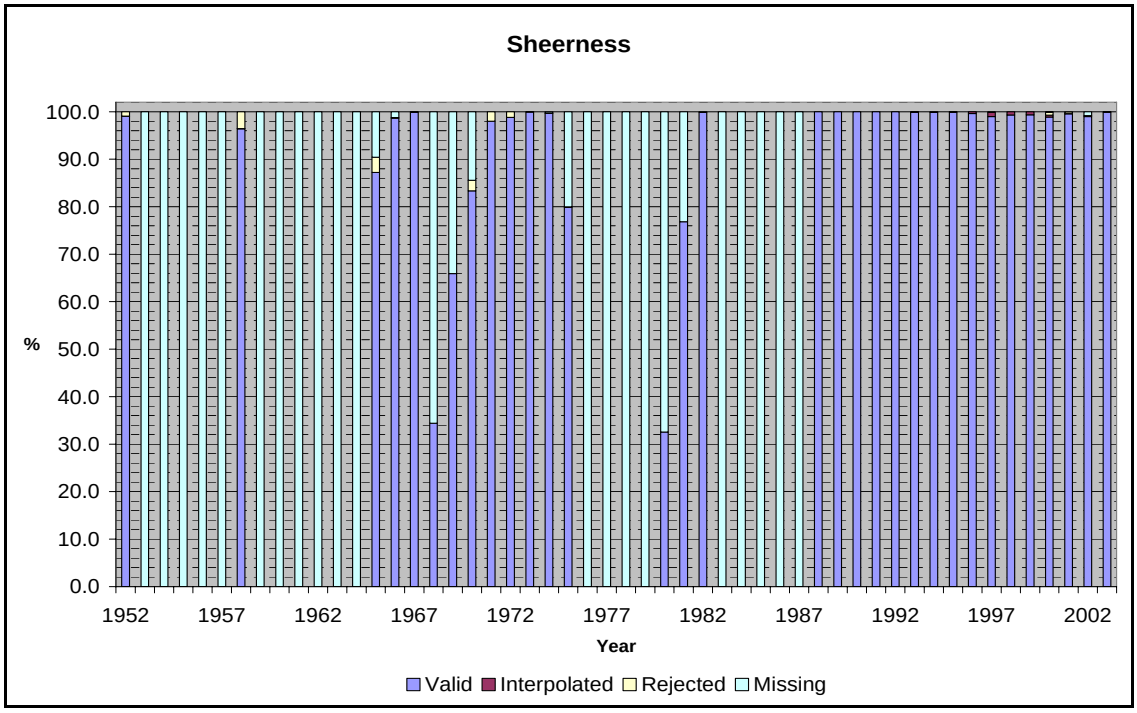

Figure A12 Validated data statistics for Sheerness tide gauge for the period from 1952 to 2003

Appendix B: CGPS height time series for 11 of the 44 stations in Great Britain and Northern France considered in the national study

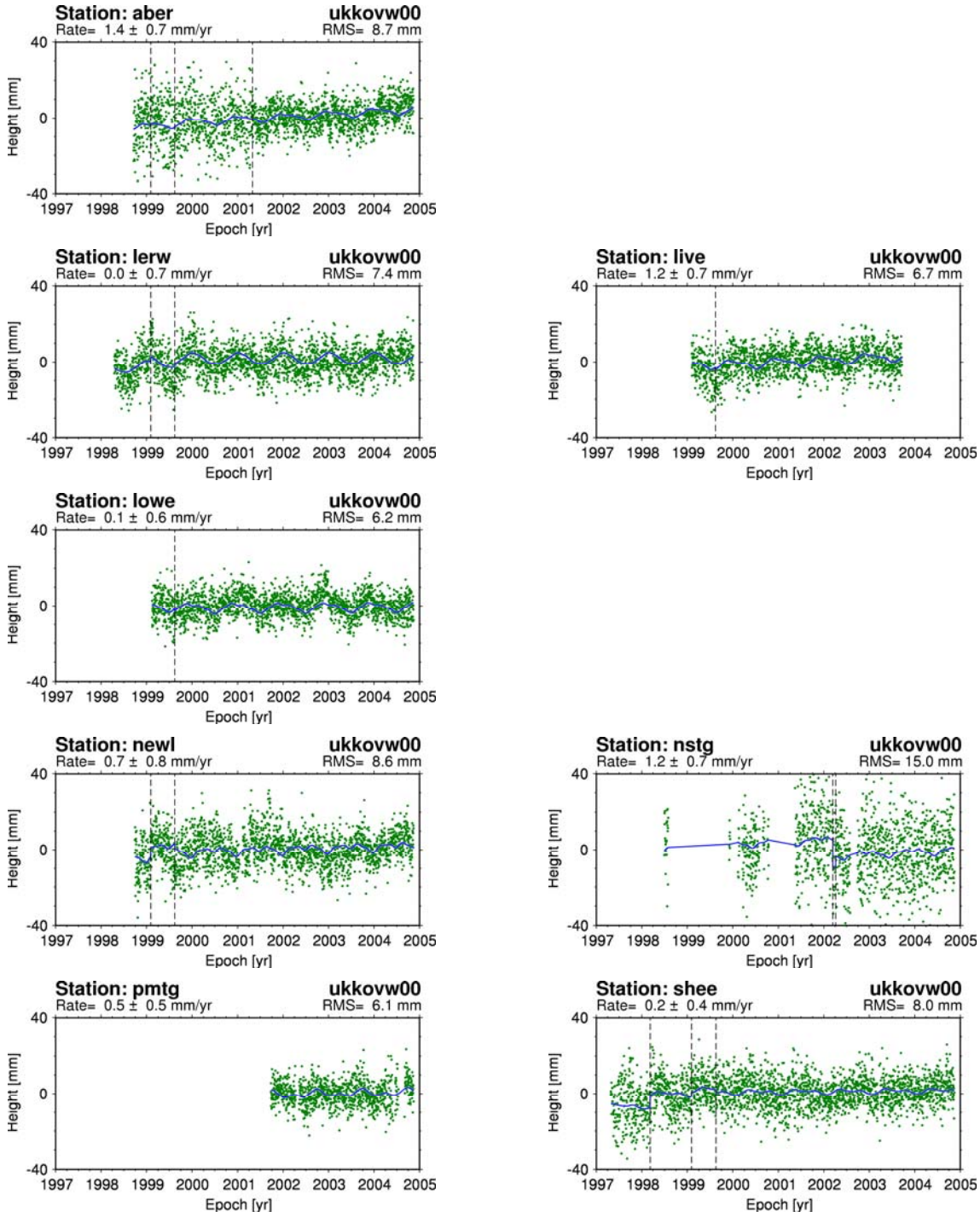

Figure B1 CGPS height time series from Solution 1 for seven of the ten CGPS@TG stations in Great Britain and the non-TG CGPS station at LERW on Shetland

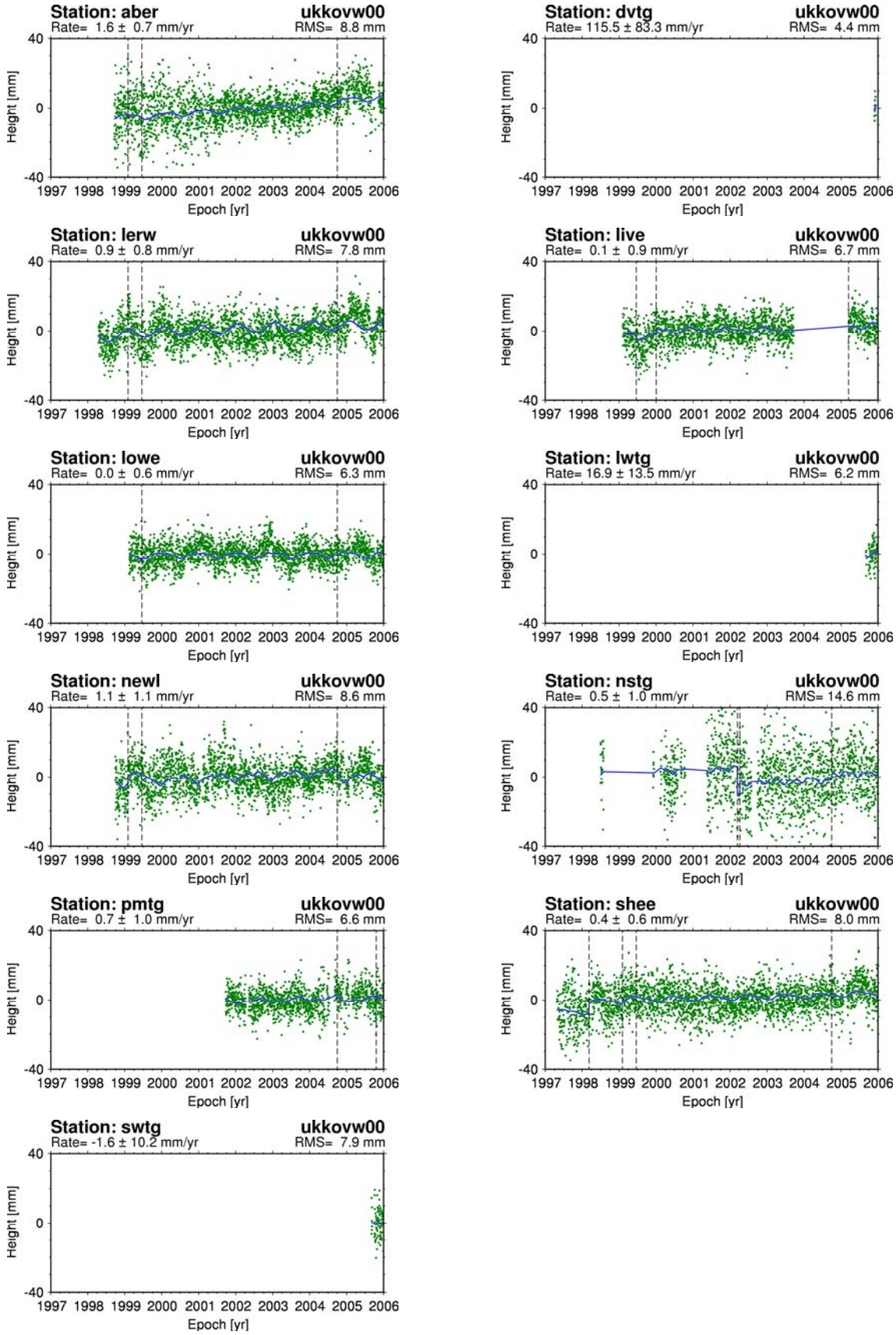

Figure B2 CGPS height time series from Solution 2 for the ten CGPS@TG stations in Great Britain and the non-TG CGPS station at LERW on Shetland

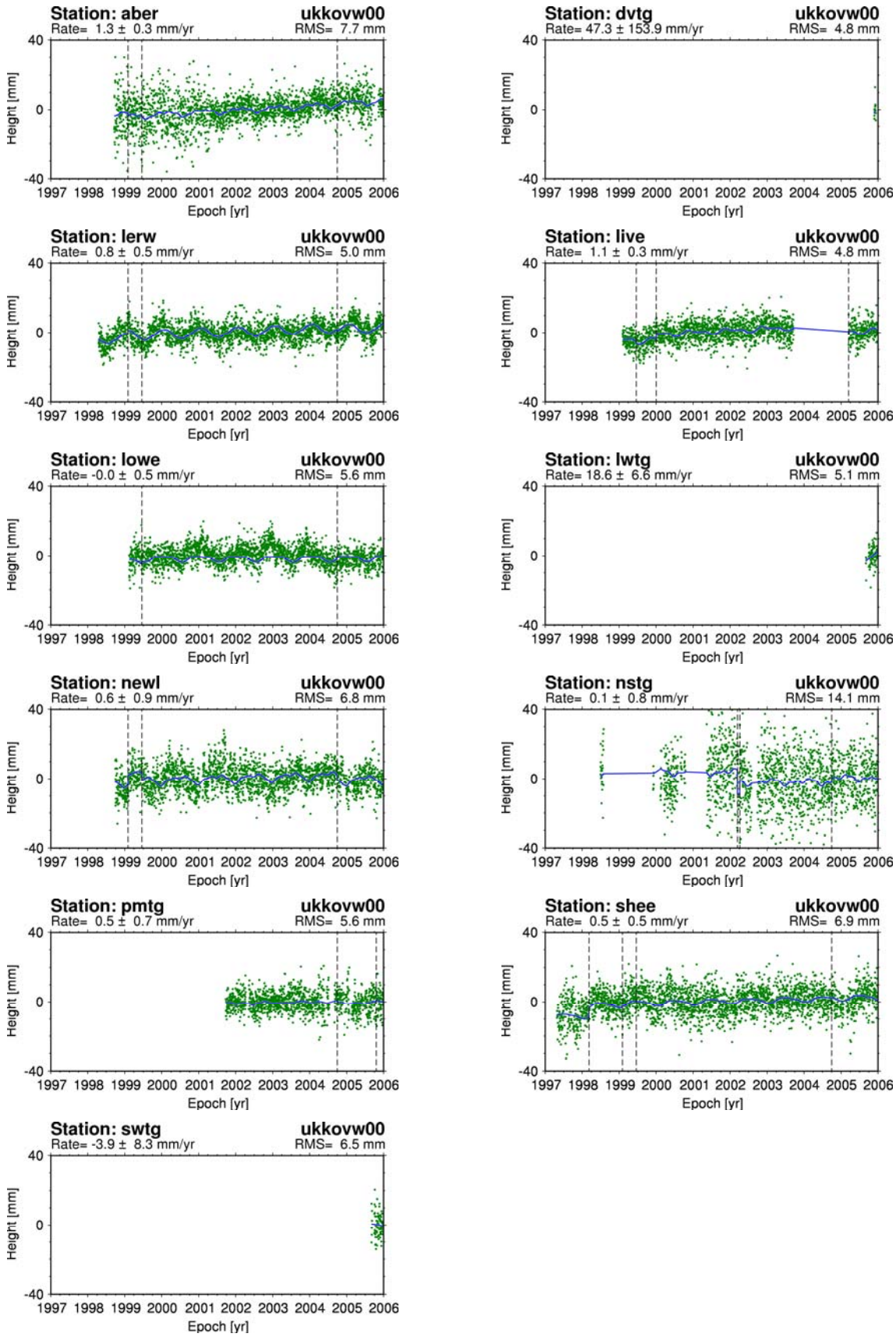

Figure B3 CGPS height time series from Solution 3 for the ten CGPS@TG stations in Great Britain and the non-TG CGPS station at LERW on Shetland

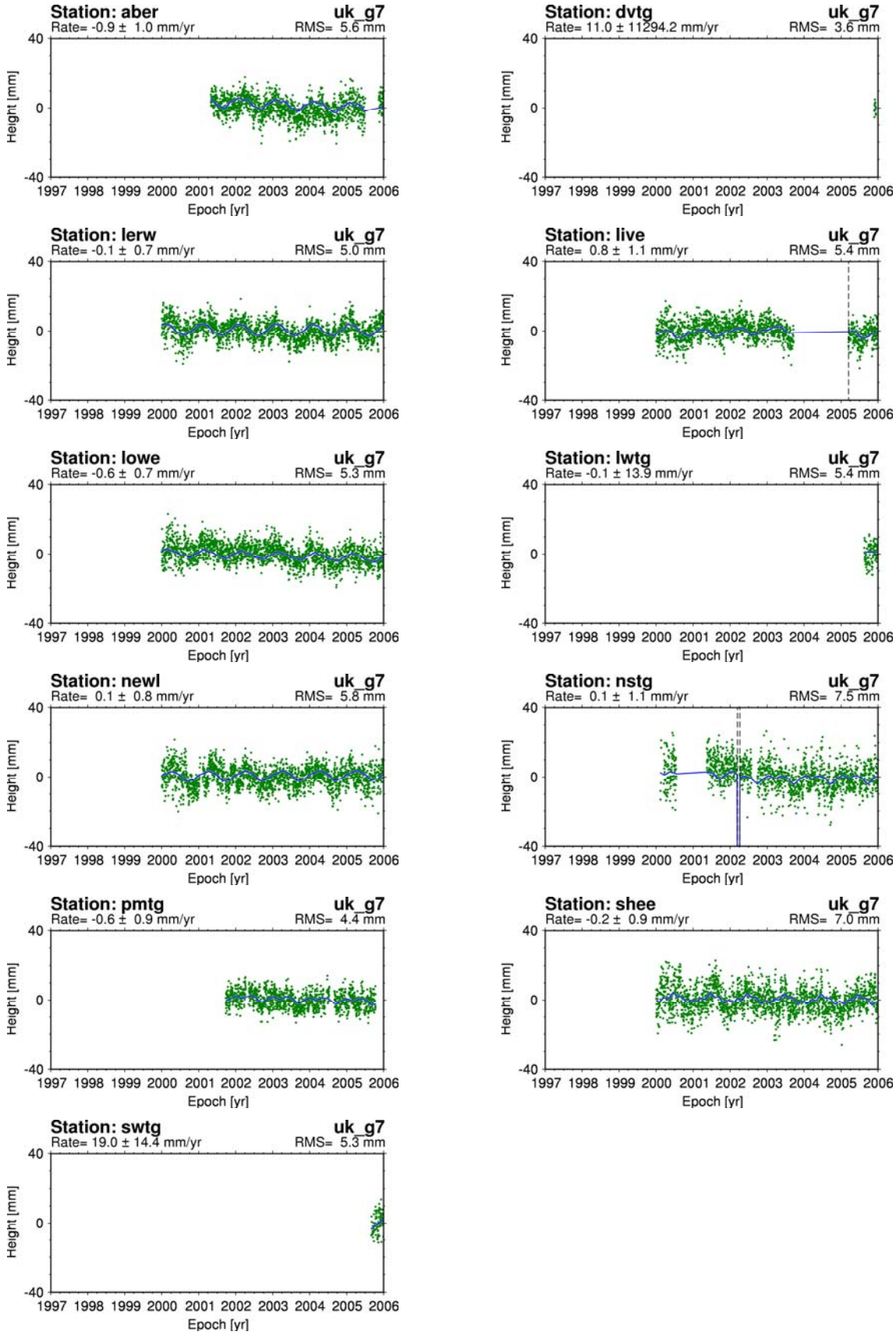

Figure B4 CGPS height time series from Solution 4 for the ten CGPS@TG stations in Great Britain and the non-TG CGPS station at LERW on Shetland

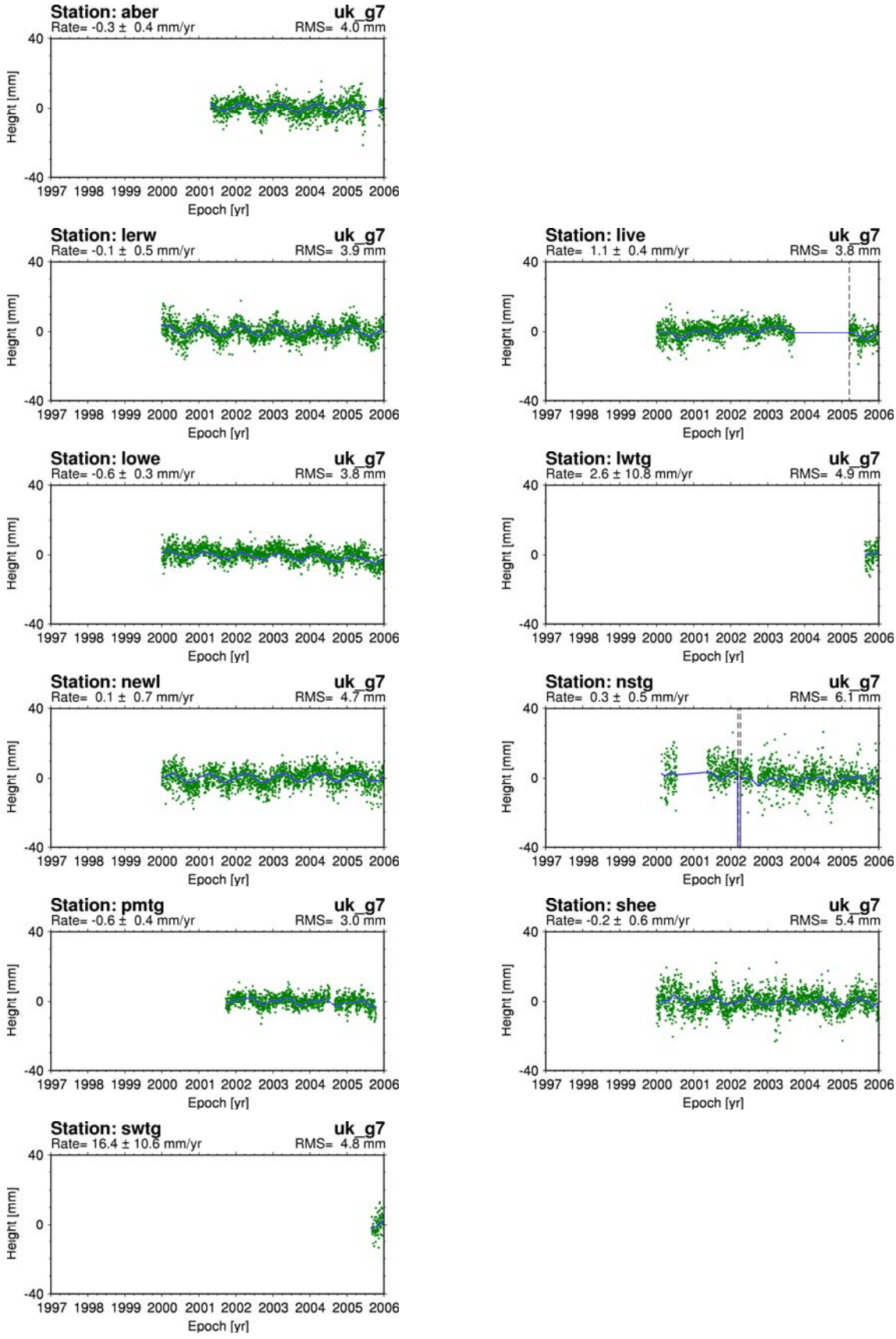

Figure B5 CGPS height time series from Solution 5 for the ten CGPS@TG stations in Great Britain and the non-TG CGPS station at LERW on Shetland

Appendix C: CGPS height time series for the three stations in the Thames Region considered in the regional study

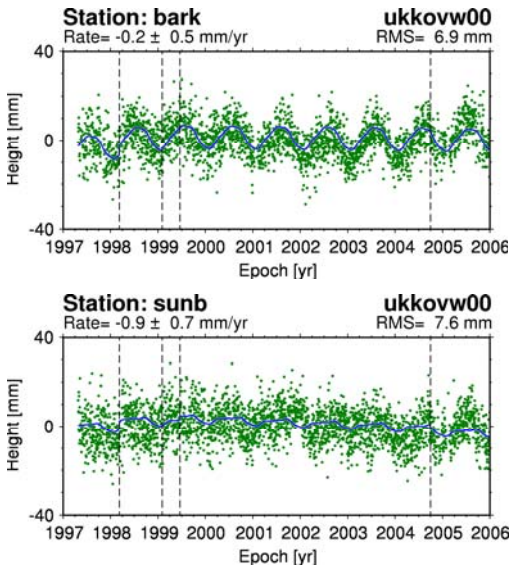

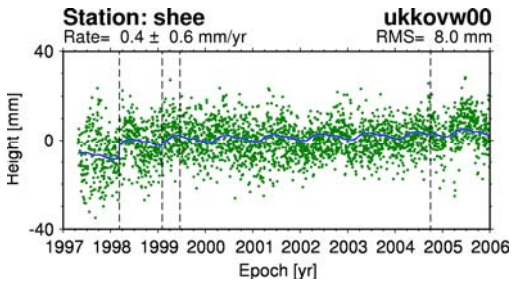

Figure C1 CGPS height time series from solution 2 for the one CGPS@TG station and two non-TG CGPS stations in the Thames Region

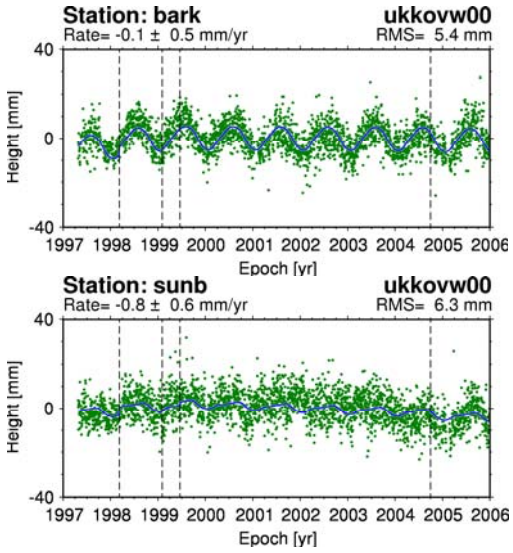

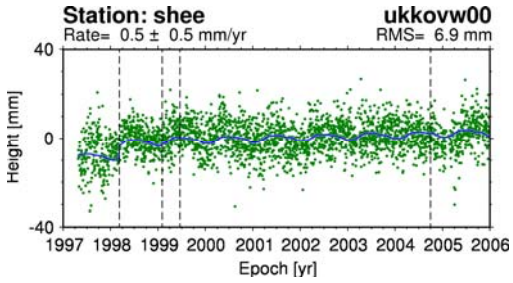

Figure C2 CGPS height time series from solution 3 for the one CGPS@TG station and two non-TG CGPS stations in the Thames Region

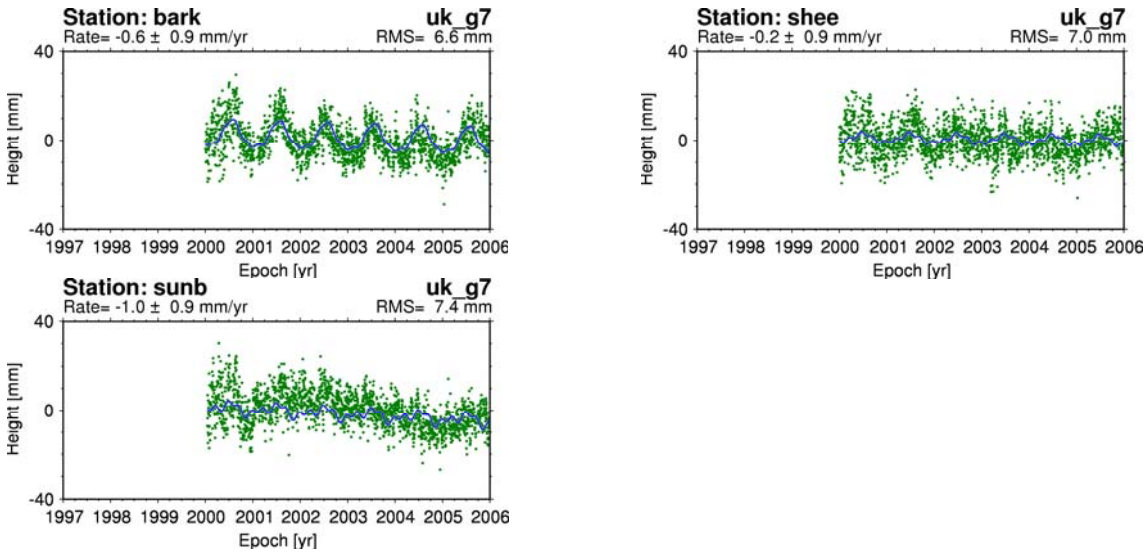

Figure C3 CGPS height time series from solution 4 for the one CGPS@TG station and two non-TG CGPS stations in the Thames Region

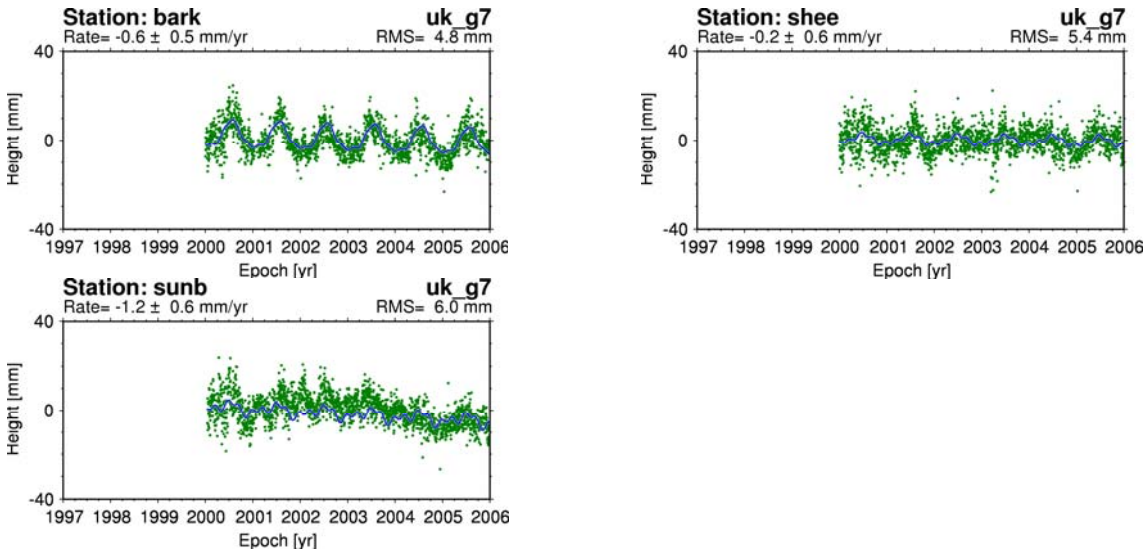

Figure C4 CGPS height time series from solution 5 for the one CGPS@TG station and two non-TG CGPS stations in the Thames Region

Appendix D: EGPS height time series for the 13 stations in the Thames Region considered in the regional study

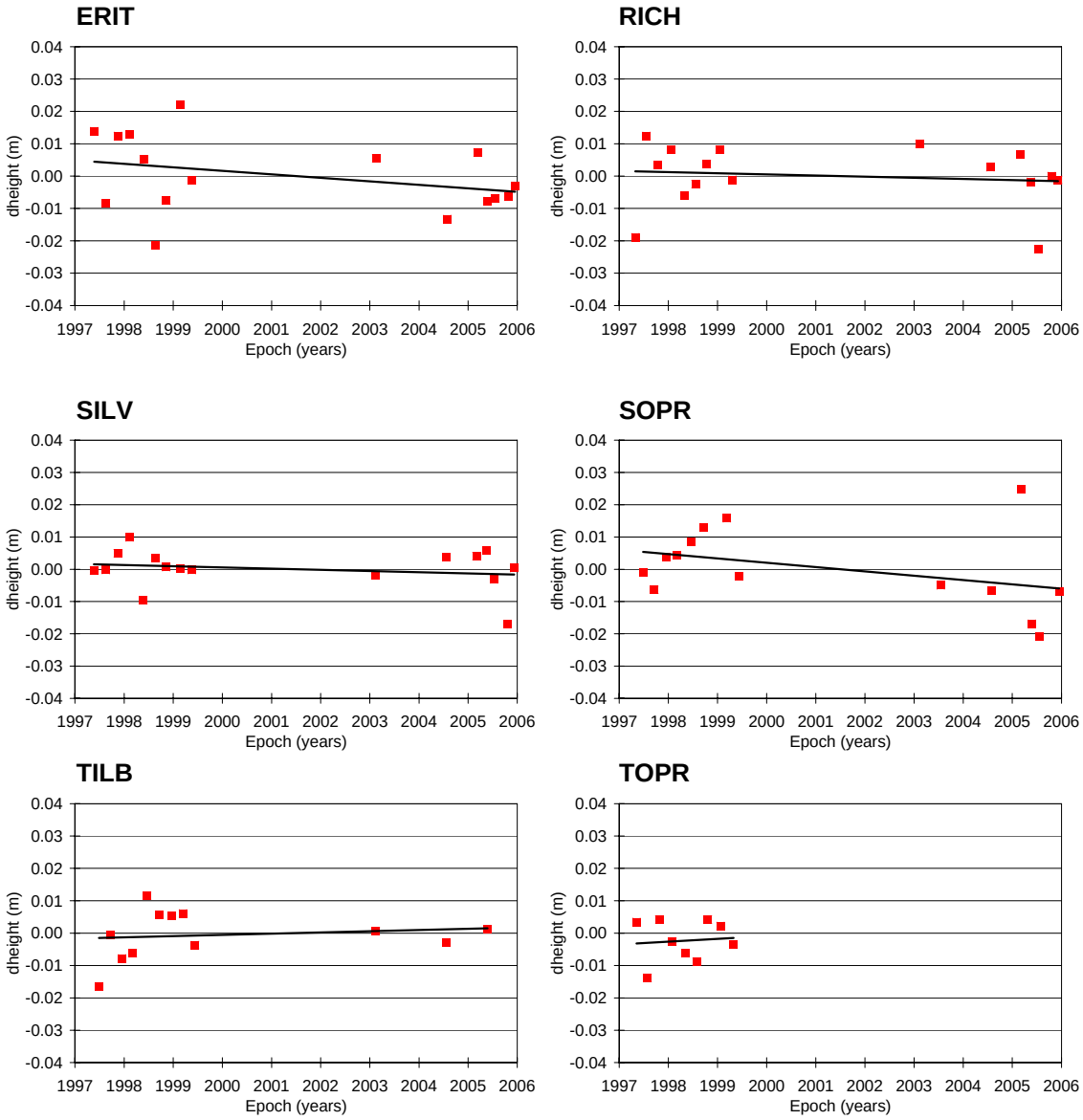

Figure D1 EGPS height time series for 6 EGPS@TG stations in the Thames Region

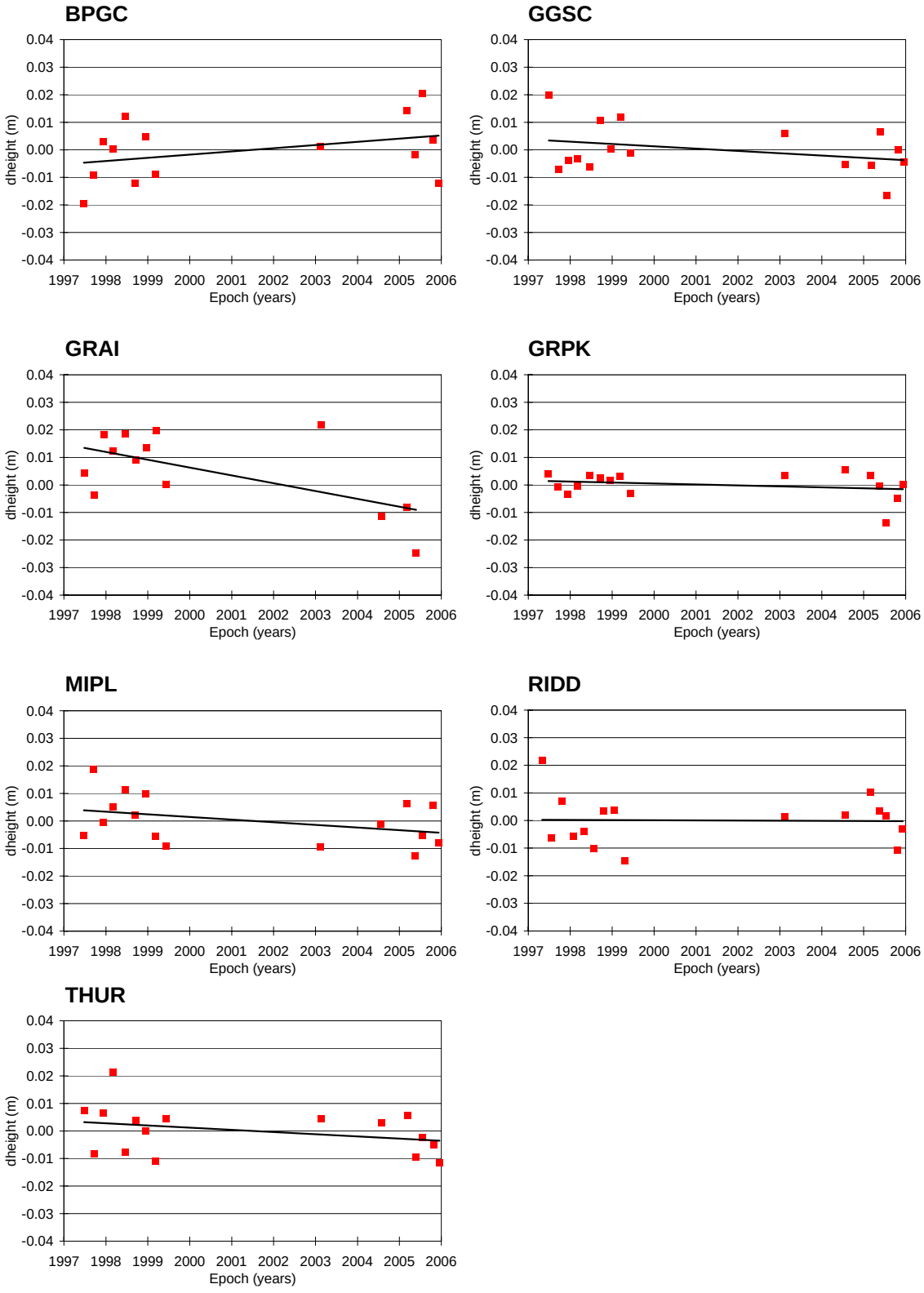

Figure D2 EGPS height time series for the other 7 EGPS stations in the Thames Region

Appendix E: Results of comparisons with geoscience datasets for the regional study

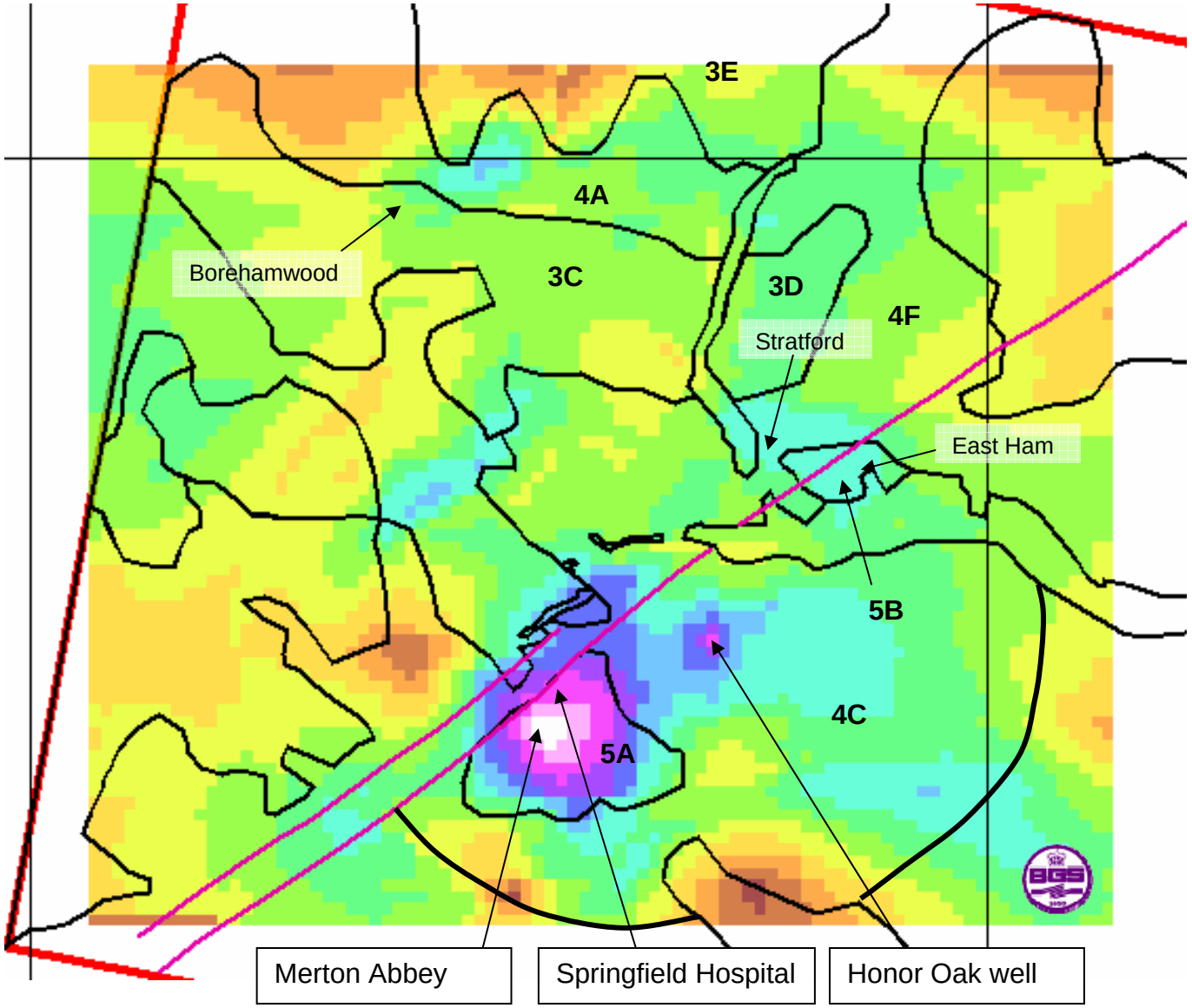

Figure E1 Change in groundwater levels in the London area, January 1997 to January 2006 and domains from the regional study

Change in groundwater level during period, in metres, based on Environment Agency data.

Positive values represent areas where groundwater has risen, and negative values show where it has fallen

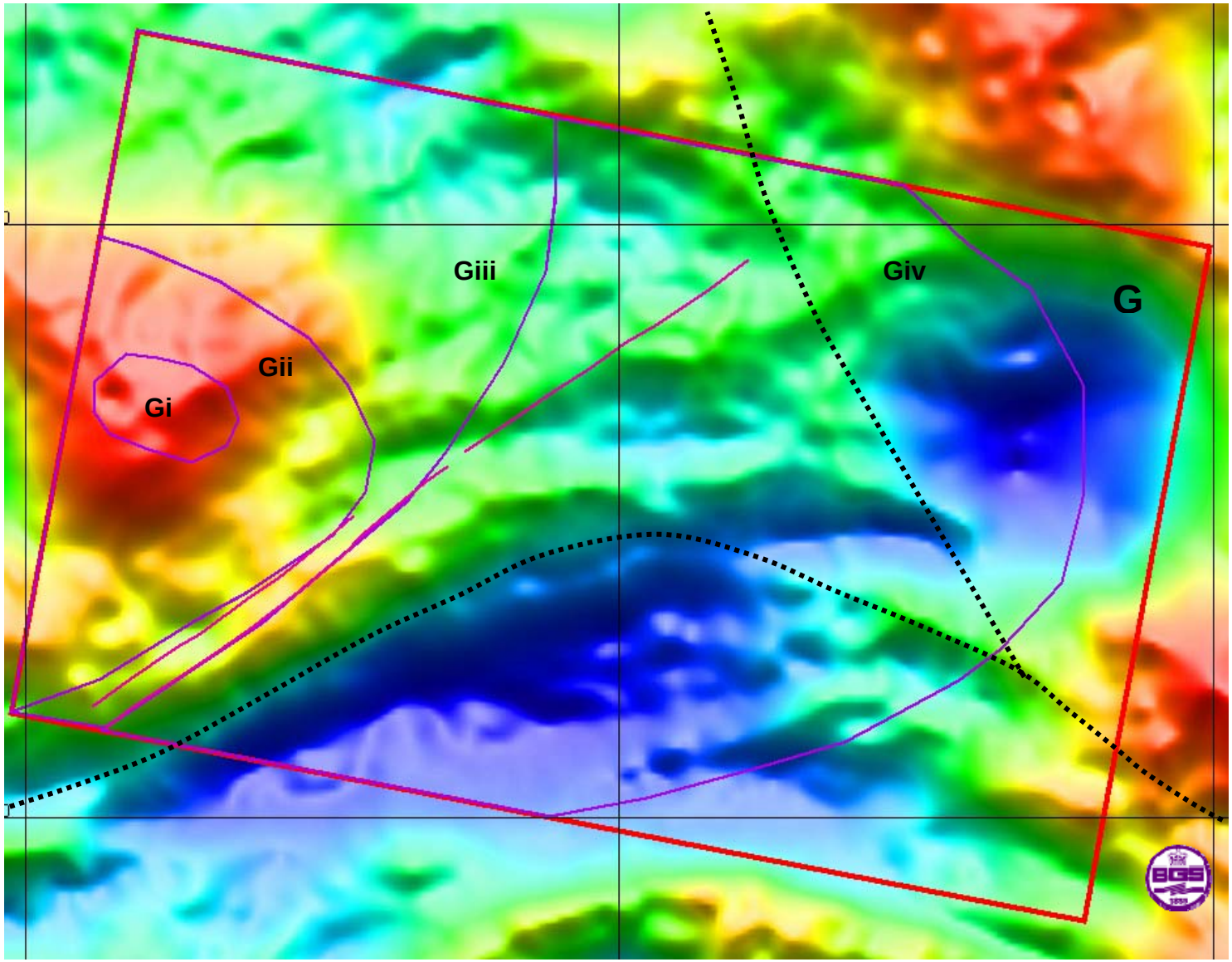

Figure E2 Regional gravity field over the AOI and generalised domains from the regional study

Red: gravity 'high' (mass of underlying rock is greater than average)

Blue: gravity 'low' (mass of underlying rock is less than average)

Appendix F: Annual tidal parameter time series and regression coefficients from the tide gauge analysis for the regional study

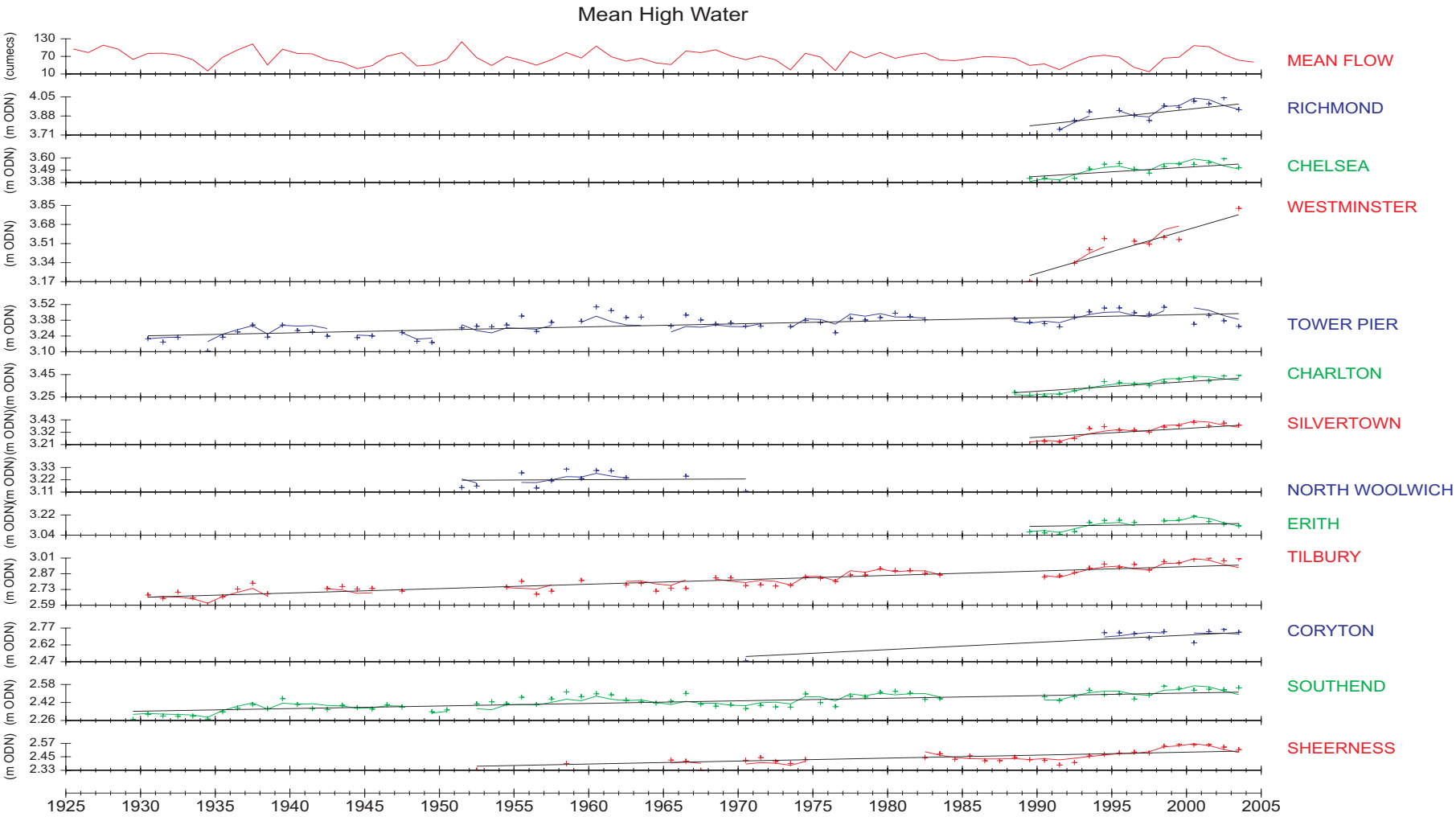

Figure F1 Annual MHW time series for the 12 tide gauges on the Thames Estuary and River Thames considered in the regional study

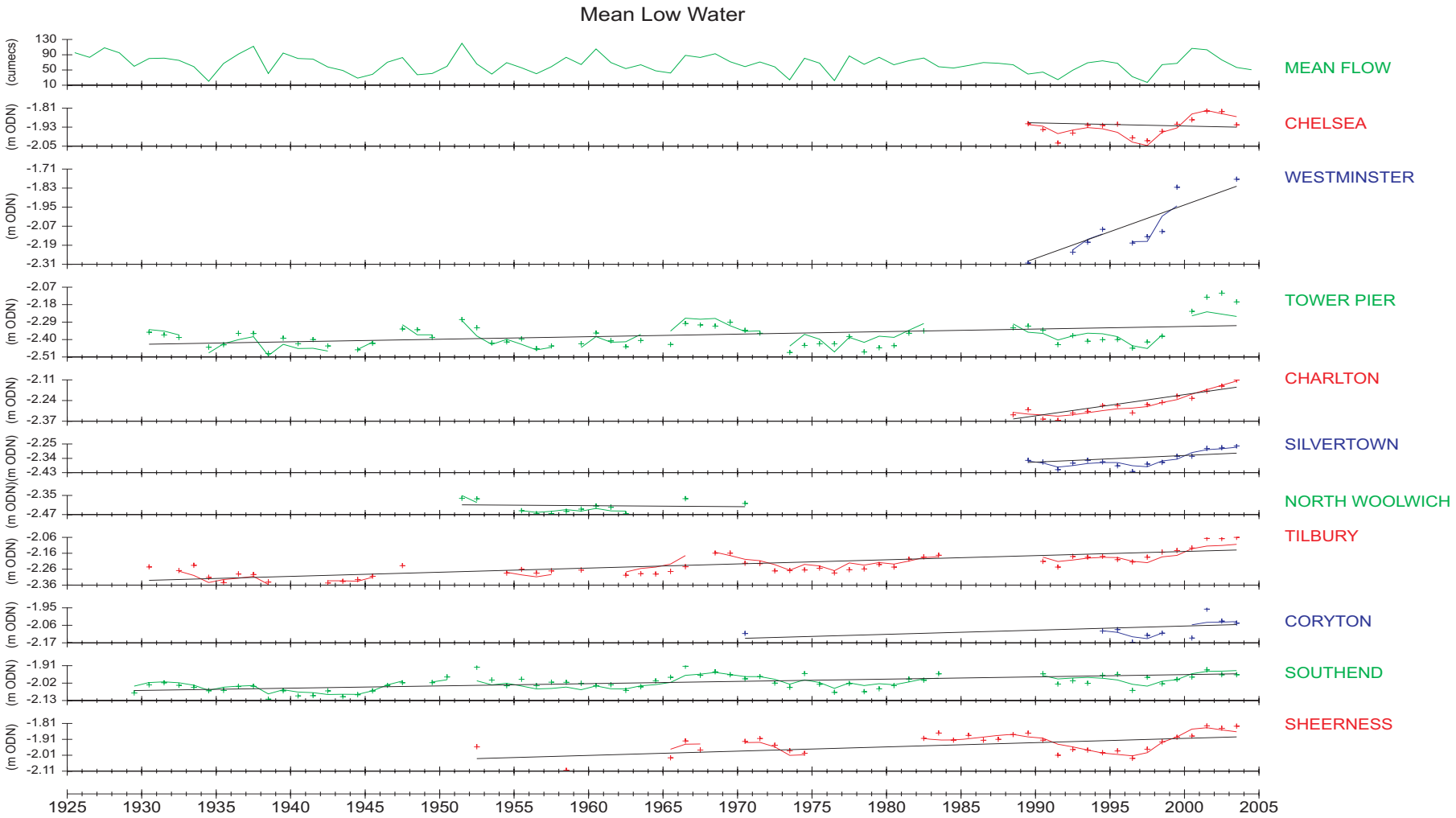

Figure F2 Annual MLW time series for 10 of the 12 tide gauges on the Thames Estuary and River Thames considered in the regional study

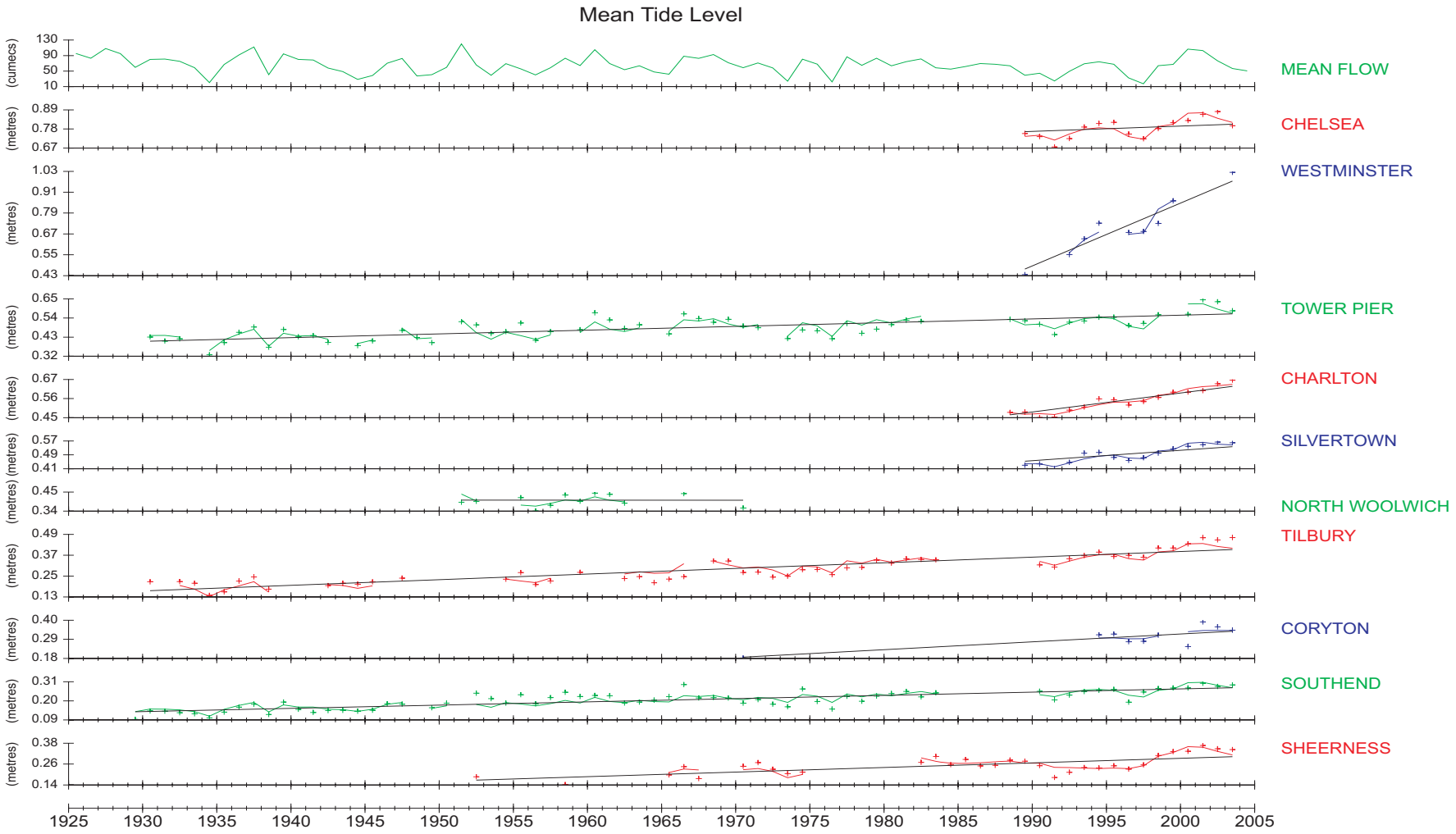

Figure F3 Annual MTL time series for 10 of the 12 tide gauges on the Thames Estuary and River Thames from the regional study

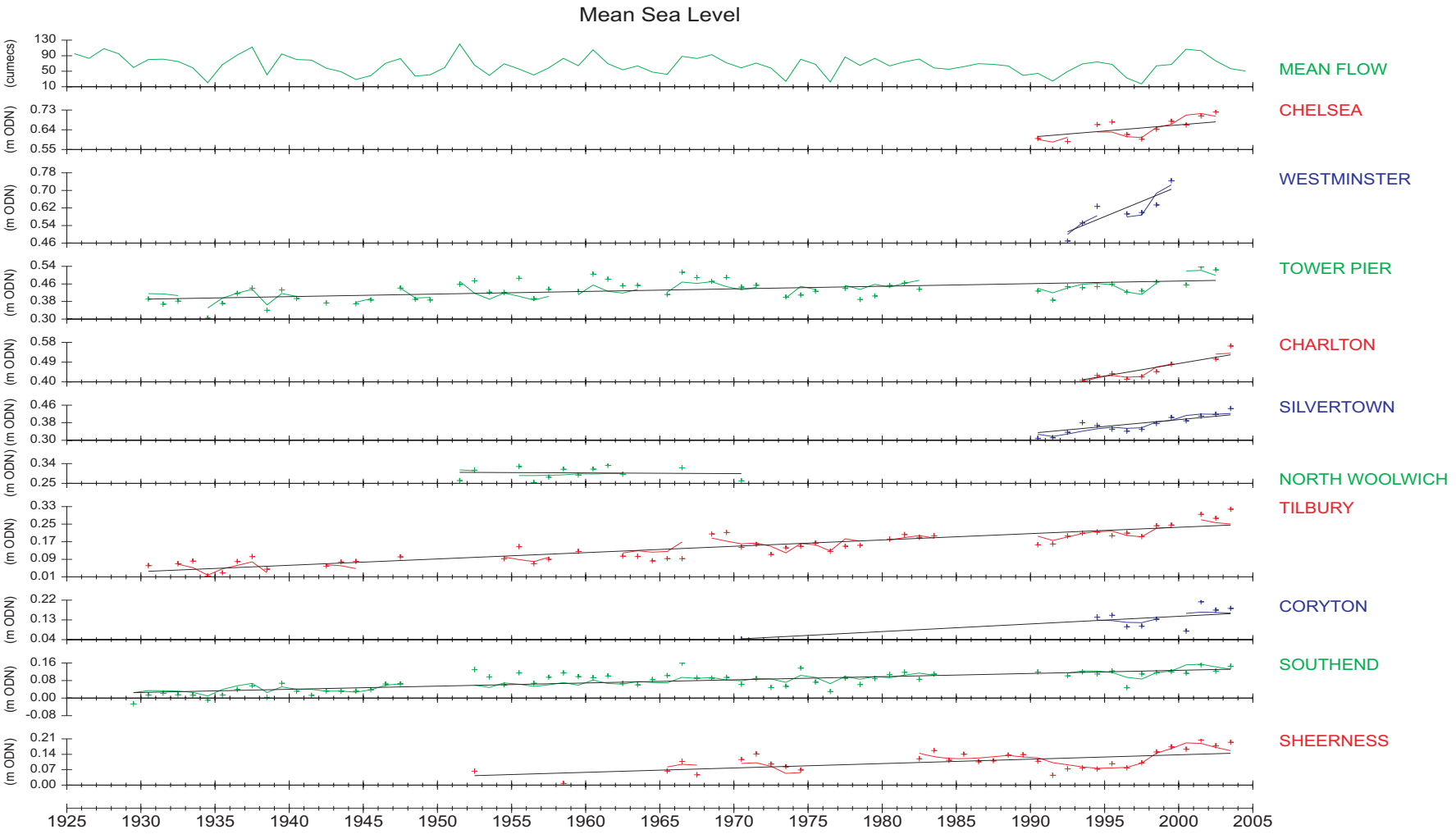

Figure F4 Annual MSL time series for 10 of the 12 tide gauges on the Thames Estuary and River Thames considered in the regional study

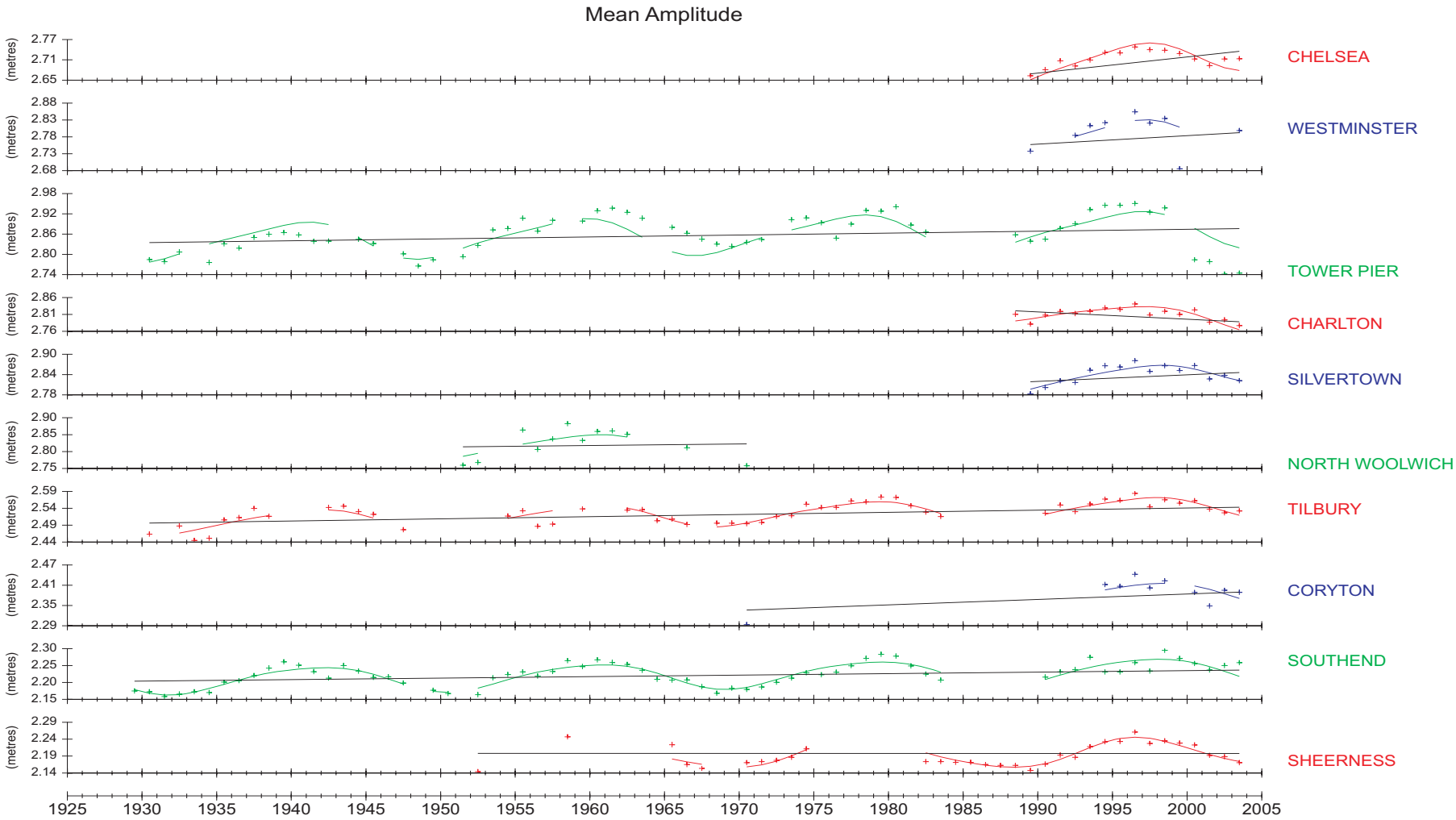

Figure F5 Annual MA time series for 10 of the 12 tide gauges on the Thames Estuary and River Thames from considered in regional study

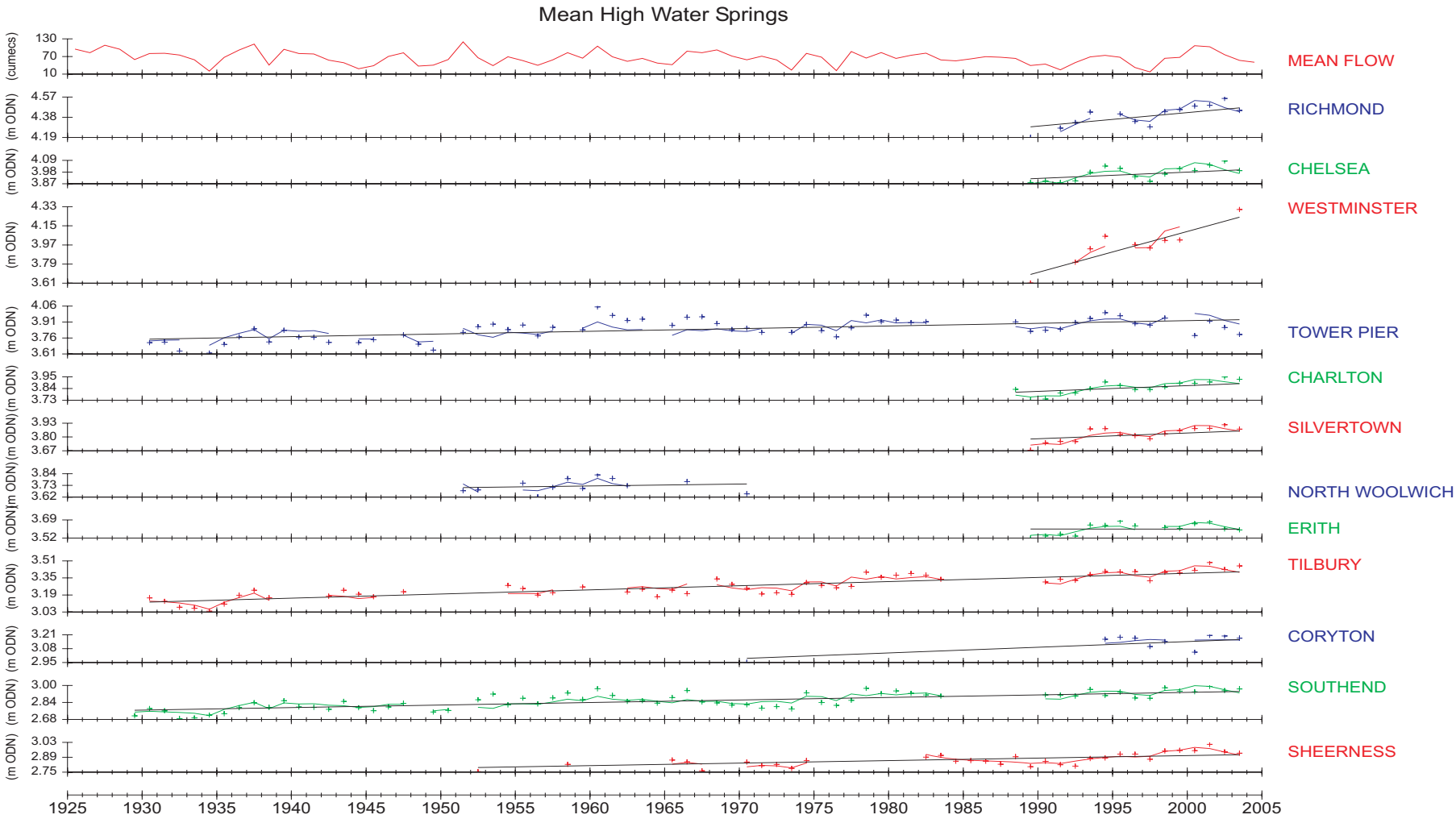

Figure F6 Annual MHWS time series for the 12 tide gauges on the Thames Estuary and River Thames considered in the regional study

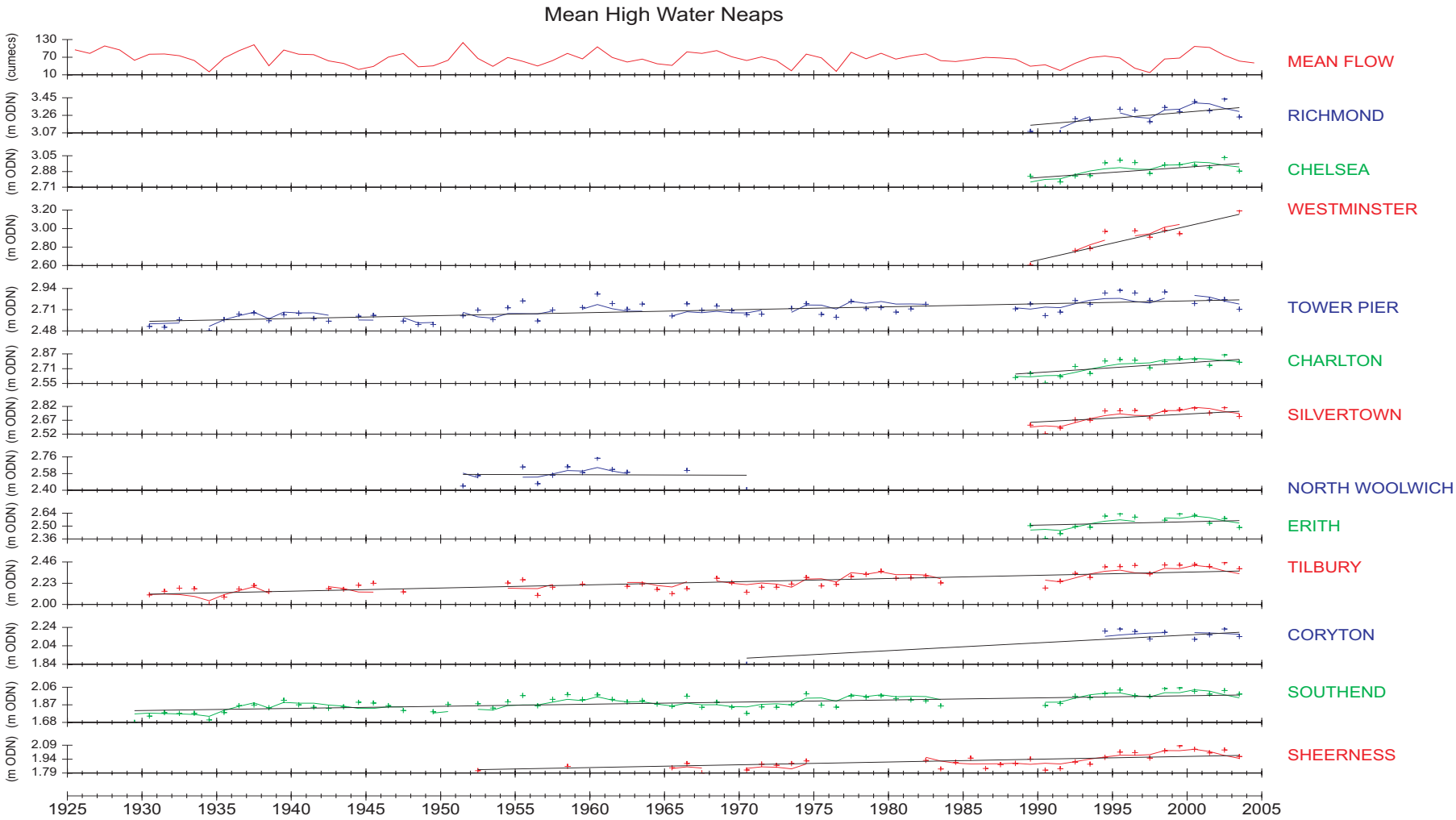

Figure F7 Annual MHWN time series for the 12 tide gauges on the Thames Estuary and River Thames considered in the regional study

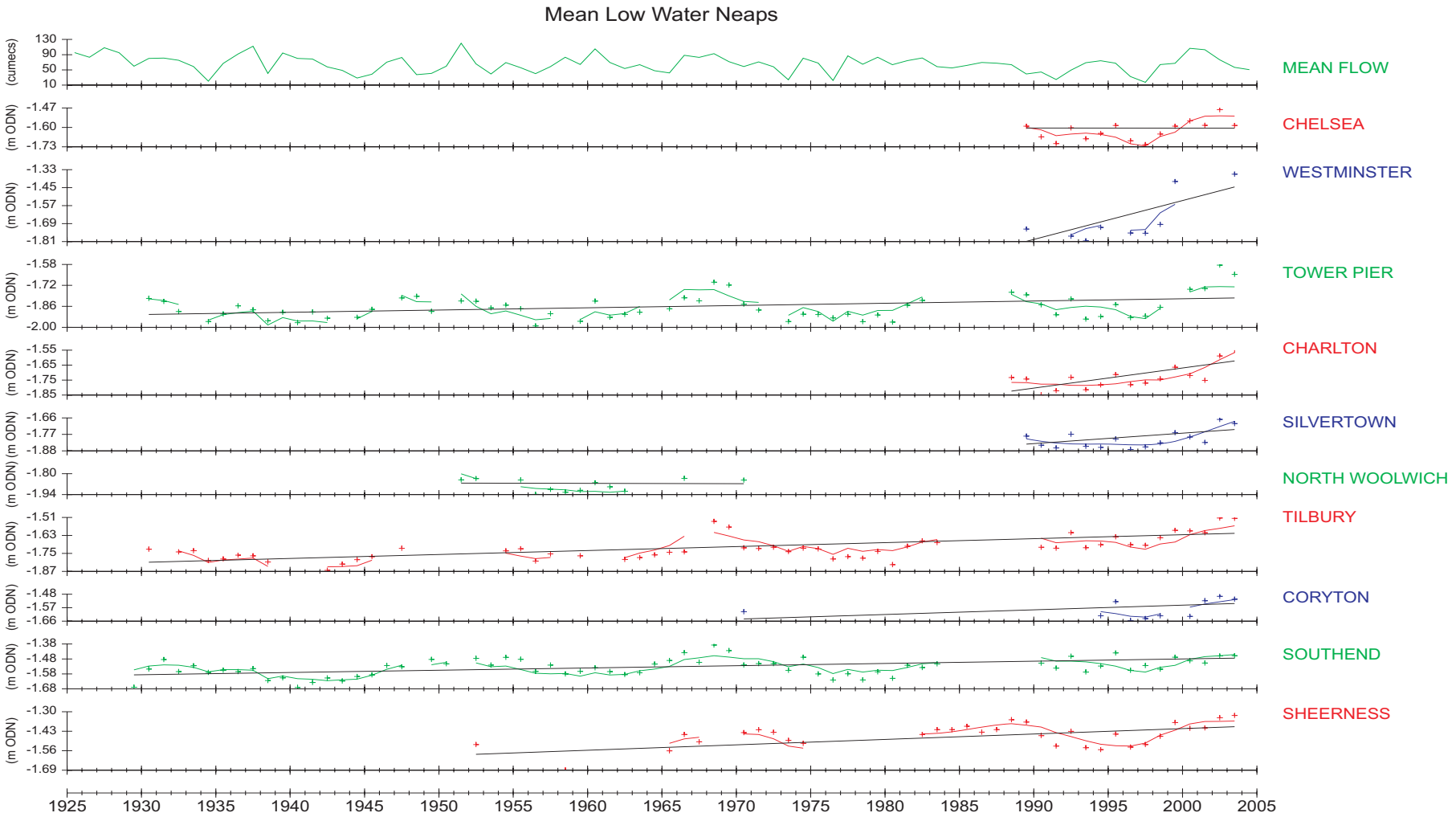

Figure F8 Annual MLWN time series for 10 of the 12 tide gauges on the Thames Estuary and River Thames considered in the regional study

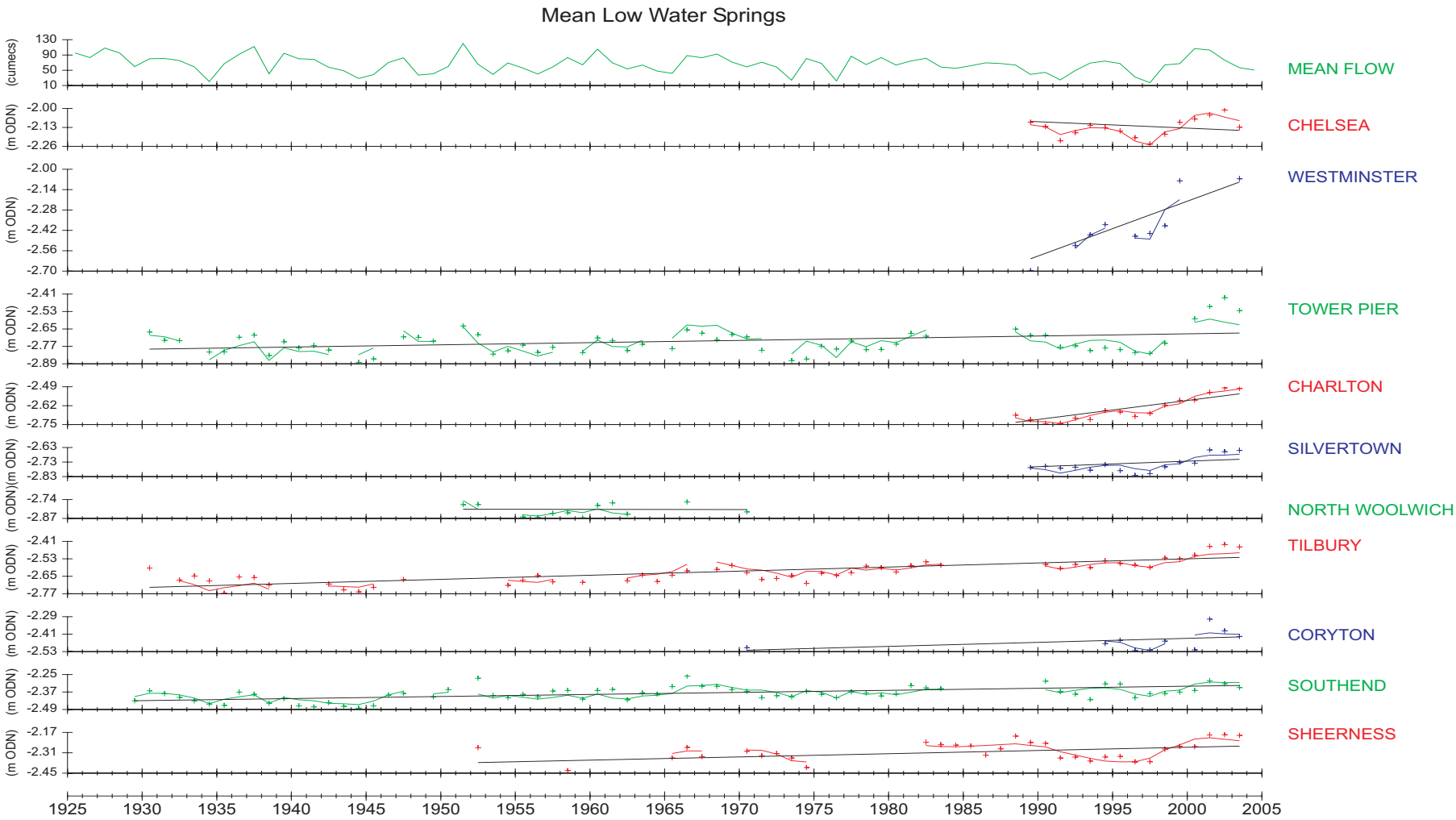

Figure F9 Annual MLWS time series for 10 of the 12 tide gauges on the Thames Estuary and River Thames considered in the regional study

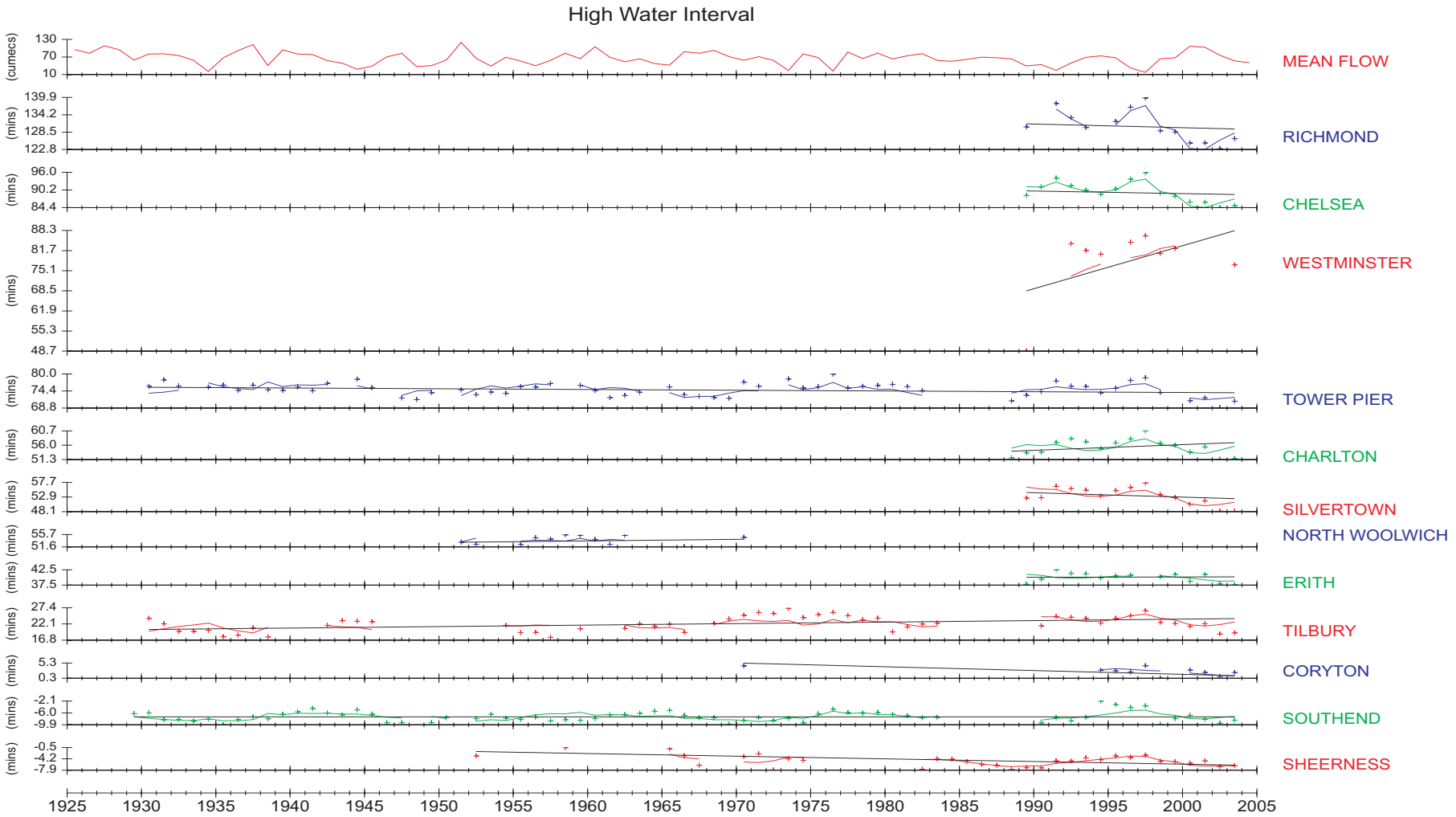

Figure F10 Annual MHWI time series for the 12 tide gauges on the Thames Estuary and River Thames considered in the regional study

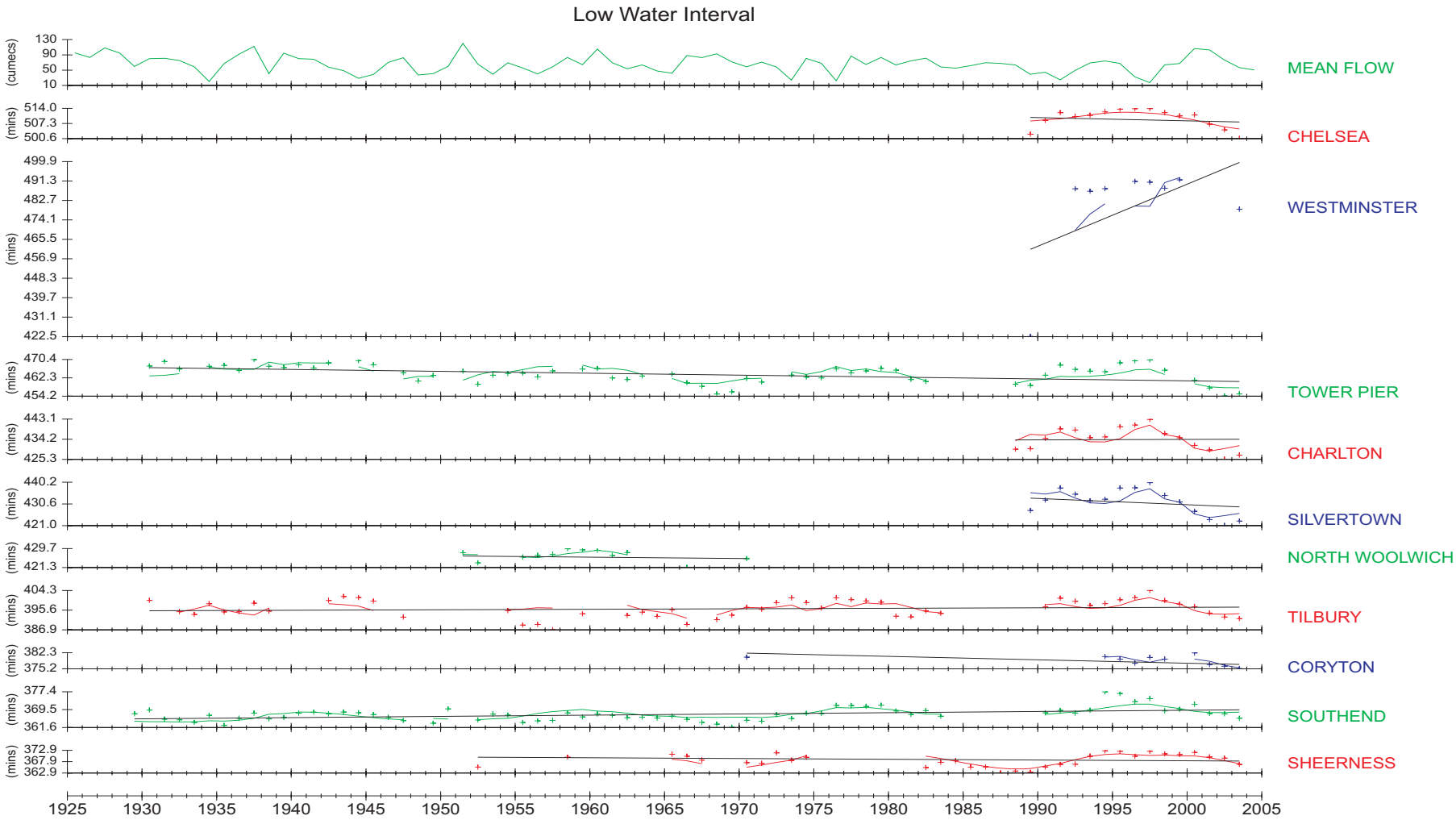

Figure F11 Annual MLWI time series for 10 of the 12 tide gauges on the Thames Estuary and River Thames considered in the regional study

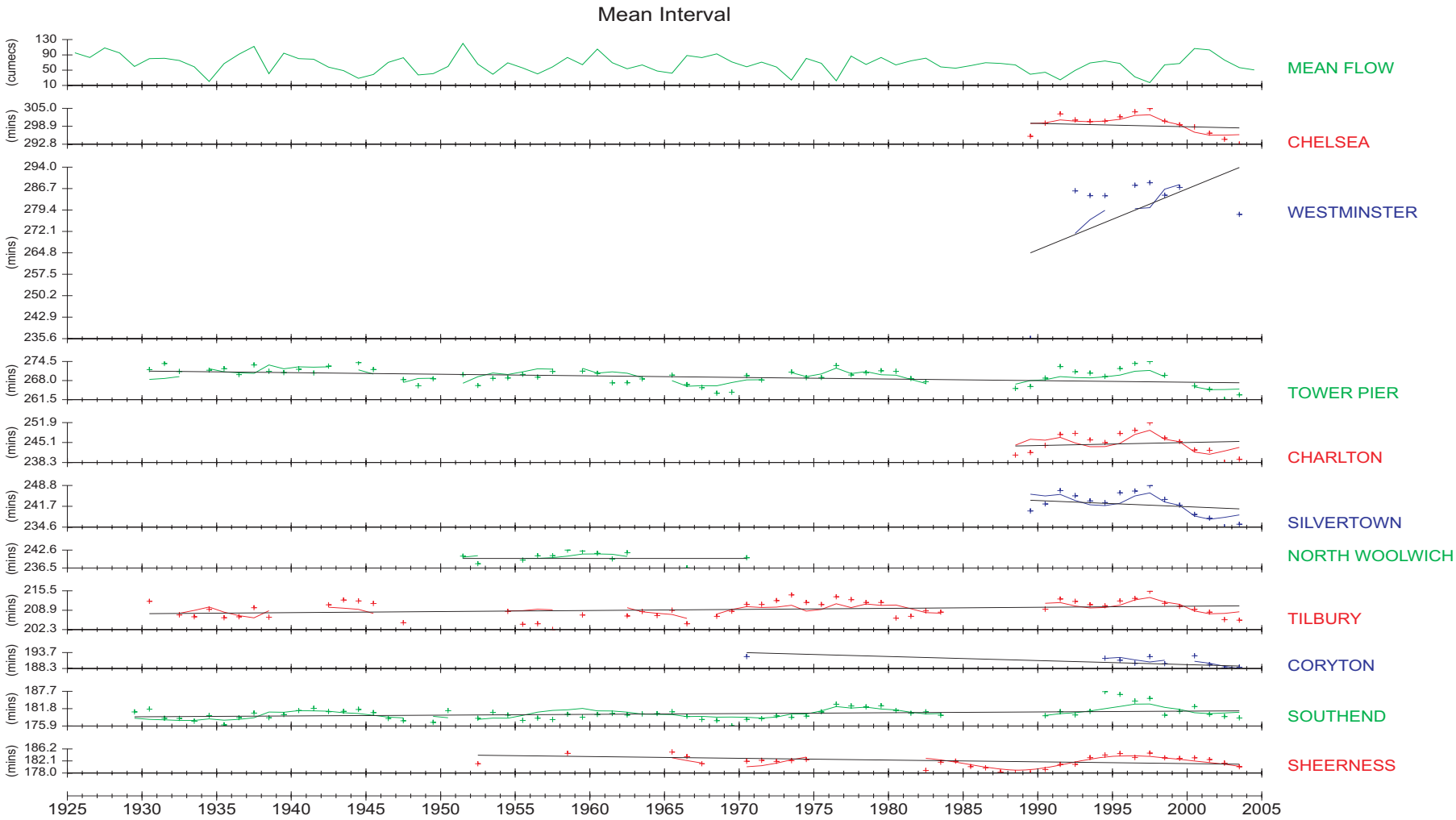

Figure F12 Annual MI time series for 10 of the 12 tide gauges on the Thames Estuary and River Thames considered in the regional study

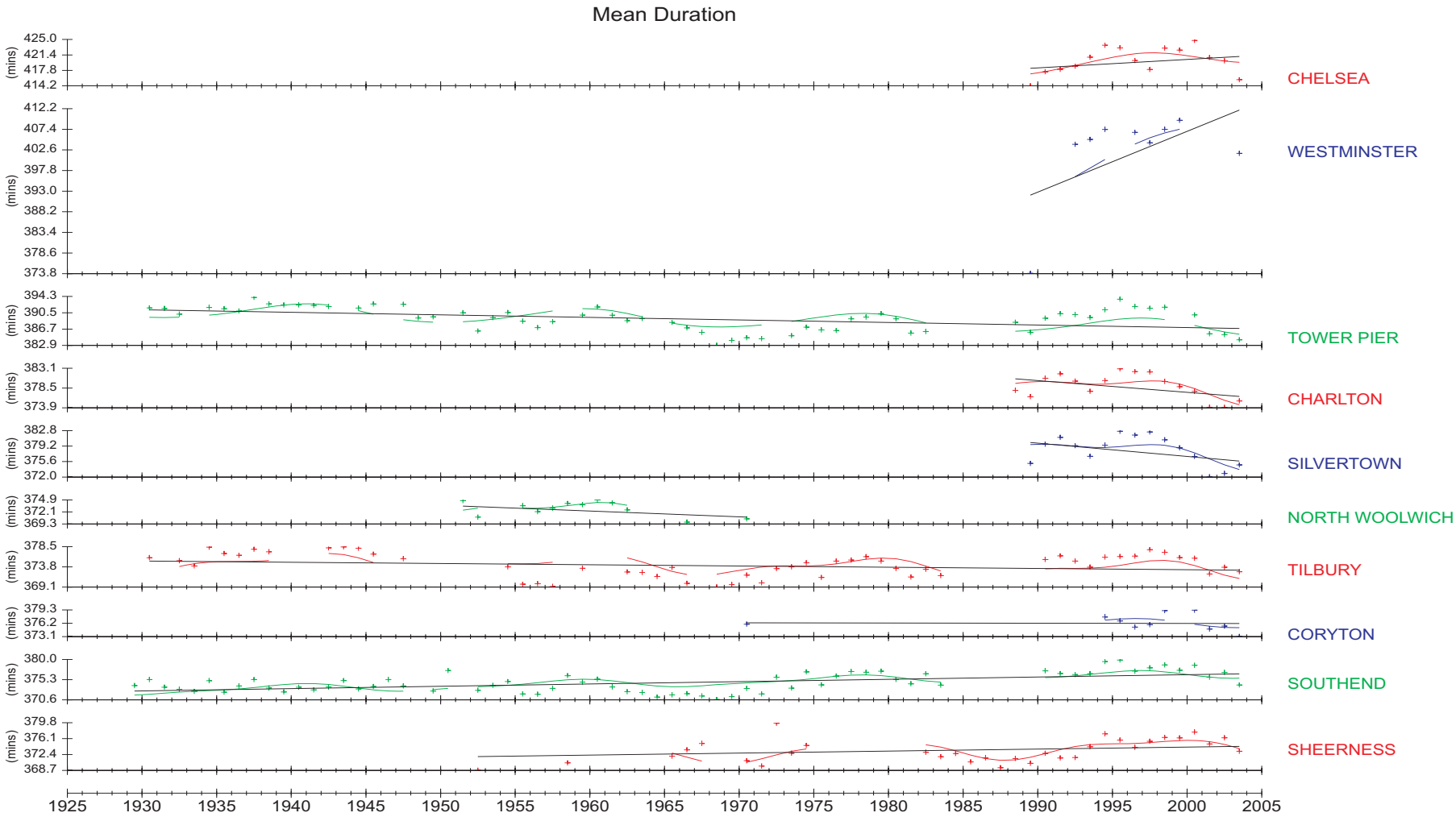

Figure F13 Annual MD time series for 10 of the 12 tide gauges on the Thames Estuary and River Thames considered in the regional study

	station	Rossiter	Bowen (1931-69)				1929-2003				
		(1934-66)									
		trend	trend	cos N	sin N	flow	years of	trend	cos N	sin N	flow
		cm/century	cm/century	cm	cm	cm/100 cumecs	data	cm/century	cm	cm	cm/100 cumecs
mean high	Sheerness						32	26.3 ± 4.0	-3.0 ± 0.8	2.6 ± 0.7	5.7 ± 2.6
water height	Southend	36.3 ± 7.6	35.1 ± 4.3	-4.3 ± 0.6	-0.9 ± 0.7	4.3 ± 2.0	67	23.2 ± 1.9	-3.6 ± 0.6	0.3 ± 0.6	9.1 ± 1.9
	Tilbury		38.1 ± 5.8	-3.6 ± 0.8	0.8 ± 0.8	7.8 ± 2.3	54	39.1 ± 2.1	-2.7 ± 0.8	0.7 ± 0.6	11.7 ± 2.1
	Tower Pier	77.5 ±11.6	68.0 ± 4.9	-4.9 ± 0.7	-1.5 ± 0.7	15.2 ± 2.1	61	27.1 ± 3.1	-3.9 ± 0.9	-1.2 ± 0.9	12.1 ± 2.8
mean low	Sheerness						32	26.7 ± 4.3	5.8 ± 0.9	3.2 ± 0.8	6.6 ± 2.7
water height	Southend	24.9 ± 7.9	25.0 ± 4.6	5.0 ± 0.6	-0.9 ± 0.6	3.8 ± 1.8	67	14.2 ± 1.6	4.0 ± 0.5	0.0 ± 0.5	6.2 ± 1.6
	Tilbury		27.7 ±17.4	4.5 ± 0.9	1.4 ± 1.2	5.9 ± 2.6	53	26.2 ± 1.9	4.1 ± 0.7	1.6 ± 0.6	7.2 ± 1.9
	Tower Pier	9.2 ± 8.9	4.3 ± 4.0	4.5 ± 0.5	1.0 ± 0.5	14.9 ± 1.6	61	16.0 ± 2.7	5.7 ± 0.8	3.3 ± 0.8	15.0 ± 2.4
mean tide	Sheerness						32	-0.1 ± 2.0	-4.4 ± 0.4	-0.3 ± 0.3	—
amplitude	Southend	5.2 ± 6.1					67	4.4 ± 0.9	-3.8 ± 0.3	0.2 ± 0.3	—
	Tilbury						53	6.4 ± 1.0	-3.2 ± 0.4	-0.3 ± 0.3	—
	Tower Pier	34.5 ± 7.0					61	5.7 ± 2.3	-4.8 ± 0.7	-2.3 ± 0.7	—
mean tide	Sheerness						32	26.5 ± 3.6	1.4 ± 0.7	2.9 ± 0.7	6.1 ± 2.3
level	Southend	31.1 ± 4.6					67	18.7 ± 1.5	0.2 ± 0.5	0.2 ± 0.4	7.7 ± 1.5
	Tilbury						53	32.5 ± 1.8	0.7 ± 0.6	1.2 ± 0.5	9.5 ± 1.8
	Tower Pier	43.4 ± 8.2					61	21.5 ± 1.7	0.9 ± 0.5	1.0 ± 0.5	13.6 ± 1.5
mean sea	Sheerness						32	19.9 ± 3.6	2.0 ± 0.7	2.7 ± 0.7	4.1 ± 2.3
level	Southend						64	14.4 ± 1.6	0.3 ± 0.5	0.0 ± 0.5	5.5 ± 1.6
	Tilbury						50	28.9 ± 1.8	1.1 ± 0.6	0.7 ± 0.5	7.5 ± 1.9
	Tower Pier						56	11.8 ± 2.1	0.9 ± 0.6	0.9 ± 0.6	9.7 ± 1.8

Table F1 A comparison of regression analyses for annual MHW, MLW, MTA, MTL and MSL with the results from the long period time series for 4 of the 12 tide gauges in the regional study (shown on the right of the table)

	station	Rossiter (1934-66) trend mins/century	1929 - 2003 years of data	trend mins/century	cos N mins	sin N mins	flow mins/100 cumecs
high water interval	Sheerness		32	-8.7 ± 2.0	-1.6 ± 0.4	0.2 ± 0.4	-1.7 ± 1.3
	Southend	0.2 ± 3.4	67	0.0 ± 0.8	-1.1 ± 0.3	0.3 ± 0.2	-1.8 ± 0.8
	Tilbury		54	4.9 ± 1.4	0.1 ± 0.5	-0.7 ± 0.4	-2.3 ± 1.4
	Tower Pier	-6.4 ± 4.7	61	-2.5 ± 1.1	-1.1 ± 0.3	-1.0 ± 0.3	-3.2 ± 1.0
low water interval	Sheerness		32	-3.3 ± 2.9	-3.4 ± 0.6	0.1 ± 0.5	1.1 ± 1.9
	Southend	-4.4 ± 5.7	67	5.4 ± 1.4	-1.9 ± 0.4	-0.2 ± 0.4	-1.1 ± 1.4
	Tilbury		53	2.2 ± 2.3	-1.6 ± 0.8	-0.9 ± 0.6	-3.8 ± 2.2
	Tower Pier	-25.1 ± 5.6	61	-8.4 ± 1.7	-3.0 ± 0.5	-1.2 ± 0.5	-3.3 ± 1.6
mean interval	Sheerness		32	-6.0 ± 1.9	-2.5 ± 0.4	0.2 ± 0.4	-0.3 ± 1.2
	Southend	-1.9 ± 4.2	67	2.7 ± 1.0	-1.5 ± 0.3	0.1 ± 0.3	-1.5 ± 1.0
	Tilbury		53	3.6 ± 1.7	-0.8 ± 0.6	-0.8 ± 0.5	-3.1 ± 1.7
	Tower Pier	-15.8 ± 5.0	61	-5.5 ± 1.3	-2.1 ± 0.4	-1.1 ± 0.4	-3.2 ± 1.1
mean duration	Sheerness		32	4.7 ± 3.3	-1.8 ± 0.7	0.2 ± 0.6	—
	Southend	-4.6 ± 5.7	67	5.4 ± 1.0	-0.8 ± 0.3	-0.5 ± 0.3	—
	Tilbury		53	-2.9 ± 1.6	-1.7 ± 0.6	-0.3 ± 0.5	—
	Tower Pier	-18.7 ± 4.0	61	-5.9 ± 1.4	-1.9 ± 0.4	-0.3 ± 0.4	—

Table F2 A comparison of regression analyses for annual MHWI, MLWI, MI and MD with the results from the long period time series for 4 of the 12 tide gauges in the regional study (shown on the right of the table)

	station	Bowen (1931-69)				1929 - 2003				
		trend cm/century	cos N cm	sin N cm	flow cm/100 cumecs	years of data	trend cm/century	cos N cm	sin N cm	flow cm/100 cumecs
mean high water springs	Southend					67	23.9 ± 2.5	-2.9 ± 0.8	0.5 ± 0.7	9.2 ± 2.5
	Tilbury					54	39.1 ± 2.6	-2.6 ± 0.9	1.2 ± 0.8	11.6 ± 2.6
	Tower Pier	75.8 ± 6.1	-4.8 ± 0.8	-2.0 ± 0.9	15.6 ± 2.4	61	25.0 ± 4.2	-3.2 ± 1.3	-0.7 ± 1.3	13.2 ± 3.8
mean high water neaps	Southend					67	22.8 ± 2.4	-4.7 ± 0.8	-0.1 ± 0.7	9.7 ± 2.4
	Tilbury					54	34.3 ± 3.4	-3.8 ± 1.2	0.7 ± 1.0	12.8 ± 3.4
	Tower Pier	65.1 ± 6.4	-5.5 ± 0.9	-1.7 ± 0.9	14.2 ± 2.5	61	31.8 ± 3.6	-4.1 ± 1.1	-1.2 ± 1.1	11.6 ± 3.3
mean low water neaps	Southend					67	15.0 ± 2.3	5.5 ± 0.7	-0.4 ± 0.7	5.8 ± 2.3
	Tilbury					53	26.4 ± 2.8	6.3 ± 1.0	1.2 ± 0.8	7.1 ± 2.8
	Tower Pier	3.4 ± 4.3	6.1 ± 0.6	1.6 ± 0.6	14.3 ±.1.7	61	15.1 ± 2.9	7.0 ± 0.9	3.7 ± 0.9	11.4 ± 2.6
mean low water springs	Southend					67	14.1 ± 1.9	2.9 ± 0.6	0.4 ± 0.6	7.7 ± 1.9
	Tilbury					53	28.1 ± 2.5	2.9 ± 0.9	1.6 ± 0.7	6.8 ± 2.4
	Tower Pier	2.4 ± 5.5	4.2 ± 0.7	1.0 ± 0.7	18.6 ± 2.1	61	15.1 ± 3.2	5.1 ± 1.0	3.8 ± 1.0	17.1 ± 2.9
amplitude springs	Southend					67	4.9 ± 1.1	-2.9 ± 0.4	0.1 ± 0.3	—
	Tilbury					53	5.6 ± 1.6	-2.6 ± 0.6	-0.1 ± 0.4	—
	Tower Pier	38.7 ± 3.4	-4.3 ± 0.5	-1.1 ± 0.5	–	61	5.2 ± 3.0	-4.1 ± 0.9	-2.3 ± 0.9	—
amplitude neaps	Southend					67	3.8 ± 1.1	-5.1 ± 0.3	0.2 ± 0.3	—
	Tilbury					53	4.2 ± 1.4	-5.0 ± 0.5	-0.1 ± 0.4	—
	Tower Pier	32.6 ± 3.4	-5.6 ± 0.5	-1.6 ± 0.5	–	61	8.3 ± 2.0	-5.6 ± 0.6	-2.5 ± 0.6	—
mean level springs	Southend					67	19.0 ± 1.9	0.0 ± 0.6	0.5 ± 0.6	8.5 ± 1.9
	Tilbury					53	33.6 ± 2.1	0.1 ± 0.7	1.4 ± 0.6	9.2 ± 2.0
	Tower Pier	41.1 ± 4.6	-0.1 ± 0.6	-0.9 ± 0.6	18.0 ± 1.7	61	20.1 ± 2.2	1.0 ± 0.7	1.6 ± 0.7	15.1 ± 2.0
mean level neaps	Southend					67	18.9 ± 2.2	0.4 ± 0.7	-0.2 ± 0.6	7.8 ± 2.1
	Tilbury					53	30.5 ± 2.9	1.2 ± 1.0	0.9 ± 0.8	9.9 ± 2.8
	Tower Pier	36.0 ± 4.3	0.5 ± 0.5	-0.1 ± 0.5	14.7 ± 1.6	61	23.4 ± 2.5	1.4 ± 0.8	1.2 ± 0.8	11.5 ± 2.3

Table F3 A comparison of regression analyses for annual MHWS, MHWN, MLWN, MLWS, MAS, MAN, MLS and MLN with the results from the long period time series for 3 of the 12 tide gauges in the regional study (shown on the right of the table)

	station	1988 - 2003				
		years of data	trend cm/century	cos N cm	sin N cm	flow cm/100 cumecs
mean high water height	Sheerness	16	42.8 ± 10.9	-3.0 ± 0.8	2.6 ± 0.7	7.5 ± 2.1
	Southend	14	46.4 ± 23.0	-3.6 ± 0.6	0.3 ± 0.6	4.9 ± 3.7
	Tilbury	14	80.8 ± 16.0	-2.7 ± 0.8	0.7 ± 0.6	7.8 ± 2.6
	Erith	14	17.5 ± 16.1	-2.7 ± 0.8	0.7 ± 0.6	11.1 ± 3.1
	Silvertown	15	78.3 ± 16.8	-2.7 ± 0.8	0.7 ± 0.6	9.0 ± 2.9
	Charlton	16	85.4 ± 14.6	-2.7 ± 0.8	0.7 ± 0.6	5.8 ± 2.8
	Tower Pier	15	-9.0 ± 28.0	-3.9 ± 0.9	-1.2 ± 0.9	6.0 ± 5.3
	Westminster	9	387.0 ± 64.8	-3.9 ± 0.9	-1.2 ± 0.9	17.4 ± 14.2
	Chelsea	15	81.2 ± 22.5	-3.9 ± 0.9	-1.2 ± 0.9	12.6 ± 3.9
	Richmond	13	138.4 ± 25.5	-3.9 ± 0.9	-1.2 ± 0.9	18.1 ± 4.2
mean low water height	Sheerness	16	43.8 ± 16.6	5.8 ± 0.9	3.2 ± 0.8	5.6 ± 3.2
	Southend	14	13.4 ± 23.6	4.0 ± 0.5	0.0 ± 0.5	5.4 ± 3.8
	Tilbury	14	78.5 ± 13.6	4.1 ± 0.7	1.6 ± 0.6	6.6 ± 2.2
	Silvertown	15	41.5 ± 13.1	4.1 ± 0.7	1.6 ± 0.6	6.8 ± 2.3
	Charlton	16	133.5 ± 13.6	4.1 ± 0.7	1.6 ± 0.6	2.5 ± 2.6
	Tower Pier	15	93.8 ± 26.7	5.7 ± 0.8	3.3 ± 0.8	13.3 ± 5.0
	Westminster	9	336.3 ± 56.8	5.7 ± 0.8	3.3 ± 0.8	23.9 ± 12.5
	Chelsea	15	-20.1 ± 24.0	5.7 ± 0.8	3.3 ± 0.8	15.5 ± 4.2

Table F4 Results of short period regression analyses for annual MHW and MLW for 10 of the 12 tide gauges in the regional study

	station	1988 - 2003				
		years of data	trend cm/century	cos N cm	sin N cm	flow cm/100 cumecs
mean tide level	Sheerness	16	43.3 ± 12.7	1.4 ± 0.7	2.9 ± 0.7	6.5 ± 2.4
	Southend	14	29.9 ± 15.2	0.2 ± 0.5	0.2 ± 0.4	5.1 ± 2.4
	Tilbury	14	79.2 ± 10.5	0.7 ± 0.6	1.2 ± 0.5	7.3 ± 1.7
	Silvertown	15	59.7 ± 11.4	0.7 ± 0.6	1.2 ± 0.5	8.0 ± 2.0
	Charlton	16	109.5 ± 11.3	0.7 ± 0.6	1.2 ± 0.5	4.2 ± 2.2
	Tower Pier	15	42.4 ± 15.4	0.9 ± 0.5	1.0 ± 0.5	9.7 ± 2.9
	Westminster	9	361.7 ± 35.7	0.9 ± 0.5	1.0 ± 0.5	20.7 ± 7.8
	Chelsea	15	30.5 ± 19.3	0.9 ± 0.5	1.0 ± 0.5	14.0 ± 3.4
mean sea level	Sheerness	16	39.3 ± 12.9	2.0 ± 0.7	2.7 ± 0.7	4.2 ± 2.5
	Southend	13	15.6 ± 16.5	0.3 ± 0.5	0.0 ± 0.5	2.8 ± 2.7
	Tilbury	13	81.6 ± 11.7	1.1 ± 0.6	0.7 ± 0.5	6.4 ± 2.1
	Silvertown	14	62.1 ± 14.4	1.1 ± 0.6	0.7 ± 0.5	4.3 ± 2.3
	Charlton	9	113.2 ± 20.5	1.1 ± 0.6	0.7 ± 0.5	6.8 ± 3.5
	Tower Pier	12	46.3 ± 22.0	0.9 ± 0.6	0.9 ± 0.6	5.2 ± 3.1
	Westminster	7	276.3 ± 61.5	0.9 ± 0.6	0.9 ± 0.6	14.3 ± 7.6
	Chelsea	12	55.7 ± 28.5	0.9 ± 0.6	0.9 ± 0.6	7.7 ± 4.0
mean amplitude	Sheerness	16	2.5 ± 5.2	-4.4 ± 0.4	-0.3 ± 0.3	—
	Southend	14	14.3 ± 14.9	-3.8 ± 0.3	0.2 ± 0.3	—
	Tilbury	14	0.4 ± 8.4	-3.2 ± 0.4	-0.3 ± 0.3	—
	Silvertown	15	19.6 ± 8.1	-3.2 ± 0.4	-0.3 ± 0.3	—
	Charlton	16	-21.5 ± 7.0	-3.2 ± 0.4	-0.3 ± 0.3	—
	Tower Pier	16	-59.0 ± 19.9	-4.8 ± 0.7	-2.3 ± 0.7	—
	Westminster	10	25.2 ± 45.9	-4.8 ± 0.7	-2.3 ± 0.7	—
	Chelsea	15	47.7 ± 10.7	-4.8 ± 0.7	-2.3 ± 0.7	—

Table F5 Results of short period regression analyses for annual MTL, MSL and MA for 8 of the 12 tide gauges in the regional study

Appendix G: Monthly tidal parameter time series and regression coefficients from the tide gauge analysis for the regional study

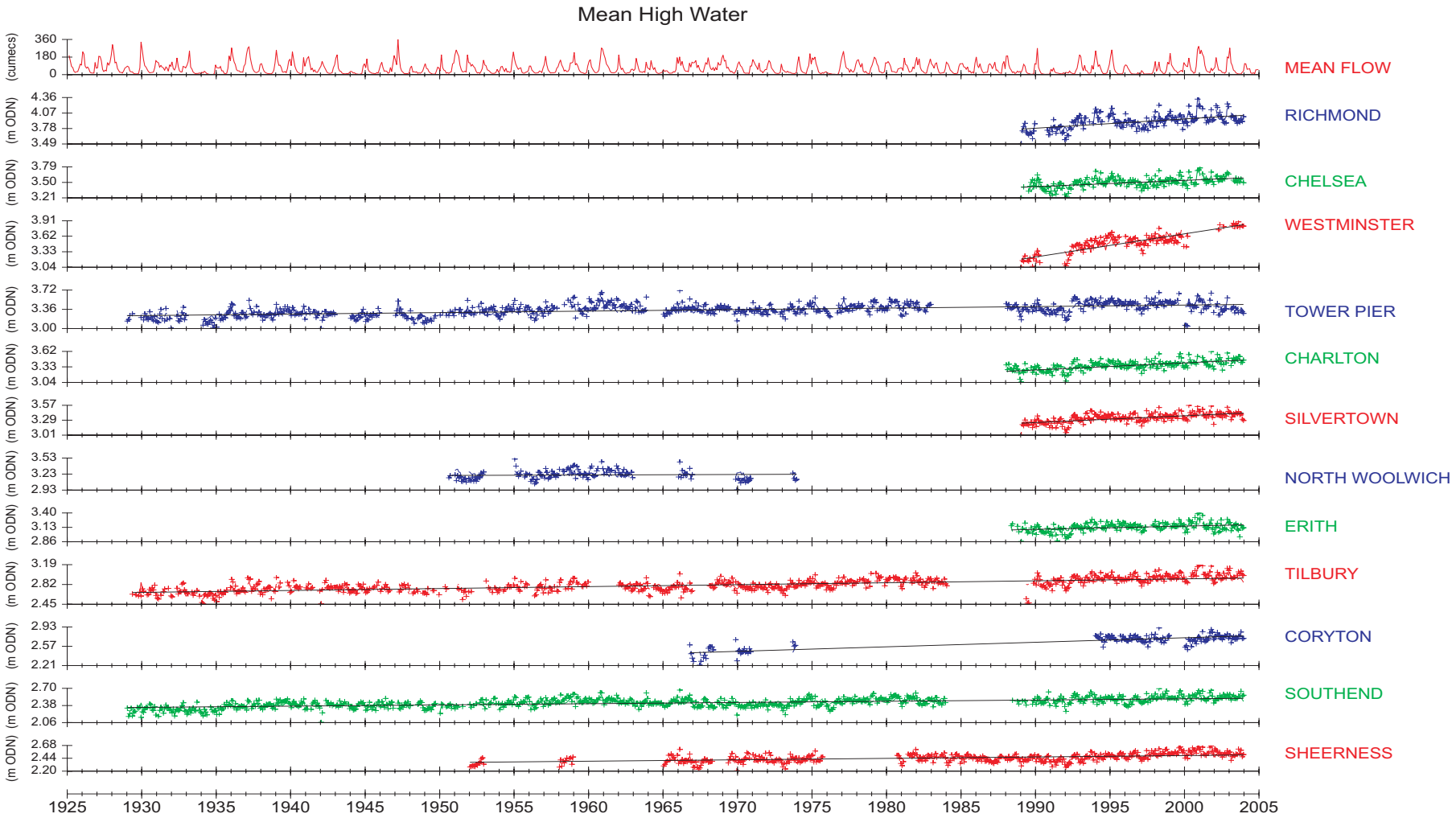

Figure G1 Monthly MHW time series for the 12 tide gauges on the Thames Estuary and River Thames considered in the regional study

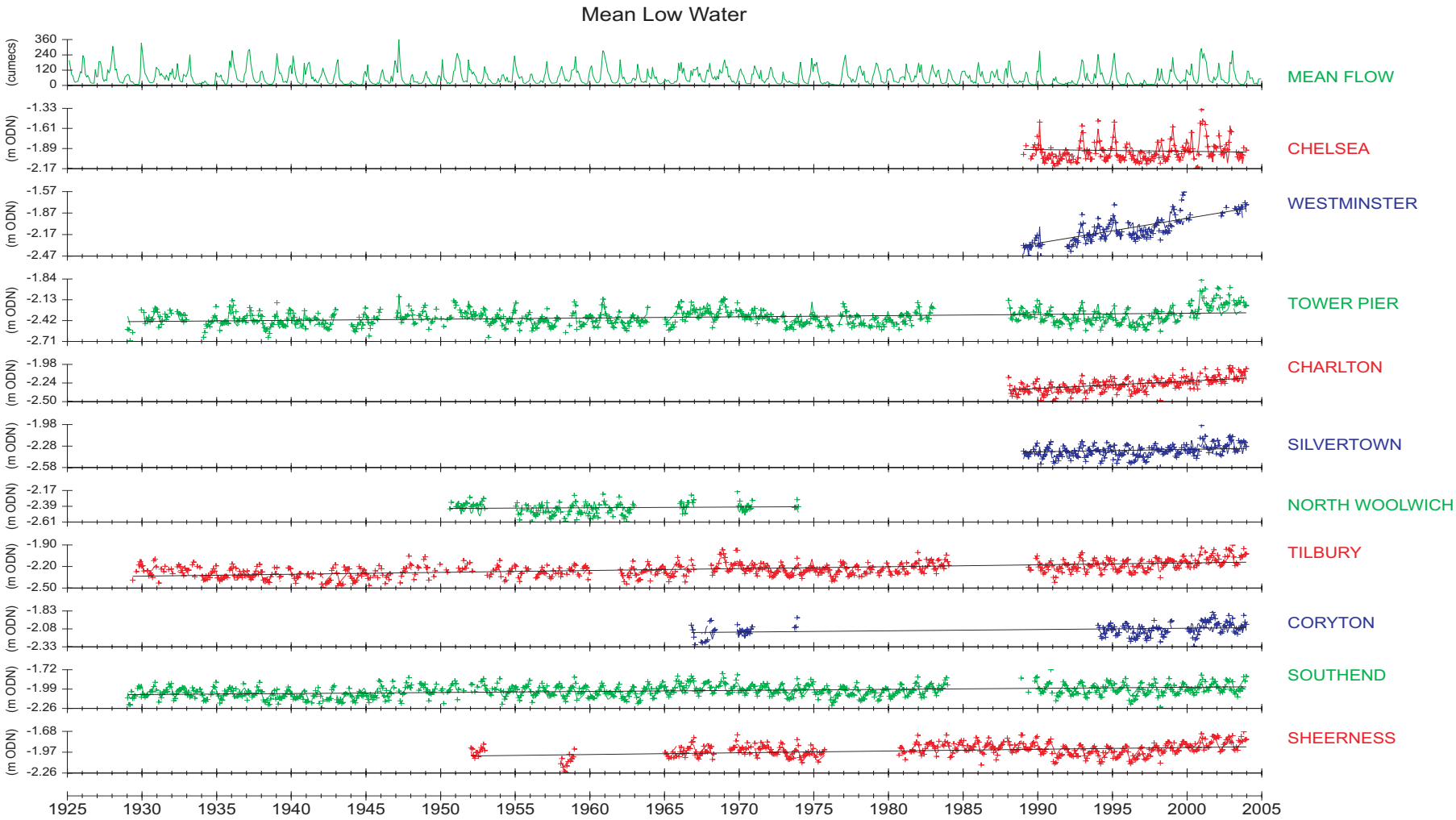

Figure G2 Monthly MLW time series for 10 of the 12 tide gauges on the Thames Estuary and River Thames considered in the regional study

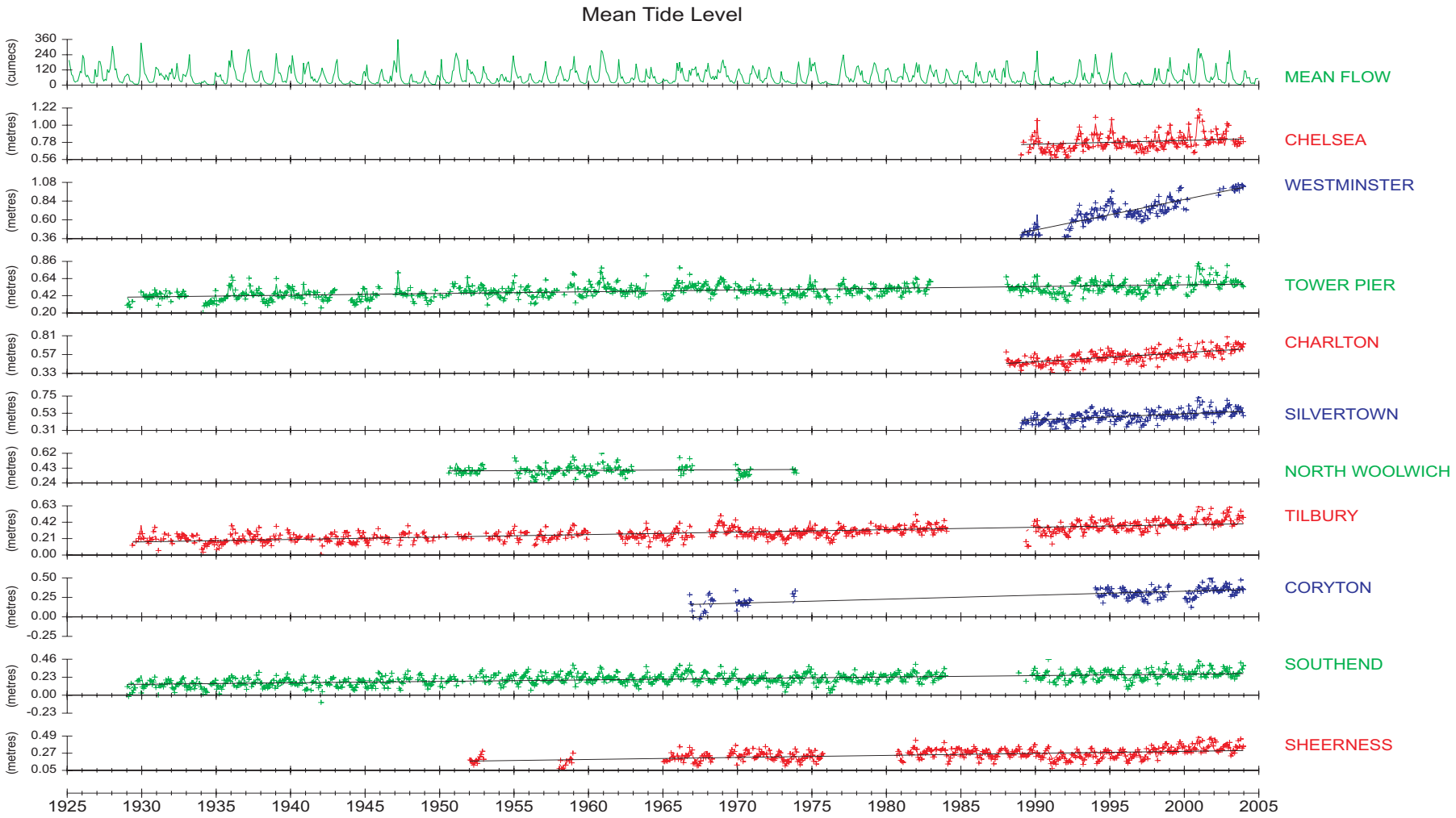

Figure G3 Monthly MTL time series for 10 of the 12 tide gauges on the Thames Estuary and River Thames from the regional study

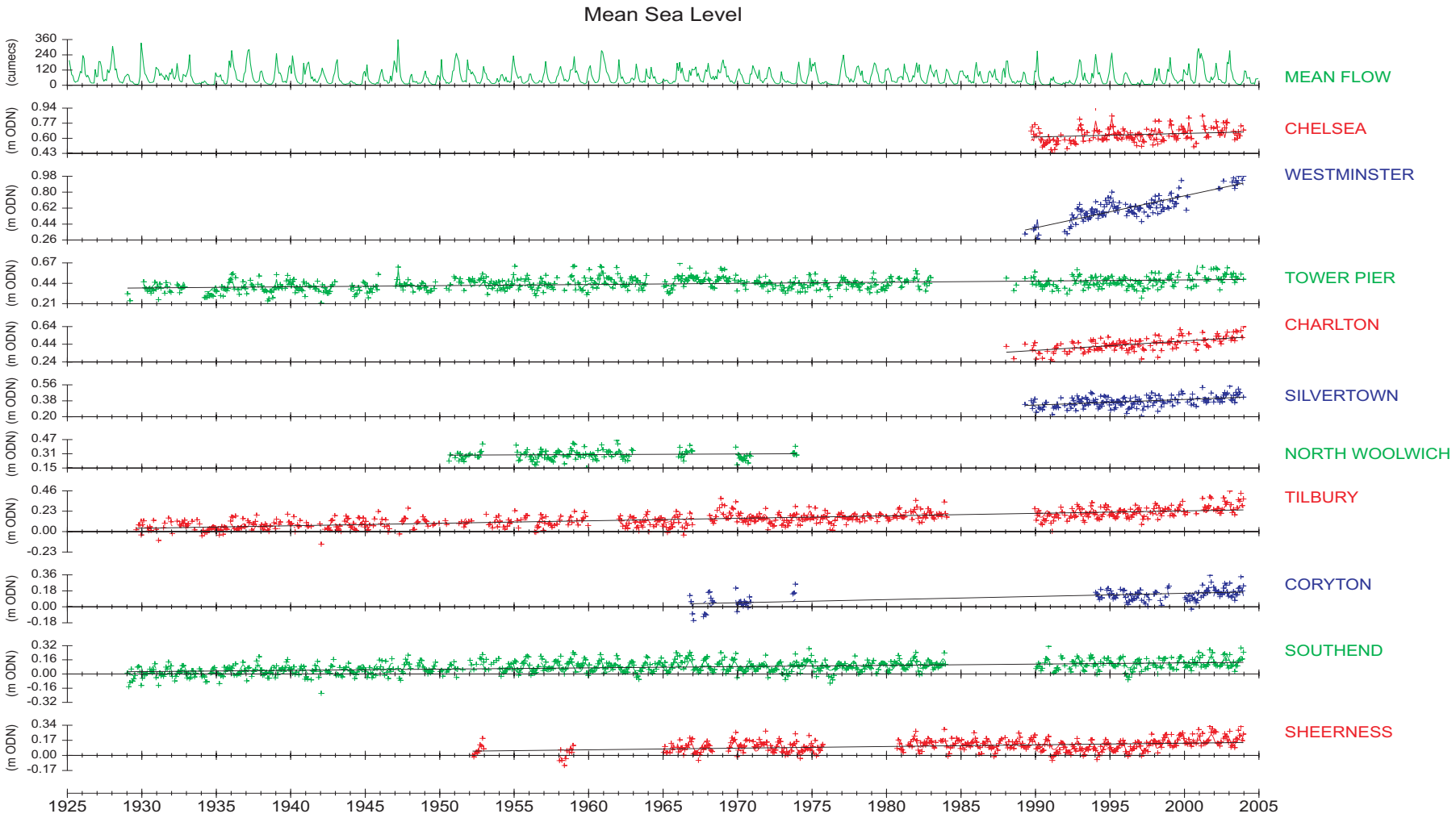

Figure G4 Monthly MSL time series for 10 of the 12 tide gauges on the Thames Estuary and River Thames considered in the regional study

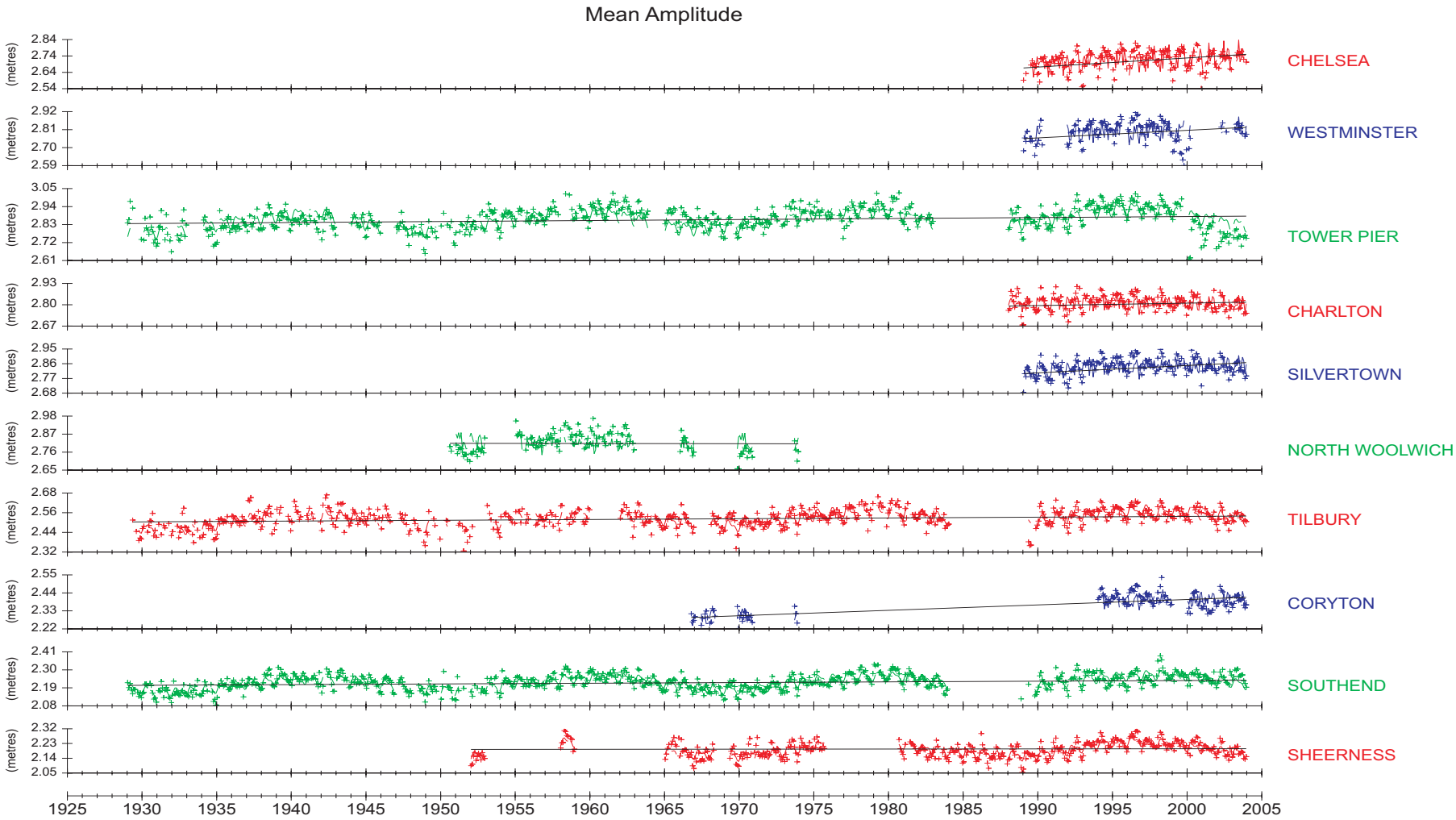

Figure G5 Monthly MA time series for 10 of the 12 tide gauges on the Thames Estuary and River Thames from considered in regional study

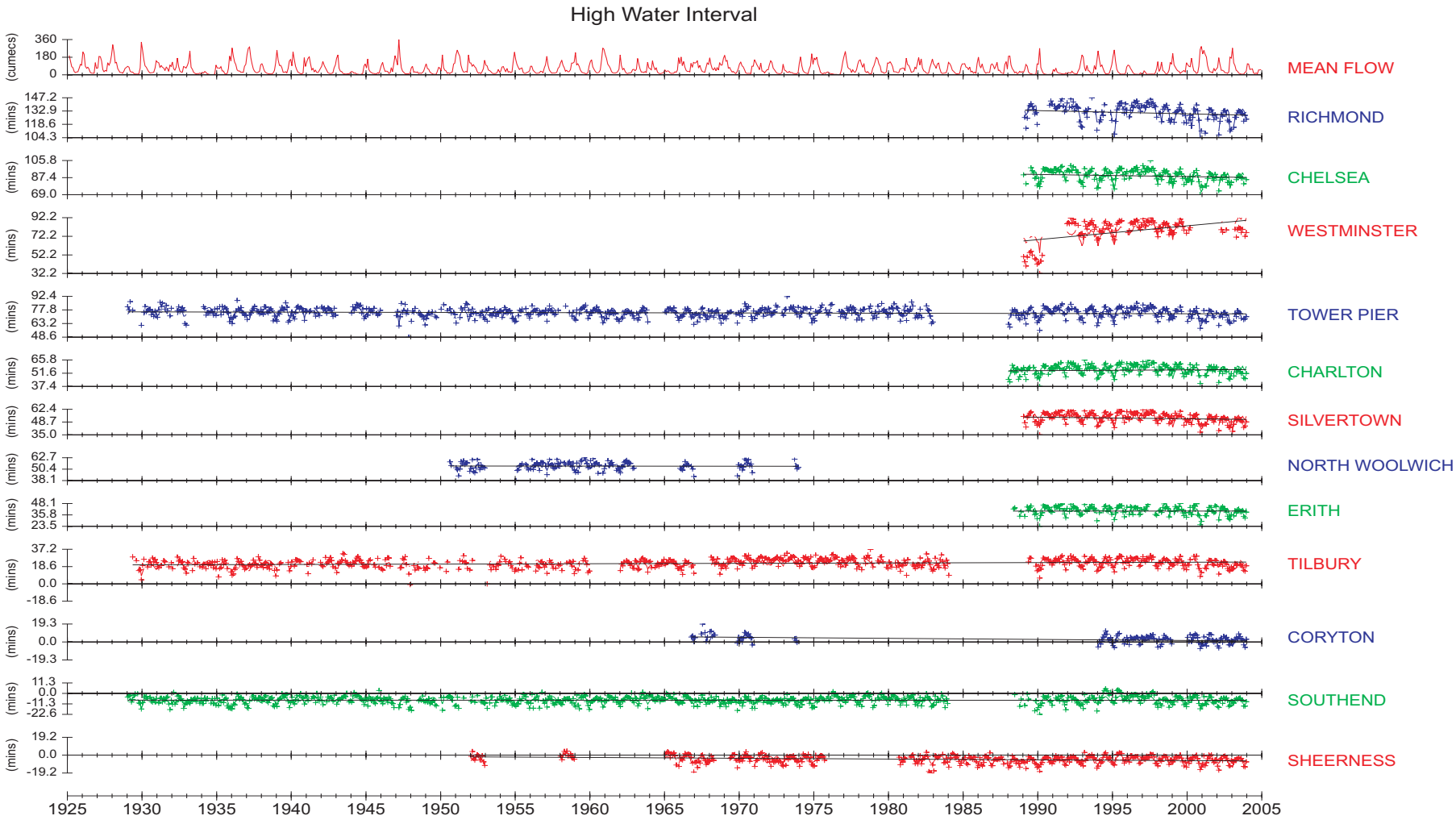

Figure G6 Monthly MHWI time series for the 12 tide gauges on the Thames Estuary and River Thames considered in the regional study

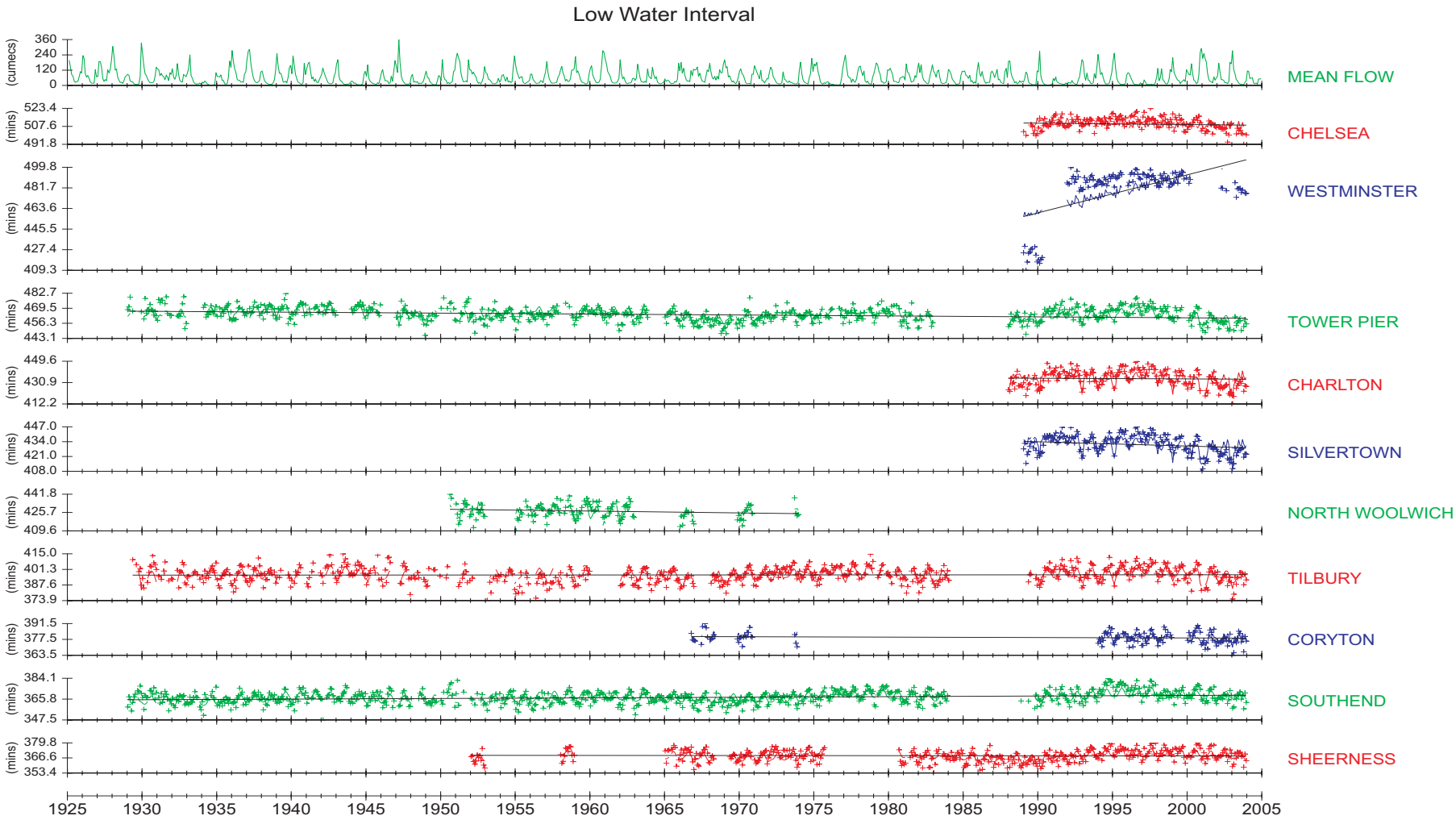

Figure G7 Annual MLWI time series for 10 of the 12 tide gauges on the Thames Estuary and River Thames considered in the regional study

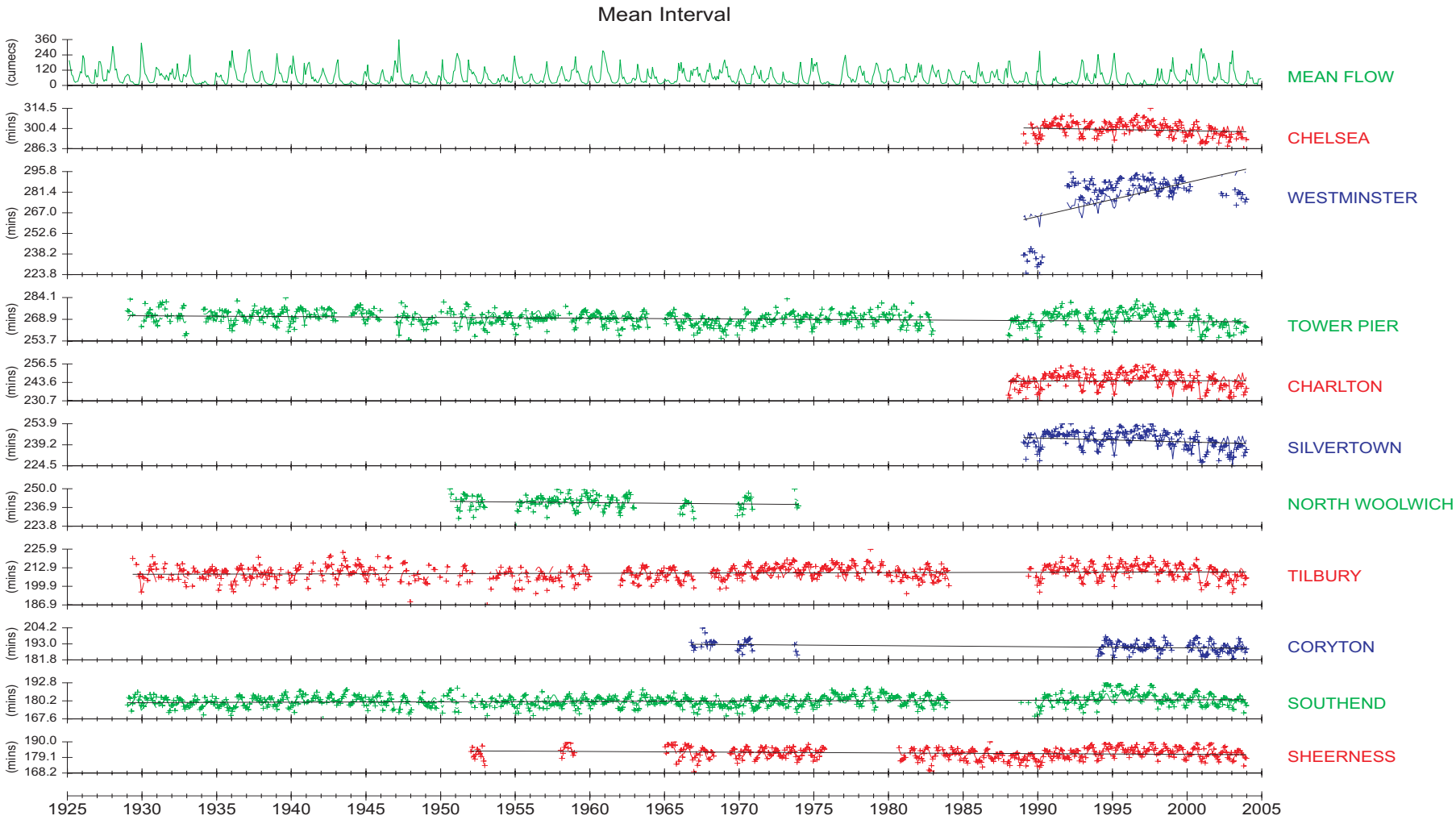

Figure G8 Annual MI time series for 10 of the 12 tide gauges on the Thames Estuary and River Thames considered in the regional study

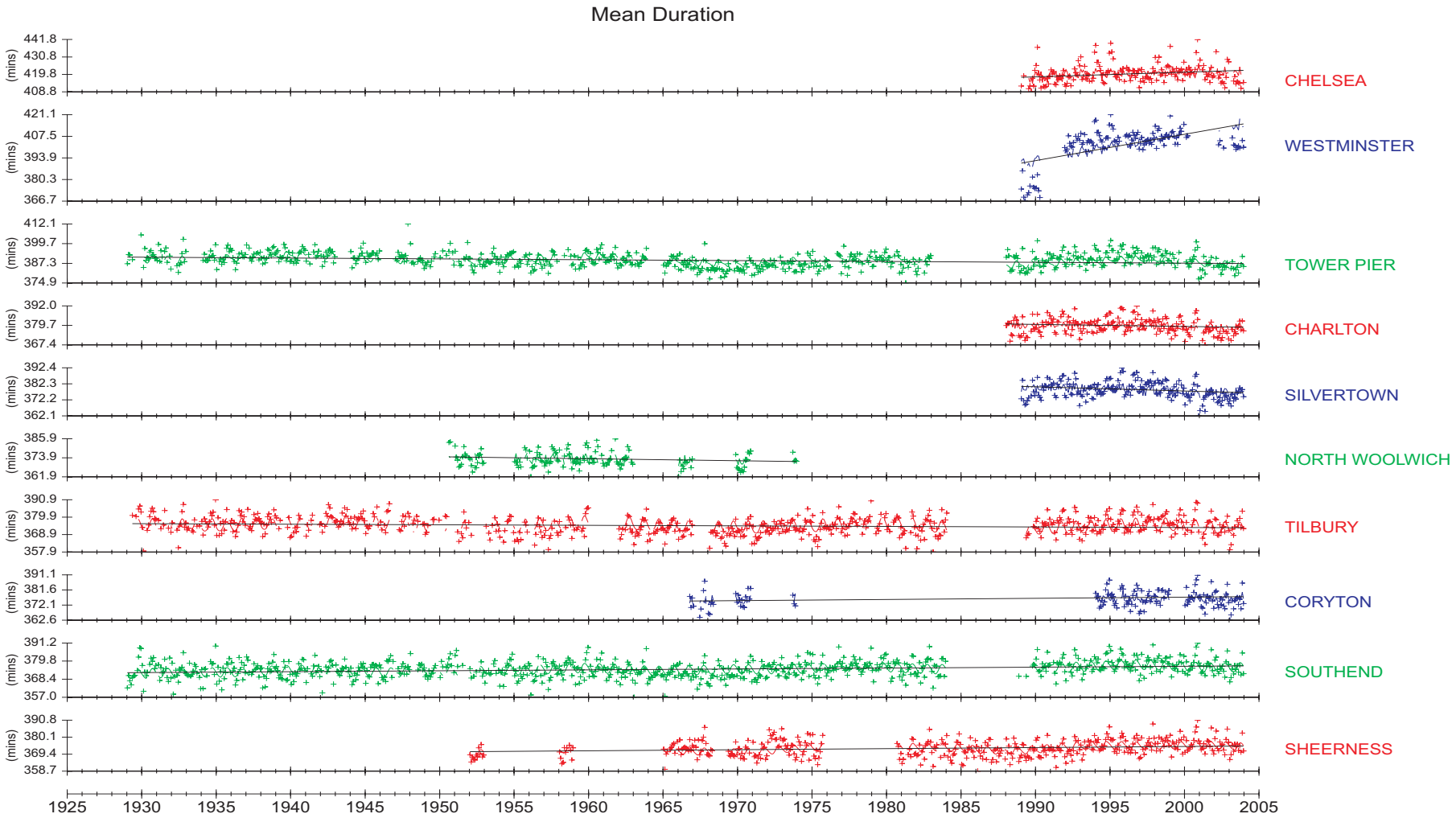

Figure G9 Monthly MD time series for 10 of the 12 tide gauges on the Thames Estuary and River Thames considered in the regional study

	station	Rossiter (1934-66)	Bowen (1931-69)				1929 - 2003				
		trend cm/century	trend cm/century	cos N cm	sin N cm	flow cm/100 cumecs	months of data	trend cm/century	cos N cm	sin N cm	flow cm/100 cumecs
mean high	Sheerness						410	26.8 ± 2.3	-2.6 ± 0.4	2.3 ± 0.4	5.4 ± 0.7
water height	Southend	36.3 ± 7.6	35.1 ± 4.3	-4.3 ± 0.6	-0.9 ± 0.7	4.3 ± 2.0	787	23.0 ± 1.0	-3.6 ± 0.3	0.6 ± 0.3	5.1 ± 0.5
	Coryton†						134	84.6 ± 5.5	-3.6 ± 0.3	0.6 ± 0.3	1.2 ± 1.1
	Tilbury		38.1 ± 5.8	-3.6 ± 0.8	0.8 ± 0.8	7.8 ± 2.3	654	36.3 ± 1.3	-3.6 ± 0.4	1.1 ± 0.4	9.2 ± 0.6
	North Woolwich†						135	8.3 ± 13.8	-3.6 ± 0.4	1.1 ± 0.4	5.0 ± 1.6
	Tower Pier	77.5 ±11.6	68.0 ± 4.9	-4.9 ± 0.7	-1.5 ± 0.7	15.2 ± 2.1	697	28.2 ± 1.4	-3.9 ± 0.4	-0.9 ± 0.4	10.8 ± 0.6
mean low	Sheerness						410	24.2 ± 2.3	5.8 ± 0.5	3.3 ± 0.4	2.1 ± 0.7
water height	Southend	24.9 ± 7.9	25.0 ± 4.6	5.0 ± 0.6	-0.9 ± 0.6	3.8 ± 1.8	784	14.4 ± 0.9	4.1 ± 0.3	0.2 ± 0.3	2.2 ± 0.4
	Coryton†						134	18.1 ± 6.6	4.1 ± 0.3	0.2 ± 0.3	3.4 ± 1.4
	Tilbury		27.7 ± 17.4	4.5 ± 0.9	1.4 ± 1.2	5.9 ± 2.6	657	26.5 ± 1.1	4.5 ± 0.4	1.6 ± 0.3	5.0 ± 0.5
	North Woolwich†						134	10.0 ± 12.6	4.5 ± 0.4	1.6 ± 0.3	7.4 ± 1.5
	Tower Pier	9.2 ± 8.9	4.3 ± 4.0	4.5 ± 0.5	1.0 ± 0.5	14.9 ± 1.6	698	16.5 ± 1.3	5.4 ± 0.4	3.3 ± 0.4	11.3 ± 0.6
mean	Sheerness						409	0.8 ± 1.3	-4.3 ± 0.3	-0.4 ± 0.2	—
amplitude	Southend	31.1 ± 4.6					783	4.2 ± 0.5	-3.9 ± 0.2	0.2 ± 0.2	—
	Coryton†						134	33.1 ± 3.6	-3.9 ± 0.2	0.2 ± 0.1	—
	Tilbury						652	4.8 ± 0.7	-4.0 ± 0.2	-0.1 ± 0.2	—
	North Woolwich†						134	-1.3 ± 9.8	-4.0 ± 0.2	-0.2 ± 0.2	—
	Tower Pier	43.4 ± 8.2					693	6.1 ± 0.9	-4.7 ± 0.3	-2.1 ± 0.3	—
mean tide	Sheerness						409	25.9 ± 1.9	1.6 ± 0.4	2.8 ± 0.3	3.8 ± 0.6
level	Southend	5.2 ± 6.1					783	18.6 ± 0.8	0.2 ± 0.3	0.4 ± 0.2	3.7 ± 0.4
	Coryton†						134	51.3 ± 4.9	0.2 ± 0.3	0.4 ± 0.2	2.3 ± 1.0
	Tilbury						652	31.3 ± 0.9	0.5 ± 0.3	1.4 ± 0.3	7.1 ± 0.5
	North Woolwich†						134	7.7 ± 8.7	0.5 ± 0.3	1.4 ± 0.3	6.3 ± 1.0
	Tower Pier	34.5 ± 7.0					693	22.2 ± 0.9	0.7 ± 0.3	1.2 ± 0.3	11.1 ± 0.4
mean sea	Sheerness						400	18.6 ± 2.1	2.0 ± 0.4	2.8 ± 0.3	1.2 ± 0.6
level	Southend						752	14.2 ± 0.9	0.4 ± 0.3	0.3 ± 0.3	1.2 ± 0.4
	Coryton†						119	35.5 ± 5.3	0.4 ± 0.3	0.3 ± 0.3	0.3 ± 1.1
	Tilbury						590	28.0 ± 1.1	1.0 ± 0.4	0.9 ± 0.3	2.8 ± 0.5
	North Woolwich†						127	7.0 ± 7.8	1.0 ± 0.4	0.9 ± 0.3	4.4 ± 0.9
	Tower Pier						618	12.9 ± 1.1	1.1 ± 0.3	1.1 ± 0.3	6.7 ± 0.5

Table G1 A comparison of regression analyses for monthly MHW, MLW, MTA, MTL and MSL with the results from the long period time series for 6 of the 12 tide gauges in the regional study (shown on the right of the table)

	station	Rossiter (1934-66) trend mins/century	1929 - 2003 months of data	trend mins/century	cos N mins	sin N mins	flow mins/100 cumecs
high water interval	Sheerness		410	-8.7 ± 1.3	-1.6 ± 0.3	0.3 ± 0.2	-2.7 ± 0.4
	Southend	0.2 ± 3.4	787	-0.1 ± 0.6	-1.1 ± 0.2	0.4 ± 0.2	-2.7 ± 0.3
	Coryton†		134	-11.3 ± 2.6	-1.1 ± 0.2	0.4 ± 0.2	-2.7 ± 0.5
	Tilbury		654	4.0 ± 0.8	-0.5 ± 0.3	-0.9 ± 0.2	-3.3 ± 0.4
	North Woolwich†		135	-1.3 ± 6.0	-0.5 ± 0.3	-0.9 ± 0.2	-3.9 ± 0.7
	Tower Pier	-6.4 ± 4.7	697	-3.0 ± 0.7	-1.0 ± 0.2	-0.7 ± 0.2	-4.5 ± 0.3
low water interval	Sheerness		410	-1.1 ± 1.8	-2.8 ± 0.3	0.0 ± 0.3	0.8 ± 0.5
	Southend	-4.4 ± 5.7	784	5.5 ± 0.7	-1.8 ± 0.2	-0.1 ± 0.2	0.6 ± 0.3
	Coryton†		134	-3.7 ± 3.4	-1.8 ± 0.2	-0.1 ± 0.2	-2.1 ± 0.7
	Tilbury		657	0.4 ± 1.0	-1.9 ± 0.3	-0.6 ± 0.3	-3.5 ± 0.5
	North Woolwich†		134	-16.2 ± 8.2	-1.9 ± 0.3	-0.6 ± 0.3	-5.8 ± 1.0
	Tower Pier	-25.1 ± 5.6	698	-8.1 ± 0.9	-2.8 ± 0.3	-1.0 ± 0.3	-2.9 ± 0.4
mean interval	Sheerness		409	-4.9 ± 1.3	-2.2 ± 0.2	0.1 ± 0.2	-1.0 ± 0.4
	Southend	-1.9 ± 4.2	783	2.7 ± 0.5	-1.4 ± 0.2	0.1 ± 0.2	-1.1 ± 0.2
	Coryton†		134	-7.5 ± 2.4	-1.4 ± 0.2	0.1 ± 0.2	-2.4 ± 0.5
	Tilbury		652	2.2 ± 0.8	-1.2 ± 0.3	-0.7 ± 0.2	-3.4 ± 0.4
	North Woolwich†		134	-9.2 ± 6.4	-1.2 ± 0.3	-0.7 ± 0.2	-4.8 ± 0.7
	Tower Pier	-15.8 ± 5.0	693	-5.6 ± 0.7	-1.9 ± 0.2	-0.8 ± 0.2	-3.7 ± 0.3
mean duration	Sheerness		409	6.7 ± 2.0	-1.2 ± 0.4	0.0 ± 0.3	—
	Southend	-4.6 ± 5.7	783	5.6 ± 0.8	-0.7 ± 0.3	-0.4 ± 0.2	—
	Coryton†		146	7.6 ± 3.5	-0.7 ± 0.2	-0.5 ± 0.2	—
	Tilbury		652	-3.5 ± 0.9	-1.5 ± 0.3	0.3 ± 0.3	—
	North Woolwich†		134	-12.4 ± 6.8	-1.5 ± 0.3	0.3 ± 0.3	—
	Tower Pier	-18.7 ± 4.0	693	-5.4 ± 0.8	-1.8 ± 0.2	-0.2 ± 0.2	—

Table G2 A comparison of regression analyses for monthly MHWI, MLWI, MI and MD with the results from the long period time series for 6 of the 12 tide gauges in the regional study (shown on the right of the table)

PB 12643

Nobel House
17 Smith Square
London SW1P 3JR

www.defra.gov.uk